

WL-TR-91-4032
DOT/FAA/CT-91/23
VOL II, Part 1

AD-A250 521



COMPOSITE FAILURE ANALYSIS HANDBOOK
VOL II - TECHNICAL HANDBOOK
PART 1 - PROCEDURES AND TECHNIQUES

R.J. Kar
Northrop Corporation
One Northrop Avenue
Hawthorne, California 90250-3277

February 1992

Final Report for Period January 1987 - October 1990



U.S. Department
of Transportation
Federal Aviation
Administration

Approved for public release; distribution unlimited.

MATERIALS DIRECTORATE
WRIGHT LABORATORY
AIR FORCE SYSTEMS COMMAND
WRIGHT-PATTERSON AIR FORCE BASE, OH 45433-6533

and

FEDERAL AVIATION ADMINISTRATION TECHNICAL CENTER
U.S. DEPARTMENT OF TRANSPORTATION
ATLANTIC CITY, NEW JERSEY 08405

DTIC
ELECTE
MAY 07 1992
S B D

92-12348

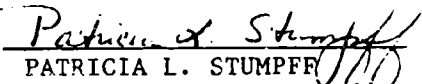


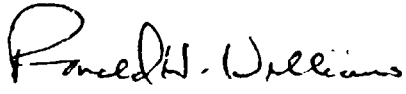
NOTICE

When Government drawings, specifications, or other data are used for any purpose other than in connection with a definitely Government-related procurement, the United States Government incurs no responsibility or any obligation whatsoever. The fact that the Government may have formulated or in any way supplied the said drawings, specifications, or other data, is not to be regarded by implication, or otherwise in any manner construed, as licensing the holder, or any other person or corporation; or as conveying any rights or permission to manufacture, use, or sell any patented invention that may in any way be related thereto.

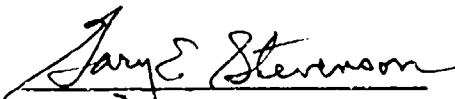
This report is releasable to the National Technical Information Service (NTIS). At NTIS, it will be available to the general public, including foreign nations.

This technical report has been reviewed and is approved for publication.


PATRICIA L. STUMPF
Project Engineer
Materials Integrity Branch


RONALD H. WILLIAMS
Technical Manager
Structural and Electronic
Failure Analysis

FOR THE COMMANDER


GARY E. STEVENSON, Actg Br Chf
Materials Integrity Branch
Systems Support Division

If your address has changed, if you wish to be removed from our mailing list, or if the addressee is no longer employed by your organization please notify WL/MLSA, WPAFB, OH 45433-6533 to help us maintain a current mailing list.

Copies of this report should not be returned unless return is required by security considerations, contractual obligations, or notice on a specific document.

REPORT DOCUMENTATION PAGE			Form Approved OMB No 0704-0188	
<small>Public reporting burden for this collection of information is estimated to average 1 hour per response, including the time for reviewing instructions, searching existing data sources, gathering and maintaining the data needed, and completing and reviewing the collection of information. Send comments regarding this burden estimate or any other aspect of this collection of information, including suggestions for reducing this burden, to Washington Headquarters Services, Directorate for Information Operations and Reports, 1215 Jefferson Davis Highway, Suite 1204, Arlington, VA 22202-4302, and to the Office of Management and Budget, Paperwork Reduction Project (0704-0188), Washington, DC 20503.</small>				
1. AGENCY USE ONLY (Leave blank)		2. REPORT DATE February 1992		3. REPORT TYPE AND DATES COVERED Final for 1 Jan 1987 to 31 Oct 1990
4. TITLE AND SUBTITLE Composite Failure Analysis Handbook Volume II: Technical Handbook Part 1 - Procedures and Techniques			5. FUNDING NUMBERS Contract Number F33615-87-C-5212	
6. AUTHOR(S) R.J. Kar				
7. PERFORMING ORGANIZATION NAME(S) AND ADDRESS(ES) Northrop Corporation Aircraft Division One Northrop Avenue Hawthorne, California 90250-3277			8. PERFORMING ORGANIZATION REPORT NUMBER	
9. SPONSORING / MONITORING AGENCY NAME(S) AND ADDRESS(ES) Wright Laboratory (WL/MLSA) Materials Directorate Wright-Patterson AFB, Ohio 45433-6533			10. SPONSORING / MONITORING AGENCY REPORT NUMBER WL-TR-91-4032, DOT/FAA/CT-91-23 Volume II - Part 1	
11. SUPPLEMENTARY NOTES Additional Funding/Sponsorship Provided By: FEDERAL AVIATION ADMINISTRATION TECHNICAL CENTER U. S. DEPARTMENT OF TRANSPORTATION ATLANTIC CITY, NEW JERSEY 08405				
12a. DISTRIBUTION / AVAILABILITY STATEMENT Approved for public release; distribution is unlimited			12b. DISTRIBUTION CODE	
13. ABSTRACT (Maximum 200 words) The objective of this program was to create a comprehensive handbook for use in conducting failure analysis investigations on failed composite structure. This program builds upon previous efforts as documented in the "Compendium of Post-Failure Analysis Techniques for Composite Materials," AFWAL-TR-86-4137. The purpose of creating this handbook was to document the techniques, the fractographic and material property data and case history studies currently being utilized in the analysis of failed composite structure. The major tasks on this program included: (1) procedural guidelines for field investigation techniques; (2) an expanded fractographic data base for carbon/epoxy materials tested under known conditions, (3) a fractographic data base for resin based composite materials other than carbon/epoxy; (4) fractographic documentation of composite material and processing defects; (5) documentation of fracture characteristics in adhesive and mechanical joint failures; (6) compilation of material property data for composite materials; and (7) documentation of case histories recently conducted on failed composite structure.				
14. SUBJECT TERMS Composites; Composite Structures; Failure Analysis; Fractography; Adhesive Joints; Mechanical Joints; Case History Studies			15. NUMBER OF PAGES 246	
			16. PRICE CODE	
17. SECURITY CLASSIFICATION OF REPORT UNCLASSIFIED	18. SECURITY CLASSIFICATION OF THIS PAGE UNCLASSIFIED	19. SECURITY CLASSIFICATION OF ABSTRACT UNCLASSIFIED	20. LIMITATION OF ABSTRACT	

SUMMARY

The objective of this program was to develop a comprehensive handbook for failure analyses of fiber-reinforced composites. The program objectives were accomplished through technical tasks that resulted in the compilation of a reference manual for evaluating failed composite structures.

A field handling logic network was prepared for on-site handling of composites during accident investigations. Procedural guidelines were developed from inputs provided by key field personnel from several government agencies, and from the results of tests performed in-house at Northrop. Several current and new fractographic techniques were evaluated to identify methods for initiation site determination and failure sequence identification in failed composite specimens. Macrophotography, ply-sectioning, and photographic methods were determined to be valuable supplemental techniques but could not directly provide initiation site/fracture propagation direction when used alone. The microchemical analysis technique of Fourier Transform Infrared Spectroscopy was determined to be useful in contaminant failure investigations but will require development of a database of chemical "signatures."

Northrop expanded the fractographic database originally developed by the Boeing Company for AS4/3501-6 graphite/epoxy (Gr/Ep) under Air Force Contract No. F33615-84-C-5010 to include the effects of load, manufacturing, processing, and environmental variables on simple interlaminar and translaminar test coupons. It was determined that applied load was the principal parameter that altered the fracture surface characteristics in Gr/Ep. Material form and processing variables indirectly affected the fracture characteristics in that these caused localized variations in applied load, thereby altering fractographic features. No significant effects of environment on fracture surface features were determined. The fractographic database also included documentation of manufacturing and processing defects that occur in Gr/Ep. The flaws were characterized using optical microscopy, and macrophotography techniques.

Failure modes in adhesively bonded Gr/Ep and graphite/bismaleimide (Gr/BMI) specimens were also characterized. Variations in ply thickness, orientation, and loading were carried out to develop mixed cohesive-adhesive, and singular cohesive or adhesive failures. It was determined that specimen geometry, lap/strap ratios, and test load played roles in controlling fracture surface characteristics. Fracture characteristics in the failed adherends served as indicators of fracture direction in mixed and total adhesive failure modes. The crack directions could not be readily determined in pure cohesive joint failures.

A test matrix was developed for characterizing the six different failure modes in mechanically joined composite structures. A computer code entitled SAMCJ (Strength Analysis of Multifastened Composite Joints), previously developed by Northrop for the USAF, was run to develop the matrix for quasi-isotropic ASR/3501-6 Gr/Ep joined with titanium "Hi-Lok" tension or shear-type flush head

fasteners. Failure tests and fractographic evaluation were carried out on the specimens. It was determined that the failure modes were a function of applied load, specimen, and fastener geometries.

Detailed in-plane shear tests were also carried out for Gr/Ep. This failure mode was characterized by the occurrence of hackles on fractured resin and tension fracture characteristics on fractured fiber ends. Processing variables did not significantly alter the fracture surface characteristics for Gr/Ep tested under in-plane shear. The information gained from the Northrop and Boeing Gr/Ep studies was used in initiating a fractographic database for other material systems. The material systems chosen were kevlar 49/3501-6 epoxy (K/Ep), AS4 graphite/5250-3 bismaleimide (Gr/BMI), and AS4 graphite/APC-2 PEEK thermoplastic (Gr/PEEK). Testing and fractographic evaluation were carried out for baseline and several variable conditions. The results for these systems indicated that the type of resin and fiber played strong roles in controlling the resulting fracture surface characteristics. As for Gr/Ep, environment and processing variables did not significantly alter fracture characteristics.

Northrop reviewed formats previously used for reporting metallic and composite fractography and failure analysis data. Based on an assessment of existing report schemes, Northrop proposed three data formats for (1) reporting fractographic data, (2) failure analysis information, and (3) organization of the Composite Failure Analysis Handbook. These were subsequently approved by the Air Force with minor modifications.

Northrop compiled material properties on current and near-term composite structural materials. Literature searches were carried out on government and commercial databases for product information and properties. Properties obtained were incorporated into database files using a personal computer. The data were organized into tabular formats for reporting in the Handbook. The properties for several classes of fiber, prepreg, and laminates were compiled and organized into the Handbook.

Under an engineering services agreement between Northrop and the university of Utah, Professor Willard Bascom of the University of Utah performed a literature search and made on-site visits to several government agencies to gather information on composite fractography and failure analysis that may have been performed at these agencies. No other information was found other than that previously reported by Boeing. Dr. Bascom also reviewed stress analysis methods and failure micromechanisms for use in failure analysis investigations. A new failure criterion developed by Dr. Richard Christensen of Lawrence Livermore Laboratories was determined to be of utility in composite failure investigations.

Verification of the composite failure analysis logic system was performed through evaluation of several failed structural items provided by the Air Force. The structural items represented "real-world" configurations and included (1) a vertical stabilizer, (2) a horizontal torque box assembly, (3) a canopy support fitting, and (4) two simple components. All the results are presented as case histories in the Handbook.

As part of the verification process, two simple Gr/Ep structures containing intentional defects were fabricated and tested to failure under controlled laboratory conditions. The failed specimens and related test documentation were shipped to the Air Force for subsequent evaluation by the Boeing Company.

The Composite Failure Analysis Handbook is divided into two volumes. Volume I is the Program Overview. Volume II comprises the Technical Handbook, and is divided into three parts. Part 1 describes all the techniques and procedures for performing composite failure analysis. Part 2 represents

an atlas of fractographs. Part 3 is a compilation of case histories of investigations performed by Northrop, Boeing, and General Electric.

In summary, Northrop has achieved the objective of producing a Handbook containing all the known techniques, procedures, sample data, and reference supporting data for performing post-failure analysis of fiber-reinforced composite structures.



Accession For	
NTIS GRA&I	<input checked="checked" type="checkbox"/>
DTIC TAB	<input type="checkbox"/>
Unannounced	<input type="checkbox"/>
Justification	
By _____	
Distribution/	
Availability Codes	
Dist.	Avail and/or Special
A-1	

FOREWORD

The final report documents work performed under Contract F33615-87-C-5212 from January, 1987 through October, 1990 by the Northrop Corporation, Aircraft Division, Hawthorne, California for the United States Air Force Systems Command. The program was administered under the technical direction of Ms Patricia Stumpff, Materials Directorate, Wright Laboratory, Wright-Patterson Air Force Base, Ohio 45433-6533. The majority of funding for this program was provided by the Federal Aviation Administration Technical Center, Aviation Safety Division, Atlantic City, New Jersey 08405. Mr Lawrence Neri, ACD-210, acted as the Federal Aviation Administration technical manager. Mr Joseph Soderquist, National Resource Specialist, Advanced Materials, Federal Aviation Administration, AIR-103, 800 Independence Avenue, S.W., Washington, D. C. 20591, also provided technical direction for this program.

The work was performed by Northrop's Materials Analysis Laboratory. Dr R. J. Kar was the Program Manager and Principal Investigator. The contributions of the following members of the Materials Analysis Laboratory are gratefully acknowledged: Ms L. M. Concepcion (Co-Principal Investigator), Mr O. P. DeCastro (SEM and materialography), Mr J. M. Dobson (case histories), Mr T. N. Gindraux (materialography and SEM) Mr L. J. Havemann (SEM), Mr M. D. Ensminger (FTIR), Mr L. S. Dhillon (materialography) and Mr E. E. Ramirez (materialography). Mr P. J. Dager of Northrop's Mechanical Testing Laboratory and Mr R. J. Isberner of Northrop's Structures Test Laboratory performed the mechanical testing of laminate coupons and real-world elements. Mr R. B. Deo, and Mr T. A. Dyer of Northrop's Structures Research Department participated in the selection of test laminates.

Professor W. D. Bascom, Department of Materials Science and Engineering at the University of Utah, also made significant contributions by conduction of literature survey on composite fractography and identifying new composite failure criteria.

The results of additional work in composites failure analysis by the Boeing Military Airplane Company under Air Force Contracts F33615-84-C-5010 and F33615-86-C-5071 from 1984 through 1988 have been included in this report for the purpose of providing the most complete Composite Failure Analysis Handbook. Mr R. A. Grove, Mr B. W. Smith, and Ms C. T. Hua were Principal Investigators, and Mr D. F. Sekits was the Program Manager of these programs. The author wishes to thank Boeing and the numerous publishing houses and authors who granted permission to include their works in this document.

TABLE OF CONTENTS

Section	Page
1 INTRODUCTION AND PURPOSE	1-1
2 SOURCES OF FAILURE	2-1
2.1 Design Errors	2-1
2.1.1 Critical Parameters	2-1
2.1.2 Common Errors	2-2
2.2 Materials and Process Discrepancies	2-2
2.3 Anomalous Service Conditions	2-3
2.4 Examples	2-3
3 FAILURE ANALYSIS LOGIC NETWORKS	3-1
3.1 General Concepts	3-1
3.2 Major Failure Analysis Logic Networks	3-1
4 FIELD GUIDELINES	4-1
4.1 Avionics Hazards	4-1
4.2 Health and Safety Issues	4-1
4.3 Safety Guidelines	4-2
4.4 Safety Equipment	4-3
4.5 On-Site Crash/Wreckage Reconstruction and Handling	4-4
4.6 Cleaning Methods	4-5
4.7 Visual Examination	4-5
5 NONDESTRUCTIVE EVALUATION TECHNIQUES	5-1
5.1 Ultrasonic Methods	5-6
5.1.1 Through-Transmission Ultrasonic	5-6
5.1.2 Pulse-Echo Ultrasonics	5-8
5.1.3 Single-Sided Ultrasonic (Backscatter)	5-10
5.2 X-Ray Radiography	5-11
5.2.1 Classical Radiography	5-11
5.2.2 Penetrant-Enhanced Radiography	5-12
5.3 Eddy Current	5-14
5.4 Edge Replication	5-14

TABLE OF CONTENTS (Continued)

Section		Page
6	MATERIALS CHARACTERIZATION	6-1
6.1	Laminate Layup and Ply Orientation Analyses	6-5
6.1.1	Optical Microscopy (For Determination of Layup and Ply Orientation)	6-6
6.1.2	Image Analysis (For Determination of Layup and Ply Orientation)	6-7
6.1.3	Radiography (For Determination of Layup and Ply Orientation)	6-8
6.2	Determination of Fiber, Matrix, Void, and Moisture Content	6-8
6.2.1	Fiber and Matrix Content	6-10
6.2.2	Void Content	6-11
6.2.3	Moisture Content	6-11
6.3	Material Identification	6-11
6.3.1	Uncured Material Identification	6-11
6.3.2	Cured Material Identification	6-17
6.4	Degree of Cure Analysis	6-19
6.4.1	Glass Transition Temperature Analysis	6-21
6.4.2	Extent of Unreacted Material	6-25
6.5	Cured Material Contamination Analysis	6-28
6.5.1	Particulate Contamination	6-28
6.5.2	Weak Boundary Contamination	6-28
6.5.3	Scanning Electron Microscopy and Electron Microprobe Analysis ..	6-33
6.5.4	X-Ray Photoelectron Spectroscopy	6-37
6.5.5	Infrared Spectroscopy and Fourier Transform Infrared	6-39
6.5.6	X-Ray Diffraction	6-42
6.5.7	Secondary Ion Mass Spectroscopy	6-42
6.5.8	Auger Electron Spectroscopy	6-42
6.5.9	Contamination Analysis Example	6-43
7	MECHANICAL TEST METHODS	7-1
7.1	Interlaminar Mode I Tension (DCB)	7-1
7.2	Interlaminar Mode II Shear (ENF)	7-1
7.3	Translaminar Tension (N4PTT)	7-4
7.4	Translaminar Compression (N4PTC)	7-4
7.5	Rail Shear Test:	7-4
7.6	Compression After Impact (CAI)	7-7
8	FRACTOGRAPHY	8-1
8.1	Care, Handling, and Protection of Fracture Surfaces	8-6
8.1.1	Mechanical Damage	8-6
8.1.2	Chemical Damage	8-7
8.1.3	Laboratory Cleaning	8-7

TABLE OF CONTENTS (Continued)

Section		Page
8.2	Photo Macrography	8-8
8.3	Optical Microscopy	8-9
	8.3.1 Microscope Systems	8-9
	8.3.2 Illumination	8-9
	8.3.3 Diaphragms	8-10
	8.3.4 Objective Lens	8-10
	8.3.5 Specimen Preparation	8-10
	8.3.6 Fracture Surface Inspections	8-10
	8.3.7 Cross-Section Analysis	8-11
8.4	Scanning Electron Microscopy	8-11
	8.4.1 SEM Specimen Preparation	8-12
	8.4.2 SEM Techniques	8-13
8.5	Transmission Electron Microscopy	8-20
	8.5.1 TEM Specimen Preparation	8-20
	8.5.2 TEM Techniques	8-22
9	STRESS ANALYSIS	9-1
9.1	Introduction to Composite Stress Analysis	9-1
	9.1.1 Relevance to Stress Analysis FALN	9-6
	9.1.2 Overview of Topics	9-8
	9.1.3 Analytical Prediction of Strength (of Unnotched Multidirectional Laminates)	9-8
	9.1.4 Individual Ply Failure Criteria	9-8
	9.1.5 Laminate Level Strength Criteria	9-13
	9.1.6 Summary — Unnotched Laminate Strength	9-19
9.2	Influence of Ply Thickness on Transverse Cracking	9-19
9.3	Strength Reductions Incorporated Into Design	9-20
9.4	Introduction to Delamination	9-25
	9.4.1 Fracture Analysis and Specimens (For Interlaminar Toughness) ...	9-26
	9.4.2 Interlaminar Fatigue Crack Growth	9-30
	9.4.3 Reductions in Strength Due to Manufacturing Defects	9-31
10	INVESTIGATIVE AND REPORTING FORMATS	10-1
11	GLOSSARY	11-1
12	REFERENCES	12-1

TABLE OF CONTENTS (Continued)

Appendix		Page
A	CHEMICAL AND MECHANICAL PROPERTIES OF FIBER-REINFORCED COMPOSITE MATERIALS COMPILED BY NORTHROP	A-1
B	CHEMICAL AND MECHANICAL PROPERTIES OF FIBER-REINFORCED COMPOSITE MATERIALS COMPILED BY BOEING	B-1

LIST OF ILLUSTRATIONS

Figure		Page
2-1	Rockwell Flaw Criticality Study Defect 1: External Delamination	2-5
2-2	Rockwell Flaw Criticality Study Defect 2: Blister, Internal Delamination	2-5
2-3	Rockwell Flaw Criticality Study Defect 3: Oversized Hole	2-6
2-4	Rockwell Flaw Criticality Study Defect 4: Hole Exit Side Broken Fibers Breakout	2-6
2-5	Rockwell Flaw Criticality Study Defect 5: Tearout in Countersink	2-7
2-6	Rockwell Flaw Criticality Study Defect 7: Resin-Starved Laminate (Bare Fibers)	2-7
2-7	Rockwell Flaw Criticality Study Defect 8: Resin-Rich Area at Arrow (Dark Areas Are Voids)	2-8
2-8	Rockwell Flaw Criticality Study Defect 9: Excessive Porosity, Voids	2-9
2-9	Rockwell Flaw Criticality Study Defect 10: Scratch, Handling Damage	2-9
2-10	Rockwell Flaw Criticality Study Defect 11: Dent, Handling Damage	2-9
2-11	Rockwell Flaw Criticality Study Defect 12: Fiber Breakaway From Impact Surface	2-10
2-12	Rockwell Flaw Criticality Study Defect 13: Splintering, Edge Delamination	2-10
2-13	Rockwell Flaw Criticality Study Defect 14: Overtorqued Fastener	2-11
2-14	Rockwell Flaw Criticality Study Defect 16: Edge Notch, Crack	2-11
2-15	Rockwell Flaw Criticality Study Defect 17: Corner Notch	2-12
2-16	Rockwell Flaw Criticality Study Defect 18: Mislocated Hole — Not Repaired	2-12
2-17	Rockwell Flaw Criticality Study Defects 20 and 21: Marcellled Fibers (Arrow) and Wrinkles	2-13
2-18	Rockwell Flaw Criticality Study Defect 26: Wrong Material, Correct Layup [0] ₁ 2T	2-13
2-19	Rockwell Flaw Criticality Study Defect 27: Misoriented Ply From Correct Layup [± 45/90/02/ ± 45/02/ ± 45/0] _S	2-14
2-20	Rockwell Flaw Criticality Study Defect 28: Ply Overlap	2-15
2-21	Rockwell Flaw Criticality Study Defect 29: Ply Underlap, Gap	2-15
2-22	Rockwell Flaw Criticality Study Defect 31: Improper Fastener Seating	2-16
2-23	Rockwell Flaw Criticality Study Defect 33: 8 Hole	2-16

LIST OF ILLUSTRATIONS (Continued)

Figure		Page
2-24	Rockwell Flaw Criticality Study Defect 35: Off-Axis Drilled Hole	2-17
2-25	Rockwell Flaw Criticality Study Defect 36: Countersink on Wrong Side of Laminate	2-17
2-26	Rockwell Flaw Criticality Study Defect 39: Burned Drilled Hole	2-18
2-27	Rockwell Flaw Criticality Study Defect 41: Undersized Fastener	2-18
2-28	Rockwell Flaw Criticality Study Defect 42: Dent, Hidden Fiber Breakage	2-19
3-1	Simplified Investigative Framework	3-3
3-2	Detailed Investigative Framework	3-4
4-1	Field Handling Logic Network for Composite Parts	4-2
4-2	Visual Macroscopic Fracture Surface Features	4-5
5-1	Nondestructive Evaluation Sub-FALN	5-2
5-2	Examples of an Ultrasonic Through-Transmission C-Scan	5-7
5-3	Pulse-Echo Ultrasonic C-Scan Using Time-Domain Gating Zones To Identify Damage States of Impact	5-9
5-4	Delamination Identified by a Family of Pulse-Echo Ultrasonic A-Scans	5-10
5-5	Pulse-Echo Ultrasonic B-Scan of a Delamination Region	5-11
5-6	Ultrasonic Detection of Simulated Crack in Laminate Plate	5-11
5-7	Penetrant-Enhanced X-Ray Image of Edge Delamination	5-13
5-8	Typical Inspection Procedure Using Probe to Detect Subsurface Damage in Fabric Laminates	5-15
6-1	Simplified Investigative Framework (Laboratory Examination)	6-2
6-2	Material Verification Technique Sub-FALN	6-3
6-3	Cross Section of a Laminate With Easily Differentiated Ply Separation	6-8
6-4	Identification of Ply Orientation by Fiber End Shape and Ovality	6-8
6-5	Polished Cross Section at 45-deg Angle Through the Thickness of the Part	6-9
6-6	Radiograph in Which the Tracer Yarns Are Evident for Determination of the Ply Orientation in a Thin Laminate	6-10
6-7	HPLC Test Setup Schematic and Typical Instrument Parameters	6-12
6-8	Chromatogram of Narmco Resin Matrix Showing Major Peak Assignment	6-13
6-9	Standard IR Spectrum of a Commercial Epoxy Resin Formulation	6-14

LIST OF ILLUSTRATIONS (Continued)

Figure		Page
6-10	Cross-Sectional Diagram of the DSC Cell Used by DuPont DSC Module	6-15
6-11	DSC Thermogram for 3501-6 Resin	6-16
6-12	Sample Fingerprinting of Various Systems by Way of X-Ray Fluorescence	6-17
6-13	Pyrolysis Gas Chromatography of Two Difficult Resin Systems	6-19
6-14	Gas Chromatography of DDS, Diaminodiphenyl Sulfone	6-20
6-15	IR Comparison of Resin	6-21
6-16	DRIFTS of Graphite-Epoxy (AS/3501-5) Composite Before and After Thermal Aging	6-22
6-17	Glass Transition Temperature Determination — TMA Penetration Test Setup ...	6-23
6-18	Glass Transition Temperature Determination — TMA Penetration Test Measurement	6-23
6-19	Glass Transition Temperature Determination — TMA Flexure Test Setup	6-24
6-20	Glass Transition Temperature Determination — TMA Flexure Test Measurement	6-24
6-21	Determination of Tg by Expansion Method	6-25
6-22	Typical DMA Plot for Cured Epoxy Showing Glass Transition Determination ...	6-25
6-23	Typical DSC Plot for Cured Epoxy Illustrating Determination of Tg and Heat of Additional Reaction	6-26
6-24	DMA Loss Modulus Versus Temperature Showing Effect of Undercure for Epoxy Resin	6-27
6-25	SEM Micrograph of a Teflon-Contaminated Tension Specimen	6-29
6-26	SEM Micrograph of a Frekote Release Agent Contaminated Tension Specimen (200X)	6-30
6-27	SEM Micrograph of a Frekote Release Agent Contaminated Tension Specimen (2,000X)	6-30
6-28	SEM Micrographs of a Typical Uncontaminated Fracture Specimen	6-31
6-29	SEM Micrographs of Foreign Particle Inclusions illustrating the Characteristic Fracture Surface Asperity and Radiating Fracture Lines	6-32
6-30	Initial Inspection and Determination of a Foreign Material Contamination	6-34
6-31	Logic Network for Chemical Analysis of Foreign Material Contamination of a Composite Fracture Surface	6-35
6-32	Talc Powder Contamination Along a Bond Line	6-36
6-33	Typical XPS Spectrum of an Epoxy Resin With Elements Identified	6-38

LIST OF ILLUSTRATIONS (Continued)

Figure		Page
6-34	Infrared Spectrum of an Epoxy Resin	6-40
6-35	AES Spectra of (a) Carbon Fiber and (b) Exposed Carbon Fiber on a Tensile Fracture	6-44
6-36	Optical Micrograph in Cross Section of a Laminate Skin to Core Buckling Separation	6-45
6-37	SEM Micrographs Showing a Replicated Surface Morphology	6-45
6-38	XPS Spectra of the Disbonded FM-300 Ply Surfaces	6-46
6-39	XPS Spectra of FM-300 Ply Surfaces Separated by Hand in the Laboratory	6-47
7-1	Double-Cantilever Beam Specimen Geometry	7-2
7-2	Double-Cantilever Beam Specimen	7-2
7-3	Double-Cantilever Beam Grip Fixture	7-3
7-4	End-Notched Flexural Specimen Geometry	7-3
7-5	Notched-Bend-Bar (Tension) Specimen Geometry	7-4
7-6	Notched-Bend-Bar (Compression) Specimen Geometry	7-5
7-7	Rail-Shear Specimen	7-6
7-8	Rail-Shear Test Set-Up	7-7
7-9	Impact Support Fixture	7-8
8-1	Fractography Diagnostic Technique Sub-FALN	8-3
8-2	Basic Features of the SEM	8-14
8-3	SEM Beam-Specimen Interaction Details	8-15
8-4	Contrasting Differences in SEM Photomicrographs	8-16
8-5	SEM Photomicrographs of Effect of Tilt on Striation Resolution	8-18
8-6	SEM Fractographs of Mode II Delamination Between Adjacent 0-deg Plies Illustrating the Effect of Tilt Angle	8-19
8-7	Two-Stage TEM Replication Technique	8-21
8-8	Basic Features of the Transmission Electron Microscope	8-23
8-9	High-Magnification TEM Photomicrographs Showing Fatigue Striations	8-24
8-10	TEM Photomicrograph of Striation Features From a Crack Lap Shear Specimen	8-25
9-1	Stress Analysis Sub-FALN	9-5
9-2	Maximum Stress Failure Theory	9-10

LIST OF ILLUSTRATIONS (Continued)

Figure		Page
9-3	Tsai-Hill Theory	9-11
9-4	Tsai-Wu Tensor Theory	9-13
9-5	Comparison of Calculated In-Plane Tensile Strength With Experiment	9-14
9-6	Quadratic Interaction First Ply Failure Envelope for T300/5208	9-15
9-7	Stress Gradients Resulting From Edge Effects	9-16
9-8	Through-Thickness Tensor Polynomial Distributions for Curing Stresses and Stresses at the First Failure (+/-) Laminates	9-17
9-9	Tensor Polynomial Distributions Along the Interface of (+/-) Laminates	9-18
9-10	Comparison of Experimentally Derived In Situ Lamina Elastic Strains at Onset of Matrix Cracking With 2D Shear Lag Model Predictions for (0/90) T300/934 Laminate Family	9-20
9-11	Strength Reduction of Uniaxially Loaded Plate With Circular Hole According to Average Stress Criterion	9-22
9-12	Strength Reduction of Uniaxially Loaded Hole According to Point Failure Stress Criteria	9-23
9-13	Strength Reductions as a Function of the Hole Radius for (0/ +45/-45/90 deg) Graphite-Epoxy Plates With Circular Holes Under Uniaxial Tensile Loading	9-23
9-14	Hole Geometries Analyzed With the Damaged Zone Model (DZM)	9-24
9-15	Effect of Impact Damage on the Compressive Strength of a Quasi-Isotropic Laminate	9-25
9-16	Design Details That Cause Interlaminar Stress Concentrations	9-26
9-17	End-Notched Flexure (ENF) and Double-Cantilever Beam (DCB) Specimens	9-27
9-18	Modes of Crack Propagation	9-27
9-19	Mixed Modes I and II Delamination Specimens	9-28
9-20	Crack Tip Loading Mechanisms Causing Interlaminar Normal and Shear Stress Concentrations	9-28
9-21	Mode II Fatigue	9-31
10-1	Analysis Collection and Tracking System (FACTS) Data Input Sheet	10-2
10-2	Nondestructive Examination Data Input Sheet	10-3
10-3	Materials Characterization Data Input Sheet	10-4
10-4	Materials Characterization Data Input Sheet (Figure Attachment)	10-5
10-5	Fractography Macroscopic Analysis Data Input Sheet	10-6
10-6	Fractography Macroscopic Analysis Data Input Sheet (Photo Attachment)	10-7

LIST OF ILLUSTRATIONS (Continued)

Figure		Page
10-7	Fractography Microscopic Analysis Data Input Sheet	10-8
10-8	Fractography Microscopic Analysis Data Input Sheet (Photo Attachment)	10-9
10-9	Stress Analysis Data Input Sheet	10-10
10-10	Stress Analysis Data Input Sheet (Diagram Attachment)	10-11
10-11	Fractographic Data Reporting Format	10-12
10-12	Failure Analysis Data Reporting Format	10-13
B-1	Hercules Fiber Properties at Room Temperature	B-3
B-2	Typical Epoxy Composite Properties at Room Temperature	B-4
B-3	0° Strength-to-Density Ratio of Typical Epoxy Composites	B-5
B-4	0° Tensile Properties of Typical Epoxy Composites	B-5
B-5	Tensile Properties of Graphite Fabric Prepreg	B-7
B-6	Tensile Properties of Matrices	B-9
B-7	Strength-to-Density Ratio of Matrices	B-10
B-8	Neat Resin Properties at Room Temperature	B-11
B-9	Deformation Stages of Fiber, Matrix, and Composite	B-12
B-10	Tensile Strength of Neat Resins	B-14
B-11	Young's Modulus of Neat Resins	B-16
B-12	Tensile Properties of Commercial Carbon Fibers	B-18
B-13	Strength-to-Density Ratio of Commercial Carbon Fibers	B-19

LIST OF TABLES

Table		Page
2-1	Rockwell Flaw Criticality Study Defects	2-4
5-1	Failure Analysis Techniques — Nondestructive Evaluation	5-3
5-2	Inspection Method Selection (Listed in Order of Preference)	5-4
6-1	Failure Analysis Techniques for Materials Characterization	6-4
6-2	X-Ray Emission Lines, Partial Listing	6-36
6-3	Approximate XPS Peak Positions and Emission Probabilities for Common Elements	6-38
6-4	Carbon Peak Shifts in XPS	6-39
6-5	Rules of Thumb for XPS Identification of Typical Release Agents	6-40
8-1	Failure Analysis Techniques — Fractography	8-4
8-2	Failure Analysis Techniques — Fracture Surface Material and Chemical Characterization	8-5
9-1	Stress Analysis Methods	9-3
9-2	Computer Analysis Programs	9-6
9-3	Fracture Toughness of Various Orientations	9-21
9-4	G_{IC} and G_{IIC} Values Obtained From DCB and ENF Testing Reported in Literature	9-29
9-5	Fatigue Crack Growth of AS-1/3501-6	9-30
9-6	Manufacturing Defects	9-32
A-1	Keywords, Sources and Abstracts in Literature Search of DTIC, NASA and Plastics Center Data Bases	A-2
A-2	Commercial Fiber Properties	A-3
A-3	Properties of Carbon/Epoxy Prepreg	A-4
A-4	Properties of Glass/Epoxy Prepreg	A-6
A-5	Properties of Kevlar/Epoxy Prepreg	A-8
A-6	Properties of Glass/Polyimide Prepreg	A-10
A-7	Properties of Carbon/Epoxy Laminates	A-12

LIST OF TABLES (Continued)

Table		Page
A-8	Properties of Glass/Epoxy Laminates	A-14
A-9	Properties of Kevlar/Epoxy Laminates	A-16
A-10	Properties of Glass/Polyimide Laminates	A-18
A-11	Properties of Carbon/Polyimide Laminates	A-20
A-12	Properties of Ablative/Phenolic Prepreg	A-22
A-13	Properties of Ablative/Phenolic Laminates	A-24
A-14	Properties of Glass/Phenolic Laminates	A-26
A-15	Properties of Glass/Polyester Laminates	A-28
B-1	Mechanical Properties of Hercules Fibers	B-2
B-2	Properties of Typical Epoxy Composites at Room Temperature	B-4
B-3	Physical Properties of Graphite Fabric Prepreg (Data From Fiberite Corp.)	B-6
B-4	Properties of Matrices	B-8
B-5	Table of Neat Resin Properties at Room Temperature	B-10
B-6	Properties of Graphite (Carbon) Fibers	B-12
B-7	Properties of Kevlar and Glass Fibers	B-13
B-8	Tensile Strength of Neat Resins	B-13
B-9	Young's Modulus of Neat Resins	B-15
B-10	Physical Properties of Epoxy Preimpregnated Unidirectional Tapes	B-17
B-11	Properties of Commercial Carbon Fibers	B-18
B-12	Constituent Property Data of Fibers	B-20

SECTION 1

INTRODUCTION AND PURPOSE

Advanced composites are rapidly emerging as a primary material for use in near-term and next-generation aircraft as they provide greater structural efficiency at lower weight than equivalent metallic components. Based on trends to date, the next generation of military aircraft could contain as much as 65 percent of their structural weight in advanced composite materials.

As composite materials continue to be developed and incorporated into airframe structures, needs have arisen for solving problems associated with their use. Composite structures can and will prematurely fail due to gross manufacturing defects, design errors, or severe in-service damage. Needs exist for a systematic compilation of failure analysis techniques, procedures, and supporting fractographic data — in handbook form — that can be used by experienced laboratory personnel, working in consultation with field investigators, to diagnose the cause for premature component failure and to make recommendations for preventing similar failures.

The goal of this Composite Failure Analysis Handbook is to provide a guide for conducting post-failure analysis of fiber-reinforced composite structures. It forms a compilation of the procedures, techniques, and sample data required to conduct analyses of composite structures. Volume II of this report is the Technical Handbook and it has been divided into three parts.

Part 1 of the Handbook is a summary of the procedures and techniques used to perform failure analyses of composites. This part is largely comprised of the results of work performed by Boeing under Air Force Contracts F33615-84-C-5010 and F33615-86-C-5071 and reported by Boeing in AFWAL TR-86-4137 and WRDC-TR-89-4055. Northrop expanded this summary under Air Force Contract F33615-87-C-5212 to include (1) procedures and techniques that have recently developed, (2) documentation of manufacturing and processing defects that occur in graphite/epoxy, and (3) a compilation of chemical and mechanical properties of current and near-term composite structural materials. The sequence that a laboratory investigator should follow during failure analysis of a fractured composite component (failure analysis logic network), and procedural guidelines for on-site handling and examination of composites during accident investigations (field handling logic network) have also been updated and expanded. Laboratory failure analysis techniques such as nondestructive testing, materials characterization, stress analysis methods, and the art of fractography are discussed.

Parts 2 and 3 (the Atlas of Fractographs and the Case Histories, respectively) of the Technical Handbook are discussed in the Summary (Page iii). Additional information has been presented in Introduction and Purpose sections of each of these parts.

The Handbook has been designed to be a living document that can be updated readily. This work reports the results of six years of fundamental work that has been sponsored by the United States Air Force (USAF) and the Federal Aviation Administration (FAA).

SECTION 2

SOURCES OF FAILURE

Composites can and will fail, due to service or manufacturing defects and material inhomogeneities. In general, the sources of failure in composites can be broadly classified as:

1. Design errors
2. Materials and process discrepancies
3. Anomalous service conditions

2.1 DESIGN ERRORS

Unlike homogeneous materials, most modern composite materials are fabricated by laminating together a large number of relatively thin gage woven or unidirectional plies. For structures made from such materials it is important to recognize that engineering properties, and hence the component's ability to operate without failure, depend upon the correct number, sequence, and orientation of plies being used to make up the laminate. In general, the significance of errors depends upon the particular material in question, as well as the magnitude of mistake in terms of the overall laminate construction. For example, an overall off-axis rotation of 5 degrees can reduce the ultimate compression strength of a unidirectional graphite epoxy laminate by as much 54 percent. In contrast, a 5-degree rotation of only one ply out of a 30-ply laminate probably would produce less than a 2-percent decrease in ultimate strength. From this standpoint it is critical that the impact of identified discrepancies be identified accurately and taken into consideration prior to being reported or to being identified as a significant contributor to the cause of failure.

Errors in layup can also have significant effects not directly related to those engineering properties considered as part of typical design. The materials coefficient of thermal expansion represents one such property, where variations in stacking sequence can produce significant amounts of panel warpage or internal residual stresses. These internal stresses have been found to cause damage such as gross delamination and matrix cracking within the laminate plies. Such damage, while not always directly responsible for failure, may in many cases constitute one of several contributory conditions resulting in premature failure.

2.1.1 Critical Parameters

For continuous fiber reinforced composite materials, the exact design properties which should be checked as part of a ply layup analysis will depend strongly upon the requirements of the specific

component examined. However, as a general guideline, critical parameters which should be given consideration in the event discrepancies are detected should include:

1. Young's Modulus
2. Basic laminate strength (tension, compression, shear)
3. Notch sensitivity (tension and compression)
4. Buckling stability
5. Internal thermal stress or residual stress conditions
6. Alterations in environmental susceptibility.

2.1.2 Common Errors

Some of the most common errors in ply layup include:

1. Missing or additional plies
2. Improper angular orientation
3. Improper ply type, grade or style.

2.2 MATERIALS AND PROCESS DISCREPANCIES

Errors in material layup, ply orientation, microconstituent chemical formulation, processing and the degree of matrix curing can lead, or contribute, to premature component failures. As a result, the analysis of these basic material and processing errors should be considered a standard operation in most analysis investigations. Standard techniques are available for characterizing the material integrity and for identifying anomalous conditions, if any, that may have caused or contributed to component failure. Factors that can contribute to premature failure include:

1. Incorrect materials
2. Improper material layup i.e., the number, orientation, and sequence of plies in the laminate
3. Improper fiber, matrix, and void volume fractions
4. Improper individual ply thickness
5. Improper fiber alignment
6. Improper chemical composition of the resin
7. Improper degree of cure
8. Contaminants
9. High moisture content
10. Incorrect size, placement, or poor quality of details such as holes and radii
11. Improper fastener installation, joining, bonding, etc.

In most failure analyses, the examination of part material, configuration, and quality should be considered a routine procedure, necessary for the accurate evaluation of the failure cause. These

examinations should identify any gross deficiencies that could have significant effect on material properties or the magnitude of local stresses within the part.

2.3 ANOMALOUS SERVICE CONDITIONS

Composite components can fail when operated under anomalous service conditions. Any variable that significantly affects the mechanical response of the laminate or the chemical properties of the composite constituents can be expected to lead to premature failure. Some of the environmental variables that can be considered deleterious to the service life of composite components include:

1. Temperature: Operation of composite components at temperatures above those for which the component was designed
2. Chemical Environments: Exposure of composite components to aggressive chemical environments
3. Abnormal Load Situations: Subjecting the component to abnormal loads for which the component was not designed, such as low energy-impact damage.

2.4 EXAMPLES

This subsection presents examples of manufacturing, materials, and processing defects that occur in Graphite-Epoxy (Gr/Ep). These defects have been previously identified in a study termed the Rockwell Flaw Criticality Study (Reference 1) as defects that could affect the service life of composite structural components. These defects and flaws can occur either during fabrication/manufacture of the composite component, or during subsequent service. A list of these defects is provided in Table 2-1. The corresponding Rockwell study defect number and the stage at which these occur are also given. Figures 2-1 through 2-28 are photographs illustrating the defects.

Table 2-1. Rockwell Flaw Criticality Study Defects

Defect No.	Defect	Manufacturing Stage
1	External Delamination	Layup
2	Blister, Internal Delamination	Layup
3	Oversized Hole	Attachment
4	Hole Exit Side Broken Fibers/Breakout	Attachment
5	Tearout in Countersink	Attachment
7	Resin-Starved Laminate	Fiber/Prepreg Generation
8	Resin-Rich Areas Fiber/Prepreg Generation	Fiber/Prepreg Generation
9	Excessive Porosity	Fiber/Prepreg Generation
10	Scratch, Fiber Breakage Handling	Handling
11	Dent	Handling
12	Fiber Breakaway From Impact Surface	Handling
13	Edge Delamination, Splintering	Handling
14	Overtorqued Fastener	Attachment
16	Edge Notch, Crack Handling	Handling
17	Corner Notch	Handling
18	Mislocated Hole, Not Repaired	Attachment
20	Marcelled Fibers	Layup
21	Wrinkles	Layup
26	Wrong Material	Layup
27	Misoriented Ply	Layup
28	Ply Overlap	Layup
29	Ply Underlap, Gap	Layup
31	Improper Fastener Seating	Attachment
33	Figure 8 Hole	Attachment
35	Off-Axis Drilled Hole	Attachment
36	Countersink on Wrong Side of Laminate	Attachment
39	Burned Drilled Hole	Attachment
41	Undersize Fastener	Attachment
42	Dent, Fiber Breakage From Production Mishandling	Handling



Figure 2-1. Rockwell Flaw Criticality Study Defect 1: External Delamination

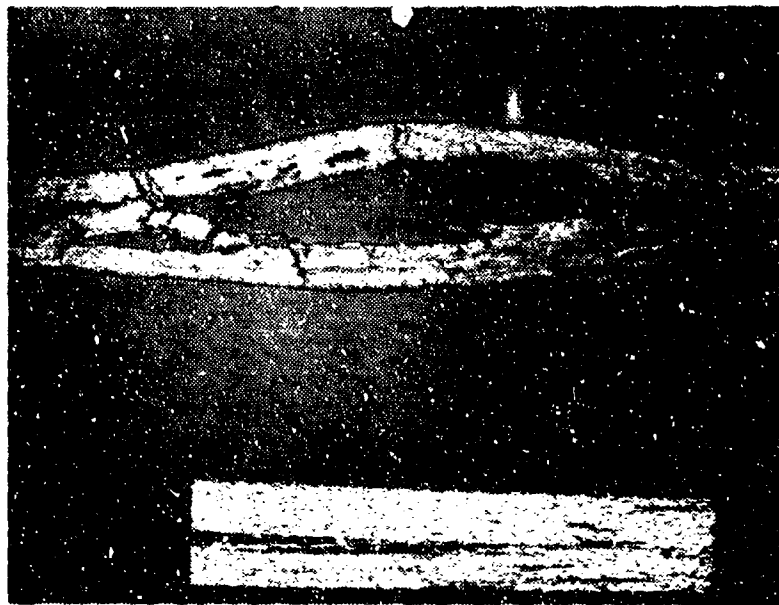


Figure 2-2. Rockwell Flaw Criticality Study Defect 2: Blister, Internal Delamination



Figure 2-3. Rockwell Flaw Criticality Study Defect 3: Oversized Hole



Figure 2-4. Rockwell Flaw Criticality Study Defect 4: Hole Exit Side Broken Fibers Breakout

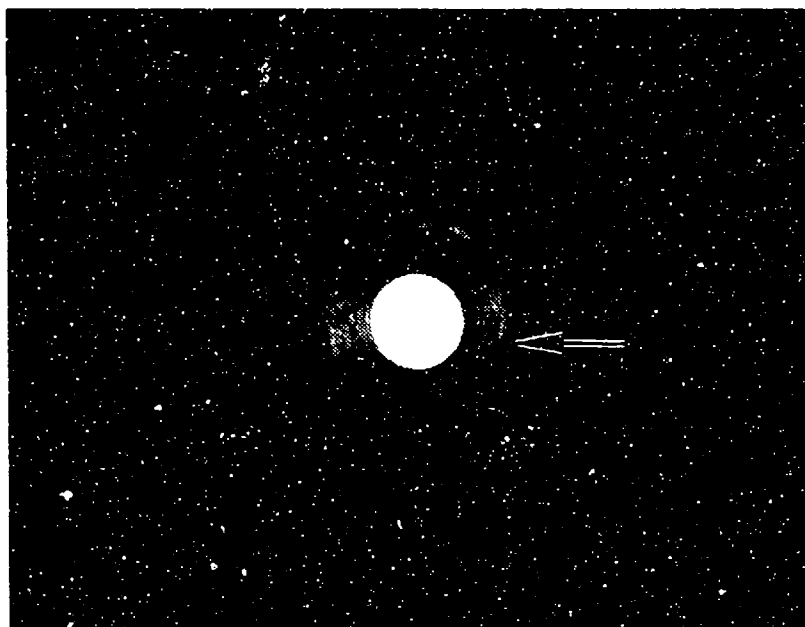


Figure 2-5. Rockwell Flaw Criticality Study Defect 5: Tearout in Countersink



Figure 2-6. Rockwell Flaw Criticality Study Defect 7: Resin-Starved Laminate (Bare Fibers)

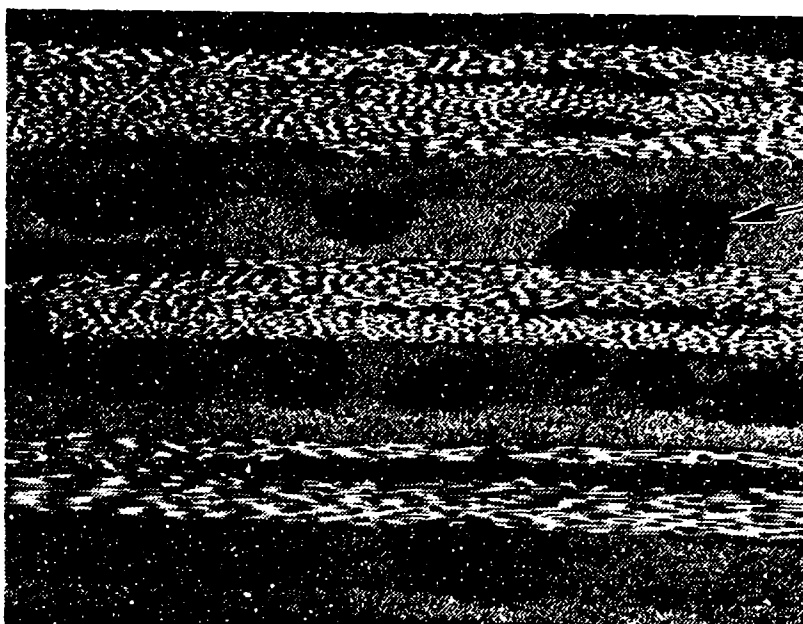


Figure 2-7. Rockwell Flaw Criticality Study Defect 8: Resin-Rich Area at Arrow (Dark Areas Are Voids)

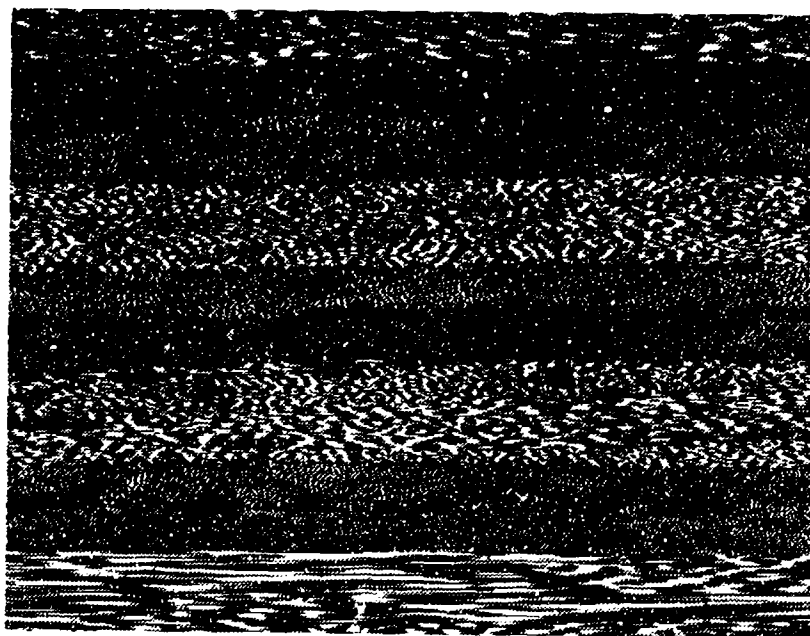


Figure 2-8. Rockwell Flaw Criticality Study Defect 9: Excessive Porosity, Voids



Figure 2-9. Rockwell Flaw Criticality Study Defect 10: Scratch, Handling Damage

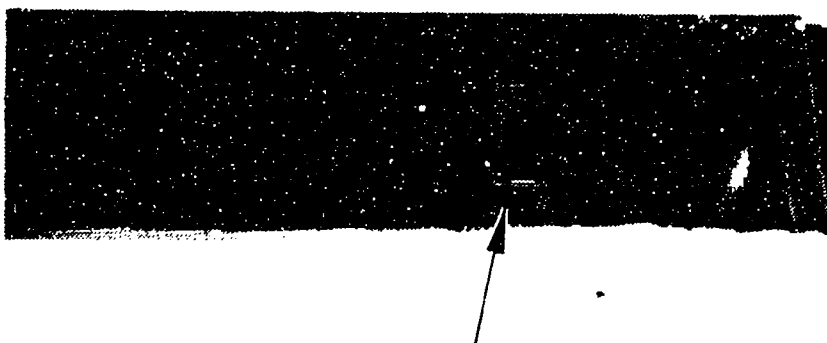


Figure 2-10. Rockwell Flaw Criticality Study Defect 11: Dent, Handling Damage

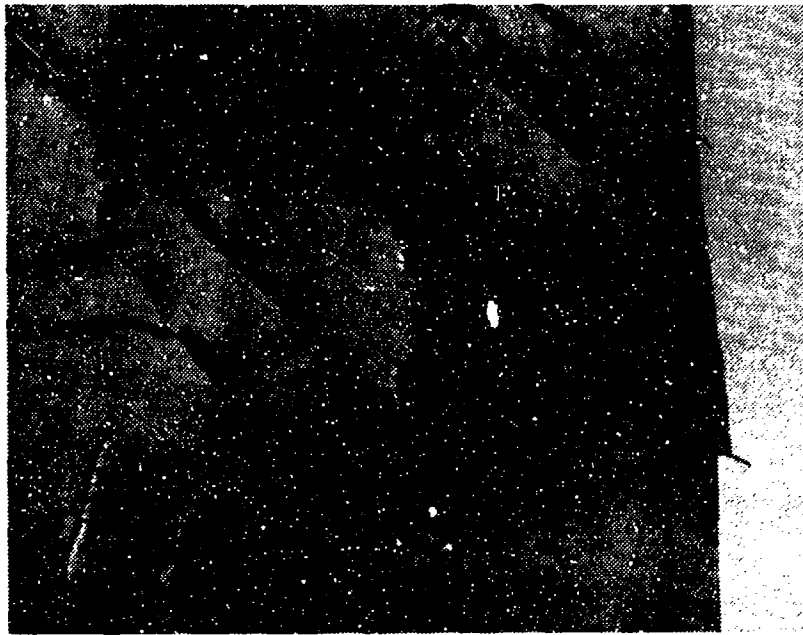


Figure 2-11. Rockwell Flaw Criticality Study Defect 12: Fiber Breakaway From Impact Surface

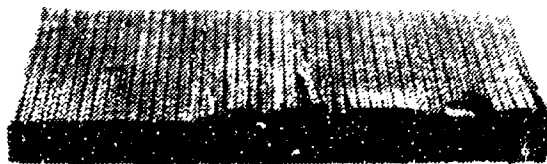


Figure 2-12. Rockwell Flaw Criticality Study Defect 13: Splintering, Edge Delamination

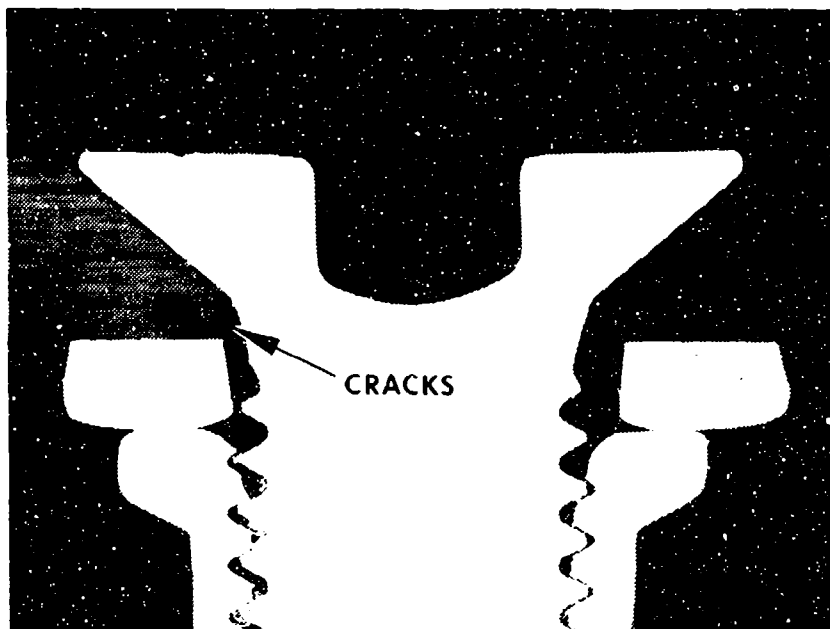


Figure 2-13. Rockwell Flaw Criticality Study Defect 14: Overtorqued Fastener

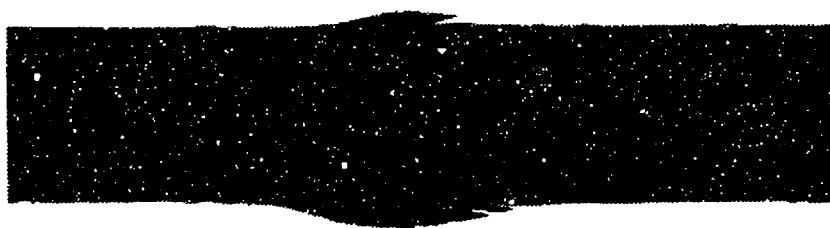


Figure 2-14. Rockwell Flaw Criticality Study Defect 16: Edge Notch, Crack



Figure 2-15. Rockwell Flaw Criticality Study Defect 17: Corner Notch



Figure 2-16. Rockwell Flaw Criticality Study Defect 18: Mislocated Hole — Not Repaired

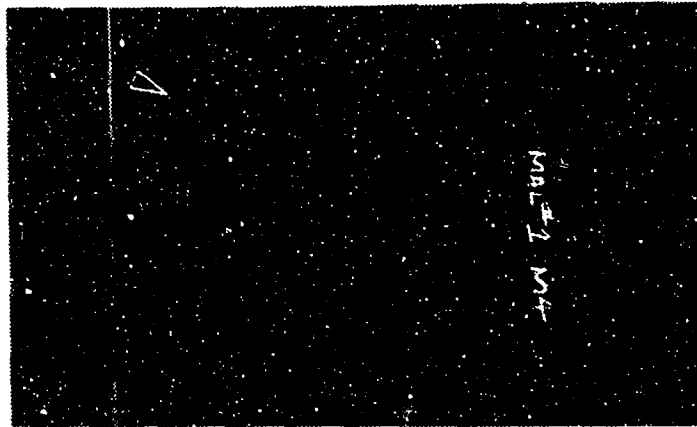


Figure 2-17. Rockwell Flaw Criticality Study Defects 20 and 21: Marcellled Fibers (Arrow) and Wrinkles

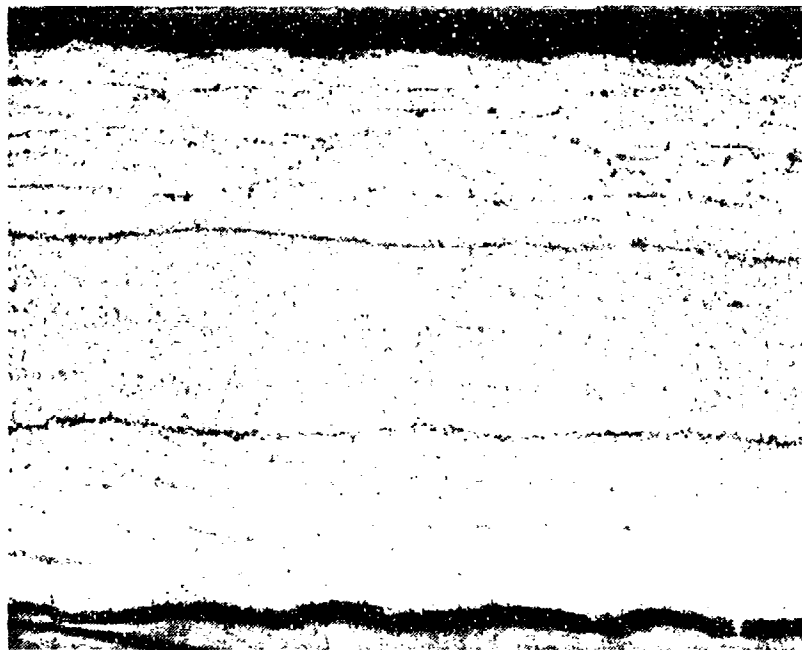


Figure 2-18. Rockwell Flaw Criticality Study Defect 26: Wrong Material, Correct Layup $[0]_{12T}$

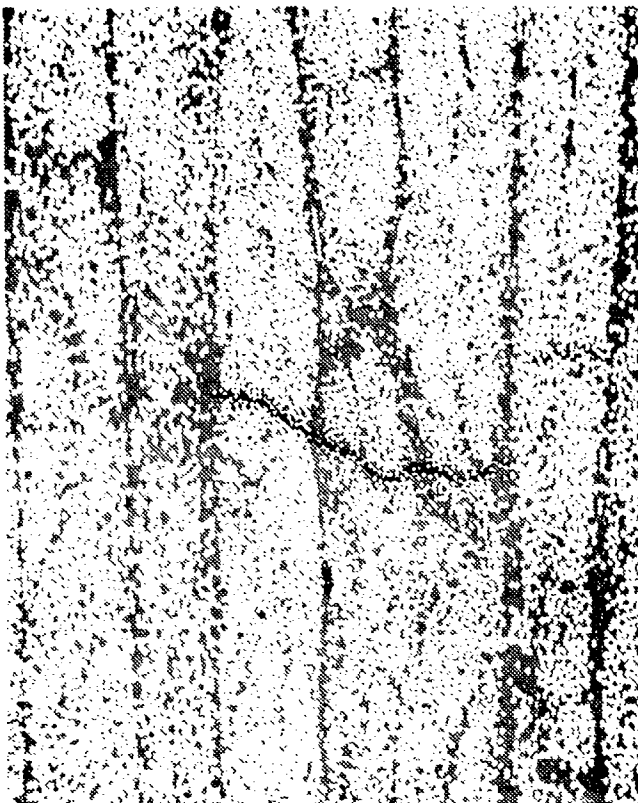
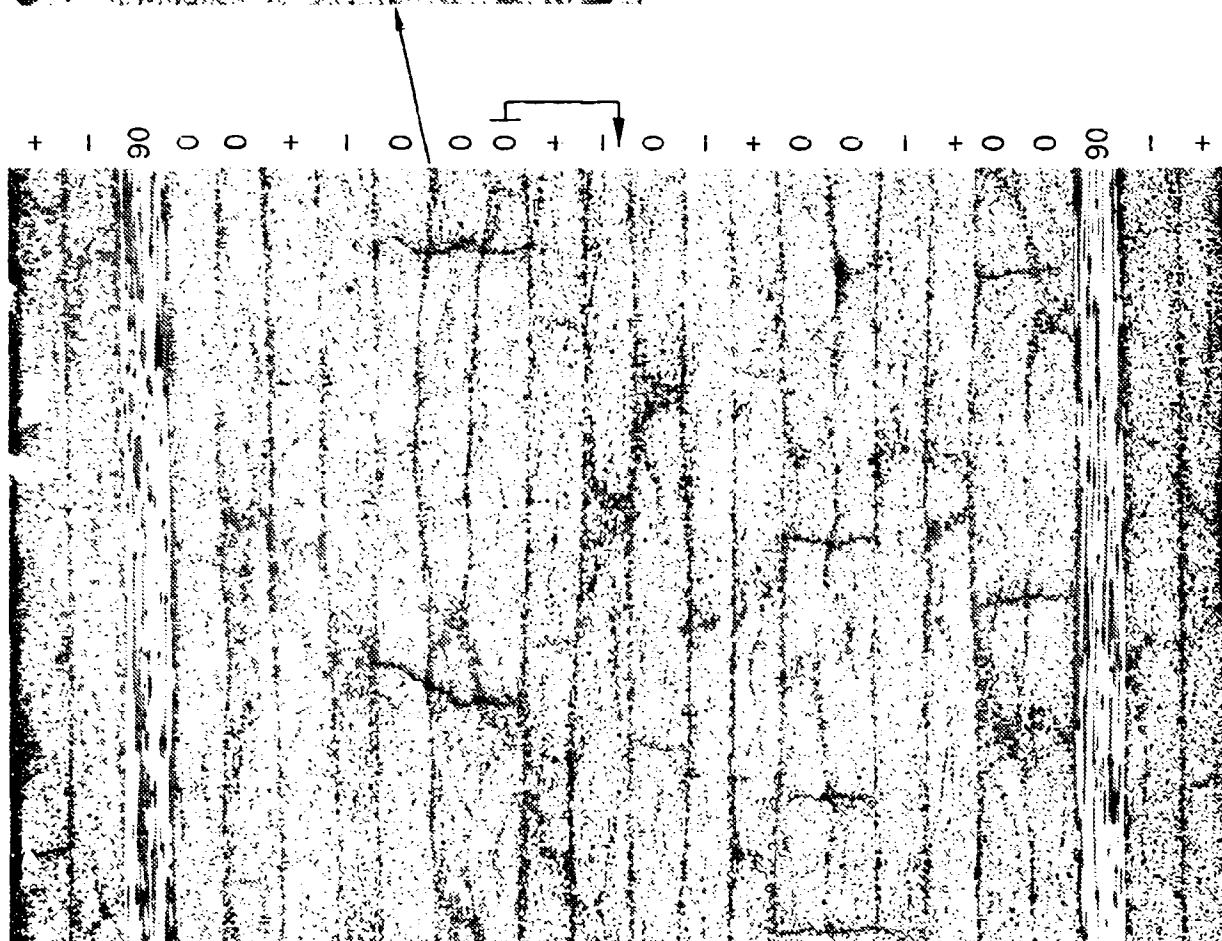


Figure 2-19. Rockwell Flaw Criticality Study Defect 27:
 Misoriented Ply From Correct Layout
 $[-45/90/0_2/ \pm 45/0_2/ \pm 45/0]_s$

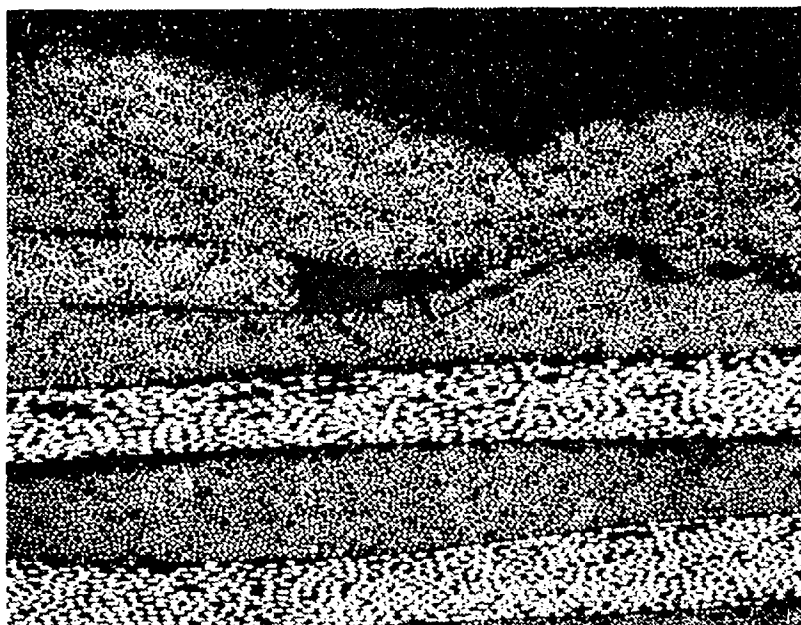


Figure 2-20. Rockwell Flaw Criticality Study Defect 28: Ply Overlap

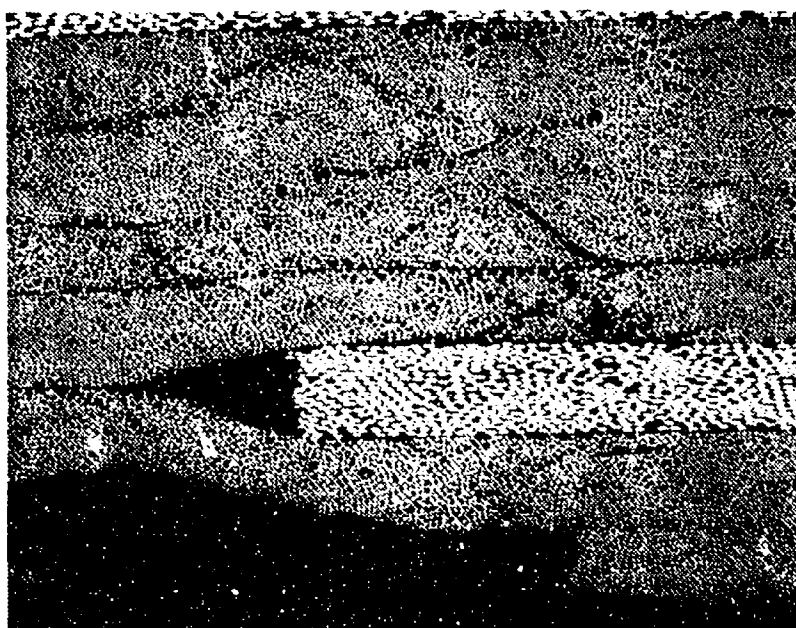


Figure 2-21. Rockwell Flaw Criticality Study Defect 29: Ply Underlap, Gap

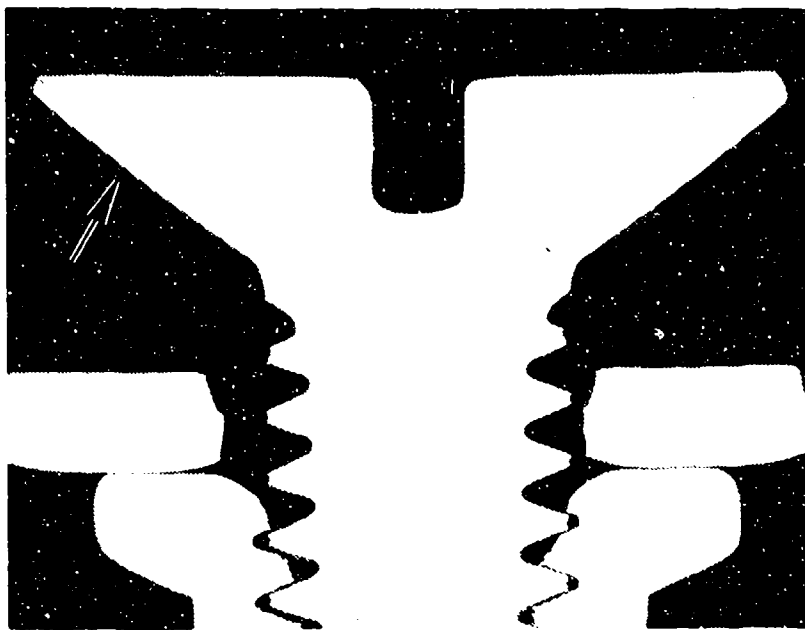


Figure 2-22. Rockwell Flaw Criticality Study Defect 31: Improper Fastener Seating

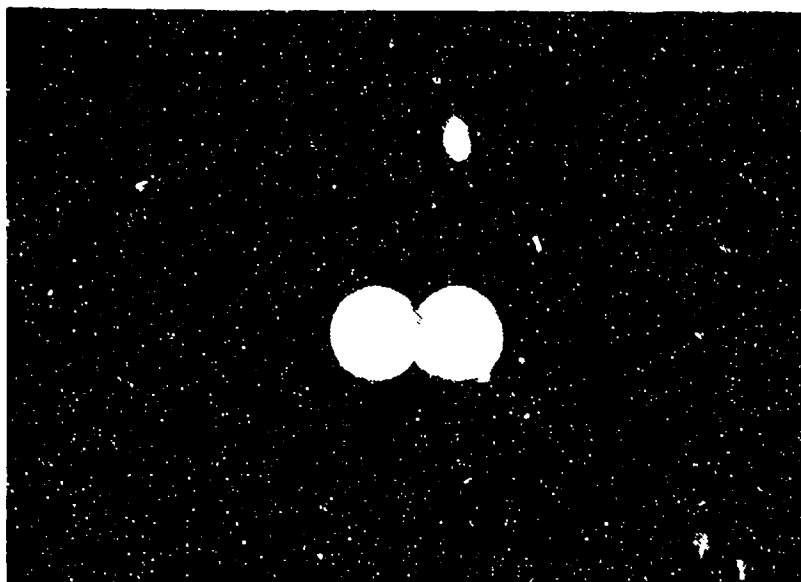


Figure 2-23. Rockwell Flaw Criticality Study Defect 33: Figure 8 Hole



Figure 2-24. Rockwell Flaw Criticality Study Defect 35: Off-Axis Drilled Hole



Figure 2-25. Rockwell Flaw Criticality Study Defect 36: Countersink on Wrong Side of Laminate

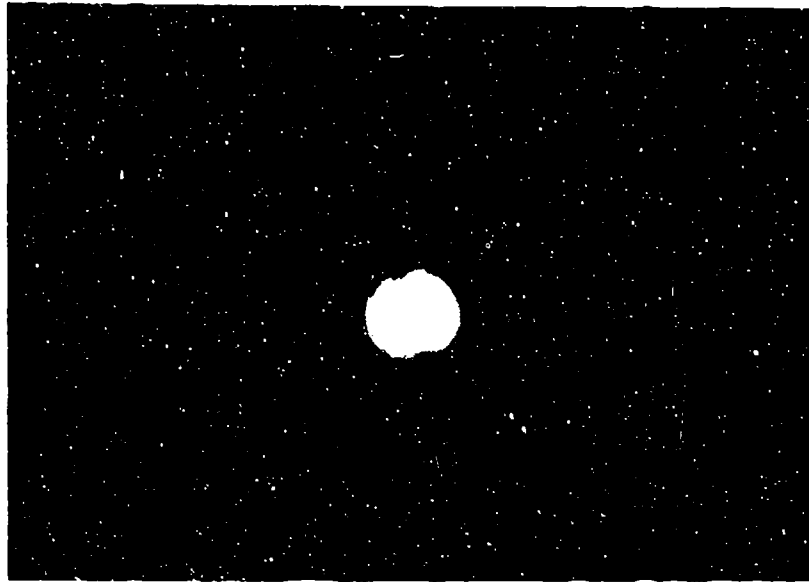


Figure 2-26. Rockwell Flaw Criticality Study Defect 39: Burned Drilled Hole

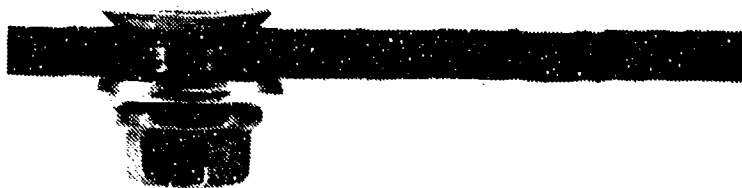


Figure 2-27. Rockwell Flaw Criticality Study Defect 41: Undersized Fastener

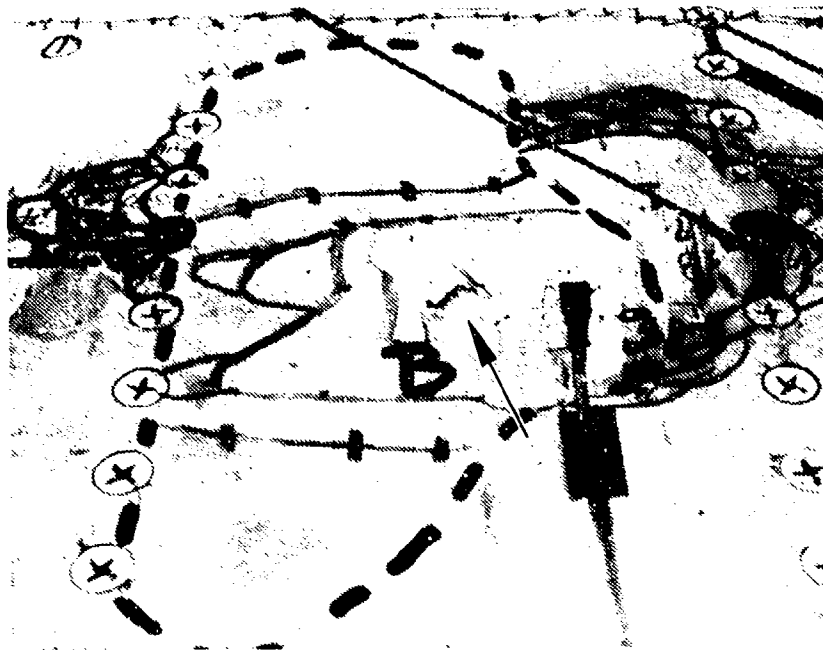


Figure 2-28 Rockwell Flaw Criticality Study Defect 42: Dent, Hidden Fiber Breakage

SECTION 3

FAILURE ANALYSIS LOGIC NETWORKS

3.1 GENERAL CONCEPTS

This section reviews the failure analysis logic network (FALN) flowcharts and supporting data tables developed to provide investigators with guidelines delineating a logical sequence of investigative operations. These flowcharts are designed to identify the analytical tools necessary for composite failure analysis. The charts, when combined with decision gates, allow an accurate, cost-effective, and timely determination of the cause of component failure. Such guidelines have not been available previously due to the relative complexity of composite materials and their fairly recent use in industry, particularly for primary structures. In developing these guidelines, specific objectives were incorporated to provide investigators with a logical sequence that:

1. Considers a variety of potential causes including design or fabrication errors, anomalies, and in-service or testing damage
2. Incorporates multiple analytical disciplines, such as nondestructive testing, materials characterization, fractography, and stress analysis
3. Avoids the premature destruction of evidence
4. Builds on gathered information and allows for redirected investigations.

In addition to the general FALN, several specific FALNs are provided for the areas of nondestructive testing, materials characterization, fractography, and stress analysis. Both types of FALNs are described in the following paragraphs.

3.2 MAJOR FAILURE ANALYSIS LOGIC NETWORKS

Identifying the logical sequence of steps for doing a post-failure analysis is often a complex and difficult process. Sufficient information must be gathered and evaluated so that the cause of fracture may be determined from positive supportive evidence rather than simply by a process of elimination. In many instances, the development of a coherent set of positive evidence is complex since: (1) numerous potential causes exist and (2) multiple contributory factors may be involved. In order to identify accurately the cause of fracture, each of these potential contributory factors must be taken into consideration. Identifying the cause of fracture and related contributory factors without examining every conceivable cause requires an organized investigation sequence. Developing this plan of attack is further complicated by the fact that many investigative steps may be destructive to remaining evidence, and thus may preclude further critical analysis. Consequently, adequate documentation to record existing evidence, as well as the logical flow of information from one analysis to another, must be considered.

To assist investigators in developing a logical plan of attack, an organizational framework was developed. This framework is based upon well established procedures utilized in the failure analysis of metallic structures, modified to meet the specific analytical requirements for fiber reinforced composite structures. This framework considers each major failure category, potential interrelationships, and the prevention of premature destruction of evidence. Because composite materials differ in many respects from metals, the specific operations involved were modified to address those characteristics specific to composites. This proven framework consists of five basic investigative operations arranged around intermediate decision points. The approach is aimed at simplifying and streamlining the number and complexity of analytical steps involved, usually lowering the overall costs of investigations. The five major investigative operations are:

1. Collection and review of background history and information
2. Nondestructive inspection
3. Evaluation of the part conformity to specified requirements
4. Detailed fractographic examinations
5. Mechanical testing and stress analysis.

An overall diagram, showing the simplified application sequence of these five operations, is illustrated in Figure 3-1. The sequence initially encourages the use of simple, inexpensive procedures, such as nondestructive examinations, followed by progressively more detailed procedures such as material verification and stress analysis. Through comprehensive hands-on application and evaluations, a significant amount of detail has been added to the original investigative framework. The expanded version, shown in Figure 3-2, establishes a more detailed and accurate path for investigators. It delineates most of the widely used techniques that may be used and the required decisions involved in carrying out a postmortem analysis.

Each initial examination is directed toward identifying items of significance early in the investigation. Through an iterative process, the number of steps can be minimized and future efforts concentrated on items of interest. During the initial stages of investigation, background information on material, fabrication, design, loads, environment, and service or test history is collected and reviewed with the intention of identifying areas of concern. This process helps develop a familiarity with the component, its operation, and its service environment. Nondestructive inspections are then performed to identify and further delineate the extent and nature of nonvisible fracture or damage. The data are documented for later reference. This operation establishes the groundwork to plan more detailed examinations and helps in selection of specimens that may require destructive sectioning. After nondestructive examination, the part is evaluated for conformity with engineering, material, and process specifications. This includes such items as material verification, ply layup, and degree of cure.

Detailed fractographic and stress examinations are the next analytical steps. These operations identify more specific details and assess their significance. Typically, fractographic examinations are used principally to identify the origin and load conditions involved in failure. In many cases, the main benefit of fracture examination is the identification of material defects or anomalies. As such factors are identified, sufficient information may be developed to identify either a specific cause for failure or a point of interest (that is, an origin) for further analyses. After inputs from fractographic analysis have been developed, stress analysis may be performed to evaluate stress states, out-of-compliance conditions, or the critical nature of identified

defects. In cases where questions may remain, additional specialized tests or further, more detailed, stress analyses may be required from the stress specialist to model previously indeterminate conditions.

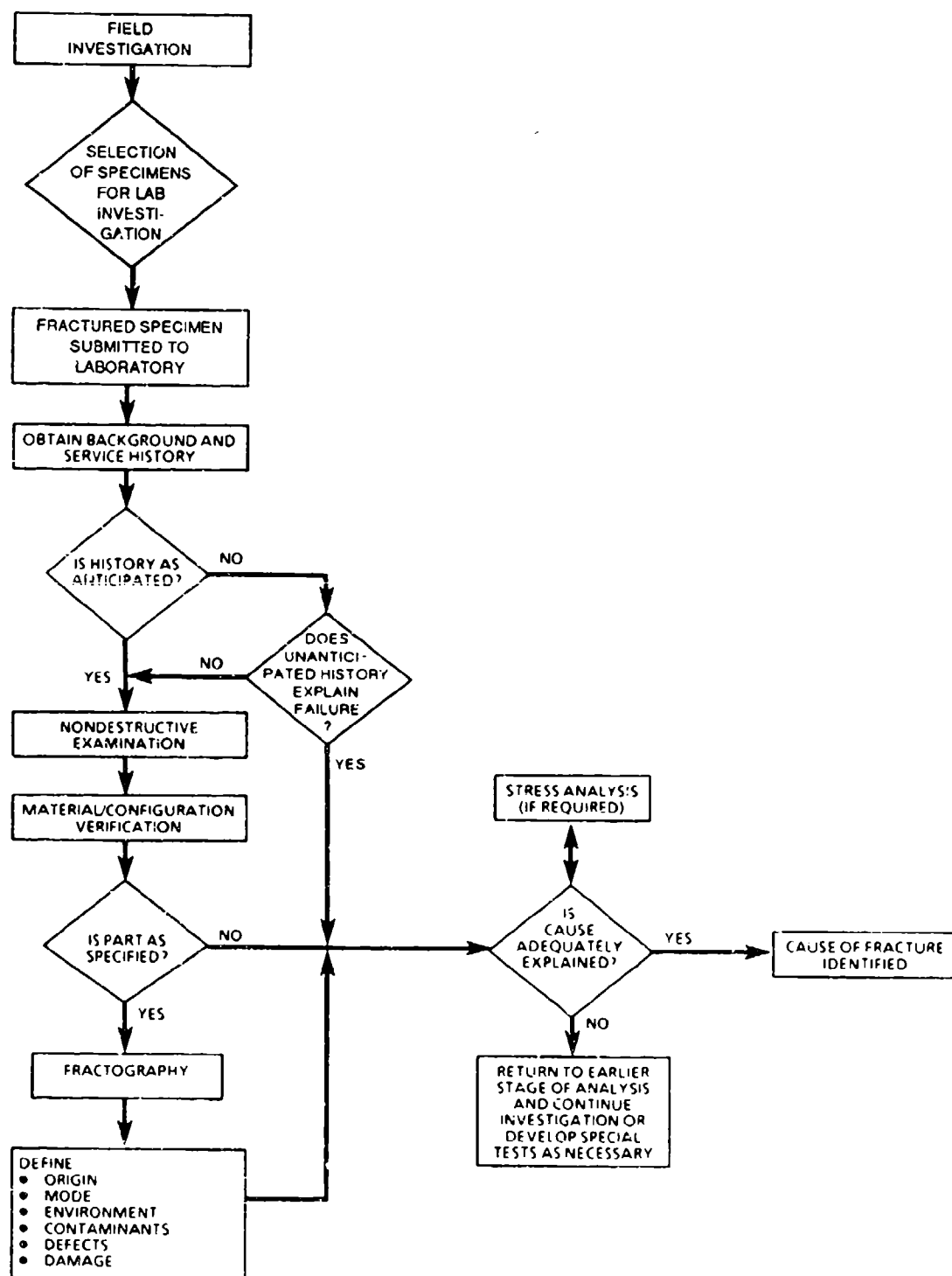


Figure 3-1. Simplified Investigative Framework

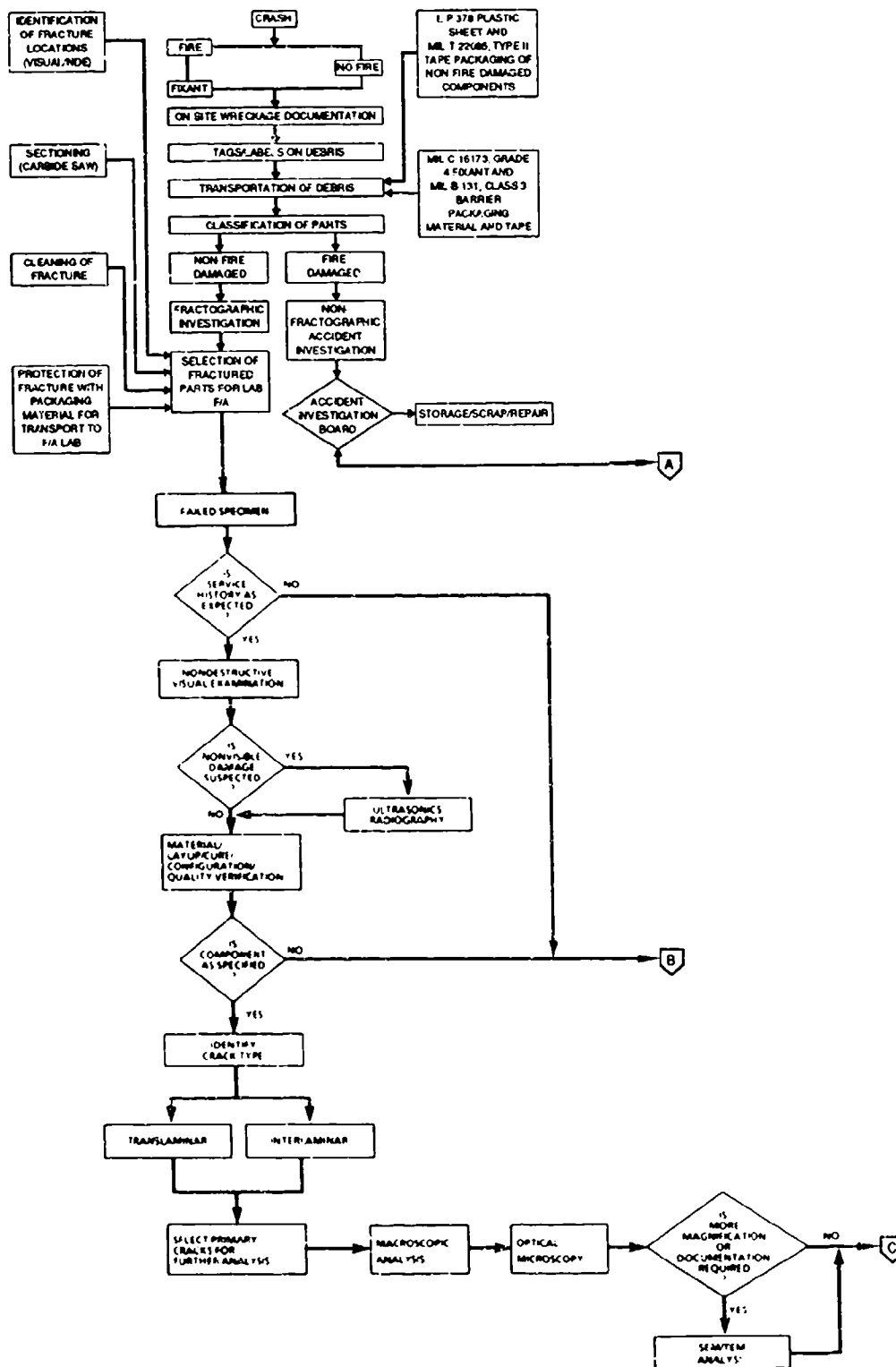


Figure 3-2. Detailed Investigative Framework (Page 1 of 2)

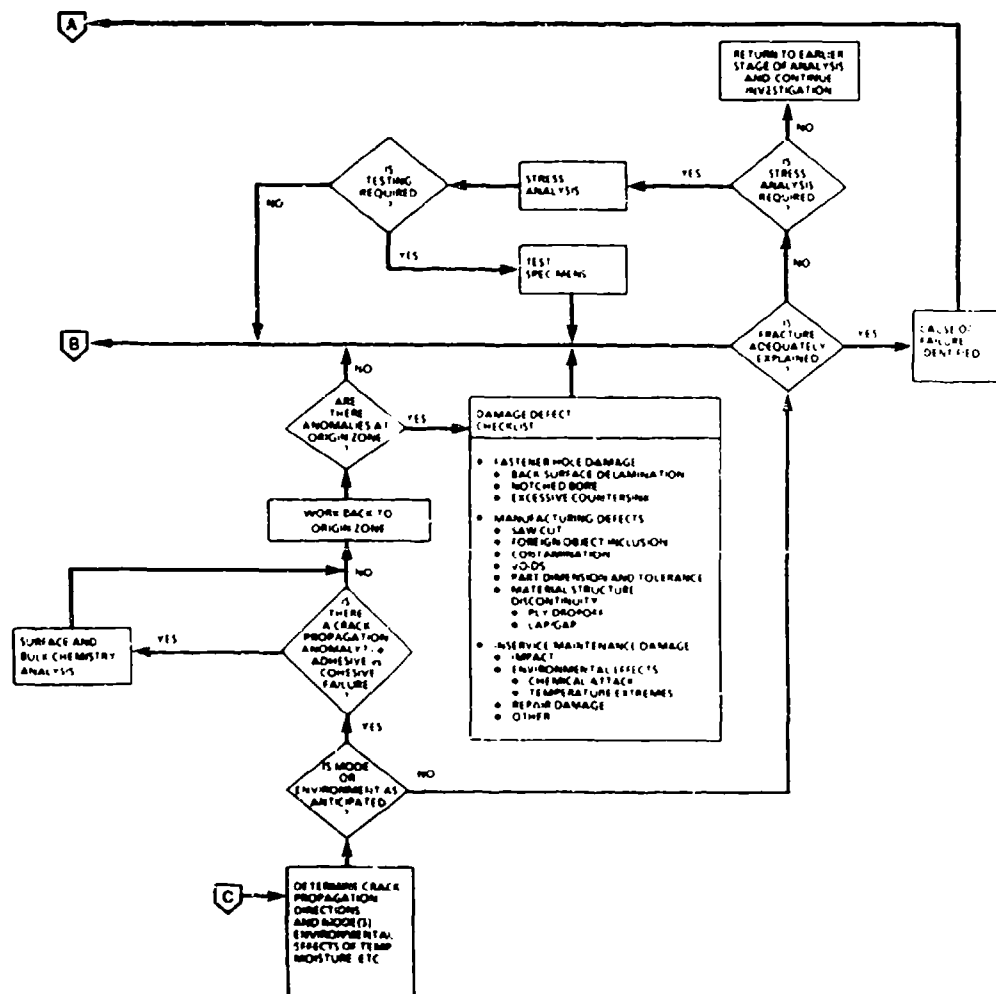


Figure 3-2. Detailed Investigative Framework (Page 2 of 2)

SECTION 4

FIELD GUIDELINES

This section describes the procedural guidelines that have been developed for field investigators to use for handling and selecting fractured components for subsequent laboratory investigations. These guidelines have been developed based on inputs and suggestions from several DOD agencies as well as representatives from the National Transportation Safety Board (NTSB) and Federal Aviation Administration (FAA).

Figure 4-1 shows the field handling logic network which defines the recommended safety steps and associated handling, packaging and shipping procedures that are being suggested to field investigators. Failed parts that have not been damaged by fire proceed to laboratory failure analysis. The failure analysis report ultimately goes to the Accident Investigation Board. A description of several of the issues used in this network follows.

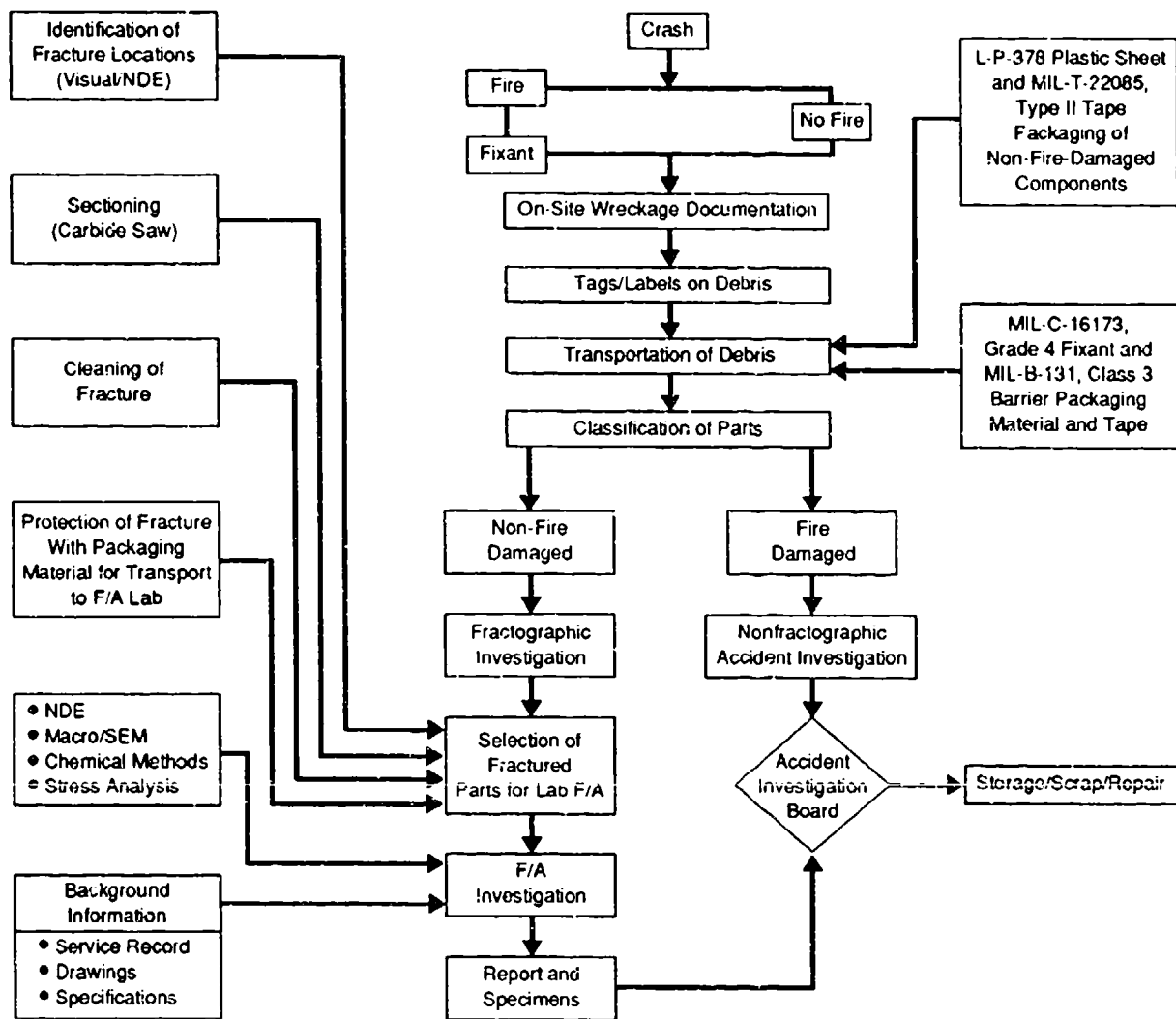
4.1 AVIONICS HAZARDS

Fibers released in aircraft crashes or from machining/handling of fire damaged composite materials can cause damage in electrical or avionics equipment. Released fibers settling on or across electrodes or circuits can short out low power electrical systems or cause severe electrical arcs in high power systems.

4.2 HEALTH AND SAFETY ISSUES

Fibers may be released during airplane accidents which can be a health hazard. Primary release occurs during post-crash aircraft fires, although some release may occur during an on-site crash investigation, during transportation of components to a safe-area, or during scrap disposal. Graphite fibers act as skin, eye, and lung irritants in a manner similar to exposure to moderate/heavy amounts of glass fibers. Except for skin irritation, no evidence exists that any serious effects could result from graphite fibers being imbedded in human skin.

With regard to other health threats associated with carbon fibers, the National Institute for Occupational Safety and Health (NIOSH) has determined that fiber particles, including carbon fibers, fiberglass, and asbestos, will not cause malignant disease if they exceed 3.5 microns. The average size of carbon fibers currently in use in composite structures ranges between 4 and 7 microns. Based on these observations, it is generally believed that carbon fiber-based composite panels fractured in aircraft crashes but not subjected to fire are biologically benign and would constitute no more hazard than fractured aluminum aircraft pieces.



T90-31/B/A

Figure 4-1. Field Handling Logic Network for Composite Parts

4.3 SAFETY GUIDELINES

The following guidelines are recommended as minimum safety precautions in the handling of carbon fiber-based composites in crash/fire incidents:

1. Base/squadron safety officers should:
 - a. Determine if the aircraft contains carbon fiber materials
 - b. Identify specific carbon fiber components/panels
2. Pre-mishap training should include:
 - a. Identifying locations of carbon fiber
 - b. Proper handling of components with regard to accidents without post-crash fires and those involving a post-crash fire

3. For aircraft mishaps where carbon fibers are released by fire:
 - a. Firefighters and rescue personnel should be the only personnel in the immediate vicinity of the burning/smoking wreckage.
 - b. Personnel should be prevented from approaching the crash site and should be restricted from assembling down-wind of the fire at the crash site.
 - c. Once the fire is completely out and the wreckage has cooled, all carbon fiber should be sprayed down with a fixant to contain the release of carbon fibers.
 - d. The area should be roped off as soon as possible and a single entry/exit point be established to the mishap site.
4. For aircraft mishaps where no carbon fibers are released by fire:
 - a. Leather palmed gloves should be worn.
 - b. Carbon fiber panels can be handled similarly to handling of aluminum panels.
5. All personnel involved with crash/fire-damaged composite parts should be provided with a suitable shower facility before going off duty to preclude injury from loose fibers.

4.4 SAFETY EQUIPMENT

1. In a crash involving fire/burning wreckage, personnel required to enter wreckage to neutralize hazards should wear adequate protection to minimize irritation. These should include:
 - a. NIOSH-approved industrial dust masks
 - b. Disposable paper coveralls with hoods
 - c. Goggles or visors
 - d. Leather palmed gloves.
2. For aircraft mishaps where no carbon fibers are released by fire, leather palmed gloves should be worn. If breaking or ripping apart of carbon fiber components with carbide saws is to be performed, mono-goggles or face shield protection should be used.
3. Safety officers should ensure that the following items are readily available at all operating sites or included in premishap kits:
 - a. An adequate supply of industrial fixant, preferably commercially procured polyacrylic acid (PAA) such as B. F. Goodrich "Carboset" XL-11. If not available, acrylic floorwax or light oil is an acceptable fixant.
 - b. Industrial dust masks (NIOSH approved), disposable coveralls or equivalent, leather palmed gloves, and mono-goggle eye protection for use if fire is present.

4.5 ON-SITE CRASH/WRECKAGE RECONSTRUCTION AND HANDLING

1. Once fixant has contained carbon fiber material, the use of industrial dust masks and gloves is considered sufficient for work around the crash site where large amounts of carbon fiber material are not being stirred up.
2. Complete documentation of all debris at the crash site should be carried out using conventional photographic equipment. Aerial photography of the crash site to include a "global" perspective of the crash investigation is also useful.
3. Inspection of the crash-damaged aircraft to identify crash/fire-damaged composite parts should be carried out. Classification of all composite components into fire-damaged and non-fire-damaged is also useful. Tagging and labeling of all debris should be carried out, preferably at the crash site or prior to transport to an accident reconstruction area.
4. Sectioning of crash/fire-damaged components for further engineering investigation should be performed using carbide saws and mono-goggle protection. Sectioning should be performed in areas well away from visible fracture and areas that contain internal damage as determined by nondestructive tests (coin-tap, portable ultrasonic, X-ray, etc).
5. Crash/fire-damaged parts which require laboratory evaluation and/or repair should have fibers contained by wrapping the affected area with 0.006 inch thick plastic sheet (MIL Specification L-P-378) and taped in place with aircraft preservation tape (MIL-T-22085, Type II tape).
6. Crash/fire-damaged parts which do not require evaluation as part of the accident investigation and/or are to be scrapped should have fibers contained (to ensure that fibers are immobilized) by using Corrosion Preventative Compound, MIL-C-16173, Grade 4 spray applied as a fixant material.
7. Transport of the wreckage to a "safe-area" for accident/wreckage reconstruction should be carried out as soon as possible. During the accident investigation/repair disposition operations, the crash-damaged aircraft should be in an enclosed area not subject to the elements of weather. This prevents degradation of the tape/plastic sheet fiber containment system and precludes the spread of loose fibers.
8. Crash/fire-damaged aircraft to be stored locally, awaiting repairs, should have crash/fire-damaged parts wrapped or preserved as previously described. All sharp projections from damaged composite parts should be covered and padded to prevent accidental injuries. Damage or abrasion to the cover assembly can be minimized by applying foam with tape.
9. Those crash/fire-damaged hulks to be scrapped should have fibers contained as stated previously and should be wrapped in barrier material and taped. The hulk thus preserved is suitable for outside storage.
10. Those operations performed on crash/fire-damaged parts which generate loose fibers (such as sectioning of parts using carbide saws) require that personnel be protected from fiber exposure. Control of loose fibers is provided by vacuuming with a vacuum system containing a high efficiency particulate air filter (HEPA) designed to provide filtration levels down to 0.3 microns in particle size. Respiratory protection is provided by portable respirators containing HEPA filters with the same filtration levels as the vacuum system.

11. Composite material that is not required for investigation should be disposed of at an approved hazardous material waste site.

4.6 CLEANING METHODS

As much as possible, cleaning should be avoided for subsequent laboratory examination of fracture surfaces. However, under extreme requirements, conventional cleaning methods such as ultrasonic rinsing in soap or alcohol used in metal fractography can usually be successfully used for fiber/resin composite material without damaging fracture details.

4.7 VISUAL EXAMINATION

Failures in composites can be described in terms of the failure mechanism exhibited on trans-laminar, interlaminar, and intralaminar fracture types. The first evaluation method available to define and differentiate between these fracture types is visual macroscopic. The ability to define fracture types at the macroscopic level can often be the most valuable capability for many investigators, particularly for those performing field investigations. When examining a failed composite structure, the investigator must assess the nature and direction of the applied load, identify the significance and time of fracture, and select portions of the structure for laboratory analyses. Visual examination alone can often provide sufficient information to answer these questions. However, this extremely valuable capability is very much in its infancy compared to the metals field. Figure 4-2 presents a brief overview of the relationships that various investigators have observed between fracture mode/load conditions and macroscopic fracture surface features.

MODE	ENVIR. CONDITION	MACROSCOPIC FRACTURE FEATURES
Interlaminar Tension Dominated	Low Temperature/Dry	<ul style="list-style-type: none">• Smooth, glassy fracture surface• Major portion of fracture between plies
	Hot or Hot/Wet	<ul style="list-style-type: none">• Smooth but with loose fibers strewn on surface• A majority of the fracture within plies• May be permanent deformation of laminate
Interlaminar Shear Dominated	Low Temperature/Dry	<ul style="list-style-type: none">• Surface flat, but with "milky" appearance when held at angle to light• Major portion of fracture between plies
	Hot or Hot/Wet	<ul style="list-style-type: none">• Also exhibits "milky" appearance• Tends to fracture within a ply• Loose fibers on surface
Translaminar Tension	—	<ul style="list-style-type: none">• Rough, jagged fracture surface with individual fibers protruding from surface
Translaminar Compression	—	<ul style="list-style-type: none">• Extreme surface damage. Large regions of fibers fractured on same plane• Very few, if any, fibers protruding from surface
Translaminar Flexure	—	<ul style="list-style-type: none">• Two fairly distinct regions, one exhibiting translaminar tension and the other translaminar compression, the regions being separated by a neutral axis line

Figure 4-2. Visual Macroscopic Fracture Surface Features

SECTION 5

NONDESTRUCTIVE EVALUATION TECHNIQUES

In the broadest sense, nondestructive evaluation (NDE) includes any examination that assesses material integrity without damaging or destroying a component. It is used for a variety of tasks such as in-process quality control, in situ test monitoring, and fleet service inspection. For failure analysis, nondestructive evaluations are useful for identifying the conditions of invisible fracture for documentation and for planning subsequent destructive evaluations.

Following preliminary visual and macroscopic analysis of the failed component, invisible damage can be identified and evaluated by various techniques outlined below. Figure 5-1 and Tables 5-1 and 5-2 present a summary of the various methods commonly used for failure analyses. Note that the methods are listed in the order of preference for evaluating and defining each defect condition. The NDE FALN is structured such that inspections involve progressively more detail of the damage condition, including:

1. Initial plan view inspections
2. Detailed plan view inspections
3. Through-thickness inspections.

It should be noted that many of the failure analyses investigations do not require detail beyond the initial plan view inspections. Usually failure of the part denotes that some fairly extensive fracture, often visible, has occurred. The main responsibility of NDE inspection is to define the damage region around the primary fracture. More detailed analyses, if performed, are usually confined to other regions on the component, away from the principal fracture region, so as to identify other sites of damage or contributory defects.

Evaluation Plan

Nondestructive evaluations can be extremely useful to the failure investigator by revealing visible damage as well as areas of fracture not readily discernable through the most intensive visual examination. Nondestructive evaluation is of particular importance with composite materials primarily because of their susceptibility to invisible internal delaminations within or between the laminate plies. Other identifiable defect or damage conditions found by NDE include:

1. Translaminar surface and subsurface fractures
2. Core cell damage and fluid ingestion
3. Porosity
4. Disbonds
5. Impact damage

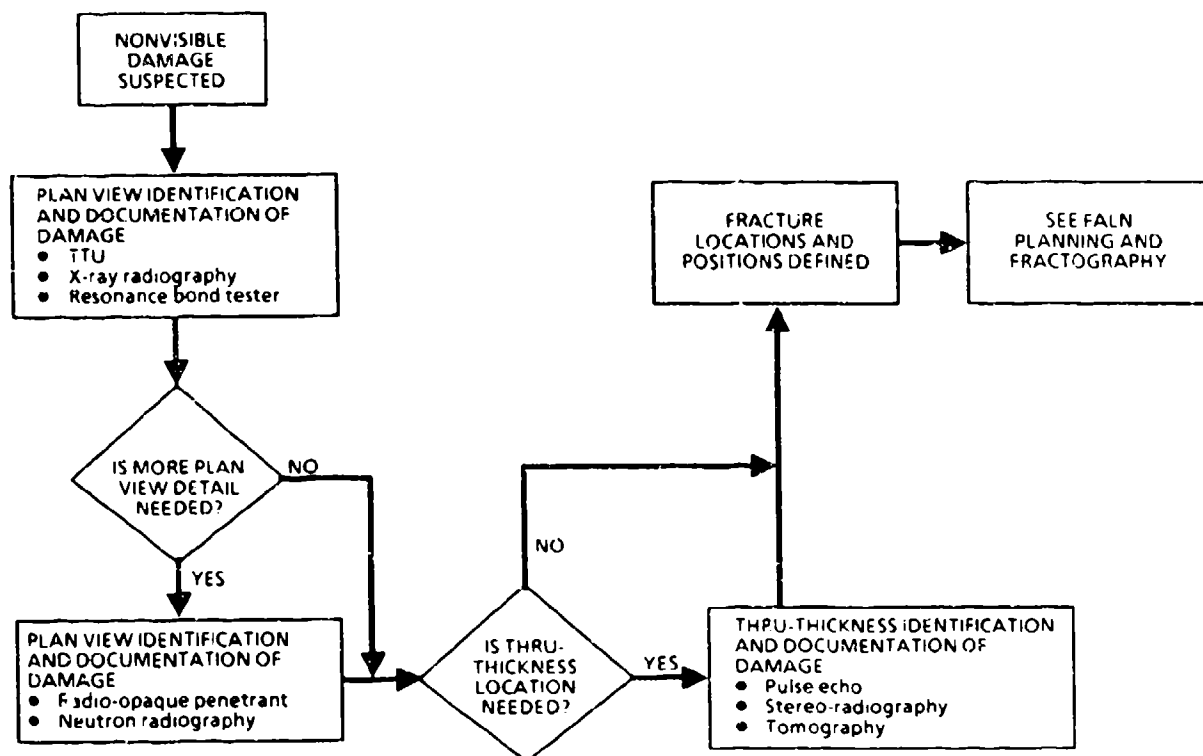


Figure 5-1. Nondestructive Evaluation Sub-FALN

6. Fastener hole drilling damage
7. Lightning damage
8. Heat or fire damage.

In addition to its primary benefits, NDE has several other notable advantages. Providing adequate documentation prior to destructive sectioning is of particular importance in failure analysis. With many modern and well-developed nondestructive analysis techniques available for composites (ultrasonics and X-ray being the most common), a permanent record is made of both visible and invisible areas of fracture. This record, somewhat like optical photography, provides invaluable documentation for later perusal. In addition to documentation of the extent of invisible damage, the investigator often gets an added benefit of identifying the type of construction such as locations of core splicing, potting regions, and ply dropoffs or pickups. Finally, since NDE is usually performed by a support specialist, the failure analyst is freed to establish a coherent plan for more detailed evaluation prior to destructive operations (such as specimen removal by sectioning).




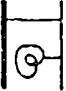



To provide the investigator with a better definition for the sequence of steps involved in the nondestructive evaluation of a part, the FALN presented in Figure 5-1 was developed. Several goals were considered in creating this FALN; first, the chart should provide the most basic information first, and second, the techniques should progress from the most easily interpreted to the most complex. The chart begins by documenting the fracture in general terms using relatively simple techniques. Next, two operations provide additional plan-view and through-the-thickness information using more complex techniques.

Table 5-1. Failure Analysis Techniques – Nondestructive Evaluation

TECHNIQUE*	DESCRIPTION	USE	VALUE
Thru-transmission ultrasonic (TTU) • C-Scan	Measures ultrasonic sound attenuation • C-Scan – plan view presentation	Determines size and location of nonvisible damage, defects, fracture in plan view	<ul style="list-style-type: none"> • Plan view documentation of failure • Plan view assessment of part quality • Planning analyses
Pulse ultrasonic • B-Scan • C-Scan	Measures ultrasonic sound reflection • B-Scan – thru-transmission view presentation • C-Scan – plan view presentation	Determines size and location of damage, defects, fracture in both a plan and thru-thickness view	<ul style="list-style-type: none"> • Plan view documentation of failure • Thru-thickness view documentation of failure • Plan view assessment of part quality • Thru-thickness assessment of part quality • Planning analyses
Reasonance bond testers: • Bondascope 2109 • Sondicator • Acoustic flaw detector • MIA 3000	Measures mechanical resonance changes caused by defects, meter or CRT display	Determines size and location of nonvisible damage	<ul style="list-style-type: none"> • Determining of size and location of part damage • Method can be used when only one side is accessible
X-ray radiography (tomography)	Measures X-ray attenuation plan view presentation	<ul style="list-style-type: none"> • Determines size and location of transiaminar fractures and radio-opaque defects – plan view presentation • Delamination size and location determined with radio-opaque penetrant • Thru-thickness position determined by stereo-radiography or X-ray tomography 	<ul style="list-style-type: none"> • Plan-view documentation of failure • Plan view assessment of part quality and defects • Planning analyses
Neutron radiography	Measures neutron attenuation plan view presentation	<ul style="list-style-type: none"> • Determines size and location of transiaminar fractures and neutron opaque defects – plan view presentation • Delamination size and locations determined with neutron-opaque penetrant • Used often where metal structure overlays composite material – neutrons are not as attenuated by metal as X-ray, and are relatively sensitive for polymers with hydrogen 	<ul style="list-style-type: none"> • Plan-view documentation of failure • Plan view assessment of part quality and defects • Planning analyses
Eddy current	Measure conditions which interrupt the flow of eddy current induced in the part	Determines differences between paint scratches and surface cracks in Gr/E fabric structures	<ul style="list-style-type: none"> • Plan view documentation of fracture with single-side access • Planning analyses

* Techniques are listed in order of preference, based on applicability, reliability, cost and sample requirements.

Table 5-2. Inspection Method Selection (Listed in Order of Preference)

STRUCTURES	DEFECTS						
	DELAMINATION/ DISBOND	IMPACT DAMAGE	FASTENER HOLE DAMAGE	LIGHTNING DAMAGE	BURN DAMAGE	TRANSLAMINAR FRACTURES, SURFACE	TRANSLAMINAR FRACTURES, SUBSURFACE AND SUBSTRUCTURE
LAMINATED SKIN 	C, D, E	A, C, D, E, G	A, C, G, H	A, C, D, E	A, C, D, E	A, B	C, G, F, D, E
SKIN/HONEYCOMB PANEL 	C, E, D	A, C, E, D	A, C, G, H	A, C, F, D	A, C, E, D	A, B	C, G, F, D, E
SKIN-TO-STIFFENER JOINT 	C, D, E	A, C, D, E, G	A, C, G, H	A, C, D, E	A, C, D, E	A, B	C, G, F, D, E
SKIN-TO-METAL JOINT 	C, D, E	A, C, D, E	A, C, H	A, C, D, E	A, C, D, E	A, B	C, I, D, E
SKIN-TO-SKIN TRAILING EDGE JOINT 	C, E, D	A, C, E, D, G	A, C, G, H	A, C, E, D	A, C, E, D	A, B	C, G, F, D, E
LAMINATED RIBS, SPARS, AND SKIN STIFFENERS 	D, E	D, E, G	A, D, E, G, H	A, D, E, G	A, D, E, G	A, B	C, G, F, D, E
LUGS AND THICK SECTIONS 	C, D, E	A, C, D, E	A, C, G, H	A, C, D, E	A, C, D, E	A, B	C, G, F, D, E

KEY: INSPECTION METHOD

- | | |
|-------------------------|-----------------------|
| A VISUAL | F LOW KV X-RAY |
| B PENETRANT | G DIB-ENHANCED X-RAY |
| C ULTRASONIC TTU | H EDDY CURRENT |
| D ULTRASONIC PULSE ECHO | I NEUTRON RADIOGRAPHY |
| E BOND TESTER | |

Initial Plan View Inspections

For preliminary inspections, the major emphasis is to determine the basic outline of the damage regions such that part breakdown and sectioning can be performed without destruction of evidence or to minimize the sectioning damage if a repair scheme is considered. Plan view analyses such as ultrasonics, through transmission ultrasonic (TTU) or pulse echo, and radiography are by far the most versatile and encompassing techniques for overall determination of the basic outline of the damage region. Commonly, this coarse damage assessment is necessary for field inspection prior to part breakdown, sectioning, and subsequent detailed NDE techniques performed in the laboratory. In the field, pulse echo is the preferred method, particularly desirable in conditions where only one side of the structure is accessible. When this initial inspection can be performed in the laboratory on a fairly flat panel, the TTU C-scan method is by far the most preferable method due to its ability to provide a full scale, plan view, hard copy record of the defect conditions that are aligned normal to the interrogating beam (delaminations). Defects aligned parallel to the beam direction (translaminar cracking) do not often create appreciable or detectable attenuation, and thus should be examined by X-ray methods.

Detailed Plan View Identification

When more plan view details are required, enhanced X-ray and neutron radiography should be used. Each technique can identify both translaminar and delamination damage, although the X-ray technique requires a free edge or surface-intersecting damage so that the penetrant can be introduced. However, when such a surface defect is present, enhanced radiography is probably the single most sensitive and accurate inspection technique for composite structures. Neutron radiography, on the other hand, can be used where metal structure overlays composite material, since neutrons are not as attenuated by metal as X-rays and are relatively sensitive to polymeric materials containing hydrogen. This method, however, has not been proven to generate radiographs that exhibit much contrast or resolution. Another available technique is eddy current, in which small translaminar cracks can be identified without the requirement of a free edge.

Through-Thickness Identification

Where through-thickness determinations of the location of planar defects such as delaminations are required, either ultrasonics (A-scan, B-scan, or time-domain gated C-scan) or X-ray (stereo radiography) can be used. This provides the investigator with information similar to cross-sectional viewing of the planar defect locations.

Several techniques such as X-ray tomography, neutron radiography, and resonance/impedance bond testing are available, although their application to failure analyses is extremely limited due either to immaturity, expense, or limitation of field investigation. Holography, acoustic emission, thermography, and speckle photography are not used for post-failure analyses investigations since they require some sort of mechanical loading of the part to define damage states. For these reasons, these paragraphs describe in detail the proven and directly applicable NDE techniques such as ultrasonics, X-ray, eddy current, and edge replication. The basic operational modes and uses are presented, along with some fundamental theory with regard to evaluating fractured composite structures.

5.1 ULTRASONIC METHODS

Ultrasonic inspection techniques are useful in characterizing material flaws such as delaminations, cracks, voids, matrix rich pockets, and changes in thickness. For homogeneous materials such as metals, the techniques and the interpretation of the data are well developed and relatively simple. The anisotropic nature of composites presents an added dimension of complexity to ultrasonic inspection.

The variables affecting an ultrasonic high frequency sound source that is directionally focused on the material to be inspected include the acoustic properties of the material and the transporting medium that the beam passes through. Any variation of the acoustic properties of these materials can produce changes in the attenuation (transmission loss), velocity, reflection amplitude, refraction angle phase, and diffraction of the beam. These changes form the basis of various ultrasonic techniques.

The four primary factors that affect the ultrasound transmission in composite structures include (1) the inherent physical properties of the material, (2) the microstructural features, (3) the condition of the surface, and (4) the thickness of the material. The first and foremost parameters that affect transmission are the physical properties of the material such as stiffness and density, which determines the directions and energy breakdown of the ultrasonic beam within the material. Second, the microstructural features such as resin content, porosity, matrix cracking, delaminations, and ply orientation affect the ultrasonic sound propagation characteristics. It is the measurement and interpretation of the ultrasonic information that constitutes the major task involved.

Typical ultrasonic inspection of homogeneous isotropic materials is a process that requires a trained operator using precision and care to avoid errors in the assessment of the damage conditions. The complexities that arise from analyses of extremely anisotropic materials such as composites require knowledge of the above-mentioned factors that can have pronounced effects on the information obtained. Although these factors tend to complicate the analyses, they can also contribute in a constructive manner to provide valuable information regarding the microstructure and basic construction of the component.

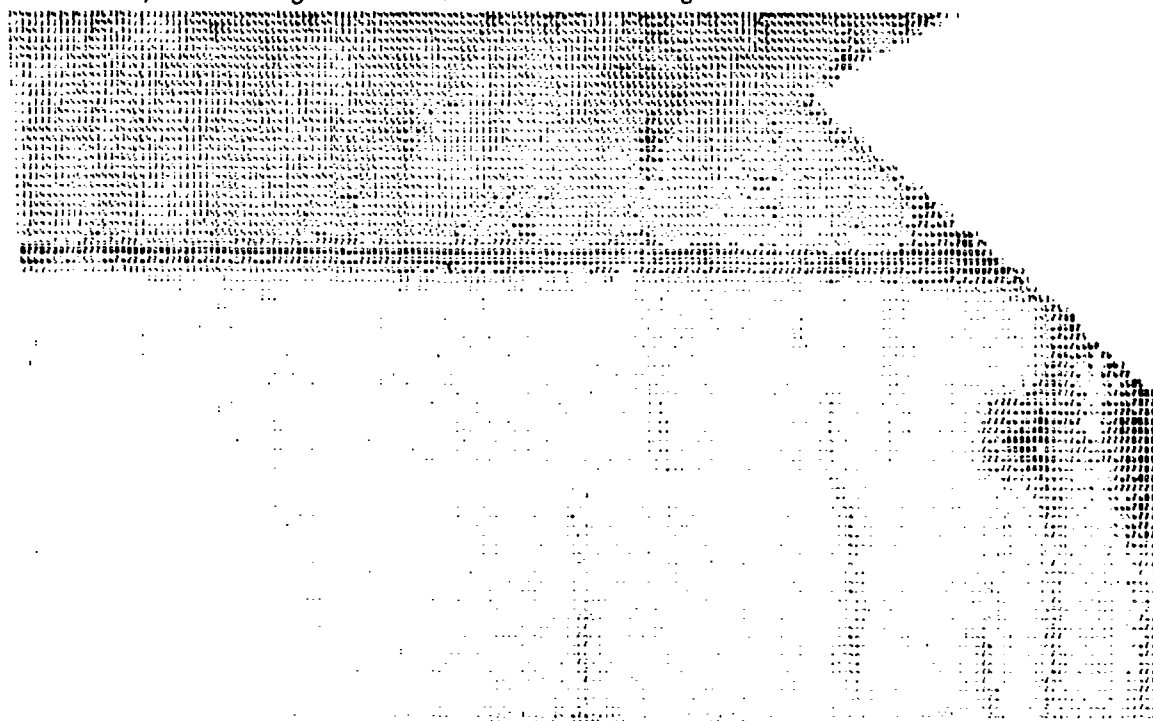
There are two primary methods which are recognized as the most flexible and efficient methods for obtaining ultrasonic sound propagation data from composite structures, through-transmission ultrasonic (TTU) and pulse-echo.

5.1.1 Through-Transmission Ultrasonic

In the TTU method, an ultrasonic transducer is placed on one side of the material and emits an acoustic pulse. The pulse travels through the material and is received by a second transducer located on the other side of the material. These transducers are placed in axial alignment so that their common axis is perpendicular to the surface of the specimen. With this placement, the amount of energy transmitted through the material is maximized and can be monitored easily as a function of position when the material is scanned by the transducers. For a C-scan, the entire surface is inspected by moving the transducer in a series of closely spaced traverses with a mechanical system. Most mechanical systems only allow planar scanning motions of flat or circular symmetric shapes. Water jet techniques have been developed which allow inspection of parts too large to be immersed in a tank. Current technology exists for robot controlled manipulators which track complex surface geometries,

but such systems are not yet commonplace. Since the speed of the test is limited primarily by the speed of the scanning, several arrayed transducers are often used for large scale inspection tasks to reduce scan times; however, for most failure analyses a single transducer can inspect a large part in a few hours.

The transmitted sound can then be evaluated and broken down into several sublevels, or grey scales, with each level equivalent to a certain amount of attenuation. This energy loss can be related to either voltage or decibels (dB). Each of these sublevels can then be assigned numbers or colors and graphically presented as a plan view of the part. Regions of attenuation greater than a standard, such as in the 6 to 18 dB range, indicate the presence of significant damage conditions that reflect the energy of the sound beam. Through the use of real-time computer monitoring of the attenuation, a map of the sound transmission relative to the part geometry can be produced by a plotter in which an image is formed by burning the surface layers of an ink-impregnated conductive paper. Figure 5-2 presents such a map, with a delamination identified in the areas of high attenuation. The numbers denote a range of dB sound loss, with the larger and darker numbers indicating more attenuation.



Note: Larger numbers denote higher levels of sound attenuation.

Figure 5-2. Examples of an Ultrasonic Through-Transmission C-Scan

In TTU, the sound attenuation results from three sources: viscoelastic effects, geometric dispersion due to material anisotropy, and dispersion due to geometric internal damage. By proper selection of the sound frequency, the attenuation due to delamination and cracks can be maximized and the attenuation due to material viscoelasticity and heterogeneity can be minimized. The use of 1 MHz has been recognized to provide the best transmittance since it has a fairly long wavelength and thus is less susceptible to scattering from smaller structural details, particularly for parts with honeycomb core. When increased sensitivity for smaller details is desired, the use of smaller wavelengths should be

used; however, frequencies in this range (5 to 15 MHz) do not transmit through honeycomb structure and require a more critical alignment of the two transducers.

The transporting medium is usually water, which provides a uniform coupler to transmit the sound waves between the transducers and the specimen. This requirement for a water coupler basically limits the TTU inspections to the laboratory, but a few portable units are available. The specimen is either immersed or water jets at the transducers supply a stream of the coupling agent. With composite failures, surface damage in the form of edge delaminations or translaminar cracking is often present. This surface damage, if extensive, can allow water to penetrate into the cracks. Since the attenuation is commonly due to air at the crack impeding the transmittance of sound, the water penetration can displace the air and eliminate, or significantly reduce, the attenuation at these defects. Hence, special precautions are required to prevent the intrusion of water into these areas, particularly for those specimens where a contaminant is suspected and water would be very undesirable. Normally, the open surface cracks are edge sealed with adhesive tape to inhibit entry of water.

Inspection of the TTU C-scan plan view records can provide a full scale assessment of the major defect conditions. Usually this inspection method is adequate to define the general outline of the delamination, particularly surrounding the major damage region that is visible. Although the C-scan method is best used to define delaminations, much smaller defects such as porosity can also be identified in extreme cases. This technique is limited by four factors: (1) both sides of the material must be accessible; (2) the depth of defects within the laminate cannot be determined; (3) extreme variations in thickness cannot be evaluated at the same time; and (4) defects aligned parallel to the incident beam are not easily identifiable (such as translaminar cracking). Where a more detailed inspection of the damage is needed or when there is access to only one side of the part, or when laboratory analysis is not possible, the pulse-echo method should be employed.

5.1.2 Pulse-Echo Ultrasonics

In the pulse-echo method, a single transducer transmits and receives the acoustic pulse. The transducer emits a gated pulse through the material, which is reflected by the far side of the part and then is detected by the transducer again. Since the full dynamic range of the receiver is available to amplify any backscattered acoustic energy, this technique can be made quite sensitive to subtle defect conditions. The reflections from the front and back surface provide known time-related endpoints so that the depth of the defect can be determined by its time function. A potential disadvantage of this method is that flaws one ply away from the front or back surface can be hidden by the reflections from the surfaces. This problem can be alleviated by properly adjusting the instrument to distinguish between these reflections, in combination with using a delay line transducer. Additionally, it is necessary to record the returned echo trace and section it at various periods of time in order to have an accurate representation of the location of the flaws. Breaking down the echo trace allows the differentiation and separation between closely arranged flaws and prevents the investigator from mistaking several small flaws as a single large one.

For use in the C-scan format, the inspection is usually performed either in a water bath or by using columns of water sprayed upon the surface of the specimen. The water serves as the coupler and delay line for the ultrasonic signals. Information is generally recorded in which the signal levels at each (and time or depth) are printed or displayed as the transducer is moved over the specimen. The C-scan

pulse echo is a plan view, two-dimensional image of the internal structure of a material. With gating of the amplitude-based digital signal, imaging of defects can be identified, related to the position within the thickness of the material, as shown in Figure 5-3. The use of a combination of two gating zones can allow the differentiation of delaminations near the front surface (light) and the back surface (dark).

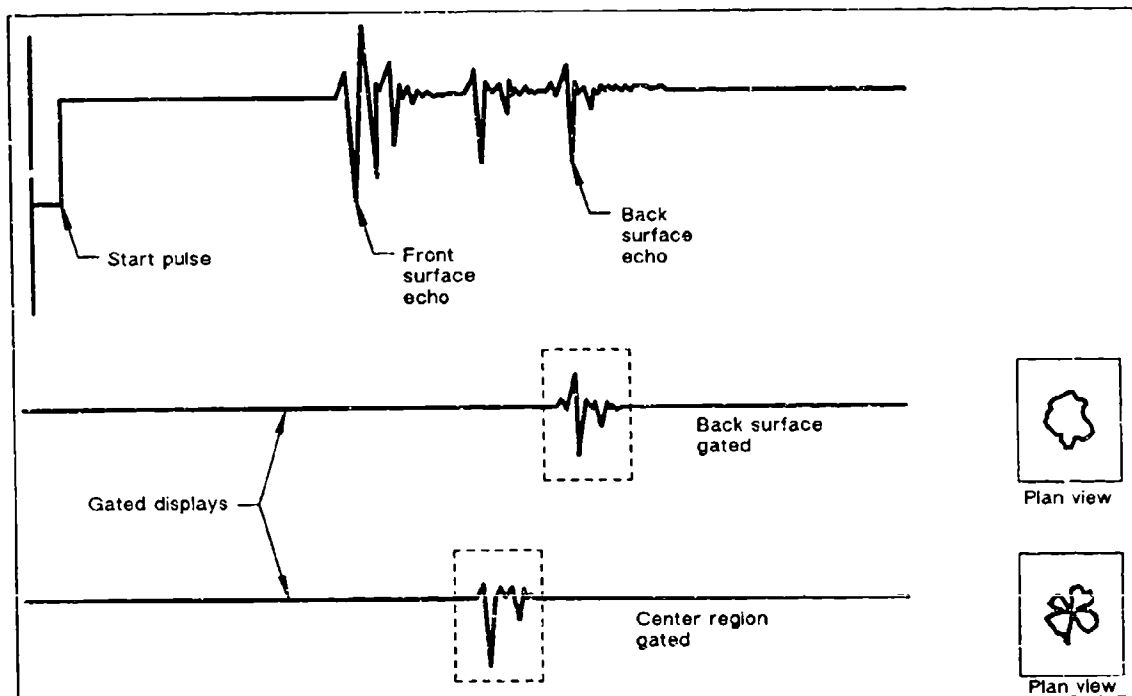


Figure 5-3. Pulse-Echo Ultrasonic C-Scan Using Time-Domain Gating Zones To Identify Damage States of Impact

Short pulse (shock wave) methods can also produce a considerable amount of information, although it is limited to linear plotting of the data instead of the two-dimensional C-scan. In A-scan, the reflected pulses can be real-time displayed on a cathode ray tube or can be permanently recorded. By comparing the reflected pulse information from a region of damage with an area containing no damage (often a calibration sample), the depth of the defect condition can be fairly accurately determined. Similar to C-scan, this method produces an image delineating the reflections between the front and back surfaces. By taking several parallel passes of the transducer over the part, a better feeling of the three-dimensional geometry of the defect can be obtained, as shown in Figure 5-4.

While the A-scan provides data regarding all reflections through the thickness, the B-scan indicates only the first echo after entering the surface. It is therefore incapable of displaying second and higher multiple reflections, as the other two methods can. The B-scan is somewhat similar to a transverse cross-section, in that it provides a record of the depth location on a line across the specimen surface. By taking several of these scans, they also can be combined to provide a more complete view of the through-thickness damage in the material. An example of a B-scan is presented in Figure 5-5, illustrating the extent of damage in a laminate at several locations along the surface of the part. For

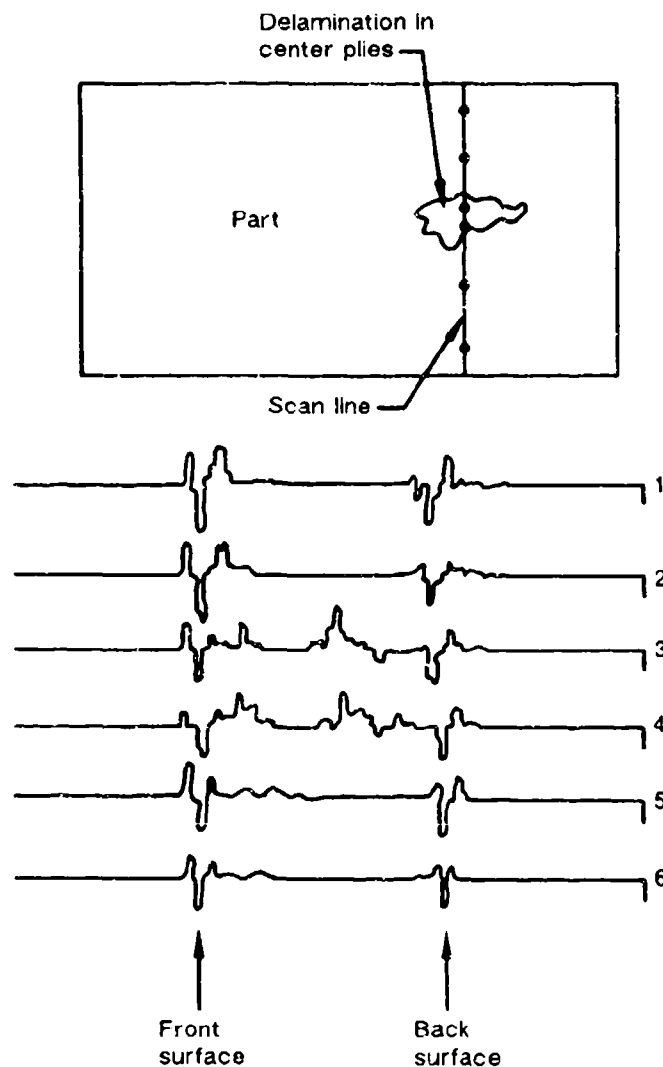


Figure 5-4. Delamination Identified by a Family of Pulse-Echo Ultrasonic A-Scans

field or initial inspections, the A-scan method using a cathode ray tube for imaging can be performed without a permanent record of the damage. For instance, in early NDE investigations in large failed structures with visible damage and delamination, hand-held pulse echo can be used to define quickly the perimeter of the delamination damage. In this case the couplant is usually a light grease, oil, or commercially available gel.

5.1.3 Single-Sided Ultrasonic (Backscatter)

Recent developments have provided a method of identifying transverse cracking, with resolution capable to identify cracking within a single ply. This technique is usually called single-sided ultrasonic angle beams (backscatter) and involves using an off-axis transducer that imparts the sound at an angle to the surface, as shown in Figure 5-6. This technique employs separate transmitting and receiving transducers housed in a single surface probe. A complex wavefront is created in the structure

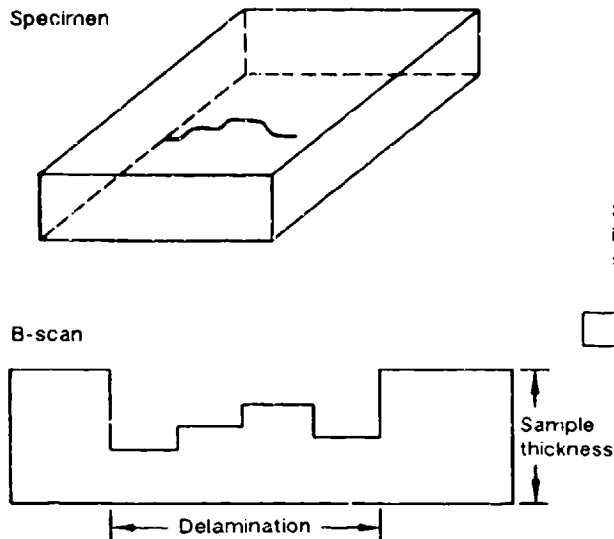


Figure 5-5. Pulse-Echo Ultrasonic B-Scan of a Delamination Region

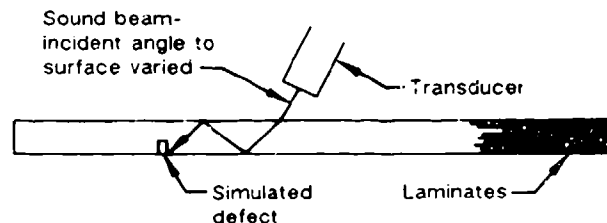


Figure 5-6. Ultrasonic Detection of Simulated Crack in Laminate Plate

by the transmitter, and is continuously monitored by the receiving transducer. With this system, delaminations create both a phase and amplitude change, allowing their detection. Because the ultrasonic signal is angled with respect to the surface, this technique has enhanced sensitivity to cracks oriented in the through-the-thickness direction. A drawback is that each ply must be scanned at a specific angle of incidence to maximize the signal amplitude and properly determine the location of the microcracks. A reference standard is also required that duplicates the materials and layup of the laminate being inspected.

5.2 X-RAY RADIOGRAPHY

X-ray techniques can be used to detect broken structure and large subsurface fractures when there is a displacement of members. Extensive cracks in which surface displacement has not occurred may not be detectable. Defects such as crushed core and fractures associated with impact damage lend themselves to radiographic evaluation. In addition to detecting cracks, the investigator can learn valuable information regarding the internal structure of the component, particularly if there are major differences in construction such as stiffeners and honeycomb core. Water in the core, if extensive, can also be detected. For failure analysis, the use of X-ray is most often considered as a secondary method to ultrasonics, although it possesses many advantages when faced with damage located parallel to the incident interrogating beam such as translaminar cracking.

5.2.1 Classical Radiography

An X-ray (radiographic) inspection is performed by transmitting a beam of penetrating radiation through an object onto a photosensitive film. This beam is partially absorbed by the composite as it passes through. Discontinuities such as translaminar cracks cause a reduction in thickness parallel to the incident beam path, and consequently result in less absorption and less reduction in the intensity of the X-ray beam. These varying beam intensities which strike the film plane

form a latent image. The film is processed to form a visible image called a radiograph. The radiograph is then evaluated for information regarding the extent and nature of the defect conditions, if they exist.

Although conventional radiography readily detects through-thickness fractures, it does not always present conclusive results. The information obtained from radiographic inspections are affected by the size and orientation of the defect relative to the incident beam. Defects presented normal to the beam result in insufficient changes in density so that interlaminar defects such as delaminations and porosity are not detected by conventional radiography. Due to these limitations, the technique has been significantly improved by the use of some form of radio-opaque penetrant, which produces probably the single most sensitive inspection technique for detecting cracks in composites that are surface related. The following paragraphs focus on this valuable technique.

5.2.2 Penetrant-Enhanced Radiography

The procedures for making radiographs of defects and damage in composites differs from the conventional ones in that an X-ray opaque penetrant is used to enhance the damage. The penetrant provides significant improvement in contrast between the damage and the intact composite, as shown in Figure 5-7. Various penetrants have been used, with tetrabromoethane (TBE) being the first solution evaluated. This penetrant was found to be highly toxic and carcinogenic so its use was discontinued. Diiodobutane (DIB) was used for a short time, but was also found to be a toxic organic halide, was expensive, and had a short shelf life. The enhancement chemical that has proven nontoxic and was relatively inexpensive is zinc iodide (ZnI_2), used with an alcohol carrier solution. The carrier solutions are as follows:

Isopropyl Solution

Zinc Iodide -- 60 grams

Water -- 10 milliliters (ml)

Isopropyl Alcohol -- 10 ml

Kodak "Photoflo" -- 1 ml

MEK Solution

Zinc Iodide -- 60 grams

MEK -- 250 ml

The isopropyl solution requires about 30 minutes after application for the penetrant to reach the end of the damage. This time is reduced to about ten minutes for the methyl ethyl ketone (MEK) solution. After saturation, excess penetrant should be removed from the open surfaces with absorbent material. These penetrant materials should be used with caution since they can potentially damage or obscure the fine microstructural fracture details and prevent detection of contaminants. For fairly chemically stable matrix systems such as epoxies, the use of these penetrants has not created any undesirable effects such as damage to the fracture surface details, particularly when removed with a clean solution of the primary solvent carrier. For other material systems such as thermoplastics, the effects have not been evaluated, and thus should be spot tested prior to application to the fracture surfaces.

Various X-ray films can be used, although a high resolution, single-coat film such as Kodak Type R industrial, low speed, fine grain film gives the best contrast and resolution. Double-coat film should be avoided since it is exposed on both emulsions, leading to a double image and loss of resolution.

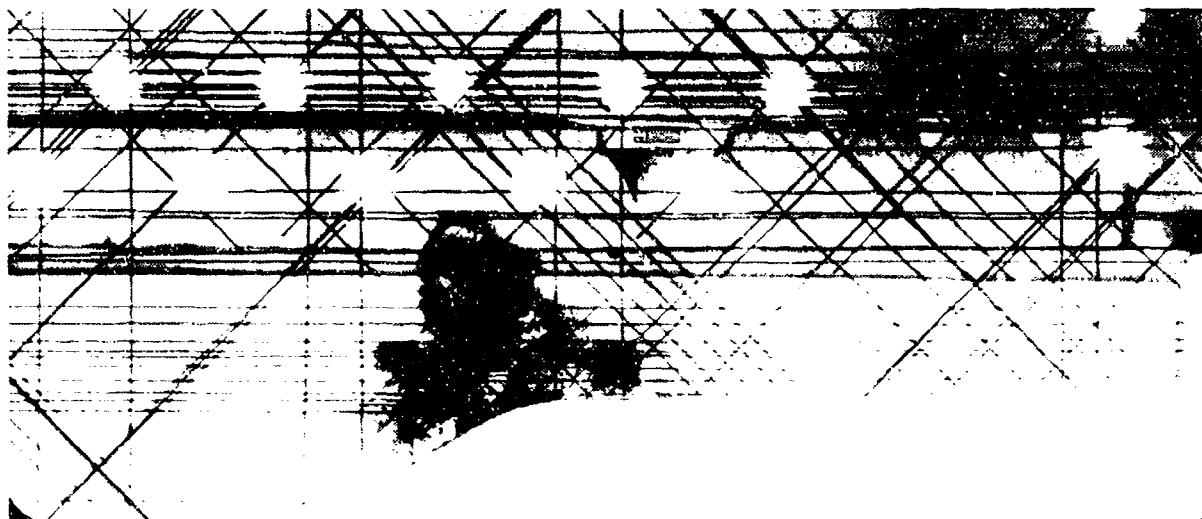


Figure 5-7. Penetrant-Enhanced X-Ray Image of Edge Delamination

X-ray units emitting soft X-rays are recommended, with a small spot size in the range of 1.5 mm by 1.5 mm or less, with an inherent filtration of 1.0 mm beryllium equivalent or less. The generator tube should be capable of producing a minimum of 20 kV at 2 mA. The low operating voltages produce soft X-rays that provide resolution of structural details within the laminate, such as porosity and fiber spacing irregularities. For applications which require positioning the X-ray tubes at tight locations, the use of an end anode side emission is recommended. The optimum exposure times are those that produce high resolution negatives from which prints can be made. These exposure times are shorter than those used for direct viewing. It should be noted that it is difficult to obtain prints of radiographs that will reproduce adequately by normal printing methods and therefore reporting and presentation of the results are more difficult and somewhat lacking.

Inspection of the films often requires an expert to differentiate artifacts from actual damage. The interpretation requires an understanding of how the penetrant affects the X-ray beam and how it enters the damaged specimen. Regions containing penetrant appear darker than regions containing no damage or defects. Regions containing no penetrant have a uniform grayness, especially on structures that have small thickness variations, since composites have relatively low radiographic scattering or absorbance due to the elements present. Cracks such as matrix or translaminar cracking appear as long, narrow, dark lines. The interpretation of artifacts corresponding to delaminations is usually more difficult. The opening displacement of the crack is the greatest at the edge and the least at the end of the delamination, and therefore one might expect a visible lightening of the image from the free edge toward the crack tip. While this change in grey level holds true at the extreme ends of the crack, the situation at the central region is such that the capillary forces are not strong enough to hold the penetrant. This condition results in a central boundary region that does not stop the X-rays and often appears light and undamaged.

Another modification to the penetrant-enhanced X-ray image involves making stereo radiographs, such that a three-dimensional view of the internal damage can be examined. The standard stereo radiography procedure consists of making two X-ray films of an object from slightly different orientations. The best method of creating the two views is to rotate the part through a small angle

(usually about 7 to 15 degrees). The part is then allowed to remain at the center of the path of the X-rays and is also centered in the radiograph. The depth of the damage can then be identified, and overlaying damage that might be masked with a single plan view can be differentiated. With the aid of a stereo viewer, the defects nearest the X-ray source have the largest relative displacement and the farthest defects are the least displaced.

5.3 EDDY CURRENT

This technique is commonly used in metals and has provided satisfactory results for fabric laminates, particularly for locations around small, localized geometric variances such as fastener holes and edge radii. Eddy current testing involves small, hand-held surface probes that produce an alternating magnetic field. This field is generated by an alternating current test instrument coil. This alternating expanding and collapsing current induces a magnetic eddy current in the specimen. The interaction of this magnetic field with the test instrument varies as the internal flaws and fractures are encountered. The use of this instrument is basically limited to solid laminates that are conductive and have appreciable magnetic permeability. This method relies on the conductivity of the carbon fiber which is, at best, limited. Figure 5-8 presents a typical inspection procedure using a probe to detect subsurface damage in fabric laminates.

5.4 EDGE REPLICATION

Edge replication has proven itself to be an accurate technique for documenting the state of damage in thin laminate sections. It is a direct application of the replication technique used for transmission electron microscopy (TEM) specimen preparation. An acetate film that has been softened with acetate solution is firmly applied to the edge, then allowed to dry. The replica can then be shadowed to enhance the surface features. The result is a mirror image of the edge that can be examined at higher magnification to assess invisible damage. Cracks such as the trans laminar cracks for the 90-degree plies and edge delaminations in the 0-degree plies can be readily identified and highlighted by shadowing.

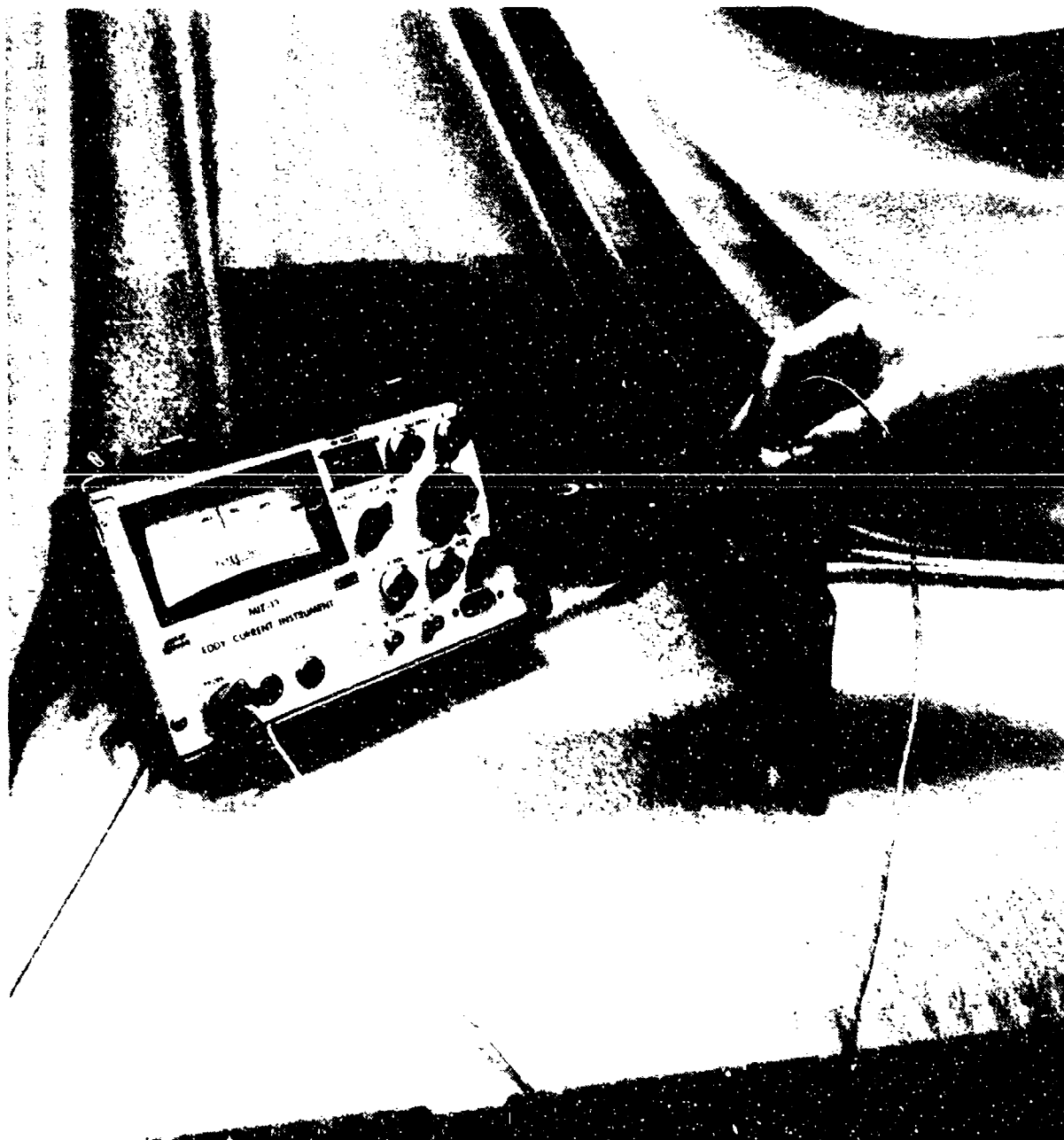


Figure 5-8. Typical Inspection Procedure Using Probe to Detect Subsurface Damage in Fabric Laminates

SECTION 6

MATERIALS CHARACTERIZATION

Errors in material layup, ply orientation, microconstituent chemical formulation, processing, and the degree of matrix curing can lead, or contribute, to premature component failures. As a result, the analysis of these basic material and processing errors should be considered a standard operation in most analysis investigations. This section presents the standard techniques currently available for characterizing the material integrity and identifying anomalous conditions, if any, that may have caused or contributed to component failure. These techniques are presented for evaluation and testing of carbon fiber/epoxy resin systems.

In this section, the principal selected topics include the following:

1. Material layup analysis: Verification of the number, orientation, and sequence of plies in the laminate
2. Fiber, matrix, and void volume fraction determinations
3. Material identification: Verification and fingerprinting of the material chemical composition for both cured laminate and uncured prepreg
4. Degree of cure analysis: Determination of glass transition temperature (T_g) and extent of reaction during the cure process
5. Contamination analysis: Analysis of surface chemicals and identification of foreign contaminants.

In most failure analyses, the examination of part material, configuration, and quality should be considered a routine procedure, necessary for the accurate evaluation of the failure cause. These examinations should identify any gross deficiencies that could have significant effect on material properties or the magnitude of local stresses within the part. For composite materials, items of concern include:

1. Incorrect materials
2. Resin content and fiber content
3. Undercure
4. Moisture content
5. Ply stacking sequence, placement, and orientation errors
6. Incorrect size, placement, or poor quality of details such as holes and radii
7. Improper fastener installation, joining, bonding, etc.
8. Void content
9. Individual ply thickness
10. Fiber alignment.

Most of these conditions are likely to be rare. However, since they require little effort to examine and have such a critical influence on failure, their inclusion in any complete analysis is a necessity. Configuration and materials characterization examinations are included in the overall FALN illustrated in Figure 6-1. Because of their potential impact on subsequent operations, these examinations have been incorporated in the early stages of analysis. In many cases, identification of a major discrepancy (such as using the wrong material), may sufficiently explain the cause of fracture, thus expediting and lowering the cost of the overall investigation, in addition to providing the rationale for appropriate corrective actions.

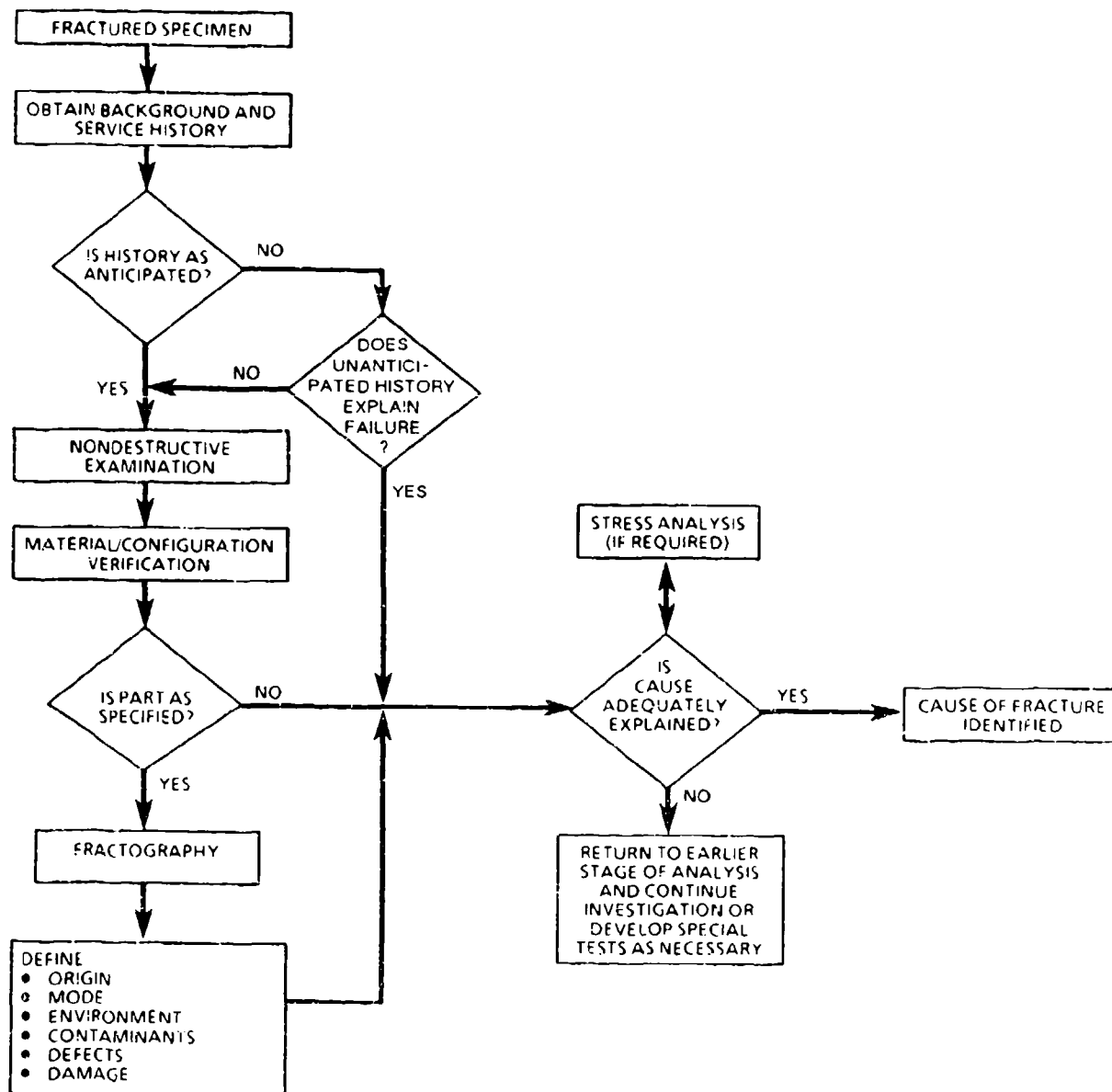


Figure 6-1. Simplified Investigative Framework (Laboratory Examination)

In support of the overall FALN, a detailed flow chart for configuration and materials characterization was developed. This chart, illustrated in Figure 6-2, provides a detailed guideline for investigators to evaluate critical items such as configuration, ply layup, degree of cure, and the type of resin system used. This FALN employs relatively simple analytical techniques. More complex and difficult analyses occur at later stages of investigation. Table 6-1 provides a detailed matrix summary of material characterization techniques.

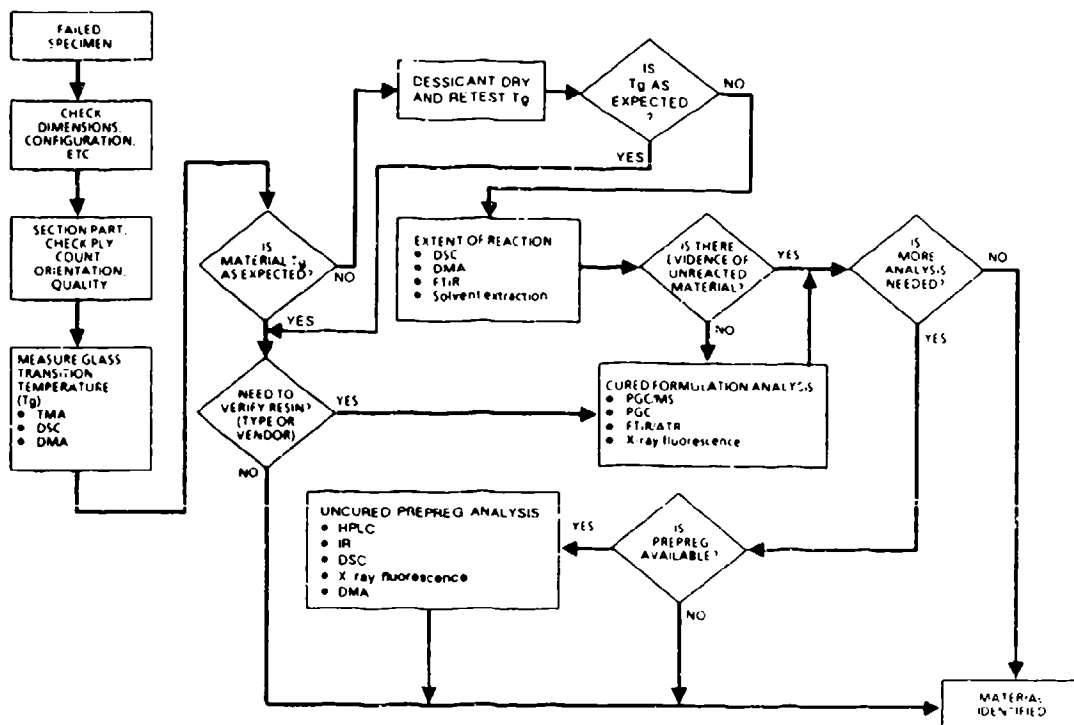


Figure 6-2. Material Verification Technique Sub-FALN

In Figure 6-2, one of the more detailed areas of a configuration and materials characterization study is illustrated. Once a thermoset resin material has cured, ascertaining its identity (such as vendor or specific resin formulation family) poses a relatively difficult problem. This is because of the generally similar chemical structure of cross-linked epoxy systems and the tendency of cured resins to resist yielding their identities by typical chemical analyses methods. However, since many of the currently used epoxies exhibit nearly identical properties (within a cure-temperature family), identification of the exact resin system used may not be as crucial as identifying a material with its proper cure-temperature family, for example 121°C (250°F) or 177°C (350°F). Through the combined use of Tg and residual heat of reaction measurements, the particular cure-temperature family of most materials can be established with relative confidence.

For example, when fully cured, most epoxies lack any appreciable residual heat of reaction and the Tg's are at or slightly above their original cure temperature. When minimum heat of reaction is observed, the measured Tg gives a fairly good indication of the cure temperature family of material used. However, in cases where significant heat of reaction still exists, and the measured Tg is well below the specified cure temperature, the indication is that the proper prepreg material was used but an

Table 6-1. Failure Analysis Techniques for Materials Characterization

	TECHNIQUE	DESCRIPTION	USE	VALUE
Degree-of-Cure Analysis	Thermomechanical Analysis (TMA)	Measure probe displacement as a function of sample temperature	Determines glass transition temperature	Indication of degree of cure or environmental effect.
	Differential Scanning Calorimetry (DSC)	Performs enthalpy measurements	<ul style="list-style-type: none"> Determines glass transition temperature Determines residual heat of reaction 	Indication of degree of cure or environmental effects
	Dynamic Mechanical Analysis (DMA)	Measures mechanical response to oscillating dynamic loading	<ul style="list-style-type: none"> Determines glass transition temperature Observes mechanical transition due to additional crosslinking 	<ul style="list-style-type: none"> Indication of degree of cure or environmental effects Indication of undercured condition
	Infrared spectroscopy	Measures IR spectrum	Distinguishes between reacted and unreacted functional groups	Indicates amount of unreacted functional groups to determine extent of cure
	Solvent extraction	Exposure to an organic solvent	Removes unreacted material leaving reacted network behind	Indication of the degree of cure
Uncured Material Identification	High-Pressure Liquid Chromatography (HPLC)	Produces liquid chromatograms of any soluble liquid	Identifies individual components of differing solubilities or size	Formulation verification
	Infrared spectroscopy	Measures IR spectra	Identifies functional groups attached to carbon backbone	Formulation verification
	Differential Scanning Calorimetry (DSC)	Performs enthalpy measurements	Determines heat of reaction	Formulation verification
	X-ray fluorescence	Measures X-ray fluorescence spectra	Determines sulfur content	Hardener content
Cured Material Identification	Pyrolysis - Gas Chromatography (PGC)	Determines gas chromatograms formed from nonvolatile organics by thermal decomposition	Qualitative and quantitative analysis of cured epoxy	Formulation/impurity verification
	Pyrolysis - Gas Chromatography / Mass Spectroscopy (PGC/MS)	Allows mass spectrometer to act as a detector for the gas chromatograph	Qualitative and quantitative analysis of cured epoxy	Formulation/impurity verification
	Infrared spectroscopy	Measures IR spectra	Functional group analysis	Formulation verification
	X-ray fluorescence	Measures X-ray fluorescence spectra	Determines sulfur content	Hardener content
	Thermomechanical Analysis (TMA)	Measures material thermal-mechanical response	Determines glass transition	Identify general resin system

insufficient degree of cure was generated during processing. In making these analyses, it is important to keep in mind that undercure can arise from several causes -- only one of which may be an improper cure procedure. Alterations in the prepreg formulation can reduce reaction rates during cure. Therefore, when a sufficient degree of undercure is detected, it is generally recommended that additional tests be carried out on the original prepreg (from that specific lot, if possible) to verify its chemistry.

In some analyses, identifying the specific resin system used may be important; however, the investigator should be aware that analytical capabilities are only partially developed, and are in their infancy for more recent resin formulations and systems. Sufficient differences exist in basic formulations so that relatively simple tests may be used to identify different systems, but for the most part, the ability to identify resin systems within the same temperature-cure family is relatively difficult.

6.1 LAMINATE LAYUP AND PLY ORIENTATION ANALYSES

Unlike homogeneous materials, most modern composite materials are fabricated by laminating together a large number of relatively thin gage woven or unidirectional plies. For structures made from such materials it is important to recognize that engineering properties, and hence the component's ability to operate without failure, depend upon the correct number, sequence, and orientation of plies being used to make up the laminate. In general, the significance of errors depends upon the particular material in question as well as the magnitude of mistake in terms of the overall laminate construction. For example, an overall off-axis rotation of 5 degrees can reduce the ultimate compression strength of a unidirectional graphite epoxy laminate by as much 54 percent. In contrast, a 5-degree rotation of only one ply out of a 30-ply laminate probably would produce less than a 2-percent decrease in ultimate strength. From this standpoint it is critical that the impact of identified discrepancies be identified accurately and taken into consideration prior to their reporting or possible identification as a significant contributor to the cause of failure.

Errors in layup can also have significant effects not directly related to those engineering properties considered as part of typical design. The materials' coefficient of thermal expansion represents one such property, where variations in stacking sequence can produce significant amounts of panel warpage or internal residual stresses. These internal stresses have been found to cause damage such as gross delamination and matrix cracking within the laminate plies. Such damage, while not always directly responsible for failure, may in many cases constitute one of several contributory conditions resulting in premature failure.

For continuous fiber reinforced composite materials, the exact design properties which should be checked as part of a ply layup analysis will depend strongly upon the requirements of the specific component examined. However, as a general guideline, critical parameters which should be given consideration in the event discrepancies are detected should include:

1. Young's Modulus
2. Basic laminate strength (tension, compression, shear)
3. Notch sensitivity (tension and compression)
4. Buckling stability
5. Internal thermal stress or residual stress conditions
6. Alterations in environmental susceptibility.

Some of the most common errors in ply layup include:

1. Missing or additional plies
2. Improper angular orientation
3. Improper ply type, grade, or style.

Several relatively straightforward methods exist for analyzing the orientation, stacking sequence, and number of plies making up a composite structure. Optical metallography is the most obvious and direct technique. Adapted from the microstructural analysis of metals, this technique involves the optical examination of finely polished cross sections using a standard reflected-light optical microscope. Other methods, although not as quick or simple, include image analysis and radiography. Specific details of each of these methods are presented in the following paragraphs.

Similar to standard metallurgical failure analysis procedures, selection of areas for examination generally constitutes the critical step involved in understanding internal material characteristics. For most failures, detailed examinations should be carried out in all areas of the part representative of the typical structure. For example, in a skin panel with attached stringers, a thorough analysis should examine both the skin as well as the stringer constructions regardless of whether the failure occurred in only one of these primary components, such as the skin. Reductions in modulus due to a layup error of one component can often produce higher loads in an adjacent part of the panel resulting in premature failure at a location not related to the original error. Generally, as a final step, metallographically prepared cross-sections should also be taken through, or adjacent to, the origin area of failure to examine for local discrepancies and ensure material uniformity.

6.1.1 Optical Microscopy (For Determination of Layup and Ply Orientation)

Sectioning. Removal of sections for metallographic preparation can be performed utilizing a wide variety of cutting devices as long as some care and forethought is given to the type and extent of damage likely to be generated. Abrasively coated band saw or circular blades are the most desirable since they generate the least damage (no further than 0.15 inch from the cut) and are widely available. If possible, a coolant such as water should be applied during the cutting operation to prevent heat damage, provided that subsequent contamination of the remaining component structure is not a concern. If abrasive cutting equipment is not available or coolant contamination is a concern, hand operated toothed blades or saws such as hack or coping saws can be used. With these blades every effort should be made to use as fine a toothed blade as possible to limit damage. With these toothed blades, a substantial amount of damage is often created adjacent to the cut edge, such as localized delaminations. The damage should be removed during subsequent sanding operations.

Metallographic Preparation. The basic preparation procedures for composites are the same as for metals. Depending upon the size of the section, mounting in a supportive resin may be necessary to provide a stable base for sanding and polishing. Resins requiring elevated temperature for cure or forming, such as bakelite, should in general be avoided since many may approach or exceed the material's original cure temperature and thereby introduce additional damage such as embrittlement, creep, or microcracking. For most applications room temperature cure systems such as two-part epoxies or methyl methacrylate resins work well.

Sanding should proceed from a relatively coarse paper (120 grit) to the finer grits (600). Typically wet-or-dry sandpapers are used during this procedure with a substantial amount of water being applied at all times to the surface being sanded to remove debris and prevent heat damage. For subsequent operations it is critical that the sanded surface produced is flat to ensure full surface contact during the final polishing operations. For most composite materials, final polishing is best accomplished by utilizing a high-speed polishing wheel covered with stretched silk (or other extremely low nap material such as nylon) in combination with either diamond paste or an equivalent alumina polishing compound. Final polishing usually does not require a large number of steps; usually 15 micron followed by 3 micron is adequate. Results are further improved by fairly heavy downward pressure and counter-rotating the specimen to the direction of wheel rotation.

Following polishing, etching is generally not required due to the distinct optical differences which exist between most fibers and the surrounding matrix systems. An exception to this is fiberglass where a dilute hydroformic or hydrofluoric acid etch may be necessary to enhance fiber visibility.

Plies. The orientation, number, and stacking sequence of plies making up the section of interest can be generally identified by optical microscopy at magnifications ranging from 50X to 400X. At the lower magnifications, individual plies can be identified by pronounced alterations in overall reflectivity due to the fiber orientation of each ply, or by the existence of a linear interfacial region of reduced fiber density (matrix-rich layer) between each ply (see Figure 6-3). Determination of the precise angular orientation of each ply requires higher magnification examinations. As illustrated in Figure 6-4, fibers intersecting the polished surface at an angle appear oval in shape. With this method, large differences between ply orientations are easily seen by large variances in the elliptical shape of the cross-sectioned fibers. In determining and reporting ply orientations, it is important to reference the measured angle against the component's defined 0-degree axis to prevent confusion and maintain consistency with other analyses such as stress analysis. Commonly, most sections are taken at 0, 45, or 90 degrees to the defined 0-degree axis, with a vertical section plane. This vertical section does not, however, allow one to distinguish between certain ply orientations such as +45 and -45 degree plies. A recent technique has been developed which provides differentiation of all ply angularities with a single cross-sectional planar view. In this method, the cross-section is prepared such that the polished sectional plane is at a 45-degree angle through the thickness of the part. This technique is presented in Figure 6-5. Small differences in fiber orientation, such as fiber waviness, can be determined by measuring the intersected fiber lengths and utilizing simple trigonometric calculations. For such measurements, the sectional plane should be vertical so that fibers from the primary reference plies are normal to the polished surface. This will result in the reference plies appearing circular and will allow measurement of nominal fiber diameter.

6.1.2 Image Analysis (For Determination of Layup and Ply Orientation)

Through the use of fairly low cost image analysis systems, both ply and individual fiber orientations can be determined. Through optical imaging of the polished cross-sections, the intersectional fiber length or the aspect ratio for each fiber is measured. Simple trigonometric calculations with these data are then used to determine overall ply orientation in each region of view or the average and worst case fiber waviness. Fiber waviness can be critical to certain product forms and applications like unidirectional or filament wound structures in which fiber nesting and tow movement occurs. One advantage of image analysis is that an automated or statistical evaluation of material integrity is available. Since fiber resolution and differentiation from the surrounding matrix resin is required, high magnification (400X or more) and various enhancement techniques such as etching (for fiberglass) or staining may be necessary.

Image analyses can also be used to determine the relative percentage of voids in the laminate. Either by cross-sectioning or by evaluation of the fracture surfaces, a quantitative assessment of the planar void content can be performed. By taking several measurements along parallel planes, a fairly accurate determination of the void shape, distribution, and percent can be made.

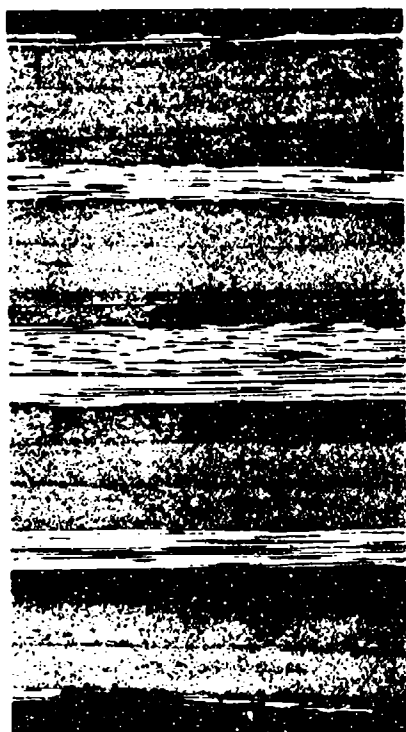


Figure 6-3. Cross Section of a Laminate With Easily Differentiated Ply Separation



Figure 6-4. Identification of Ply Orientation by Fiber End Shape and Ovality

6.1.3 Radiography (For Determination of Layup and Ply Orientation)

A nondestructive technique is available in which a plan view image of ply orientations can be determined. This involves the use of radiographically opaque tracer yarns, such that X-ray imaging can detect these doped fiber bundles. For tape prepreps, the tracer yarns are placed in the 0-degree direction parallel to the fiber orientation. For fabric, the yarns are most often placed in the warp direction. This technique is most useful for thin laminates, where the precise number of plies and orientation can be determined. Thick laminates make it difficult to identify the number of plies, although anomalous conditions such as ply orientation shift and ply dropoffs and pickups are easily detected. Figure 6-6 presents a radiograph in which the tracer yarns are evident.

6.2 DETERMINATION OF FIBER, MATRIX, VOID, AND MOISTURE CONTENT

The determination of the constituents present in the cured laminate is as important as identifying the layup of the individual plies. These details provide information regarding the microstructure which in turn can be directly related to mechanical properties of the overall laminate. For instance, a 20 percent shift in the fiber (or matrix) content has been shown to result in a decrease in mechanical properties as large as 50 percent. Similarly, void contents above 3 percent (by volume) can significantly reduce interlaminar tension and shear strength, particularly when the voids concentrate between plies.

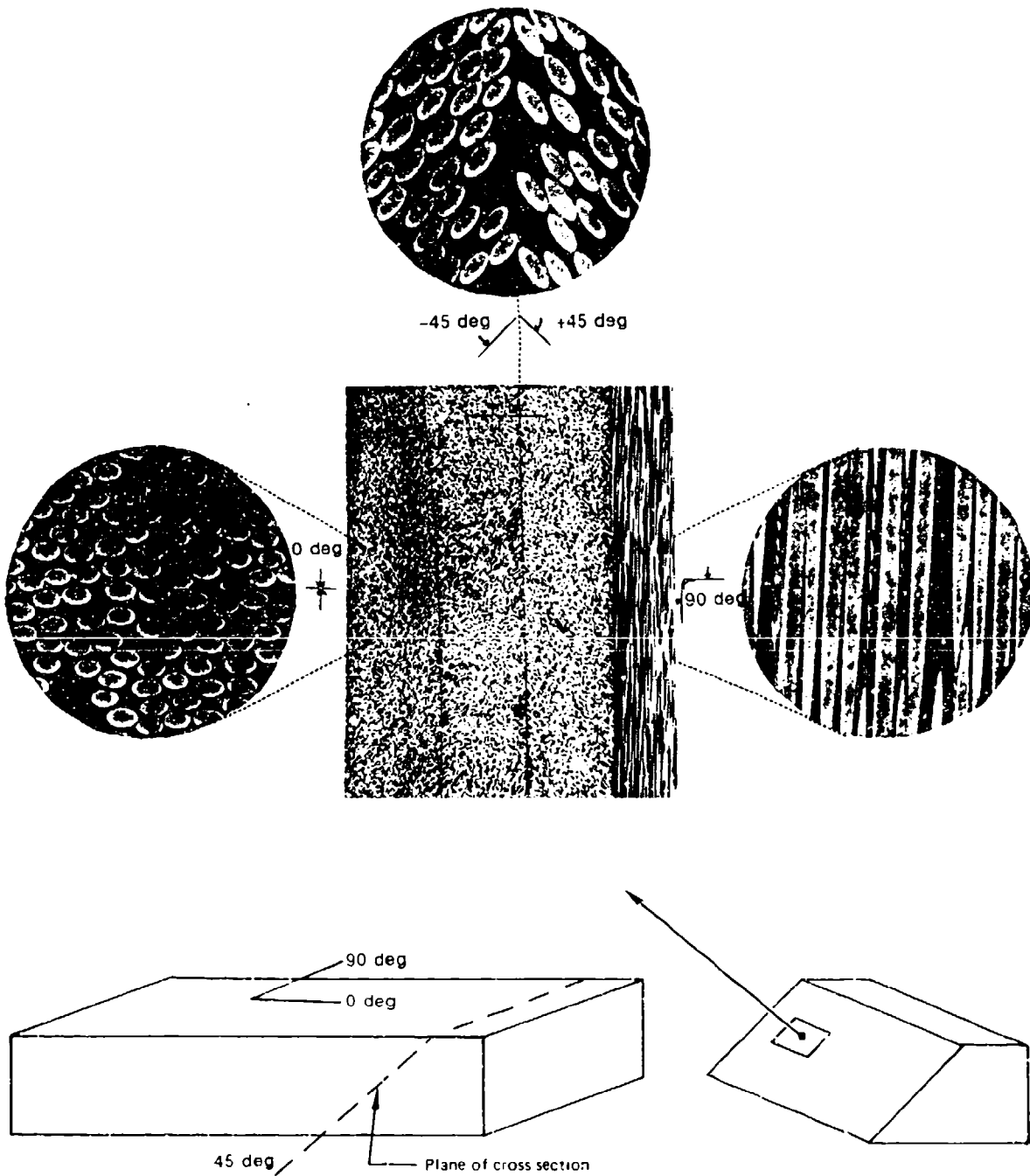


Figure 6-5. Polished Cross Section at 45-deg Angle Through the Thickness of the Part

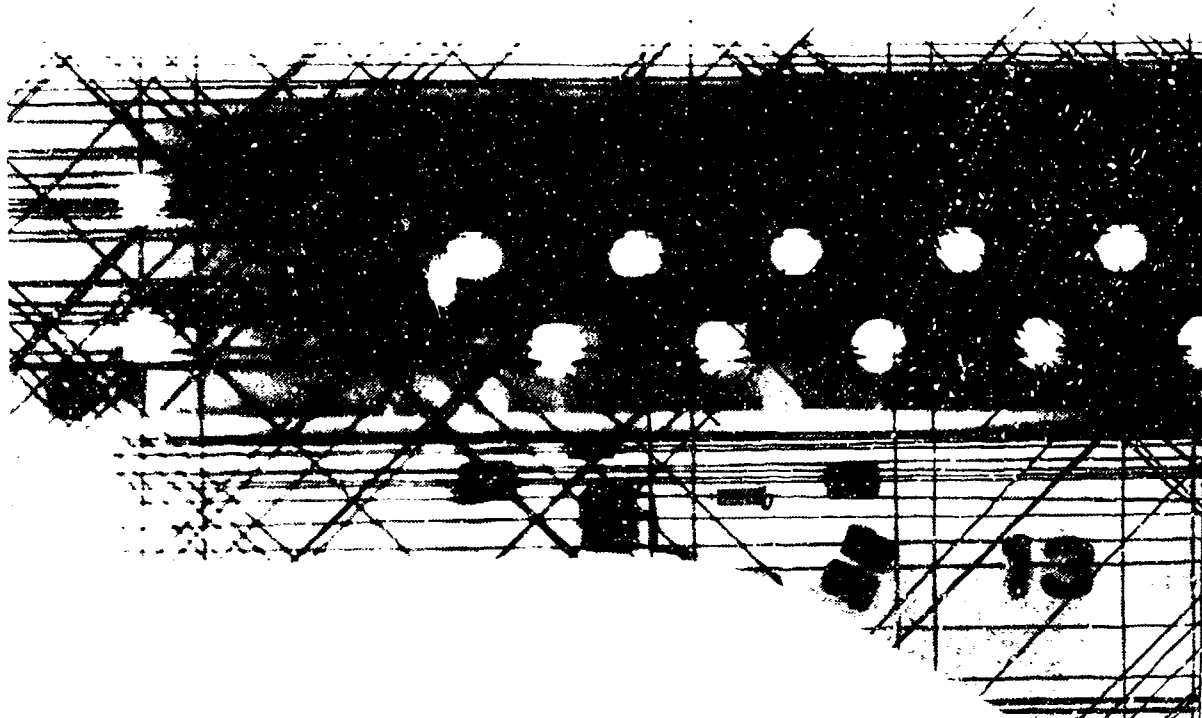


Figure 6-6. Radiograph in Which the Tracer Yarns Are Evident for Determination of the Ply Orientation in a Thin Laminate

6.2.1 Fiber and Matrix Content

The stiffness and strength of laminates are determined by the internal packing geometry of the fibers and the constitutive behavior of the fiber and matrix. The volume fractions of the fibers or matrices can be determined by three methods: (1) gradient density column, (2) chemical matrix digestion, and (3) photomicrographic.

The gradient density column method is performed by placing the sample in a graduated column containing a solution with a gradient of density from top to bottom. The height at which the sample is suspended in the solution can be used to calculate the overall density of the sample. The specimen density can then be used to calculate fiber volume and resin volume, given the resin density and fiber density as known constants.

The chemical matrix digestion method is performed by dissolving the resin with hot nitric acid and weighing the amount of fibers remaining. The volume fractions of fibers and resin can then be determined from the beginning and final weights and from the known densities of the constituents.

In the photomicrographics technique, the number of fibers in a given area of polished cross-section are counted and the volume fractions are determined as the area fractions of each constituent. Both area methods and line intercept methods can be used with an image analyzer to quickly determine fiber volume fractions.

The first two methods require a much larger specimen than the photomicrographic technique. This latter method must use many sampling areas to produce reliable results, since the area viewed is about a

hundredth of a square millimeter. It does, however, give an accurate view of the fiber-matrix distribution and void content. The first two methods do not indicate void content, which can result in erroneous data with specimens containing high void content or moisture content.

6.2.2 Void Content

The best method for determining void content is the photomicrographic analysis, as discussed in the previous paragraph. When inspecting laminates for void content, the cross-section is usually taken transverse to the laminate plane. In such cases where the voids are concentrated between plies, a polished section in the plane of the laminate can be examined to determine void content specific to the region between plies. As indicated above, a quantitative image analyzer can be used to determine void content more quickly and accurately.

6.2.3 Moisture Content

Moisture content of cured laminates can be performed by thermal drying or with a moisture analyzer. The primary difference between the two methods is that the moisture analyzer can differentiate between water vapor and other volatiles which escape from the specimen. Thermal drying only requires an accurate weighing balance and a small drying oven. The specimen is weighed before and after drying to determine moisture content. The temperature selected should be much less than the cure temperature or the Tg. For a 177°C (350°F) system, a temperature below 60°C (140°F) is recommended. The moisture analyzer is much quicker (hours versus days) and more accurate; however, the analyzer is a relatively expensive unit that also requires a trained operator.

6.3 MATERIAL IDENTIFICATION

The identification of the composite material used in a failed part may be necessary to determine the cause of failure. Material identification techniques are available which are suitable for cured or uncured material analysis. Uncured identification techniques are rarely used in failure analysis because the prepreg used in part fabrication is rarely available. Once a material has cured, identification of materials is difficult due to the intractable nature of a thermosetting polymer matrix. Since many of the currently used epoxies exhibit nearly identical properties (within a cure-temperature family), identification of the exact resin system may not be as crucial as identifying a material within a cure-temperature family. Due to the extensive vendor certification, receiving inspection testing, and quality control records maintained throughout the aerospace industry, a large amount of data usually exists on the prepreg used in any specific part. Major formulation or production errors are rare. The following paragraphs describe techniques for identification of cured or uncured composite materials.

6.3.1 Uncured Material Identification

Evaluation techniques for uncured epoxy prepreg are fairly well established. Several analytical techniques to characterize the uncured prepreg including high performance liquid chromatography (HPLC), infrared (IR) spectroscopy, differential scanning calorimetry (DSC), automatic absorption spectroscopy, and X-ray fluorescence provide detailed information to the investigator. Each technique is discussed in more detail below.

Generally, uncured material identification techniques are seldom used in failure analysis because the prepreg materials used to fabricate the failed part are not available to analysis. The most commonly used techniques, when the prepreg is available, are HPLC and IR spectroscopy. HPLC and IR are widely utilized in the aerospace industry to "fingerprint" the prepreg resin formulation. Standard HPLC chromatograms and IR spectra exist for all qualified materials. These standards provide a quick check of resin formulation. DSC is less frequently used for material identification. Although DSC can identify reaction types, specific resin system formulations are difficult. X-ray fluorescence is used to detect sulfonyl groups to verify the amount of diaminodiphenyl sulfone (DDS) hardener present. Atomic absorption spectroscopy is utilized to detect boron which verifies the level of BF_3 catalyst present. X-ray fluorescence and atomic absorption spectroscopy are usually used only if anomalies are detected in HPLC, IR, or DSC.

High Pressure Liquid Chromatography. HPLC is a common technique for chemical characterization of composite matrices. HPLC separates individual resin components according to their size or solubility using high efficiency, microparticulate columns.

HPLC test procedures are well established in the aerospace industry because of the widespread usage of HPLC for "fingerprint" inspection of resin formulation. Resin samples are extracted using an HPLC grade solvent such as 63:37 $\text{CH}_3\text{CN}:\text{H}_2\text{O}$. A schematic of a HPLC test setup and instrument parameters are shown in Figure 6-7. The extracted sample is injected into the column and analyzed using an ultraviolet detector. A typical HPLC chromatograph is shown in Figure 6-8. Components can be identified by comparing the peak positions on the chromatograms to a reference standard. Peak areas can be used to determine relative concentrations.

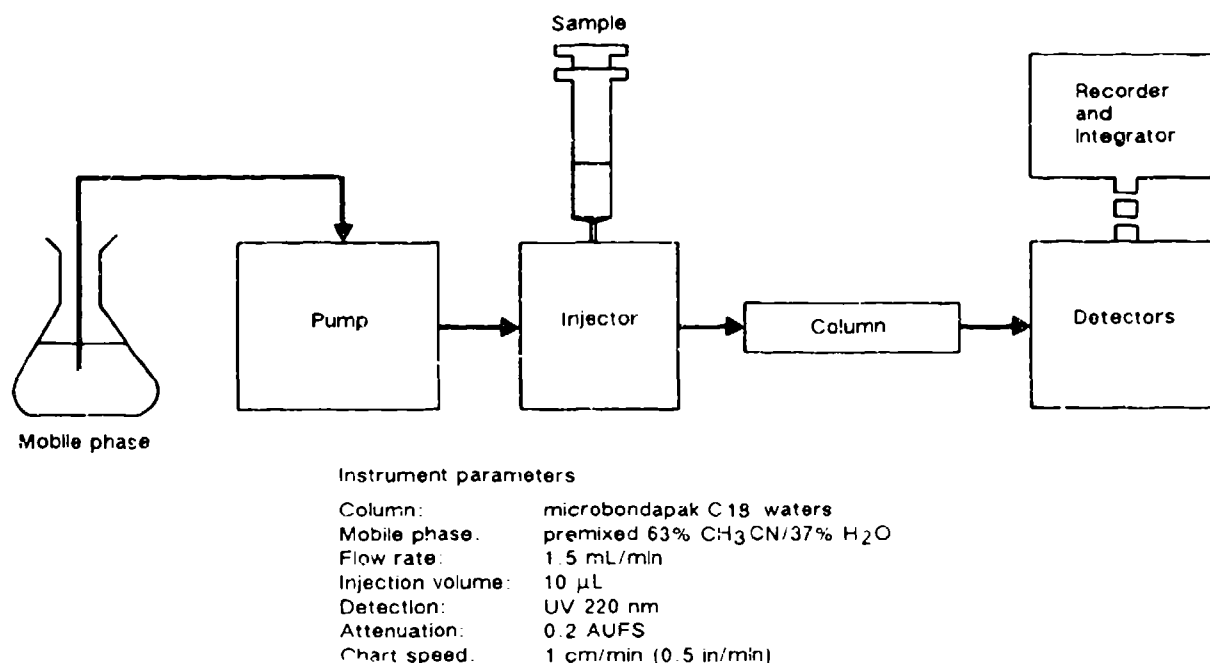


Figure 6-7. HPLC Test Setup Schematic and Typical Instrument Parameters

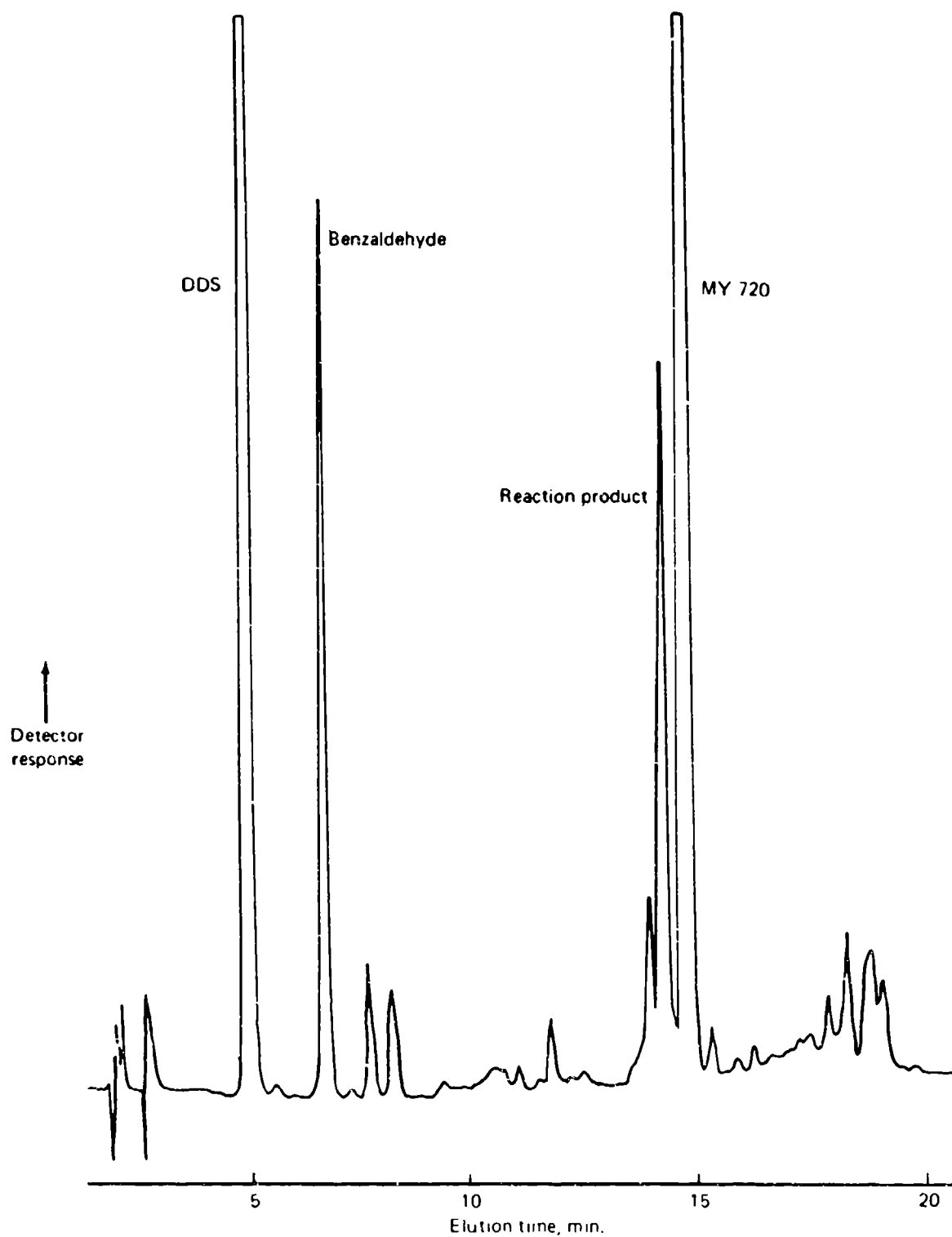
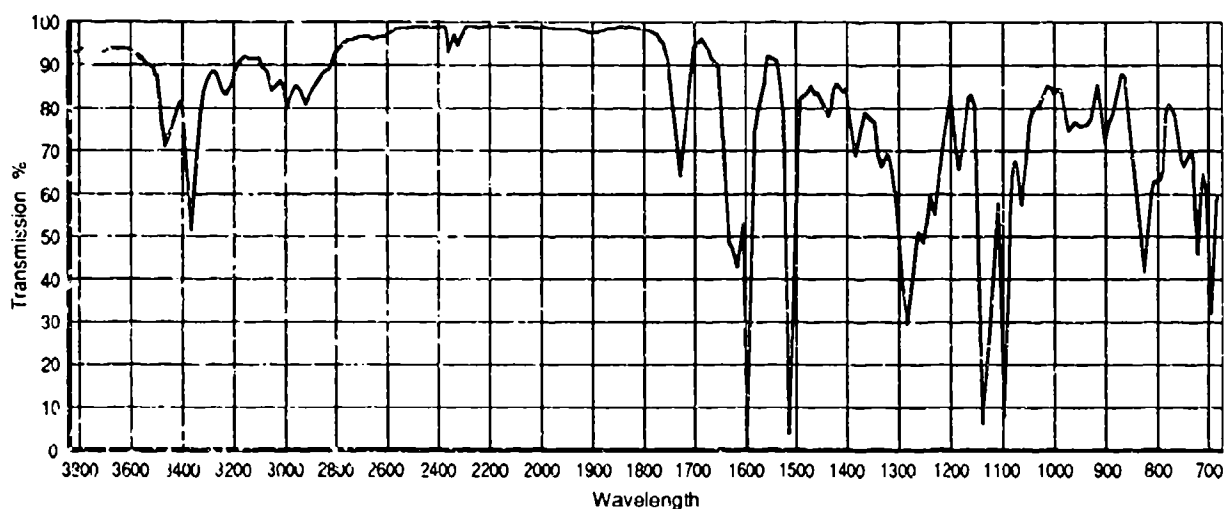


Figure 6-8. Chromatogram of Narmco Resin Matrix Showing Major Peak Assignment

Infrared Spectroscopy. IR is an organic chemical analysis tool which is extremely sensitive to the overall chemical makeup of a complex chemical formulation. IR measures the absorption of incident infrared radiation, and is used to verify epoxy resin formulation. This technique is well suited for characterizing commercial epoxy resins which often contain several components such as aromatic epoxy main, reactive epoxy diluents for flow control, aliphatic epoxy flexibilizers, elastomers, curing agents, catalysts, or accelerators. IR can accurately fingerprint the total resin formulation by detecting the absorbed frequencies of infrared light associated with the vibrations of specific molecular functional groups. The degree of absorbance is proportional to the amount of functionality in the resin formulation.

Because IR is able to fingerprint a given formulation accurately, it is used as a quality control tool to assure that lot-to-lot variations do not exceed certain limits. IR would also be useful to determine the manufacturer of the material when unidentified material is encountered. The typical application requires that the resin is extracted from the prepreg with reagent grade acetone at room temperature. The extract is then allowed to dry onto a salt pellet for IR analysis. The resultant spectrum is then compared to a standard epoxy spectrum acquired from the supplier or on a previous batch of material. The spectrum is examined for contaminants (additional peaks) or gross formulation changes (changes in the relative peak ratios). An example of a standard epoxy resin spectrum is shown in Figure 6-9. If a deviation from the standard spectrum is observed, then each subcomponent should be quantified and compared to standard formulation quantities. Quantitative methods for the curing agent and catalyst are considered below.



T90-31/1/A

Figure 6-9. Standard IR Spectrum of a Commercial Epoxy Resin Formulation

A quantitative method for determining the amount of DDS curing agent and carbonyl epoxy has been developed for the 3501 resin system (Reference 2). This involves constructing a working calibration curve for DDS concentrations in solution versus IR absorbance for the sulfone peak followed by a measurement of the absorbance of the unknown concentration of DDS in an epoxy prepreg extract. An alternate qualitative approach would rely on comparing the relative change in the ratio between these peaks as the concentration varied.

Differential Scanning Calorimetry. DSC is a thermal analysis technique which measures heat flow into or out of a sample by measuring the differential heat (energy) necessary to keep the sample at the same temperature as a reference sample. In the case of a curing epoxy system, DSC measures the heat released during the exothermic cure reactions as the specimen is heated at a constant heating rate.

DSC can be used to identify or characterize uncured prepreg. The cure of typical aerospace epoxy systems consists of several chemical reactions with different reaction rates and activation energies which cause certain cure reactions to be favored over certain temperature ranges. The reaction types occurring in a particular system depend on the formulation of the system. DSC can be used to separate the different cure reactions to help identify a particular resin system.

A typical DSC cell is shown in Figure 6-10. The sample pan and reference pan are placed in the cell. An inert atmosphere of nitrogen is then introduced into the test chamber. Heat is transferred to the pans through the sample platforms and heat flow is monitored by thermocouples. Generally, prepreg sample sizes of approximately 10 mg are used for DSC experiments depending on the size of the sample pan used. Low heating rates of about 2 to 5°C/minute are best to separate the various reaction peaks. Heat flow versus temperature or versus time at constant heating rate from ambient to 300°C is measured. An interface with a computer or microprocessor for experiment control, data acquisition, and data analysis provides greater accuracy and more information from each experiment.

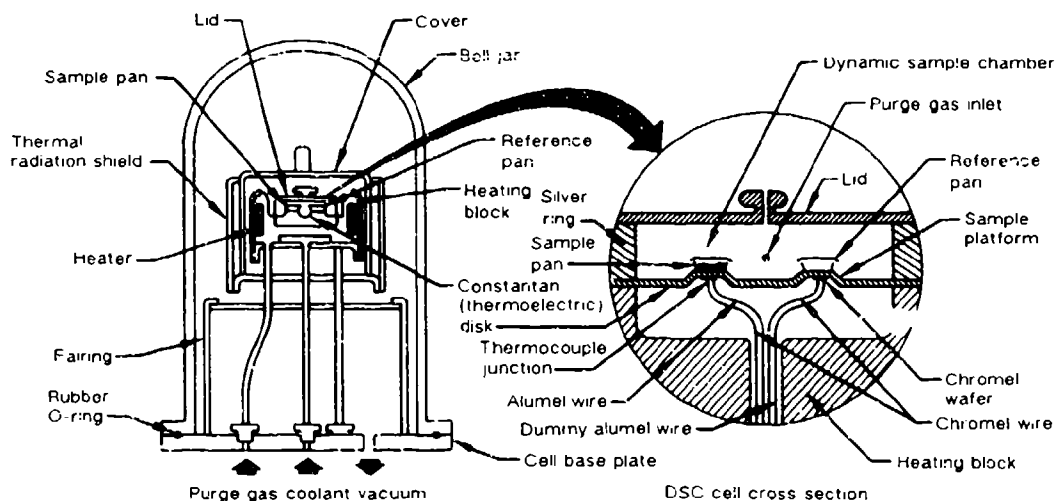


Figure 6-10. Cross-Sectional Diagram of the DSC Cell Used by DuPont DSC Module

A DSC thermogram for the Hercules 3501-6 resin system is shown in Figure 6-11. Exotherm peaks are observed at two temperatures (149°C and 213°C). The lower temperature peak is attributed to the catalyzed cure reactions while the higher temperature peak is attributed to the uncatalyzed cure reactions. The total heat of reaction (the area between the thermogram peaks and baseline T1 to T4), the relative peak size, and reaction temperature can identify resin constituents. Comparison to a standard thermogram can identify a particular resin system.

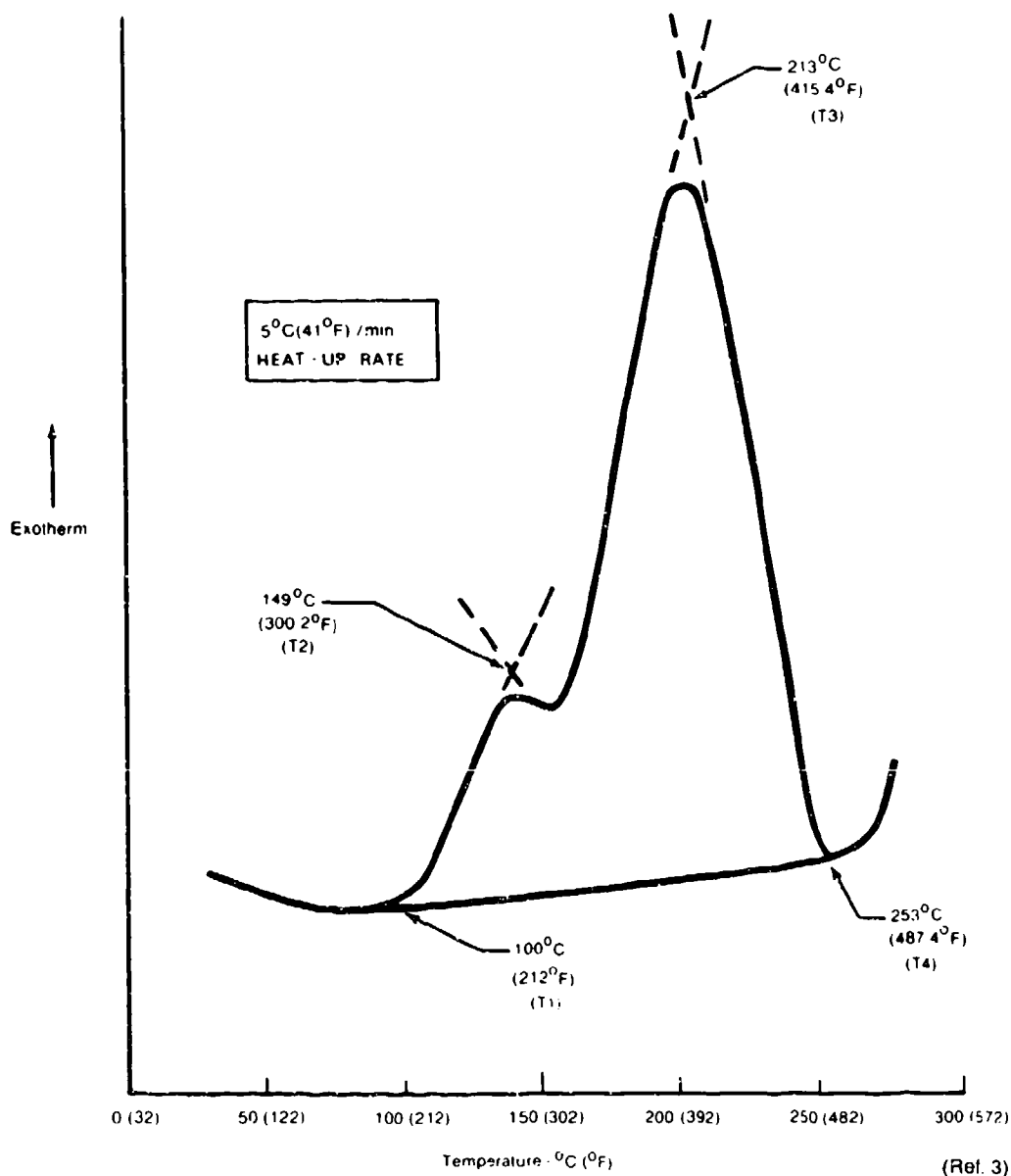


Figure 6-11. DSC Thermogram for 3501-6 Resin

The advantages of DSC formulation verification are the small sample size and the experimental ease. The disadvantage is the need for standard thermograms and background information for system identification.

Atomic Absorption Spectroscopy. Atomic absorption (AA) spectroscopy is used to quantify the amount of BF_3 containing catalyst in the epoxy resin. AA determinations for catalyst concentration are initiated when HPLC and IR indicate a significant deviation in resin formulation has occurred. The underlying principle of AA is the absorption of a discrete wavelength of light by a vaporized prepreg resin extract. For boron, 249.7 nm and 208.9 nm wavelength light will be attenuated proportionately to

the boron concentration. A boron calibration curve is established using a certified standard. Typical working range of concentrations for boron is 400 to 4,000 μl per ml of solution.

X-Ray Fluorescence Spectroscopy. X-ray fluorescence (XRF) spectroscopy can be used qualitatively or quantitatively to determine the amount of DDS curing agent in an epoxy prepreg extract by quantifying the amount of sulfur present. XRF measurements are initiated when a formulation change is suspected, based on HPLC or IR evaluation. The XRF determination is based on the emission of X-rays characteristic of sulfur (0.537216 nm) when the sample is irradiated with an X-ray source. The intensity of X-ray emission is proportional to the sulfur concentration. An example of a qualitative comparison of different epoxy resin systems is given in Figure 6-12.

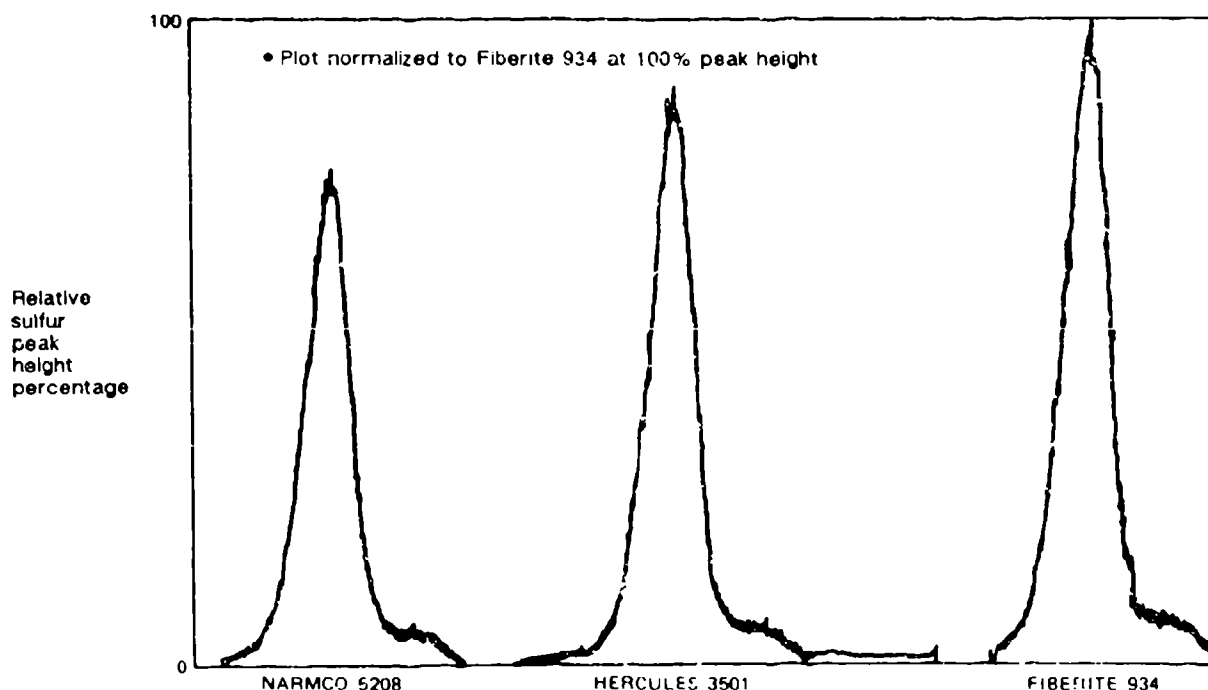


Figure 6-12. Sample Fingerprinting of Various Systems by Way of X-Ray Fluorescence

6.3.2 Cured Material Identification

Once a material has cured, ascertaining its identity poses a relatively difficult problem arising from the generally similar chemical structure of cross-linked thermosetting systems and the tendency of the cured resins to resist yielding their identities by typical analytical methods. However, since many of the currently used epoxies exhibit nearly identical properties (within a cure-temperature family), identification of the exact resin system used may not be as critical as identifying a material with its proper cure-temperature family. Through the combined use of determinations of T_g and residual heat of reaction measurements, the particular cure-temperature family can be determined.

In some isolated cases during post-failure analysis investigations, identifying the specific resin system used to fabricate the failed part may be important; however, the investigator should be aware that extensive capabilities in this area are only partially developed. Sufficient differences exist in basic formulation so that relatively simple tests, such as XRF, may be used to identify different systems. For the most part, the ability to identify resin systems within the same cure-temperature family is difficult. Two of the most promising techniques are pyrolysis gas chromatography (PGC) and diffuse reflectance (FTIR) spectroscopy. These techniques are discussed in the following paragraphs.

Pyrolysis Gas Chromatography. The PGC method is used to determine epoxy matrix chemical formulation. Pyrolysis is the vaporization and degradation of the matrix resin under controlled heating. The resulting decomposed products pass through a gas chromatograph which separates the components by physical or chemical parameters such as molecular size or polarity.

PGC requires samples of approximately 25 to 50 micrograms. Pyrolysis is accomplished at 1,000°C. Typical PGC chromatograms are shown in Figure 6-13 for two commercial epoxy systems. The resulting PGC chromatogram can be used to identify the matrix resin by comparing to a reference fingerprint standard.

PGC/Mass Spectrometry. PGC/mass spectrometry (MS) consists of PGC, as described above, coupled with a mass spectrometer. In order to identify separated pyrolysis products and to assign component structure to chromatographic peaks, the pyrolysis products are passed through a capillary column directly into the mass spectrometer. A typical PGC chromatogram with MS peak assignments is shown in Figure 6-14 for DDS hardener. Identification of resin formulation can be accomplished using PGC/MS.

Infrared Spectroscopy. Chemical characterization of a cured composite specimen is important in order to establish if the proper resin system was selected and to establish if any environmental degradation has occurred to the chemical structure. Using traditional transmission IR specimen techniques, a cured composite can be analyzed. Small particles are scraped off a resin rich area and ground to a fine particulate using a mortar and pestle. The particulate is then mixed into a potassium-bromide salt pellet for analysis. Figure 6-15 illustrates a comparison between this method for cured resin analysis and the standard spectrum for the uncured resin. Qualitatively these spectra are similar (except for the loss of epoxide groups upon curing) and may prove to be useful in a failure analysis where a database of uncured and cured resin systems has been established.

Diffuse Reflectance Infrared Spectroscopy. The diffuse reflectance infrared spectroscopy (DRIFTS) method permits direct measurement of the infrared spectrum from a cured composite resin. Infrared radiation is focused on the sample. The resulting diffusely scattered infrared radiation is collected with a large solid angle detector. The spectrum is interpreted as a normal IR spectrum would be except that a number of potential artifacts due to variations in sample geometry, peak distortions, and spectral interferences may occur. Figure 6-16 (Reference 4) illustrates DRIFTS spectra of a composite before and after thermal aging where increasing oxidation with aging is observed. Note the increased absorbance levels at 1,654 to 1,636 nm.

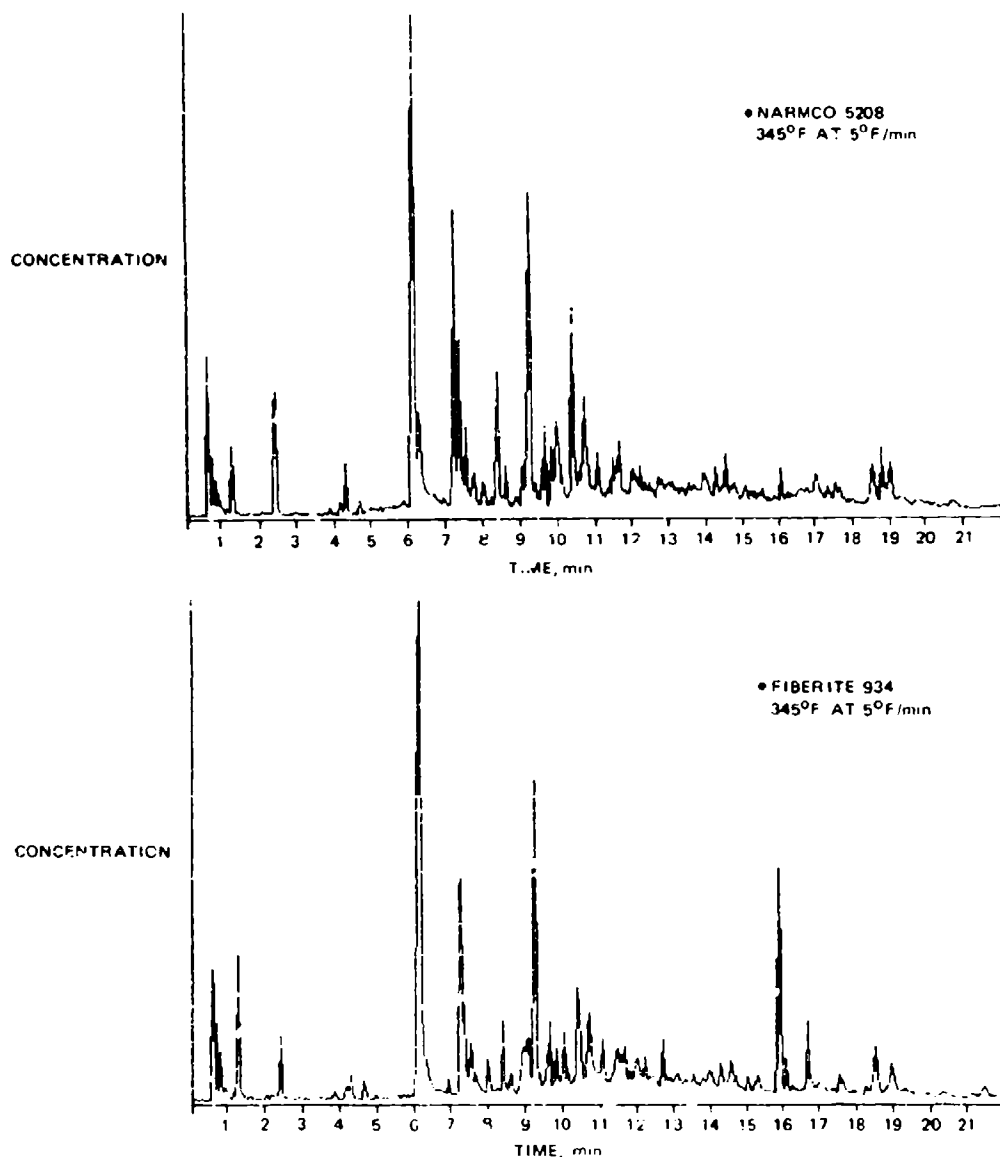


Figure 6-13. Pyrolysis Gas Chromatography of Two Difficult Resin Systems

4 DEGREE OF CURE ANALYSIS

The degree of cure of a thermosetting polymeric composite matrix is a critical variable affecting the performance of the composite, especially in elevated temperature or moist environments. Insufficient cure may occur due to lower than required cure temperatures, shorter than required cure times, or errors in resin formulation or chemistry. Errors in resin formulation or chemistry are rare because of the stringent specification requirements, vendor certification, and receiving inspection testing common throughout the aerospace industry. However, because conditions of undercure can significantly impact structural integrity and can be rapidly and easily checked, their analysis should be included as a routine step in most failure analyses. Verifying the degree of cure is analogous to checking

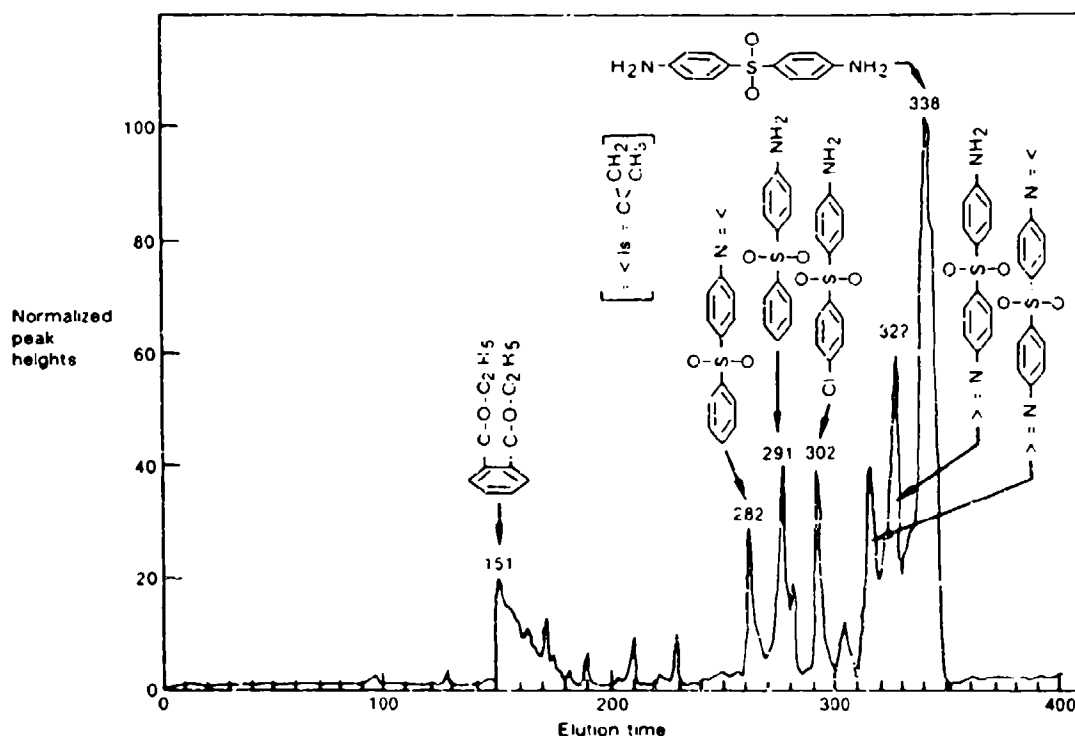
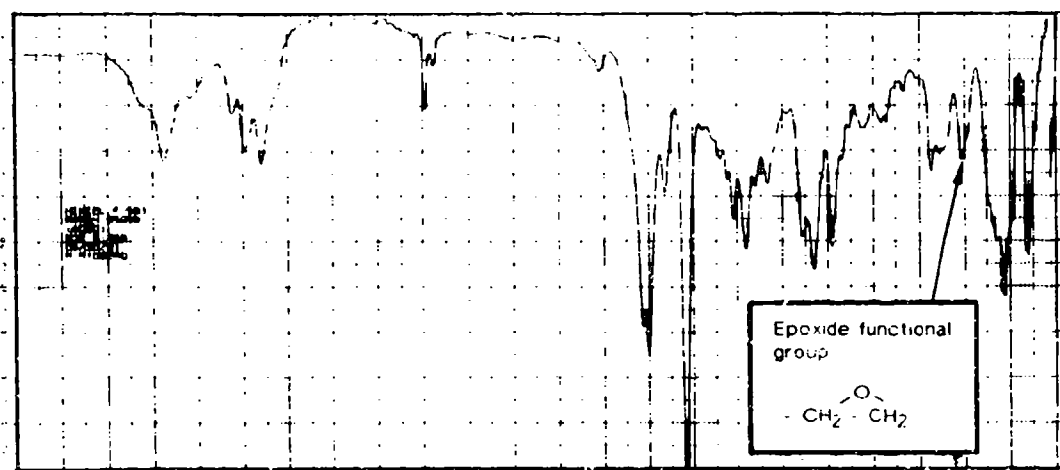


Figure 6-14. Gas Chromatography of DDS, Diaminodiphenyl Sulfone

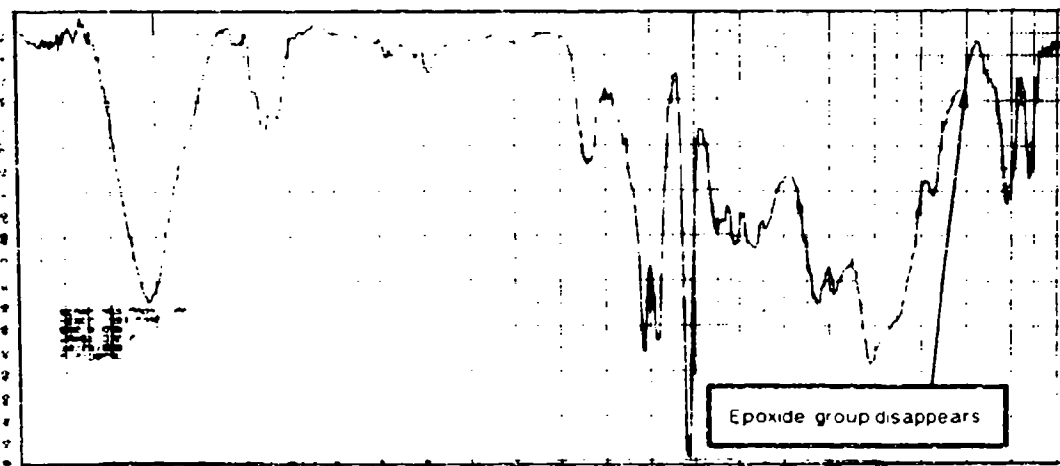
the correct heat treat condition on fractured metal components, a procedure considered routine in metals failure analysis.

As described in the materials characterization FALN contained in the beginning of Section 6, verifying the state of cure of a fractured component normally represents the first stage of materials characterization analysis. There are several reasons for performing such analyses during the initial stages of an investigation. Perhaps the most significant reason is that such analyses can be performed quickly and easily and produce results which may have a significant impact on downstream investigative operations.

In most cases, evaluation of the degree of cure of a failed component is best addressed by a two-stage process. In the first stage, Tg analysis establishes whether a lower than expected degree of cure may exist. These analyses (Paragraph 6.3.1) are generally relatively easy to perform and therefore impose a relatively small impact on the amount of effort necessary to carry-out an investigation. As with evaluating the heat treat of metals, most of the time the appropriate thermal processing has been performed, and similarly for composites, the correct degree of cure will be detected and further analyses will not be necessary. However, if the Tg of the laminate and a subsequent retest of a dried (desiccated) laminate does not match that anticipated for the material used, the second stage analyses (Paragraph 6.3.2) should be performed. This involves determination of the extent of unreacted material — can be performed to evaluate if this anomaly represents a condition of undercure. Here it should be noted that a low Tg may arise both from inadequate processing or resin formulation errors, as well as the accidental use of a wrong material such as a 250°F curing prepreg in place of a 350°F curing



(a) Uncured Resin



(b) Cured Resin

Figure 6-15. IR Comparison of Resin

prepreg. A detailed description of the logical sequence of steps (FALN) involved in assessing the materials' degree of cure was presented at the beginning of Section 6.

6.4.1 Glass Transition Temperature Analysis

The temperature at which an amorphous polymer reversibly changes from a brittle, glassy state to a more flexible, rubbery state is the glass transition temperature. In the case of thermosetting polymers this transition temperature directly reflects the degree of cure achieved by the material. This transition temperature is manifested as a change in slope of the curve obtained by plotting any of the primary thermodynamic properties against temperature. This change in slope falls in the same temperature range as that in which mechanical softening occurs. A variety of techniques exist by which the point of this softening can be determined. The most common are thermal analysis tests such as

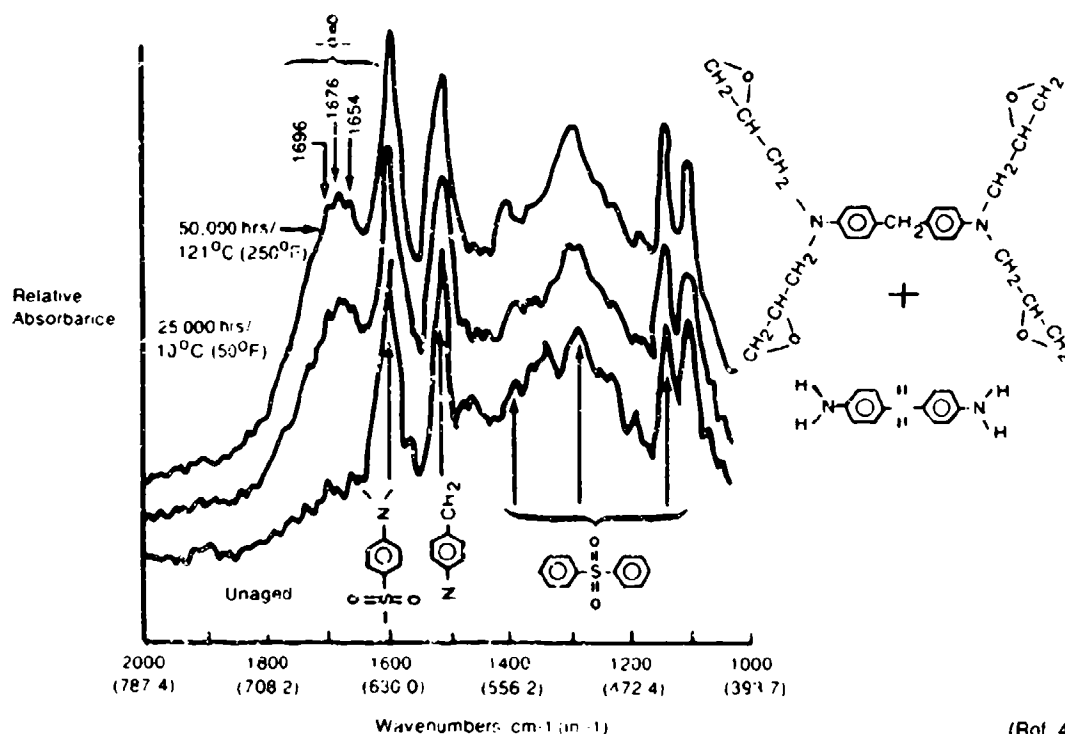


Figure 6-16. DRIFTS of Graphite-Epoxy (AS/3501-5) Composite Before and After Thermal Aging

thermomechanical analysis (TMA) and dynamic mechanical analysis (DMA), and DSC. TMA is the most common technique for failure analysis because of the small sample requirement and the ease of testing and evaluation. DMA and DSC can be used to determine the T_g , but are less attractive due to specimen preparation, performance, and interpretation difficulties. These methods are more appropriately used in failure analyses for determination of the extent of unreacted material and environmental effects, as discussed in the following paragraph.

Thermomechanical Analysis. TMA is designed to measure (with extremely high sensitivity) the relative linear displacement of a quartz probe placed in contact with the sample surface. During controlled heating, a record is generated revealing thermally dependent dimensional changes exhibited by the sample and therefore the materials' glass transition temperature. For this method several variations can be used to support the sample and measure dimensional behavior. Specific methods commonly available on most instruments include:

Penetration. In this mode, a probe is placed on the side of a small rectangular specimen cut from the sample. Typically, a cubic shaped specimen with 0.1 to 0.15 inch for each dimension is used for this technique. This small sample size lowers the concern of thermal lag. The generation of any thermal lag between the temperature of the sample (which is uncontrolled) with that of the surrounding chamber (which is controlled) can affect data accuracy. For most samples, the direction of fiber orientation does not represent a critical parameter in this test since only relative dimensional measurements are being made; however, placement of the probe directly on the carbon fibers

instead of the epoxy resin may interfere with sharp definition of the glass transition. During the test, the specimen is situated as shown in Figure 6-17, heated at a controlled rate, typically 5° to $25^{\circ}\text{C}/\text{minute}$, and the glass transition temperature determined by a pronounced downward movement of the probe indicating matrix softening, Figure 6-18. Typically, several specimens from a part are characterized. The measured T_g can then be averaged to minimize errors due to specimen inhomogeneity on a small scale.

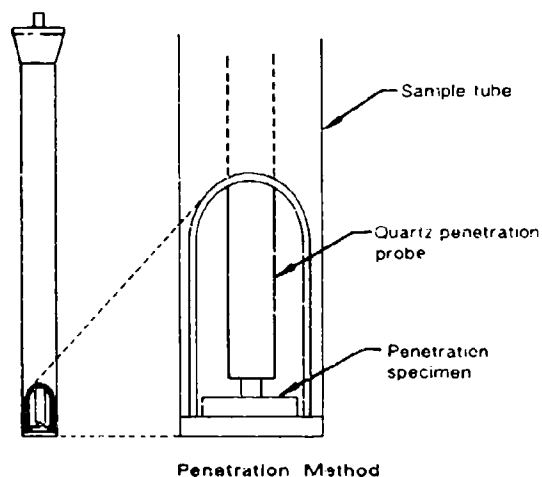


Figure 6-17. Glass Transition Temperature Determination – TMA Penetration Test Setup

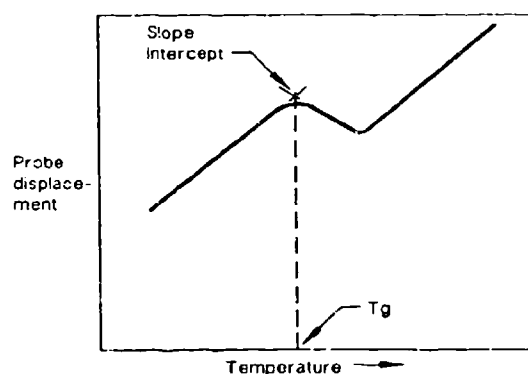


Figure 6-18. Glass Transition Temperature Determination – TMA Penetration Test Measurement

Flexure. In this test mode, a rectangular sample 0.1 inch in width by 0.25 to 0.50 inch in length by 2 to 4 plies in thickness is placed in three point flexural stress within the test chamber as shown in Figure 6-19. With this configuration the probe measures beam deflection as a function of temperature. Again, as the transition temperature is reached the resin softens, the beam (specimen) deflects, and an inflection in the slope of the thermogram being generated occurs. Nominally, the heat-up rate is approximately $20^{\circ}\text{C}/\text{minute}$ with a probe load of 10 grams. A thermogram of a 177°C (350°F) epoxy system is presented in Figure 6-20, showing the tangents to the slope. The T_g is defined as the temperature at which the tangents intercept. Care should also be taken not to remove specimens from the laminate near a surface which has a different chemistry or cure temperature material attached. This includes adhesively bonded regions, potted areas, or surfaces which have had surface prep fabric such as peel-ply.

Expansion. This test is run in much the same manner as penetration, except a larger diameter probe is utilized to prevent penetration into the sample at the point of softening. As the specimen is heated, the resin is free to expand in the transverse or lateral direction. Since a distinct increase in the rate of thermal expansion normally occurs at the glass transition, the thermogram generated by this technique typically provides an additional method by which to determine the materials' glass transition (Figure 6-21). As in the penetration method, placement of the probe directly on carbon fibers may interfere with accurate T_g determination.

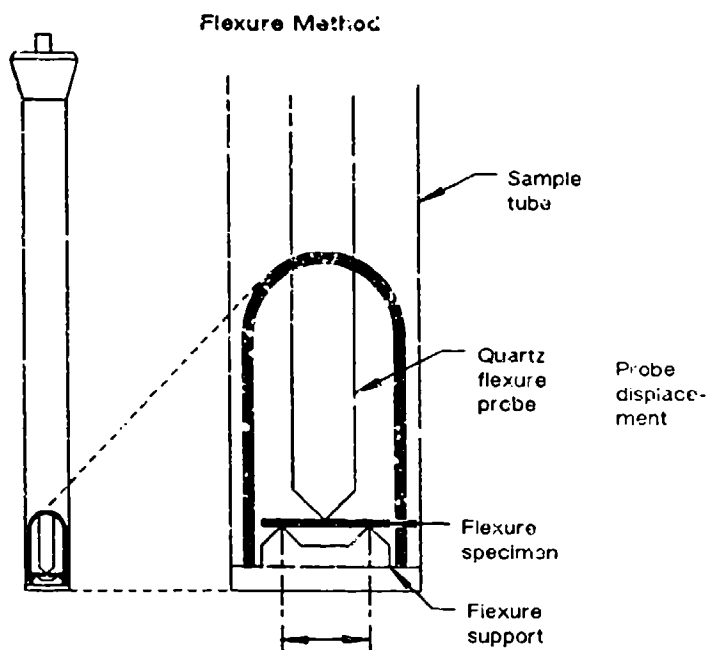


Figure 6-19. Glass Transition Temperature Determination – TMA Flexure Test Setup

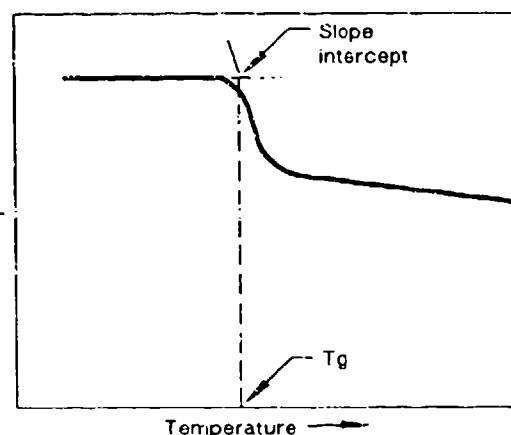


Figure 6-20. Glass Transition Temperature Determination – TMA Flexure Test Measurement

Of the three methods discussed above, the preferred method is the flexural technique. Generally, the flexural test method produces sharper, more distinct inflections and only requires a very small sample. The penetration and expansion methods are used less often because of the interference of the carbon fibers with accurate T_g determination.

Dynamic Mechanical Analysis. High performance epoxy systems used in composite matrices exhibit a viscoelastic response to applied mechanical strains. DMA techniques are a useful means of determining the viscoelastic nature of epoxy matrices. The glass transition temperature can be determined from DMA experiments.

DMA involves the application of a sinusoidally oscillating tensile, torsional, or flexural strain to a sample and measuring the response versus increasing temperature from -150°C to 400°C . Heating rates vary from 1°C per minute to 10°C per minute depending on the sample size. Data are presented in terms of storage modulus (elastic component), loss modulus (viscous component), and tangent delta (ratio of loss modulus to storage modulus) versus test temperature.

Typical DMA data are shown in Figure 6-22. The glass transition temperature can be determined as the peak temperature of the high temperature transition in tangent delta or loss modulus or as the knee of the storage modulus curve.

DMA is typically not used where only glass transition temperature measurement is required. Larger sample sizes and more difficult sample preparation and test methods limit the utility of DMA

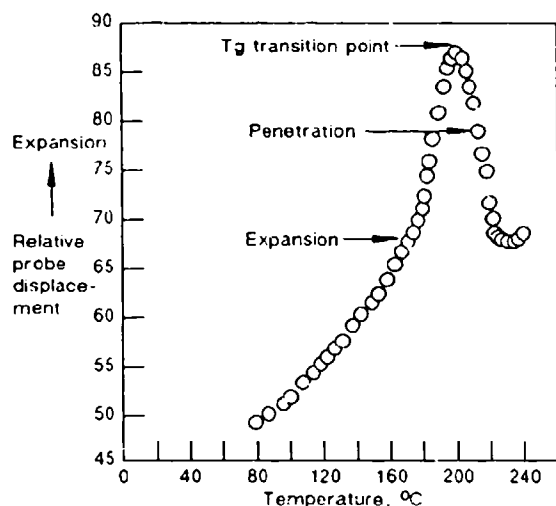


Figure 6-21. Determination of T_g by Expansion Method

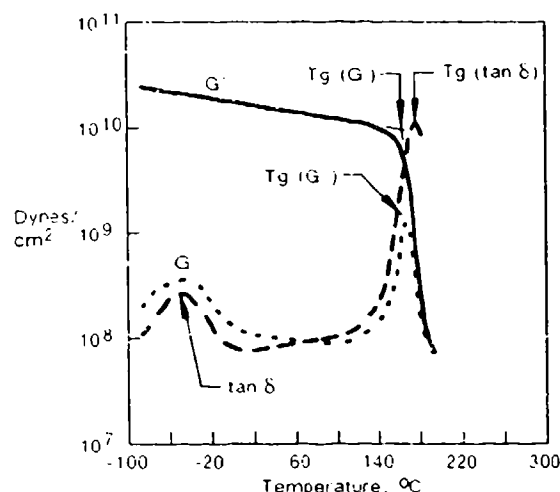


Figure 6-22. Typical DMA Plot for Cured Epoxy Showing Glass Transition Determination

for glass transition measurement. Since carbon fibers tend to diminish the viscoelastic transition magnitudes, samples should be tested in a matrix dominated direction if possible.

Differential Scanning Calorimetry. DSC techniques similar to those described in Paragraph 6.4.1 can be used to determine the glass transition temperature of a cured epoxy composite sample except that sample sizes of approximately 5 mg are tested at approximately 20°C per minute heating rate.

A typical DSC thermogram for a cured epoxy is shown in Figure 6-23. The glass transition will appear as a change in the slope of the DSC thermogram. Determination of glass transition temperature using DSC is sometimes difficult because of the exotherm peaks due to additional reaction during the DSC test.

6.4.2 Extent of Unreacted Material

An undercured condition may be indicated by a lower than expected glass transition temperature determined as described in the beginning of Section 6. However, a low glass transition temperature may also be due to environmental/moisture effects or to formulation errors. To show that the low glass transition temperature is due to undercure it may be necessary to determine the extent of reaction by analysis of the residual unreacted material, as shown in the materials characterization at the beginning of this section. Before testing for extent of reaction, glass transition temperature tests should be rerun on a desiccated laminate to eliminate moisture effects as a cause of low T_g .

The most effective means of determining the extent of unreacted material is by measuring the residual heat of reaction using DSC. This method has the advantage of small sample sizes and fast, simple experimental procedures. DMA can show the effects of both undercure and environmental exposure, although the larger sample size and difficult data analysis discourage widespread usage.

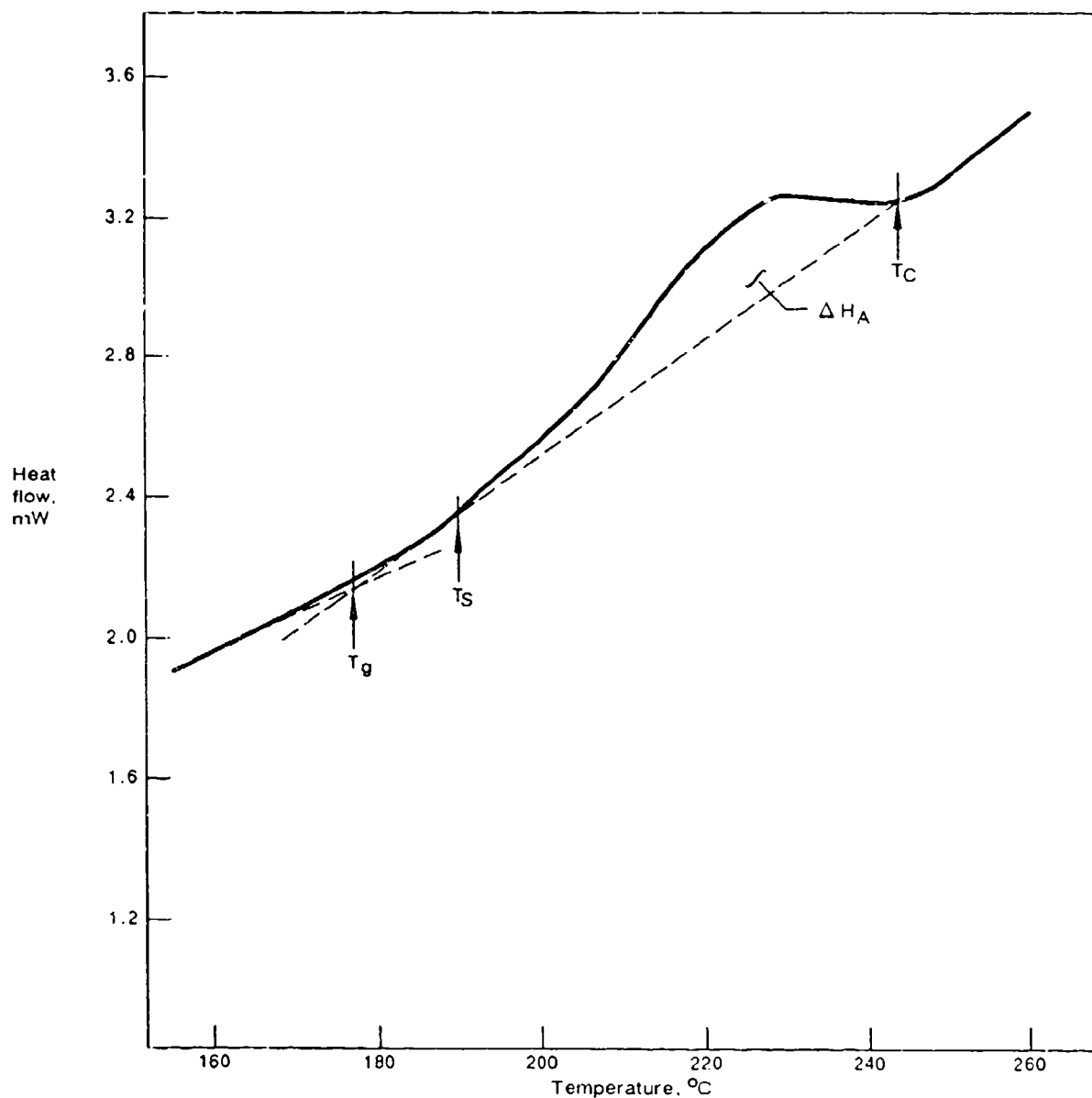


Figure 6-23. Typical DSC Plot for Cured Epoxy Illustrating Determination of T_g and Heat of Additional Reaction

Solvent extraction, with or without subsequent analysis using IR spectroscopy, may also be used to indicate extent of unreacted material. Excessive handling and analysis difficulty discourage these techniques.

Differential Scanning Calorimetry. DSC can be used to measure the heat of residual reaction in a partially cured epoxy matrix. Experimental procedures as described at the beginning of Section 6 are used on cured laminates. The heat of residual reaction is the area between the DSC thermogram and a baseline drawn from the reaction onset temperature, T_s , to the reaction completion temperature, T_c , as shown in Figure 6-23. The presence of measurable heat of residual reaction indicates some undercure.

The extent of unreacted material can be calculated by dividing the heat of residual reaction by the total heat of reaction of the prepreg.

Dynamic Mechanical Analysis. DMA can be used to detect undercure and moisture degradation of cured laminates. Experimental procedures as described earlier are used. An undercured laminate will exhibit a double high temperature peak in tangent delta and loss modulus plus an initial loss with subsequent recovery of storage modulus as shown in Figure 6-24. The initial softening (increase in tangent delta, loss modulus; decrease in storage modulus) is attributed to the glass transition temperature of the original undercured material. As the test temperature increases, the matrix undergoes further cure allowing a recovery of properties. The final softening is due to the glass transition temperature of the fully cured material. Laminates with absorbed moisture exhibit a peak in tangent delta and loss modulus at approximately 100°C due to the increased activity of moisture at this temperature. The presence of this peak indicates significant absorbed moisture in the laminate.

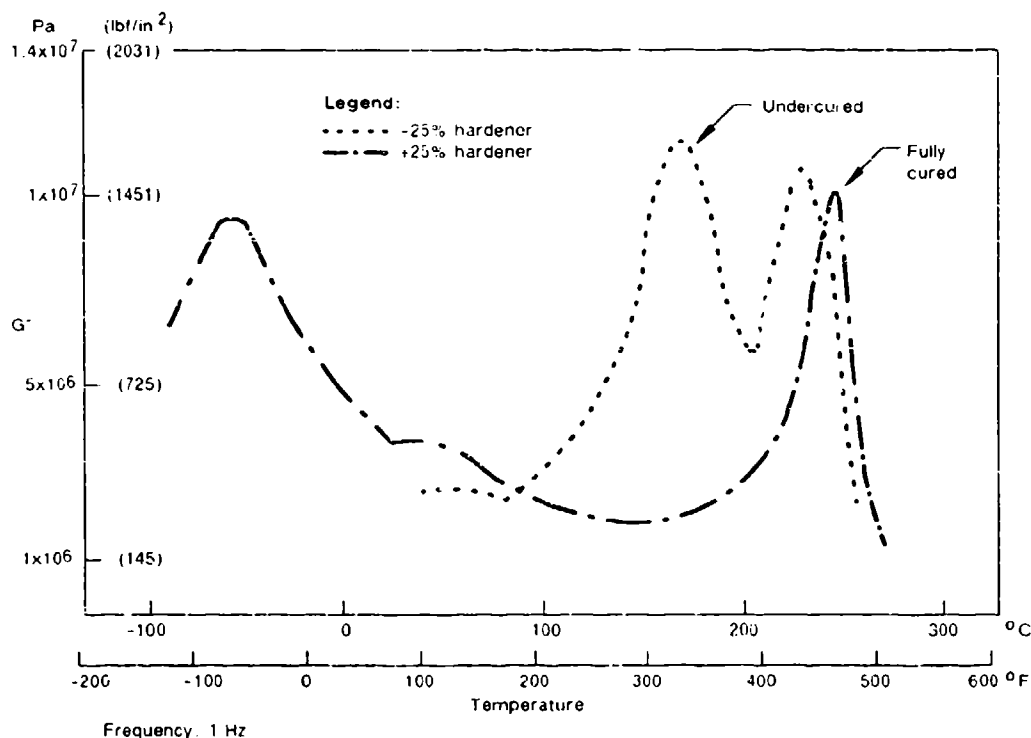


Figure 6-24. DMA Loss Modulus Versus Temperature Showing Effect of Undercure for Epoxy Resin

Solvent Extraction/Infrared Spectroscopy. This method can be used to remove low molecular weight (uncured or partially cured) polymer from the surrounding cured matrix. A solvent such as dimethyl acetamide (DMAc) or reagent grade acetone may be used to extract the uncured segments from a thin sample laminate. By weighing a solvent extracted and desiccated (moisture free) sample, the percent of unreacted material can be calculated. The extracted sample can be analyzed using IR spectroscopy. The test procedure is identical to that described in Paragraph 3.1. The unreacted functional groups can be identified by the peaks in the IR spectra. The extent of reaction can be determined from the peak intensities by comparison to standard prepreg spectra.

6.5 CURED MATERIAL CONTAMINATION ANALYSIS

Cured composites may contain defects due to contamination during manufacturing and assembly of composites structures. Foreign material contamination present in the cured composite is readily identified by an array of traditional chemical analysis tools. This paragraph addresses the methods for selecting the technique and interpreting the data. Emphasis is also placed on showing how the contaminant affects the fracture morphology and the ultimate integrity of the failed component.

The essence of a successful material contamination analysis is: (1) recognizing the anomalous fracture morphology, (2) exactly documenting and interpreting the anomalous features, (3) chemically identifying the material contamination, (4) establishing that the detected contamination is not an artifact of specimen handling or post-failure inservice exposures, (5) identifying possible sources of contamination, and (6) evaluating the criticality of the contaminant as related to crack growth and initiation.

Foreign material defects lead to lower crack propagation energies and a corresponding typical fracture morphology. Contamination analysis is initiated when anomalous crack propagation or foreign material inclusions are detected on the fracture surface during the course of the FALN execution. While performing optical microscopy or scanning electron microscopy (SEM) examination of the fracture surfaces, the specific fracture morphology allows the analyst to classify the contamination as either a particulate or weak boundary layer contamination. This step is crucial to selecting the steps needed to chemically identify the contamination and to relate the analysis to the overall failure analysis and location of the origin. It is also crucial to be able to recognize artifacts created by sample preparation or due to post-failure exposure to contamination sources. The following definitions will serve to classify contamination types.

6.5.1 Particulate Contamination

In this case, inhomogeneous resin fracture will be observed with inclusion particles on the fracture plane with the optical or electron microscope. The particulate significantly reduces the net cross-sectional load bearing area leading to lowered properties such as reduced interlaminar shear and tensile strength. Although composites with their fiber reinforced construction are less sensitive to small localized defects, large particulates have been found to initiate failure. An individual particle defect, if located at a critical location, may also act as a crack initiation site with corresponding fracture lines radiating from the defect.

6.5.2 Weak Boundary Contamination

The presence of weak boundary surfaces account for the majority of crack initiation and subsequent component failures due to contamination. The weak boundary layer acts as a barrier to adhesive bonding between:

1. Adjacent plies
2. Dissimilar materials or microconstituents such as fiber and resin or honeycomb core and laminate
3. Adhesively bonded subcomponents such as stringers and skin.

The weak boundary layer is formed by a chemical compound which interferes with the wetting and adhesion mechanism between the epoxy adhesive layers. Interfering chemicals such as hydrocarbons, fluorocarbons, and silicones are common in composite manufacturing as mold release compounds and parting agents. During the fracture event, the weak boundary layer provides a low energy crack propagation pathway through the structure. The fracture surfaces exhibit localized regions of smooth and featureless mating fracture surfaces, as opposed to normal fractures, where there is significant resin microflow deformation, hackle formation, and secondary cracking. When stress analysis has indicated that a composite structure failed at a fraction of the design limit strength, and delaminations are present, weak boundary contamination layers should be suspected.

As illustrated in Figures 6-25, 6-26, and 6-27, contamination caused by Teflon paddle and Frekote release agent along the interlaminar ply interface exhibit inhomogeneous resin fracture as compared to a typical uncontaminated baseline fracture specimen illustrated in Figure 6-28. A second example of an isolated foreign particle inclusion, in Figure 6-29, illustrates the distinctive fracture surface asperity and crack initiation lines radiating from the particle. However, isolated particles will not significantly degrade the structural integrity of the composite because the fibers already act as primary sites of crack initiation. As a result, low delamination strengths are expected and incorporated into the designs. Particulate contamination along these directions can be tolerated in moderate amounts without significantly affecting the performance.

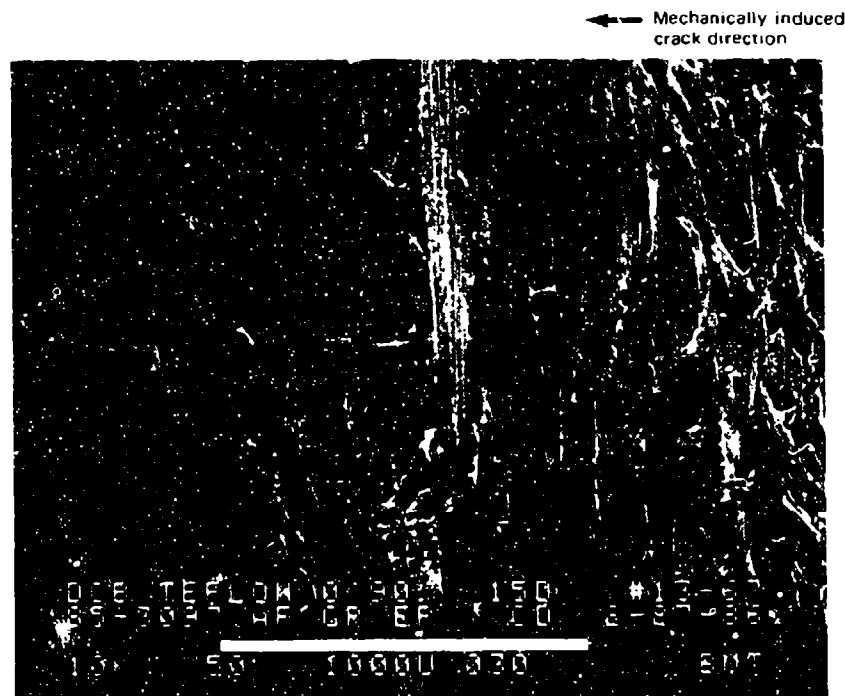


Figure 6-25. SEM Micrograph of a Teflon-Contaminated Tension Specimen

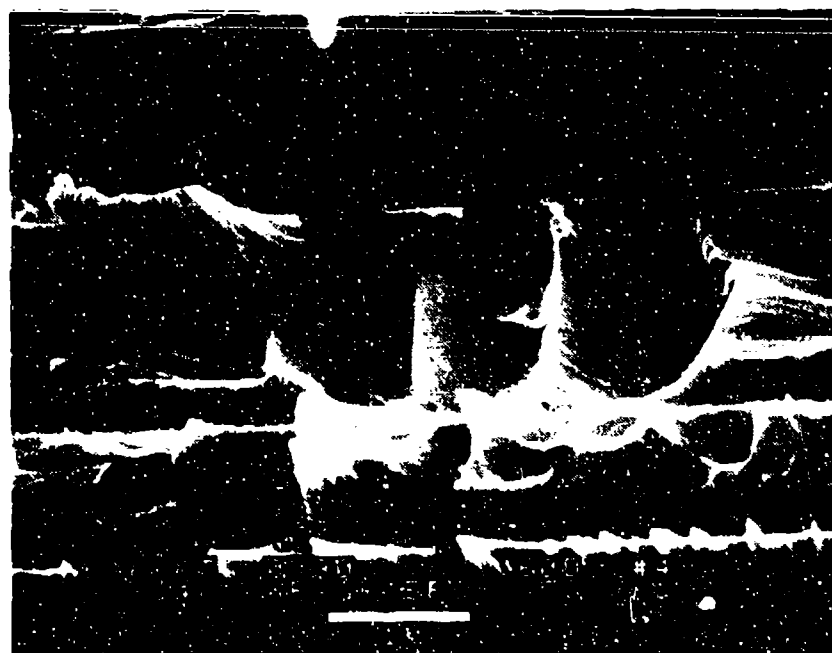
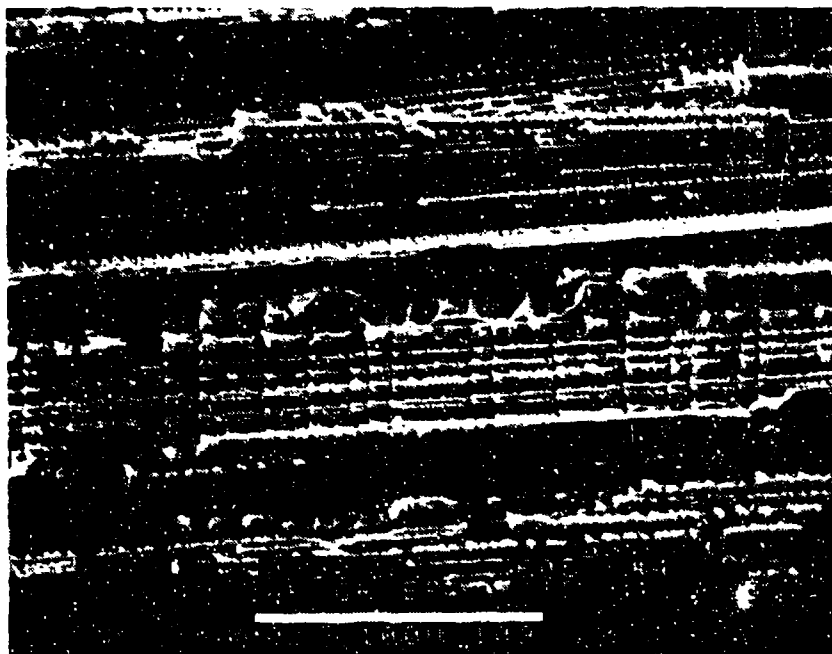


Figure 6-28. SEM Micrographs of a Typical Uncontaminated Fracture Specimen

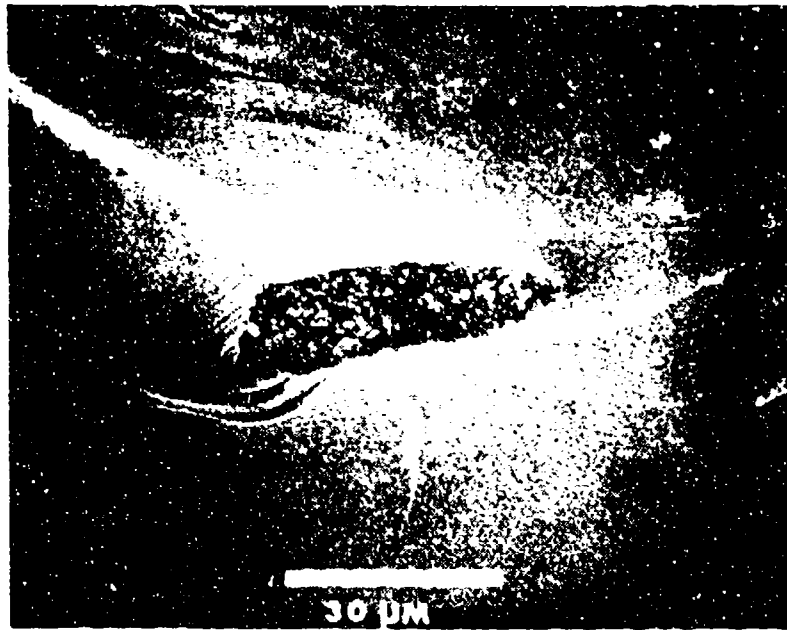


Figure 6-29. SEM Micrographs of Foreign Particle Inclusions illustrating the Characteristic Fracture Surface Asperity and Radiating Fracture Lines

Special care must be taken to avoid confusing the post-failure surface debris on the fracture surface with foreign particle inclusions in the resin. By definition, the surface debris will not initiate radiating fracture lines. This is especially a problem where the fracture surface has had a long environmental exposure or has experienced in-service cyclic loading conditions. Caution should also be exercised when extensive mechanical cutting was required to extract the specimen from the failed component. Often the particle shape can lead to identification of the contamination source where the particulate contains fractured carbon fibers and the source could be traced to machining debris. Another concern in examining a resin system with particles on the fracture surface is that the resin may have intentional particle additions (or phases) which improve properties or manufacturing characteristics. If there is a suspicion that the resin system may have been modified in this way, the analyst must prepare a lab fractured specimen for SEM examination as a reference fracture surface.

The flow diagram in Figure 6-30 reviews the sequence of steps taken to perform initial inspections and to classify the contamination type. The next sequence of steps involve selection of the appropriate analytical techniques to make an accurate chemical identification of the contaminant. Direct chemical analysis probes can be very decisive in providing a chemical identification in a cost efficient manner. The flow diagram in Figure 6-31 for analytical work reflects this emphasis. A number of analytical techniques are recommended in order of decreasing information per unit analysis time for each application. There are specialists for each analytical technique whose expertise in instrumentation and spectroscopy will be required. The following paragraphs on analytical techniques are designed to inform the investigator of the special terminology used for these techniques and highlight special concerns which arise during a composite failure analysis. The section concludes with an applied example of contamination analysis during a failure analysis.

6.5.3 Scanning Electron Microscopy and Electron Microprobe Analysis

The scanning electron microscope and the electron probe microanalyzer (EPMA), commonly known as the electron microprobe, are powerful tools for identification of contaminant particles on a fracture surface. This paragraph covers the elemental detection capabilities of the SEM and EPMA for foreign particle detection. The microscopic image formation is covered in this section. These instruments are used when a quick qualitative identification is needed and provides information regarding selection of more detailed methods to be performed later.

The SEM and EPMA instruments are equipped with X-ray detectors to monitor the X-ray emission spectrum generated when a finely focused electron beam impinges on a microscopic feature of interest. Electron beam induced X-ray emission produces a spectrum unique to each element present allowing direct determination of particle composition. The analysis volume is determined by the electron beam energy and the density of the specimen surface. Typically, the analysis volume is 0.5 to 2 micrometers in diameter. If the X-rays are measured with an energy detector, then the analysis is termed energy dispersive spectroscopy (EDS). If the X-rays are measured with a wavelength detector, then the process is termed wavelength dispersive spectroscopy (WDS). Each method has its own unique advantages. Conventional EDS can acquire a spectrum for all the elements from sodium to uranium simultaneously in 30 seconds to a minute. (Ultrathin window EDS detectors can detect elements to the boron range.) Because of the limited energy resolution of the EDS detector, there are a number of spectral peak overlaps. For example, aluminum and bromine peaks occur at 1.48 KeV. WDS has

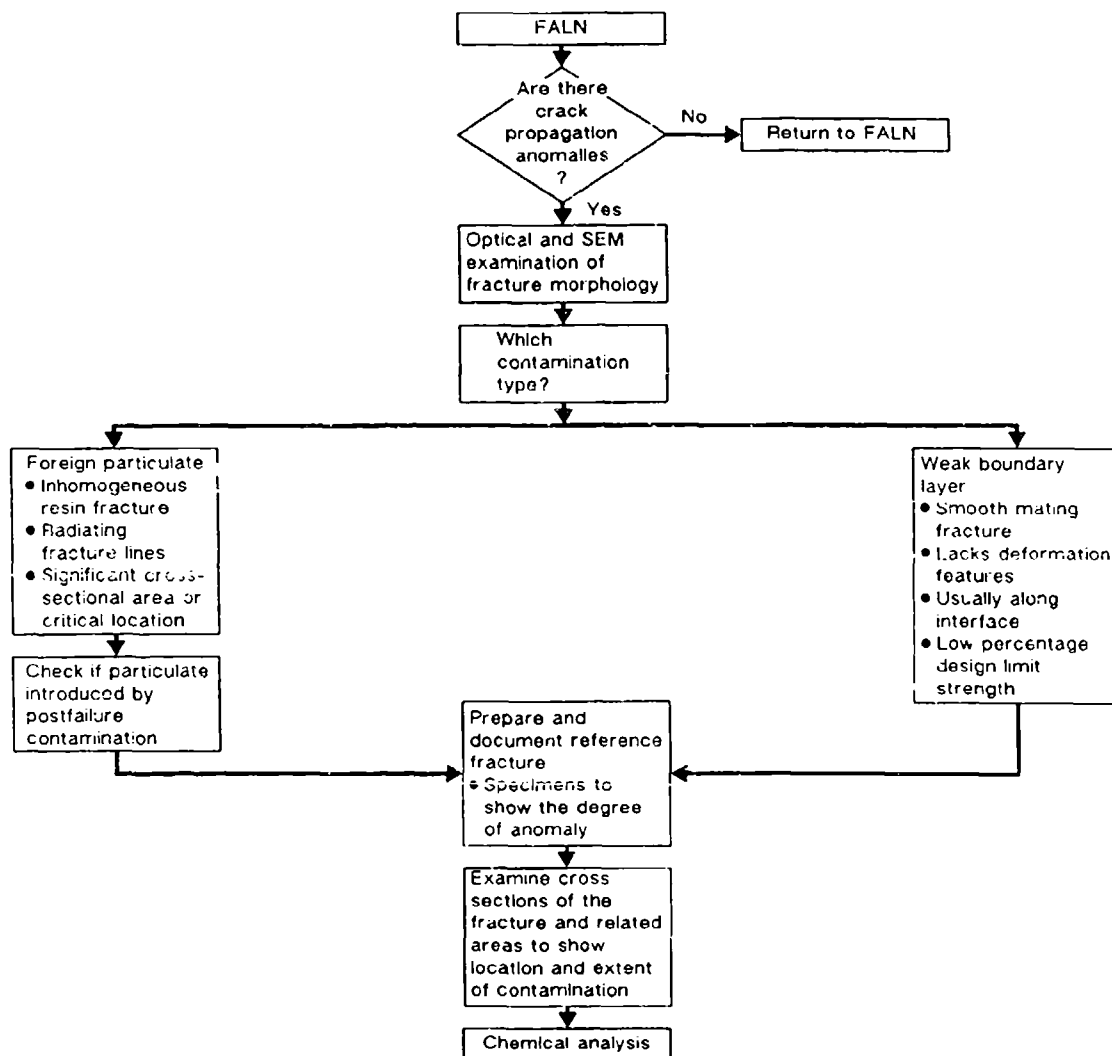


Figure 6-30. Initial Inspection and Determination of a Foreign Material Contamination

extremely high signal-to-noise sensitivity and resolution. WDS can also detect boron, carbon, oxygen, and fluorine. The disadvantages are that only a single wavelength at a time can be detected, requiring many minutes to scan even a limited range of elements. Of concern to composites failure analysis is the ability to use WDS for light element detection. A partial list to assist the analyst in identifying elements by EDS and WDS is given in Table 6-2. A SEM micrograph and EDS spectrum of talc contamination at a bondline is shown in Figure 6-32. The SEM reveals the sheet-like crystalline morphology and the EDS spectrum exhibits the primary elements typical of talc powders, magnesium, and silicon, along with other particulate impurities.

In using EDS or WDS several concerns should be mentioned. First, the composite specimen is introduced into an instrument vacuum chamber at pressure ranging from 1×10^{-8} torr to 1×10^{-4} torr. If the contaminant under investigation is volatile in the instrument vacuum chamber, there is a possibility that important elemental information will be lost before analysis. Second, these techniques were originally developed as techniques to study conducting metal specimens. Polymers which are

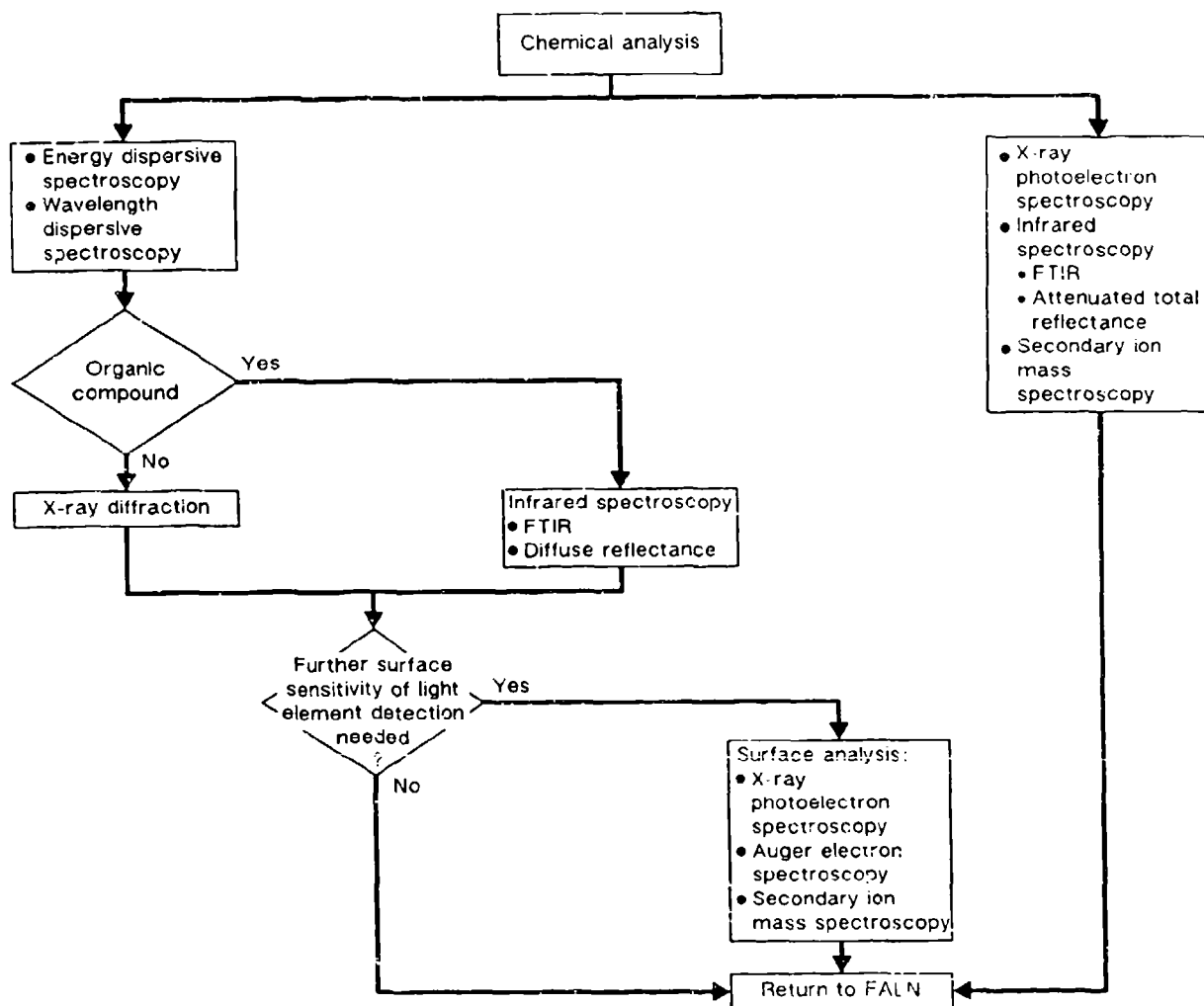


Figure 6-31. Logic Network for Chemical Analysis of Foreign Material Contamination of a Composite Fracture Surface

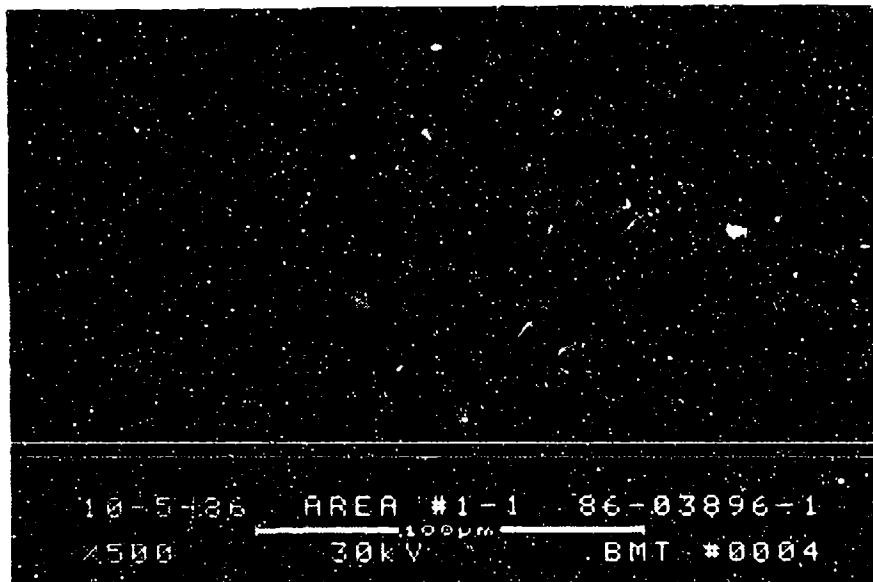
nonconductive present a specimen charge buildup problem which is reduced by vapor depositing a conductive coating on the specimen. Typically, a very thin 5 nanometer film of gold or other noble metal alloy is used. These films provide interfering peaks in the X-ray spectrum which may mask elements of interest. When analyzing composite contamination, it is sometimes useful to coat these surfaces with conductive carbon since carbon is to be expected and will not be detected in the EDS spectrum. There is a significant literature base to suggest the electron beam can induce degradation and thermal effects to polymers. The degradation can be minimized by using low electron beam accelerating voltages and low current densities. Since WDS usually requires very high beam currents, this detection method should be used as quickly as possible to reduce the detrimental beam damage effects.

Table 6-2. X-Ray Emission Lines, Partial Listing

WDS	X-ray wavelengths (K_{α}), nm	EDS	X-ray energies, keV	
			$K_{\alpha 1}$	K_{β}
B	6.76	Na	1.04	1.07
C	4.47	Mg	1.25	1.30
N	3.16	Al	1.49	1.56
O	2.36	Si	1.74	1.84
F	1.83	P	2.01	2.13
		S	2.31	2.46
		Cl	2.62	2.81

(Ref. 5)

(A)



(B)

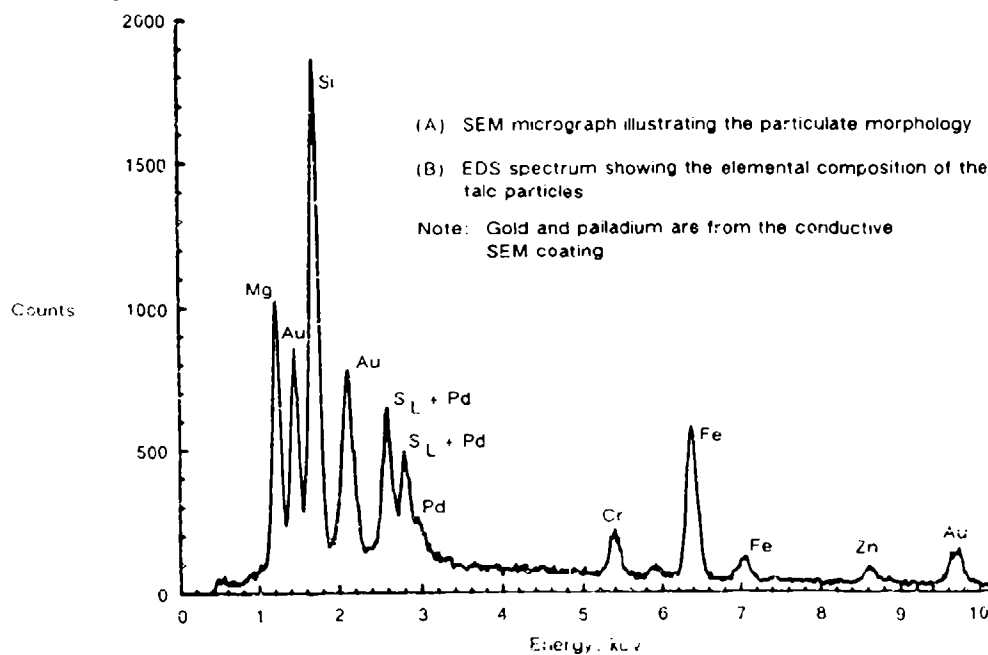


Figure 6-32. Talc Powder Contamination Along a Bond Line

6.5.4 X-Ray Photoelectron Spectroscopy

X-ray photoelectron spectroscopy (XPS) is based on electron emission when a sample is irradiated with low energy X-rays. The process called photoelectron emission causes each element to emit photoelectrons at specific energies. All elements except hydrogen and helium can be detected by this method. Typical instruments analyze a square centimeter of surface area. The latest generation of instruments has a small spot XPS capability to analyze areas 100 micrometers in diameter. This development in XPS will make it increasingly important to the failure analyst. Several unique features arise from the physics of this process. The surface sensitivity of XPS arises from the very short distance that a low energy electron can travel in a solid without losing its initial energy. Since the detected electrons must travel to the detector without losing energy, detected electrons can only originate within this short characteristic distance (called the escape depth) from the surface. Typical escape depths in organic solids are 5 nanometers.

The XPS spectrum is expressed as the detected electron number versus electron energy. The measured kinetic energy (*KE*) relationship to binding energy (*BE*) of the electron from the parent atom is expressed as:

$$BE = h\nu - KE - \phi - V \text{ charge} \quad (\text{Eq. 1})$$

where:

$h\nu$ = energy of X-ray source

ϕ = spectrometer work function

$V \text{ charge}$ = correction due to specimen charging

The binding energies of some typically encountered elements are listed in Table 6-3. Figure 6-33 is a typical spectrum of an epoxy resin where the elements carbon, nitrogen, oxygen, and sulfur are shown. If one is examining a fracture surface for a chemical contaminant, comparison of the surface relative to a fresh cohesive resin fracture surface will provide a very sensitive test for the presence of foreign elements indicative of contamination.

The details of XPS quantitation are unique to each instrument depending on design and detection efficiency. In Table 6-3, the relative probabilities for photoelectron emission, called cross-sections, are given. These factors would need to be adjusted for detection efficiency to obtain the relative sensitivity factor. Quantitation is accomplished by normalizing the observed intensities for each element and is expressed as:

$$\text{Element} \times \text{atom\%} = \frac{I_x/S_x \times 100}{\sum_i I_i/S_i} \quad (\text{Eq. 2})$$

where:

S = relative sensitivity factor

I_x = observed intensities

x = each element

Table 6-3. Approximate XPS Peak Positions and Emission Probabilities for Common Elements

Element	Binding* energy	Relative emission probability (cross section for aluminum X-rays) (Ref. 4)
Boron	195	0.49
Carbon	285	1.00
Nitrogen	399	1.80
Oxygen	531	2.93
Fluorine	689	4.43
Sodium	1072	8.52
Silicon	102	0.82
	151	0.96
Phosphorus	135	1.19
	189	1.18
Sulfur	165	1.68
	229	1.43
Chlorine	199	2.29
	264	1.69
Bromine	69	2.34

*Laminating energies change depending on how the elements are chemically bonded.

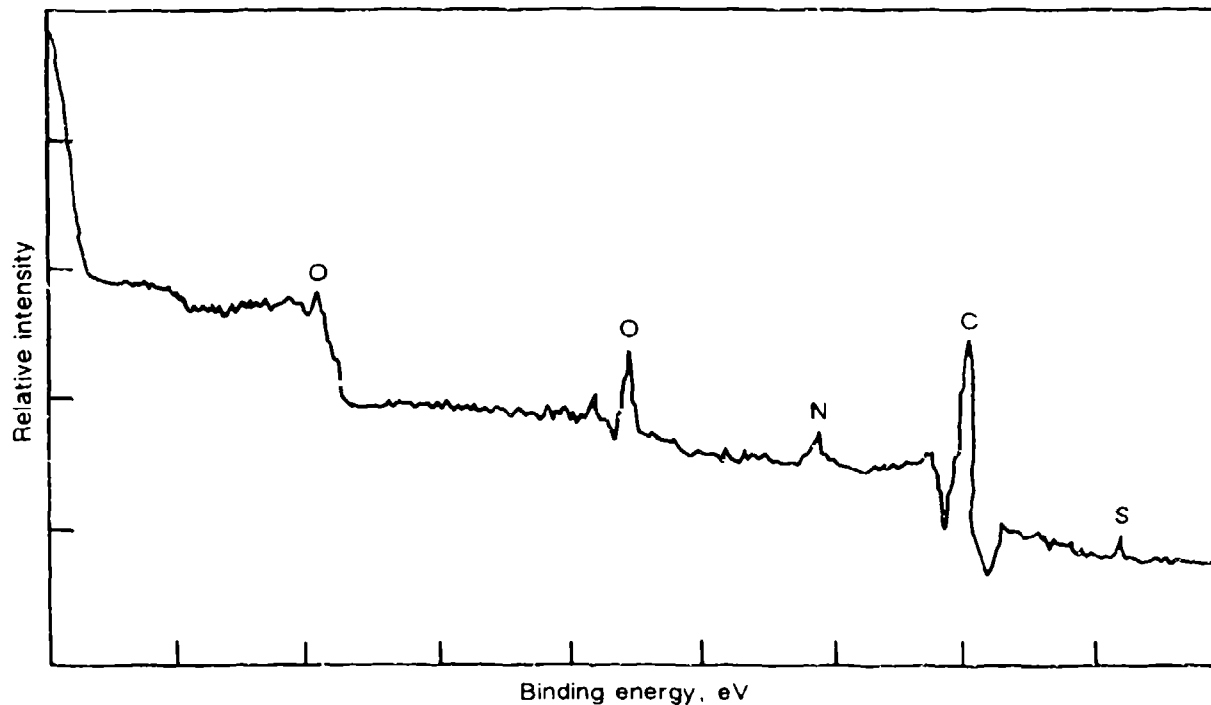


Figure 6-33. Typical XPS Spectrum of an Epoxy Resin With Elements Identified

The binding energy concept is important because XPS peaks exhibit small binding energy shifts due to the chemical bonding environment of the parent atom. Chemical functional groups on the surface can be inferred from these binding energy shifts. Inspection of the equation also shows that the binding energy is dependent on the work function constant which is a spectrometer calibration constant and the specimen charge correction factor which is determined for each non-conductive specimen (the usual case for composite specimens). A charge correction can be made by shifting the binding energies so that the carbon 1s peak due to the hydrocarbon-like chemical bond present in polymer resins occurs at 285.0 eV. Some investigators use alternate charge correction methods or a slightly different carbon 1s peak correction value (284.6 eV). So when making comparisons to published literature values, the author has to be careful. Table 6-4 gives a partial list of the carbon 1s peak shifts which might be encountered with composite materials.

Table 6-4. Carbon Peak Shifts in XPS

Functional group	Binding energy, eV
Hydrocarbon	285.0
Ether or alcohol	286.5
Ketone	288.0
Ester	288.8

(Ref. 6)

When analyzing a composite fracture surface for foreign material contaminants, low surface energy compounds or releasing agents are high on the list of potential contaminants. These compounds are typically hydrocarbon oils, fluorocarbons, or organic silicone oils. Table 6-5 summarizes a few rules of thumb in interpreting the XPS data for these compounds. Some materials which could be contamination sources are as follows:

1. Molding tool release compounds and sprays
2. Parting films and breather fabrics
3. Prepreg backing papers and films
4. Solvent impurity residues
5. Vacuum pump oils
6. Machining debris
7. Plastic resin sweeps
8. Gloves
9. Vacuum bags
10. Molding compounds, vacuum bag sealants.

6.5.5 Infrared Spectroscopy and Fourier Transform Infrared

IR spectroscopy is the primary technique for identifying the compound or chemical family in which a foreign organic contaminant belongs. Infrared spectroscopy is much less sensitive than XPS or EDS/WDS but provides more chemical information. Special techniques have been developed to apply IR

Table 6-5. Rules of Thumb for XPS Identification of Typical Release Agents

• Hydrocarbon	<ul style="list-style-type: none"> • Excessively high carbon levels on the surface compared with a cohesive resin fracture • Confirm by FTIR analysis of the residue from a solvent rinse of the fracture surface
• Fluorocarbon	<ul style="list-style-type: none"> • Carbon-shifted peak in the range 288.0 to 292.0 eV; fluorine peak at 689.0 eV • Ascertain whether there is a fluorocarbon additive to the resin • Compare with XPS spectrum of known fluorocarbon release agents or parting films used in manufacturing the part
• Silicone	<ul style="list-style-type: none"> • Silicon peak at 102.0 eV; silicon Auger parameter in the range 1708.5 to 1709.5 eV • Where there are significant silicon levels, the carbon-to-oxygen ratio will exceed the resin value • Because some inorganic minerals exhibit the same XPS shifts, verify that there are no inorganic mineral particulates on the fracture surface with SEM/EDS • Ascertain whether there is a silicon additive to the resin • Confirm by FTIR analysis of the residue from a solvent rinse of the fracture surface • Compare with XPS spectrum of known silicon release agents used in manufacturing the component

to the weak boundary layer and the particulate contamination problem. These methods are addressed in the following discussion.

Organic polymer molecules absorb infrared radiation at frequencies which relate to the chemical bonds within the molecule. The physics of this process can be attributed to a mechanism where the infrared light is absorbed at discrete frequencies associated with characteristic molecular vibrations within the molecule. This principle forms the basis of infrared spectroscopy as an analytical technique to characterize polymer resins. Each polymer molecule absorbs infrared light in a distinctive pattern which can be used to fingerprint the molecule. Figure 6-34 illustrates a typical IR spectrum of an epoxy spectrum. In a contamination analysis where one is investigating an unknown identification, it is useful to compare the spectrum of the unknown with infrared spectra of model compounds published in an atlas or stored in a database. Infrared spectra are usually plotted as intensity versus wavenumber (CM⁻¹), wavelength (micrometers or microns), or frequency (s⁻¹).

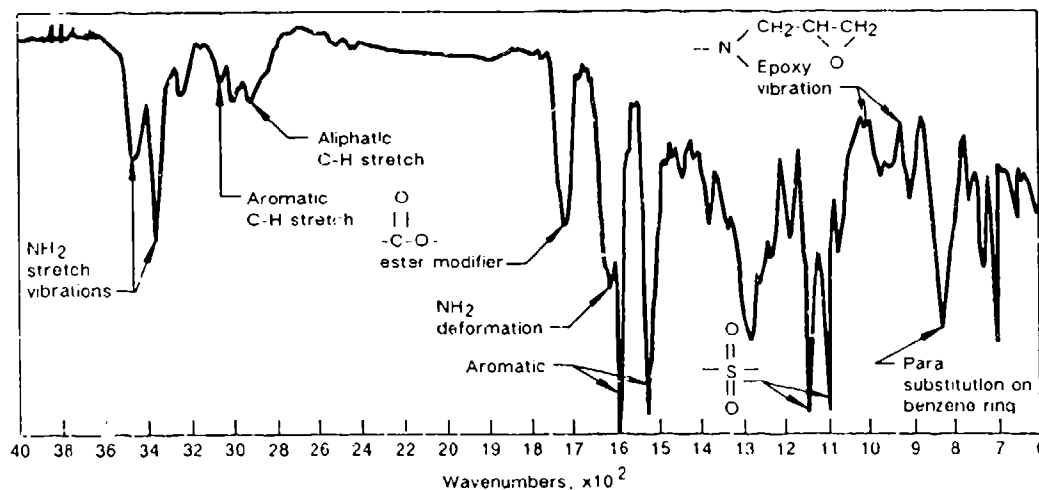


Figure 6-34. Infrared Spectrum of an Epoxy Resin

Intensity can be expressed as percent transmittance or absorbance as shown in the following equations.

Percent Transmittance

$$\%T = \frac{I}{I_o} \quad (\text{Eq. 3})$$

where:

%T = percent transmittance

I = selected radiation

I_o = incident radiation

Absorbance

$$A = \text{Log}(I/I_o) \quad (\text{Eq. 4})$$

where:

A = absorbance

I = detected radiation

I_o = incident radiation

Recently, several developments in the field of IR analysis have allowed the technique to become more practical for solid materials involved with composite failure analysis and contamination analysis. The first development is the use of FTIR instruments. It is orders of magnitude greater in sensitivity than conventional IR instruments. It is almost a necessity to select the FTIR instrument for sensitive contamination detection. The FTIR sensitivity can be used to complement the XPS in weak boundary layer identification. The analysis can be approached from several directions. First, a fracture surface can be rinsed with an ultrapure solvent, such as methylene chloride, which is allowed to evaporate on a salt pellet (the standard specimen holder). The residue can then be analyzed as in conventional FTIR transmittance analysis. Often there is enough material on a contaminated surface to be detected and the increased chemical information increases the reliability of the contamination source identification. If a large amount of particulate contamination can be isolated, then particles can be dispersed into a salt and then consolidated into a pellet. Often a reasonable spectrum can be obtained.

Reflectance methods are desirable in order to avoid the use of removal methods described above. The attenuated total reflectance (ATR) method is implemented on an FTIR instrument which uses an infrared transparent crystal with a high refractive index. The IR radiation is then caused to propagate through the crystal and the near surface region of a specimen. The depth of penetration is typically 0.5 to 2 micrometers. The method has a limited application to fracture surfaces since it requires a fairly smooth and flat surface to obtain a spectrum. Diffuse reflectance, an older reflectance method, is coming back into use on the FTIR instruments. This method relies on the detection of scattered IR radiation directly from a solid surface. The technique has seen limited application for analysis of rough surfaces which are usually encountered in composite fractures.

6.5.6 X-Ray Diffraction

X-ray diffraction (XRD) techniques are used for a wide variety of crystal structure determinations. In composite failure analysis, XRD is primarily used for crystalline foreign material particulates which can be isolated from a fracture surface. The cylindrical Debye-Scherrer or Gandolfi camera is commonly employed for crystal phases in identification of particles. The basis for X-ray diffraction is given by Braggs law:

$$\lambda = 2d \sin \theta \quad (\text{Eq. 5})$$

where:

λ = wavelength of incident X-ray beam

θ = measured angle of diffracted beam

d = crystal lattice spacing

X-rays diffracted from a particle strike a film from which the diffraction angle theta is measured and consequently the crystal lattice spacing is determined. A tabulated index of lattice planes (Reference 6) can be searched for compound identification.

6.5.7 Secondary Ion Mass Spectroscopy

Secondary ion mass spectroscopy (SIMS) can be used to obtain several information levels about the surface and near surface region of a solid material. SIMS is used in composite failure analysis of weak boundary layers when XPS cannot provide sufficient sensitivity or chemical information. SIMS is based on energetic ion beam impact (or sputtering) on a surface with subsequent ionization and removal of the surface atoms. The ejected surface ions are then detected with a mass spectrometer. The plotted spectrum of intensity versus atomic mass units (amu) can be interpreted to identify the elements or molecular fragments of the parent molecule. A number of SIMS instruments exist to perform specific functions, the simplest of which (often the most frequently encountered) requires very high sputter removal rates to provide sufficient secondary ions to the detector. These instruments operating in the dynamic SIMS mode can be used for detecting extremely low levels of elements as a function of depth into the surface. Due to the very high current densities involved, this method does not work well on nonconducting composite surfaces due to specimen charging. Static SIMS applications use very low sputter removal rates to characterize the surface molecular layer. Future improvements in this method to allow routine polymer characterization may find significant uses to complement XPS analysis of composites. The SIMS microprobe, a variation of the static SIMS instrument, has an imaging capability which can be used to characterize particulates and map chemical inhomogeneities across the surface.

6.5.8 Auger Electron Spectroscopy

Auger electron spectroscopy (AES) is a surface analysis technique based on electron beam induced Auger electron emission, characteristic energy for each element, and escape from the surface in a manner analogous to XPS. In fact, many surface analysis instruments are designed to perform AES and XPS with the same spectrometer. Since AES requires a conducting specimen, its applications are

limited in composite analysis. However, since the carbon fibers are conductive, AES can be useful in determining whether an exposed carbon fiber failed at the fiber matrix interface or in the resin. The analysis is based on the elemental differences between the fiber and the surrounding resin (which may be a sizing resin different from the nominal epoxy resin composition) as shown in Figure 6-35. Usually preparation methods are required to provide a conductive path from the fiber to the sample holder.

6.5.9 Contamination Analysis Example

A secondarily bonded composite structure was returned from service after visual inspection revealed surface cracks on the outer painted skin surface. The composite construction had a laminated skin bonded to a honeycomb core. The bonding adhesive was a FM-300 adhesive. When the composite part was sectioned, it was noted that the paint cracking resulted from the skin buckling away from the honeycomb. An optical cross section is shown in Figure 6-36. Optical microscopic examination revealed the FM-300 adhesive separated along the centerline of the adhesive layer. SEM micrographs of mating separation surfaces are shown in Figure 6-37. The smooth surfaces lack any significant evidence of fracture features or resin deformation, indicating that a low energy adhesive failure had occurred. The adhesively separated surface followed the contoured boundary between two plies of adhesive. The mating surfaces are perfect replicas of each other. Even the protruding scrim fibers of one ply made an impression on the other ply without showing any evidence of bonding.

The XPS spectra of the debonded surfaces shown in Figure 6-38 revealed a significant amount of silicon, fluorine, and carbon in addition to the expected composition of the adhesive. XPS peak shifts indicate the presence of silicone, fluorocarbon, and hydrocarbon chemical functional groups. The next step was to rinse the fracture surfaces with methylene chloride solvent and allow the soluble residues from the surfaces to precipitate on a salt pellet. The residue was then analyzed with the FTIR where hydrocarbon oils were identified in the spectrum. It was important to remember that these surfaces may have experienced a significant exposure to contaminants from the service environment. Because the SEM micrographs implied the weak boundary layer was present during the curing of the adhesive by the presence of scrim fiber impressions on the mating adhesive plies, the contaminant must have been present during manufacturing and curing of the bondline.

Using this assumption, areas of the composite part with similarities of location and construction (the disbond occurred adjacent to a core dropoff) were examined for bondline integrity. To ensure that no secondary contamination would occur, the part was cut with hand shears (cleaned in a solvent) which produces very little particulate damage. The part was also cut in the analytical lab well away from fabrication and machining areas where contaminants can be easily introduced. The result was that the adhesive bondline was easily separated by hand after being cut out with the shears. Separation occurred in a similar manner at the interface between the two adhesive plies and the mating surfaces were smooth and featureless. The advantage of finding these weak boundaries is that the specimen can be separated and introduced into the XPS spectrometer within minutes, thereby ensuring that any contaminant found is directly related to the original debonding. Figure 6-39 shows the XPS spectra in which the primary contaminant is silicon with the appropriate shift expected for a silicone release agent. Subsequent FTIR analysis of the soluble residues rinsed from the surface did not detect any anomalous functional groups, which implies the contamination is very minute.

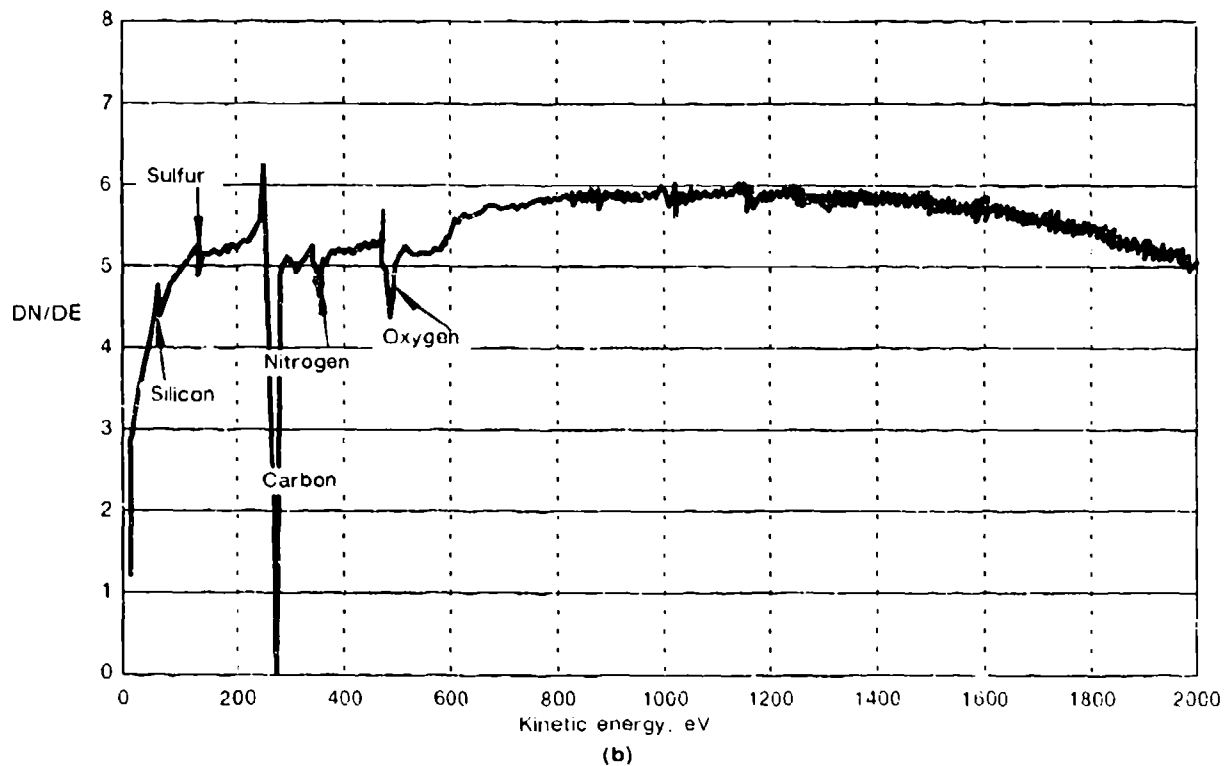
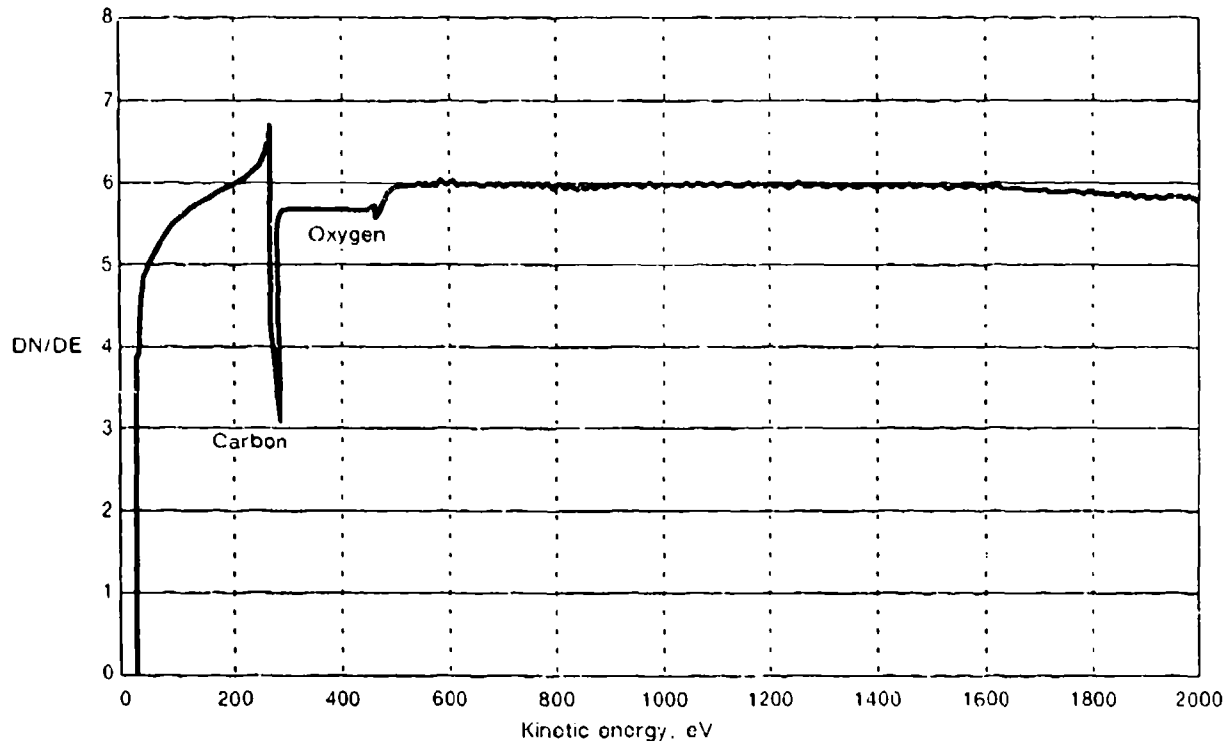


Figure 6-35. AES Spectra of (a) Carbon Fiber and (b) Exposed Carbon Fiber on a Tensile Fracture

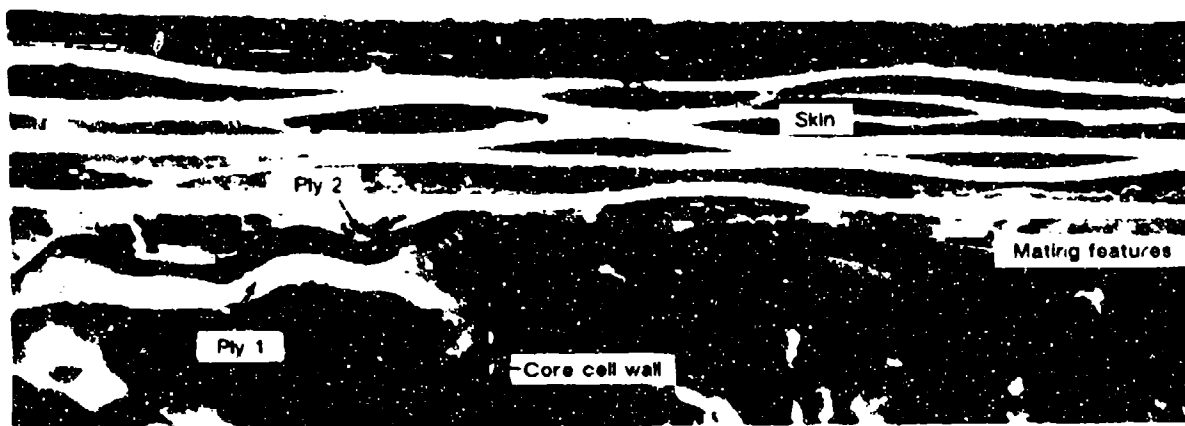


Figure 6-36. Optical Micrograph in Cross Section of a Laminate Skin to Core Buckling Separation

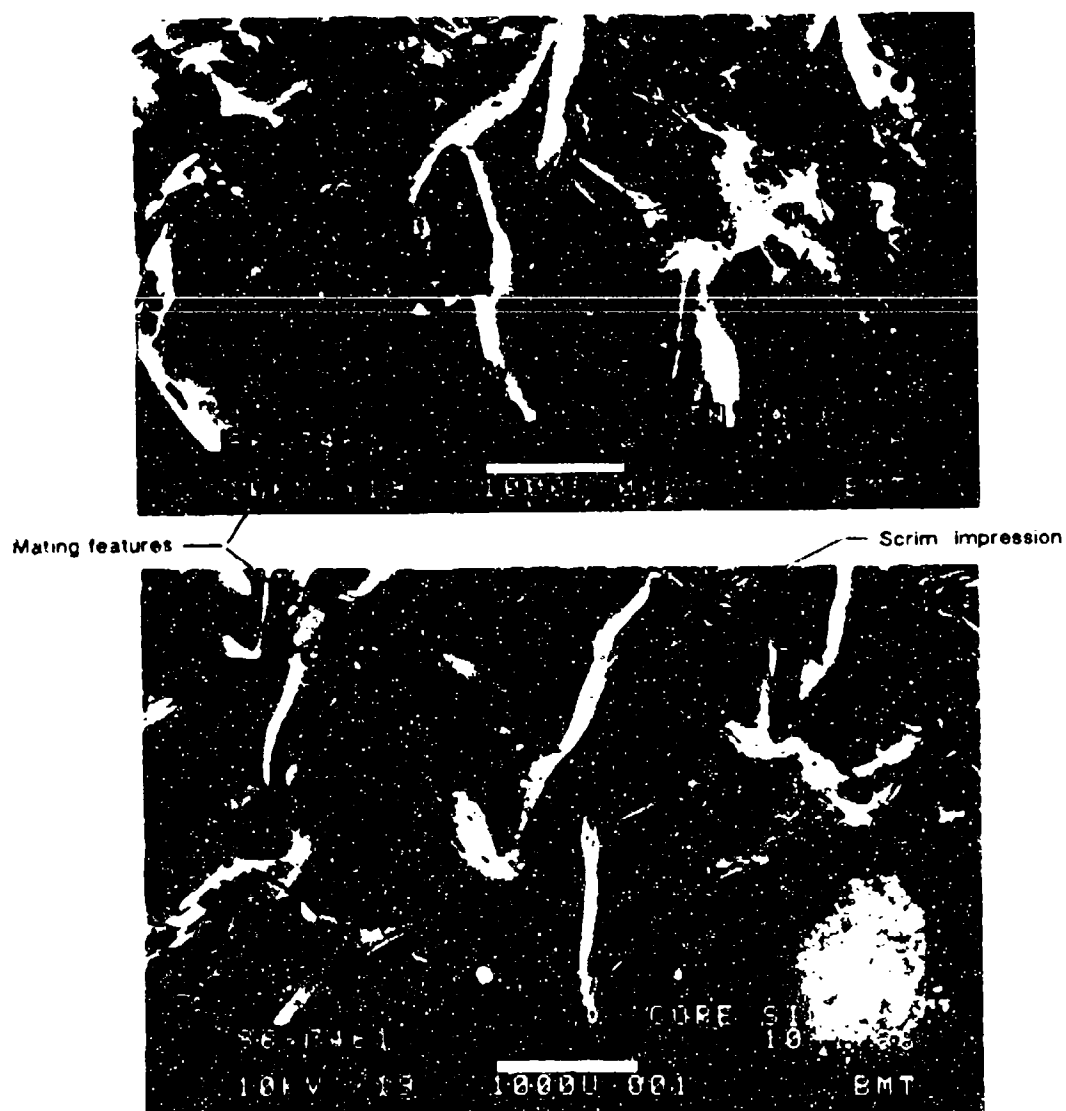


Figure 6-37. SEM Micrographs Showing a Replicated Surface Morphology

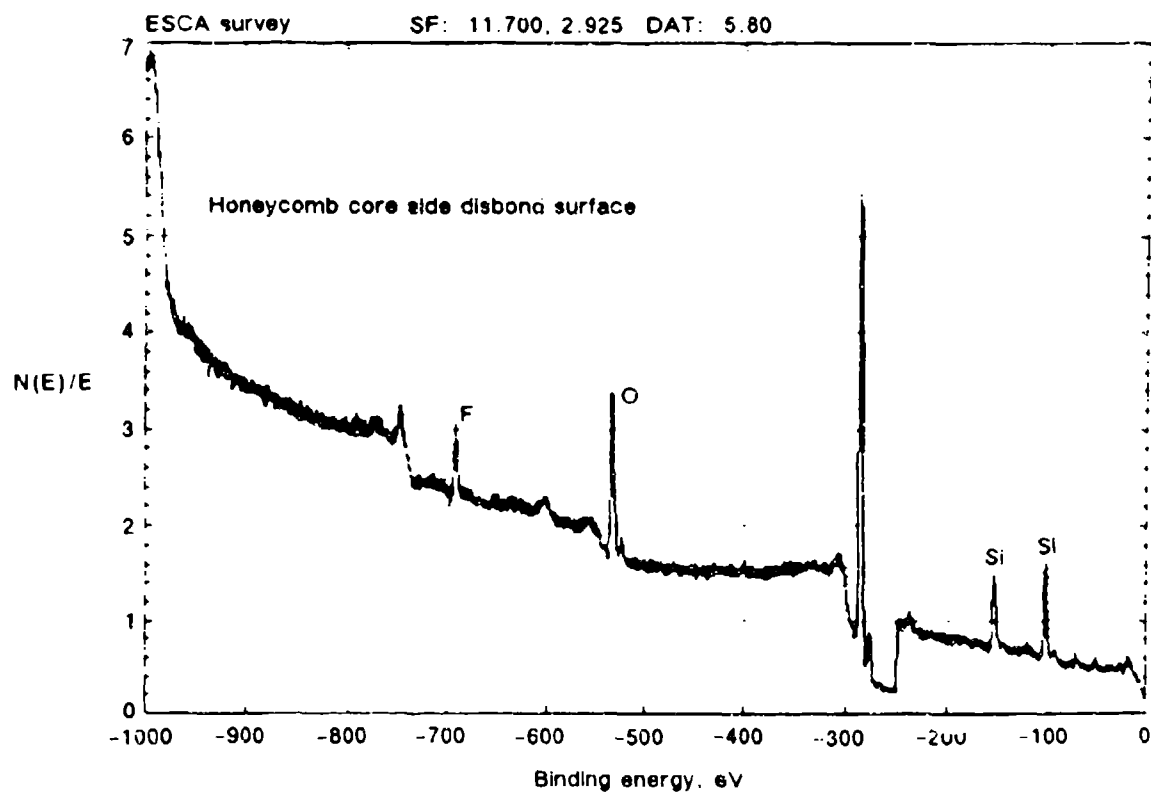
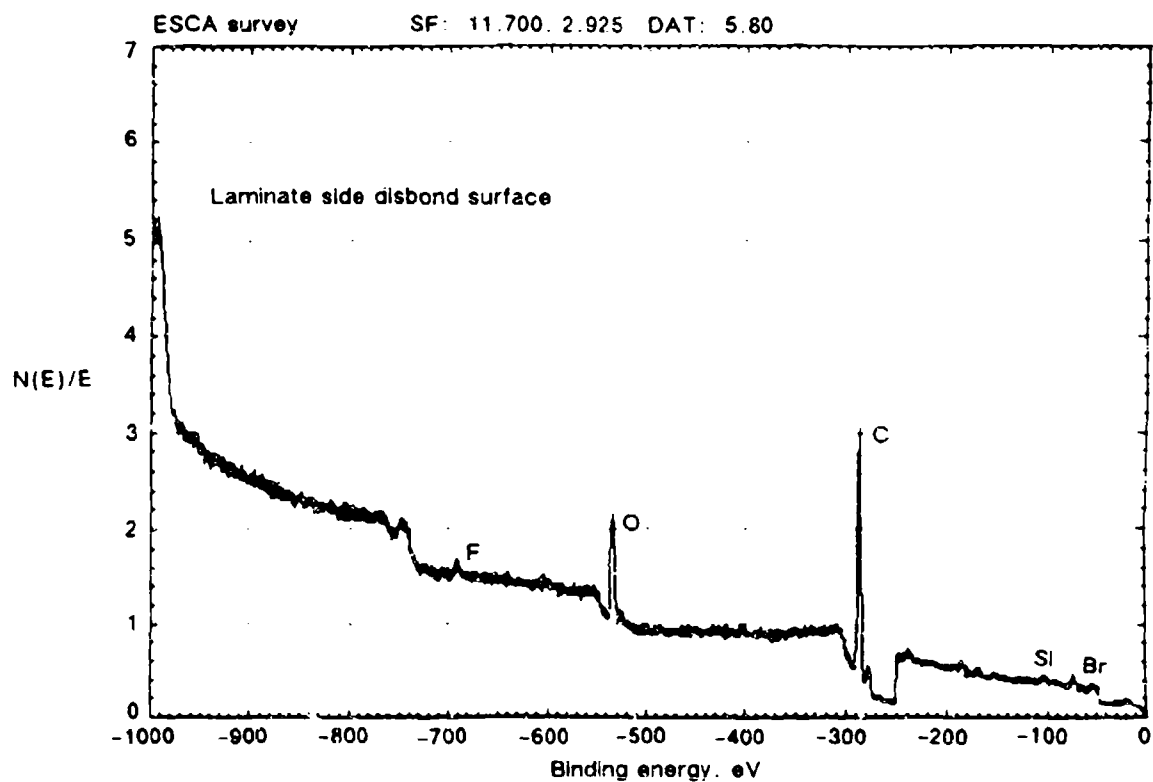


Figure 6-38. XPS Spectra of the Disbonded FM-300 Ply Surfaces

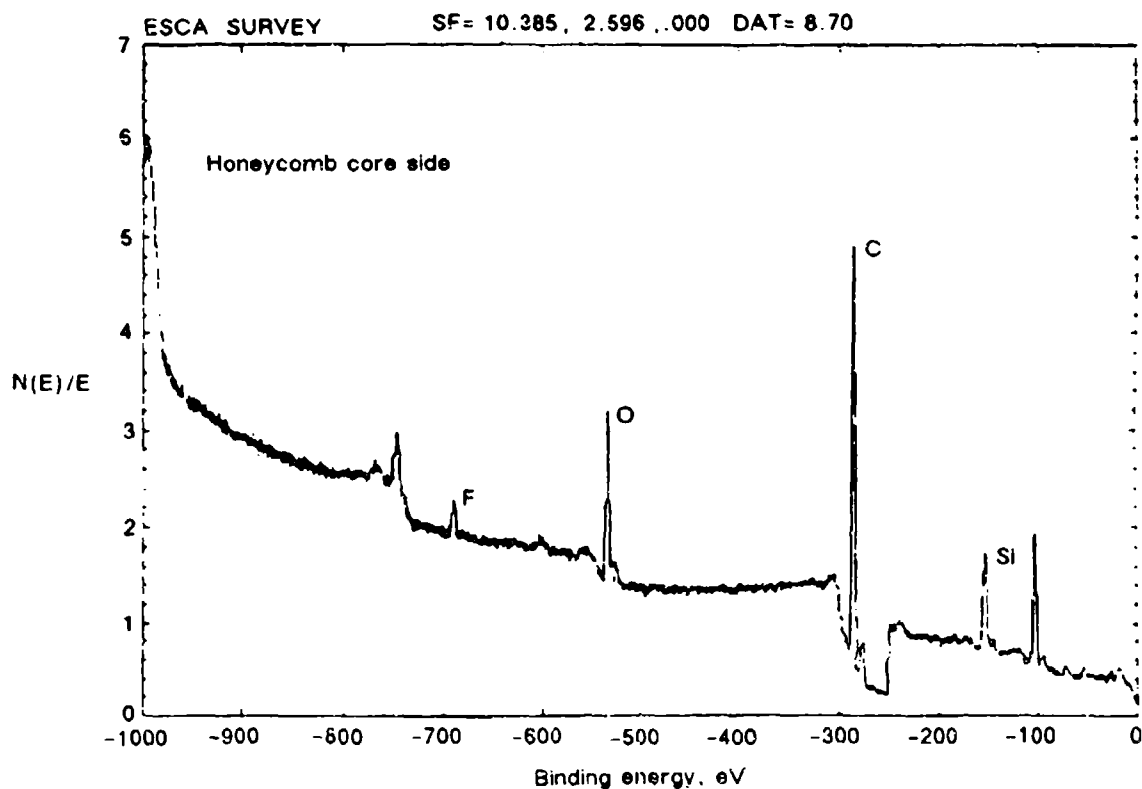
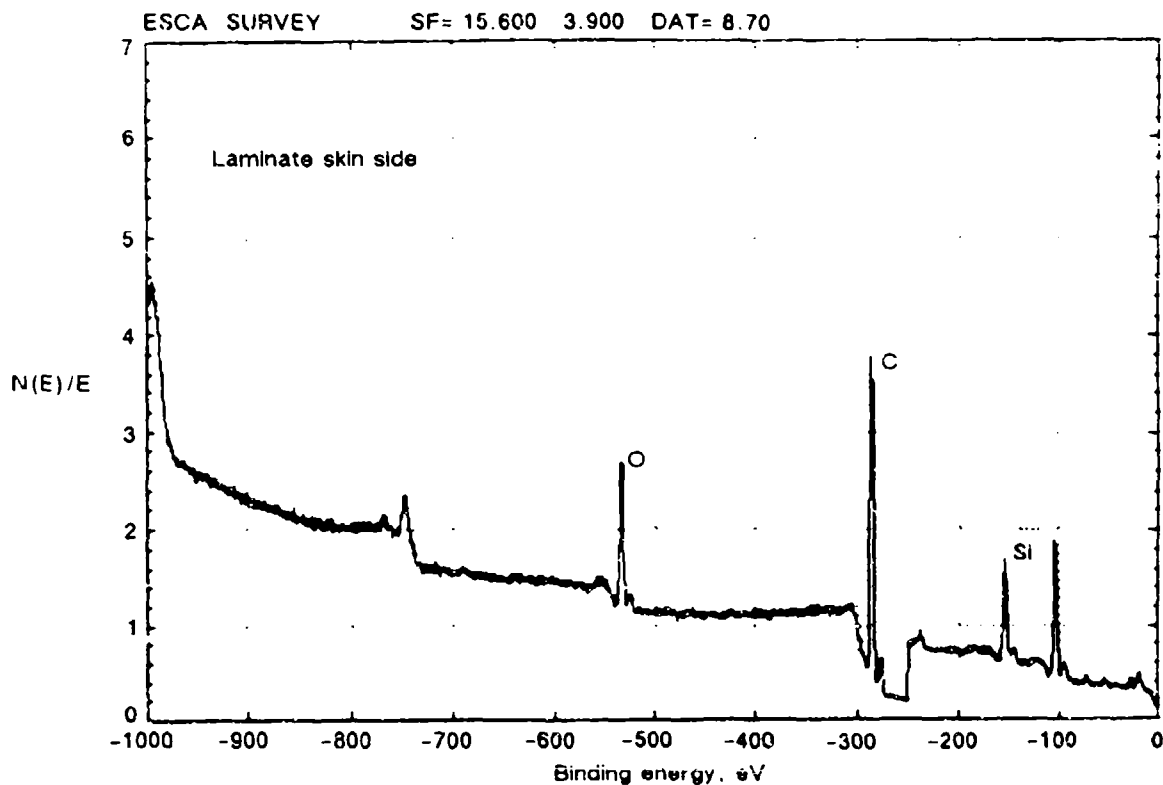


Figure 6-39. XPS Spectra of FM-300 Ply Surfaces Separated by Hand in the Laboratory

SECTION 7

MECHANICAL TEST METHODS

Different mechanical tests are used to create fracture surfaces in simple test coupons. The six mechanical tests used are:

1. Interlaminar Mode I Tension (DCB)
2. Interlaminar Mode II Shear (ENF)
3. Translaminar Tension (N4PTT)
4. Translaminar Compression (N4PTC)
5. Rail-Shear
6. Compression After Impact (CAI)

7.1 INTERLAMINAR MODE I TENSION (DCB)

Interlaminar Mode I tension fractures are produced using a double cantilever beam specimen geometry as shown in Figure 7-1. In this test, interlaminar tension conditions are generated at the specimen midplane by deflecting two beam halves at one end of the specimen. This is made possible by a release film (FEP) insert. The specimen configuration is illustrated in Figure 7-2. Special fixtures are used for the specimen to allow free-pin rotation at the beam end and mechanical grip attachment. The specimen grip fixtures, which are of a triangle grip configuration, are wedged into the crack tip formed by the FEP insert as shown in Figure 7-3. This results in mouth opening displacement at the beam end prior to mechanical testing. Any precrack observed during clamping is marked on the specimen edge. The specimen is loaded under deflection control on a Mechanical Testing System servohydraulic load frame with the rate of cross-head deflection adjusted during the test to produce a relatively constant rate of crack extension. In general, crack extension occurs in a progressive manner, with observed crack growth rates of about 1.27 to 2.54 cm (0.5 to 1.0 in.)/min. Cross-head deflection rates range from 0.25 to 0.51 cm (0.1 to 0.2 in.)/min.

7.2 INTERLAMINAR MODE II SHEAR (ENF)

Interlaminar Mode II shear fractures are produced using a modified end-notched flexural specimen geometry as shown in Figure 7-4. Tests are carried out using a cantilever geometry fixture. The uncracked end cannot rotate or move vertically, but can move horizontally. Such movement prevents the introduction of extraneous (vertical) loads as the beam shortens under deflection. With this geometry the top surface is loaded in pure compression, while the bottom surface is in pure tension resulting in pure shear at the crack tip.

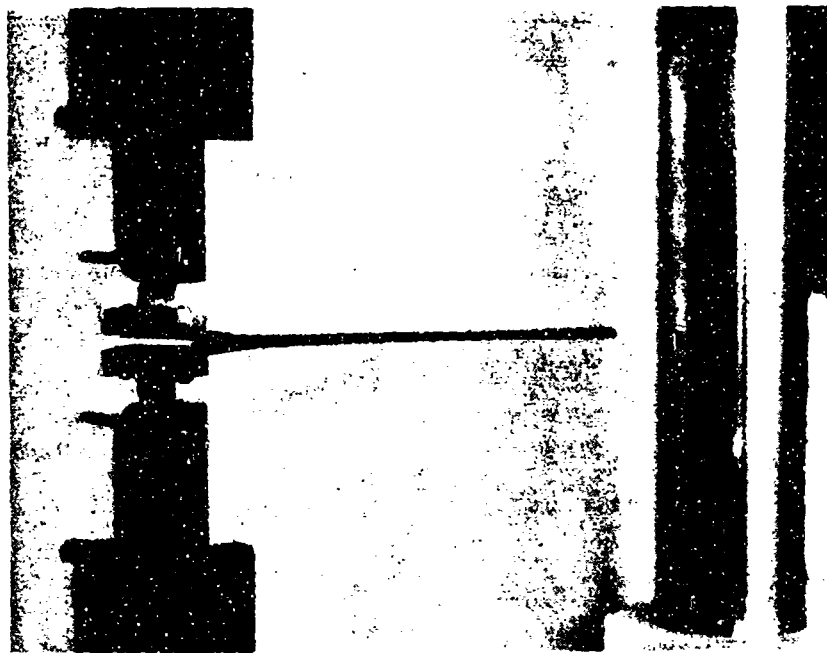


Figure 7-1. Double-Cantilever Beam Specimen Geometry

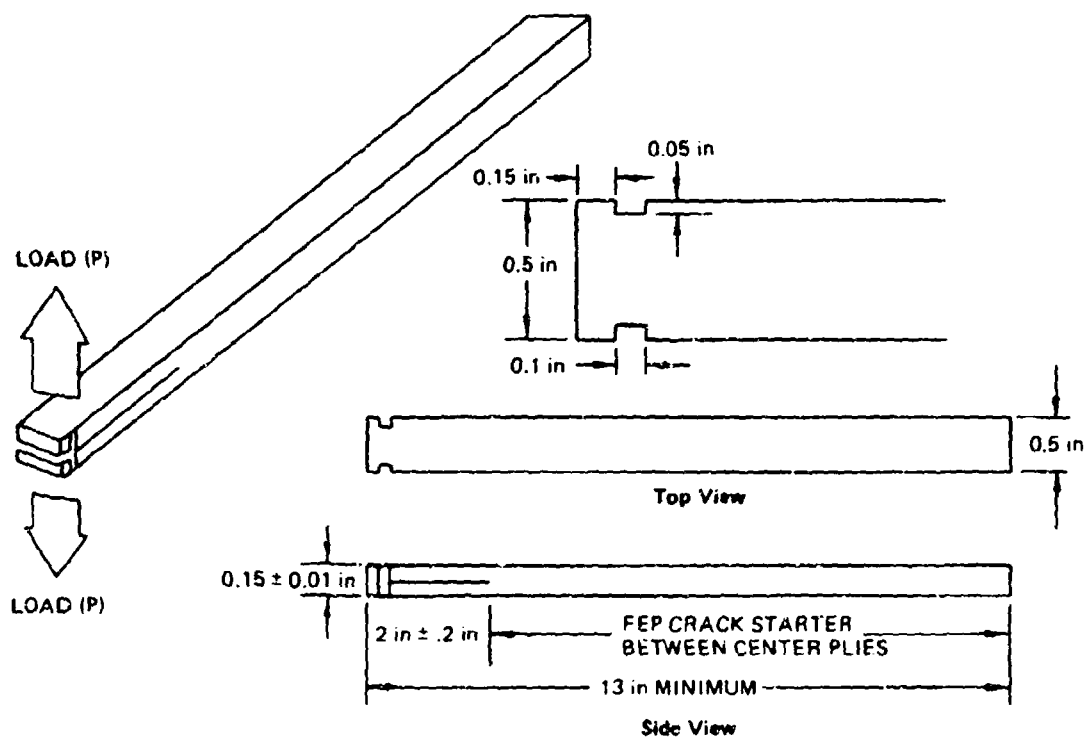


Figure 7-2. Double-Cantilever Beam Specimen

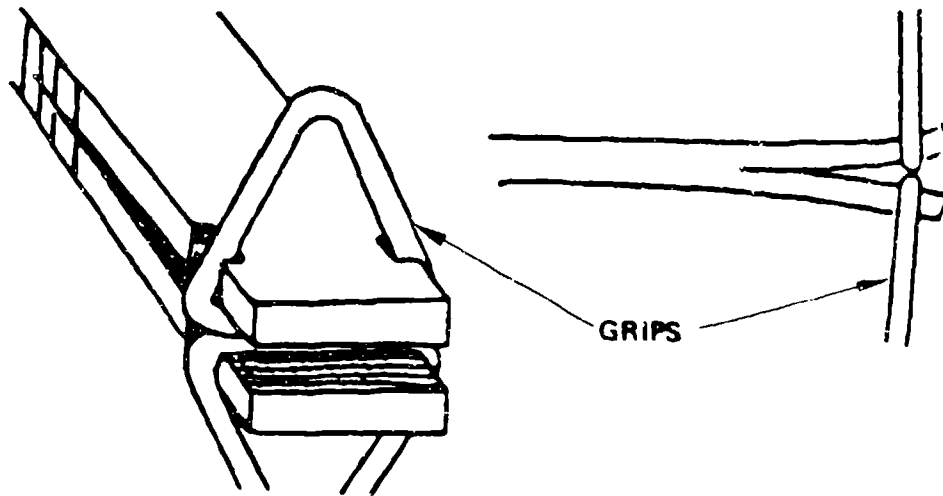


Figure 7-3. Double-Cantilever Beam Grip Fixture

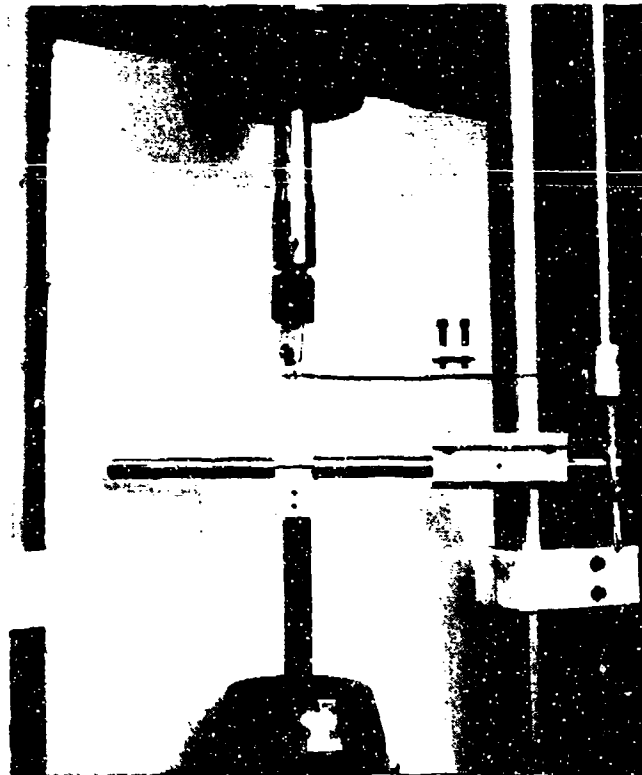


Figure 7-4. End-Notched Flexural Specimen Geometry

Crack propagation during testing typically occurs by rapid extension of the crack along the specimen midplane. In general, such rapid growth extends over 60 percent of the test span during the first crack extension, and then is followed by several increments of slower, more observable growth. Rapid crack growth precludes the full monitoring of the direction of cracking. However, during those

periods of slow, stable growth, crack extension is observed in a direction away from the FEP crack starter region, and toward the cantilever beam support fixture.

7.3 TRANSLAMINAR TENSION (N4PTT)

Conditions of controlled translaminar tension are generated using a simple, notched-bend-bar specimen geometry as shown in Figure 7-5. The conditions of translaminar tension are produced by four-point beam loading a Chevron-notched specimen with the notch located transverse to the beam's lower tensile surface.

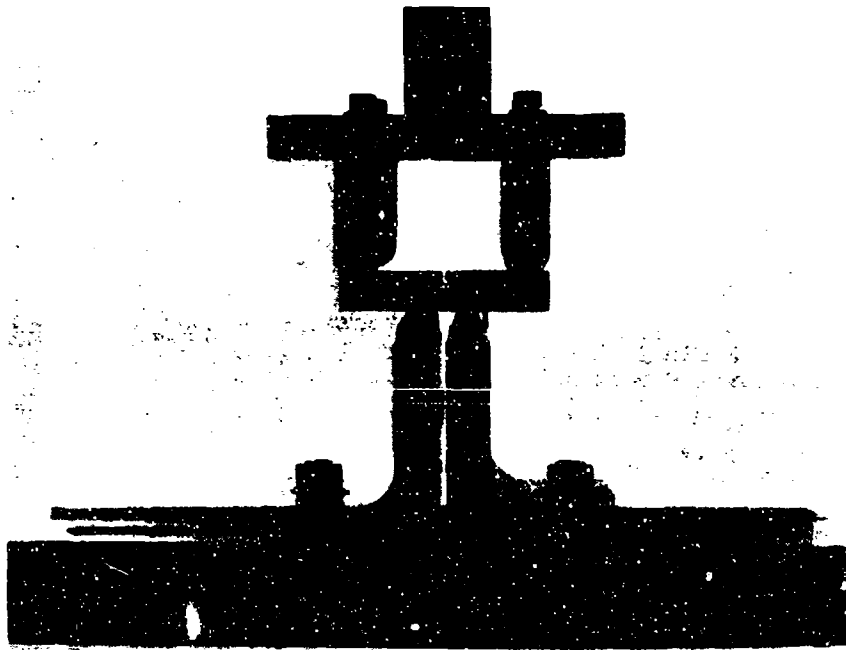


Figure 7-5. Notched-Bend-Bar (Tension) Specimen Geometry

7.4 TRANSLAMINAR COMPRESSION (N4PTC)

The conditions for this test are similar to the translaminar tension except the translaminar compression is produced by four-point beam loading a Chevron-notched specimen with the notch located transverse to the beam's upper compression surface as shown in Figure 7-6.

7.5 RAIL SHEAR TESTS

Rail-shear testing is performed on coupons having a specimen geometry as illustrated in Figure 7-7. Figure 7-8 shows the typical test configuration. In this test, the long sides of the rectangular specimen are clamped to steel rails. Stresses are transmitted to the specimen by means of a relative displacement of one rail to another. This mode of testing results in a localized in-plane shear condition in the test specimen.

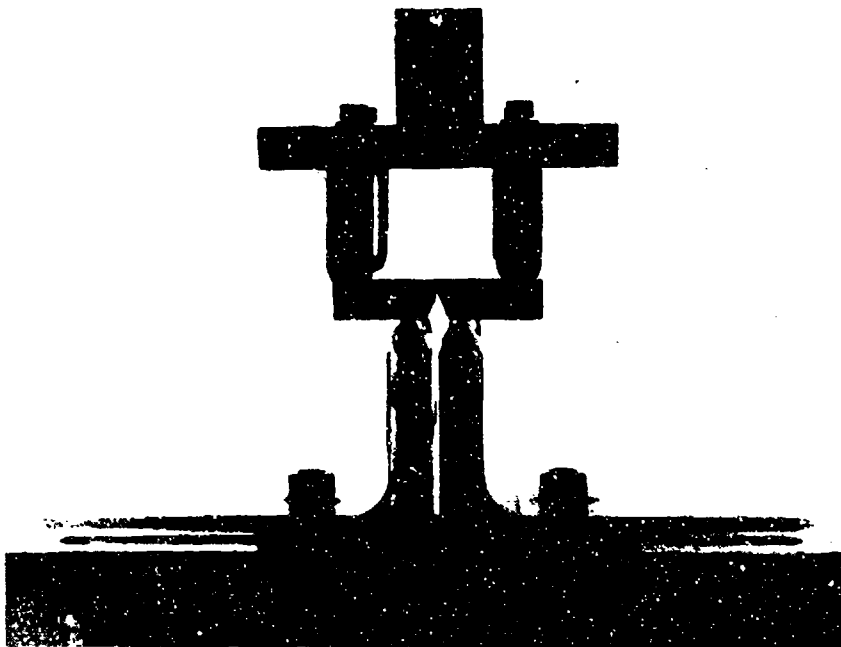
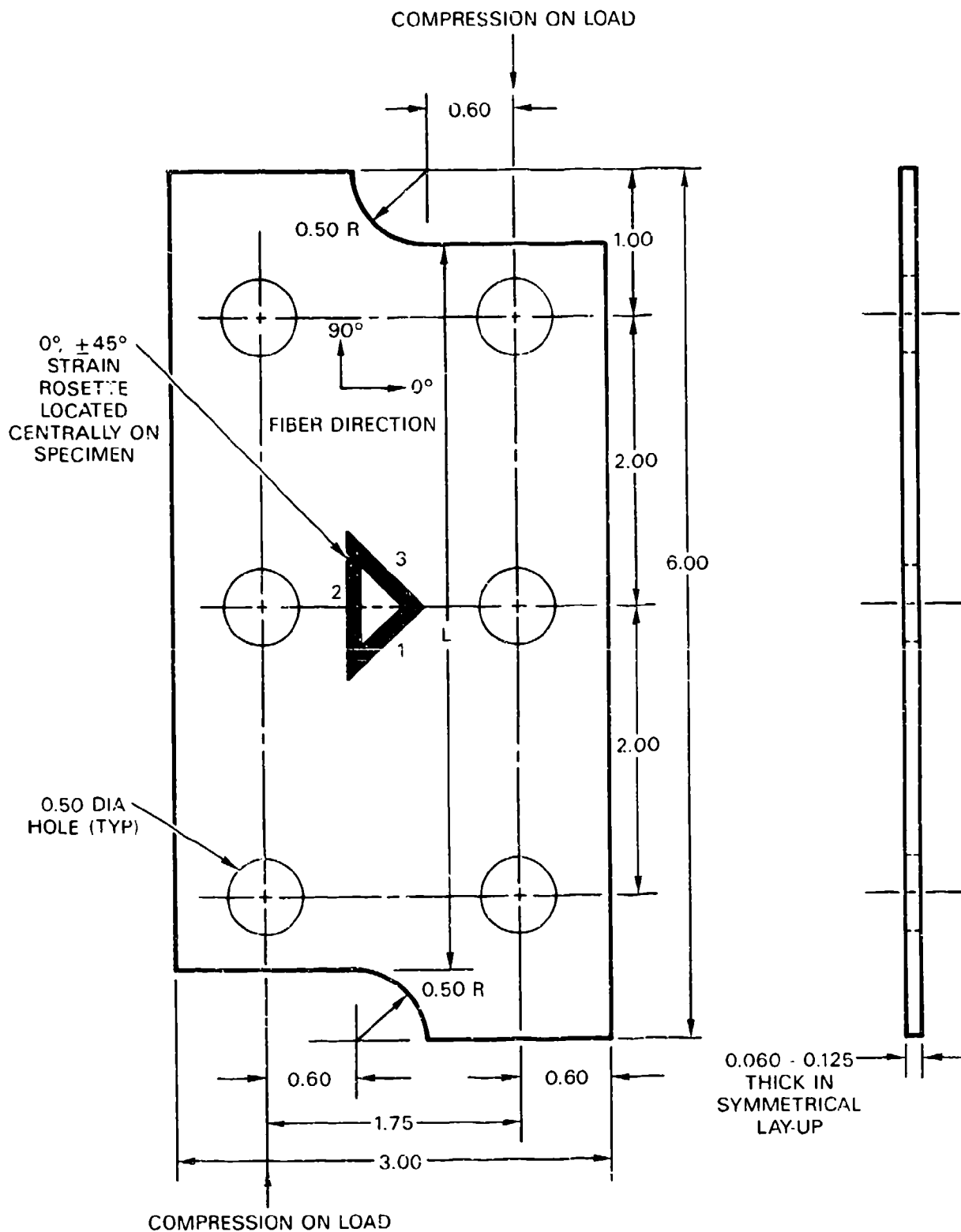


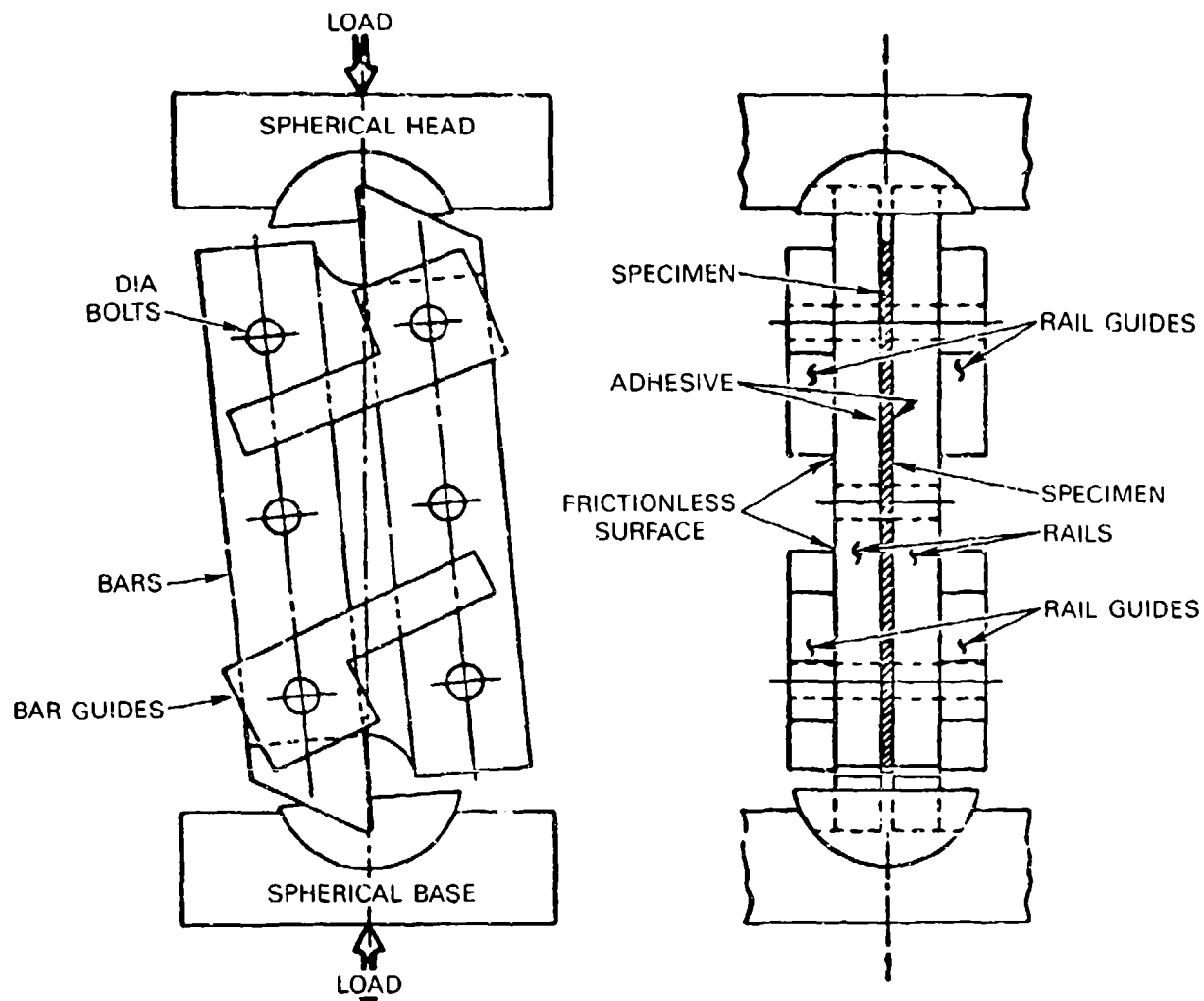
Figure 7-6. Notched-Bend-Bar (Compression) Specimen Geometry



NOTE: ALL DIMENSIONS IN INCHES

532.08

Figure 7-7. Rail-Shear Specimen



532.09

Figure 7-8. Rail-Shear Test Set-Up

7.6 COMPRESSION AFTER IMPACT (CAI)

Compression testing is performed on an impacted 4-inch by 6-inch quasi-isotropic laminate. The specimen is mounted on an impact support fixture (Figure 7-9), centrally positioned, and impacted on the tool side by an indenter with a 0.62 inch hemispherical tip at 1,200 in.-lb/in. The specimens are then placed on a 50 kip servohydraulic machine, utilizing a deflectometer, and loaded to failure with a displacement typically of the order of 0.05 in./min.

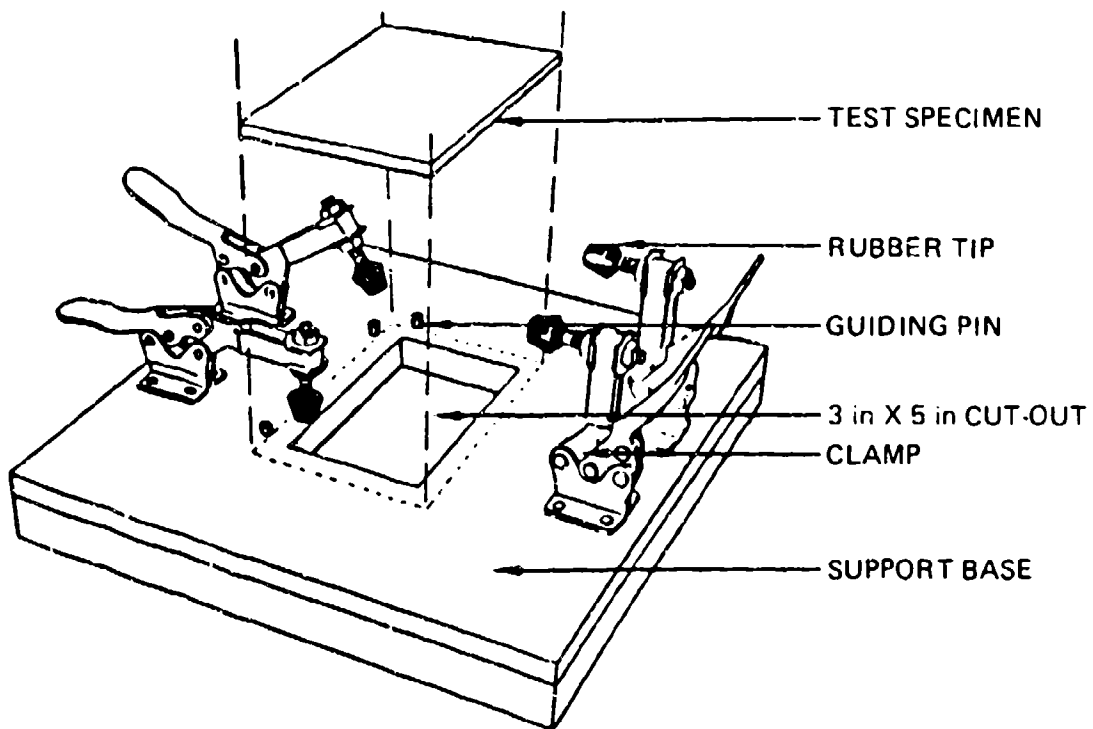


Figure 7-9. Impact Support Fixture

SECTION 8

FRACTOGRAPHY

Fractography, the science of studying fracture surfaces, is the key not only to the determination of the sequence of fracture events that took place during the failure process but also for the identification of the state of stress that existed at the time of fracture (tension, compression, and shear). Other factors such as environment, material defects, or other material anomalies that may have contributed to crack initiation, growth, and ultimate failure can also be evaluated using the tools presented in the following paragraphs.

Due to their laminated construction and high level of anisotropy, particularly on a localized scale, failures in composite materials tend to be extremely complex in appearance as well as in mechanism. The actual failure process and fundamental fracture mechanisms in this class of materials are not sufficiently well understood at this time. However, many of the analytical methods presently used for fractography of composite structures have been previously developed for use in failure analysis of metallic materials, and therefore have a fairly sound fundamental basis. Efforts within the past 10 or so years in the area of composite fractography have been directed toward modifying these well developed metals techniques, which include:

1. Visual and optical macroscopy
2. Optical microscopy
3. Scanning electron microscopy
4. Transmission electron microscopy.

Each of these analytical techniques provide the investigator with a significant amount of information regarding the fracture by examination of the morphology and other topographical features related to the fracture process. As a general rule, all failure analyses should involve each of the above techniques (with the exception of TEM) in the order of increasing magnification. Each investigation requires a combination of the above methods, dependent on variables such as size, time available, and type of fracture. Fractography, as an investigative post-failure analysis method, involves the use of the various techniques listed above in conjunction with the interpretation of the results as related to the fracture process. These paragraphs describe in detail the techniques used to identify the morphological fracture features. The physical principles involved in each technique are presented, including comments on how these principles can be used to control image type and the type of features observed in the fractographs. Specific examples of how to obtain suitable fractographs and gather data related to propagation type (interlaminar versus translaminar), crack propagation mode (tension versus shear), crack propagation relative to the fibers, and other divisions are illustrated.

In Section 4, the interpretive methods and specific examples of how the fractographic data relates to fracture mode, crack growth, and other faults are presented.

In addition to identifying the fracture morphology, the other primary responsibility of the investigator is to document the key features relevant to the determination of the cause of failure. This involves photo documentation for reports or presentations, as well as later analyses, and can often require extra effort during an investigation so that the photos convey the message to nontechnical personnel. For example, a significant portion of the analyses can be performed using optical microscopy, and although the image can be evaluated during use of the instrument, the details of resin fracture are often too fine and their fracture topography too rough (at high magnification) to be documented on optical photomicrographs. In this case, the SEM is required to document these features, although it may not be required to analyze resin fracture details. The two techniques are complimentary to one another. The value and methodology of both photo documentation and the identification of the fracture morphology are presented and considerations relative to specimen preparation prior to analyses are provided.

In fractographic analyses, primary emphasis is placed on:

1. Locating the origin of the failure
2. Establishing the direction of fracture
3. Identifying the load state and modes of crack growth
4. Determining if environmental conditions or degradation were present
5. Identifying if anomalous condition contributed to reduced material strength or premature fracture.

The use of fractography for the analysis of metals dates back to the early 1900s, and well established procedures exist for its application. Recent work has reviewed and modified these guidelines to yield the detailed fractography FALN illustrated in Figure 8-1. The chart diagrams three distinct operations: classification of failure types, crack mapping, and fracture surface chemical examinations.

The first failure classification breaks down the relatively complex nature of composite fractures into two distinct types, interlaminar and translaminar. This classification is useful because different analytical methods are best suited for each type of fracture. Interlaminar fractures, or delaminations, are best analyzed for crack growth direction using optical microscopy, whereas translaminar fracture (which break the fibers) are best analyzed by scanning electron microscopy.

Determining the direction of crack propagation is one of the most significant concerns in fractography. The recommended technique for crack mapping uses the lowest magnification capable of performing the job. This recommendation is made because one of the fundamental problems in detailed microscopy of large fractures is that there is an extremely limited perspective on how the area being examined relates to the part as a whole. The situation is similar to the old adage, "one can't see the forest for the trees." With a limited perspective, it is often possible to improperly characterize the direction, mode, or load state at fracture. By emphasizing the use of lower magnifications for early investigations, the FALN imposes a sense of perspective on later, higher magnification inspections.

The chemical analysis of fracture surface features may be required to determine the sequence of fracture events. By carrying out these examinations after identifying the fracture origin, emphasis can be placed on any anomalies encountered. Table 8-1 and Table 8-2 summarize the techniques used in fractography.

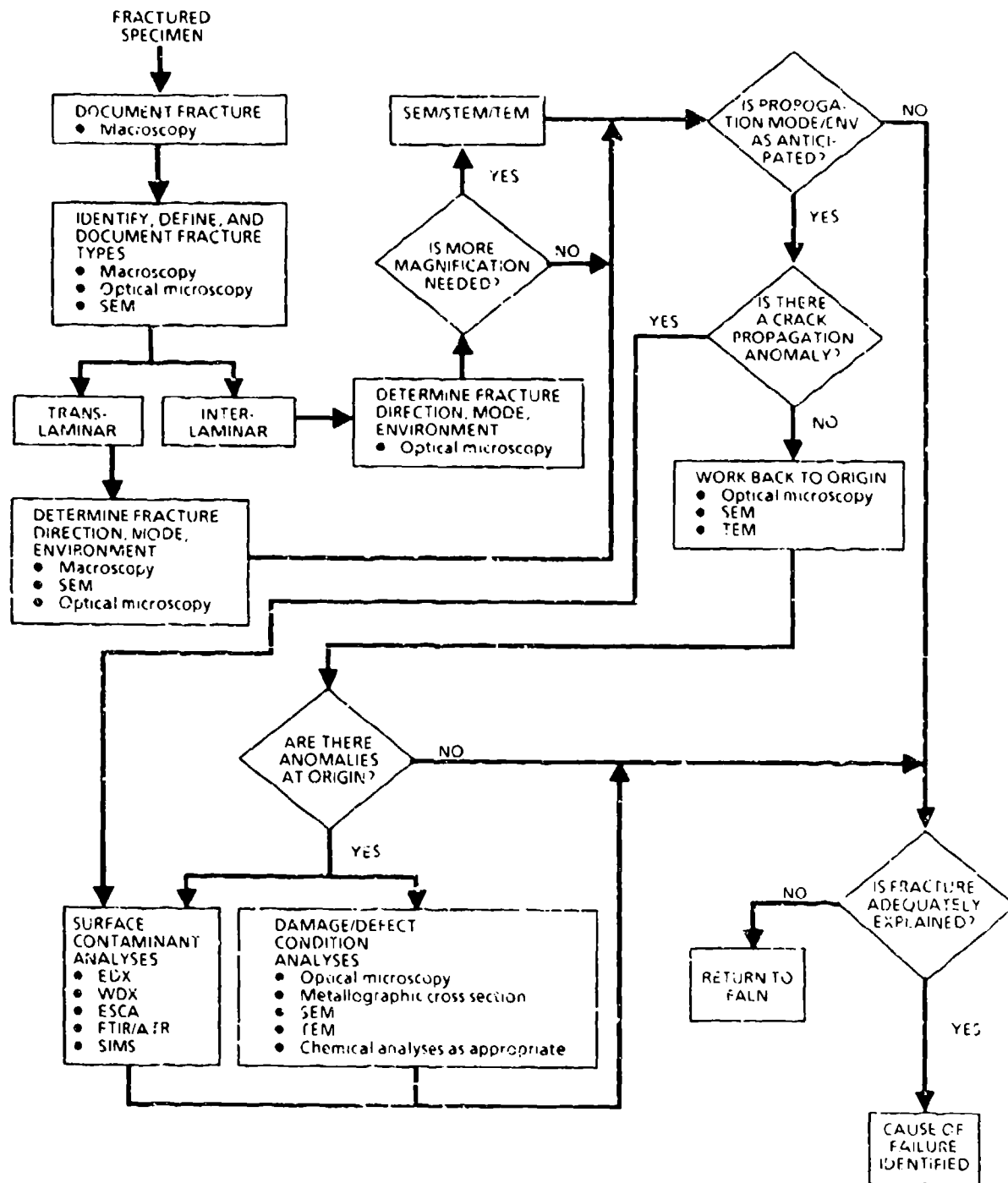


Figure 8-1. Fractography Diagnostic Technique Sub-FALN

Table 8-1. Failure Analysis Techniques – Fractography

TECHNIQUE	DESCRIPTION	USE	VALUE
Optical macroscopy	Optical examination at magnification generally at or below 10X	Plan-view examination and identification of fracture surface features, damage and defects	<ul style="list-style-type: none"> • Documentation of fracture • Identification of fracture types (translaminar vs. interlaminar) • Determination of translaminar fracture modes
Optical microscopy	Optical examination at magnifications above 10X	Plan view examination and identification of fracture surface features, damage, and defects	<ul style="list-style-type: none"> • Identification of fracture types (translaminar vs. interlaminar) • Determination of interlaminar fracture direction, mode, and environment • Determination of origin • Identification and characterization of defect and damage conditions
Optical X-section	Metallographic optical examination at magnifications above 10X	Cross-sectional examination of laminate, defect, and damage conditions	<ul style="list-style-type: none"> • Identification of fracture locations • Determination of laminate orientation and drawing compliance • Identification and characterization of defect conditions
Scanning electron microscopy (SEM)	Microscopy performed by mapping secondary electrons from the sample generated by a primary electron beam raster	High-magnification examination of fracture surfaces and defects with excellent depth of field	<ul style="list-style-type: none"> • Documentation of fracture surface • Identification of interlaminar fracture mode, direction, and environment • Identification of translaminar fracture mode, direction, and environment • Determination of origin • Identification and characterization of defect conditions
Transmission electron microscopy (TEM)	Microscopy performed by examining the focused pattern of electrons from the sample attenuated by a thin fracture surface replica	High-magnification examination of replicated fracture surfaces with better depth of field than in optical microscopy	<ul style="list-style-type: none"> • Limited to delamination fractures • Documentation of fracture surface • Identification of interlaminar fracture mode, direction, and environment • Determination of origin • Identification and characterization of select conditions
Back-scatter electron microscopy	Microscopy performed by imaging back-reflected primary beam electrons generated by a rastered electron beam	Intermediate magnification of fracture surface and defects. Back-reflected electrons are sensitive to atomic number and can be used to distinguish surface details as a function of atomic number	<ul style="list-style-type: none"> • Documentation as a function of atomic number • Identification and characterization of defect conditions

The following paragraphs describe the failure analysis methodology associated with fractography, the decision points, and the use of most of the analytical tools, all combined with the background reasoning that led to the sequencing and structure of the fractography FALN.

Beginning with a failed structural component, the initial responsibility of the investigator is to document the fracture surfaces, both by extensive photodocumentation and by visual and optical macroscopy. At this important stage, while the entire part or structure is intact, significant critical information may be gained through assessment of the overall types of fracture, their locations, and obvious anomalous production or service conditions, all of which give an investigator a feeling of the primary loading events, sequence, and other contributory conditions that occurred prior to or during

Table 8-2. Failure Analysis Techniques – Fracture Surface Material and Chemical Characterization

TECHNIQUE	DESCRIPTION	USE	VALUE
SEM/microprobe energy dispersive X-ray analysis (EDX)	Quantitative microchemical analysis, photographic mapping of X-ray energies created by primary electron beam raster	Determines microchemical elemental composition of micro-inhomogeneities and particles	<ul style="list-style-type: none"> • Identification of metallic contaminants (atomic number >1) • Particle size analyses
SEM/microprobe wavelength dispersive X-ray analysis (WDX)	Quantitative microchemical analysis, photographic mapping of X-ray wavelengths created by primary electron beam raster	Determines microchemical elemental composition of micro-inhomogeneities and particles	<ul style="list-style-type: none"> • Identification of metallic contaminants (atomic number >5) • Particle size analyses
Auger electron spectroscopy (AES)	Quantitative surface chemical analysis (top 5 nm) of Auger electrons ejected due to primary electron beam	Determines elemental chemistry of upper 5 nm of surface (requires conductive surfaces)	<ul style="list-style-type: none"> • Identification of contaminant monolayers • Identification of adhesive failure interfaces
X-ray photoelectron spectroscopy (XPS)	Quantitative surface chemical analysis (top 5 nm) of photoelectrons ejected due to primary X-ray beam	Determines elemental chemistry and chemical state of upper 5 nm of surface (does not require surface conductivity)	<ul style="list-style-type: none"> • Identification of contaminant monolayers • Identification of adhesive failure interfaces
Secondary ion mass spectroscopy (SIMS)	Qualitative surface chemical analysis of surface monolayer atoms removed by ion sputtering	Determines elemental and chemical state of surface monolayers; repeated operation allows elements to be profiled versus depth	<ul style="list-style-type: none"> • Identification of contaminant monolayers

failure. Dependent upon the size and location of the component, further fractographic analysis may be delayed for nondestructive analysis such as hand-held pulse-echo ultrasonics and part breakdown (fastener removal) into separate components such as skin and spar. As the separated pieces become available during breakdown, the investigator should identify, define, and document the individual fracture types such as translaminal or interlaminal. Visual and optical macroscopy should be employed for these analyses.

Following definition of fracture types, and more detailed NDE examinations of the damage regions, the most labor intensive and critical portion of the fractographic examinations involve the use of detailed macroscopic and microscopic analysis. These analyses require the investigator to use specialized fractographic techniques to determine the fracture directions, modes, and environmental conditions at fracture. For translaminal fractures, the majority of the analyses involve fiber fracture details, while for interlaminal fractures, resin fracture analyses predominate. Emphasis should be placed upon performing as much examination as possible at the lower magnification ranges, thereby increasing confidence and reliability in the determination of crack directions, modes, and any anomalous conditions which may exist.

If determination of the fracture origin is made, through the use of detailed crack mapping or visual and macroscopic analyses, the next step is to assess whether or not an anomalous condition exists in the origin zone. If such a defect is evident or suspected, such as adhesive separation which has a general lack of fracture features, commonly associated with contamination, then further examinations like surface chemical analysis may be required.

8.1 CARE, HANDLING, AND PROTECTION OF FRACTURE SURFACES

The preservation of the physical evidence should be viewed as one of the most important responsibilities for the investigator. Education on proper handling and protection prior to any fractographic examination is strongly recommended for anyone dealing in fractures either in the field or in the laboratory. When a fracture occurs, and there is even a slight chance that it will be submitted for laboratory examination, several important steps must be followed so that maximum information can be obtained. The important factor is prevention of damage that might preclude the use of various analytical methods. Most of the procedures described are independent of the particular fractographic techniques being employed.

The care and handling procedures that must be followed are based on general methods that have been proven for metals and modified for application to composite structures. These procedures rely on the fact that the fracture surface contains an enormous amount of valuable information and that anything done to obliterate or alter this information may obstruct important information related to the fracture. The damage that can occur can be separated into two types, either mechanical or chemical.

8.1.1 Mechanical Damage

This type may arise from several sources, including allowing the fracture to impact other objects. This can occur during the fracture process itself (for example, departure from the aircraft and subsequent ground impact), during removal of a fractured portion from the remainder of the structure, during transportation to the laboratory, or by careless accidents such as dropping the component. For composites, the consequences of damage can be detrimental to the proper determination of the cause of failure, since quite often the post-failure damage cannot be differentiated from that actually created during the failure event. Notably different than metallic structures, fractures created during rapid loading, such as impact from dropping, often cannot be differentiated from fractures created under slower loading which might be encountered during part service. Crack growth created during handling such as peeling delamination surfaces apart by hand are especially undesirable as they are often impossible to differentiate from delaminations created during the fracture event.

The fracture can usually be protected during shipment by properly crating the structure, if it is large and intact, so that motion of the component will not create rubbing or translation of the mating fracture surfaces. Where possible, particularly for components that have translaminar fractures, the amount of motion-induced damage can be eliminated by total separation of the fracture halves prior to shipment. Parts with only delamination damage can usually be left intact for shipment. To prevent contamination or fluid ingress such as rain, the structure should be wrapped with a clean plastic sheet. Smaller components or test coupons should be placed in zip lock bags or other airtight bagging to maintain the level of absorbed moisture and more completely protect the structure from contaminants. If necessary, the fracture can be protected during shipment by taping cloth or cotton to the surface, as long as loosely adhering material, commonly associated with the critical fracture regions, is not dislodged.

Touching the fracture with the fingers or rubbing it should definitely be avoided, as this can leave oils or other contaminants on the fracture surface which may alter or prevent surface chemical

analysis results. One of the most common sources of fracture surface damage is when two halves of a fracture are fit together. This accomplishes nothing important and always results in some microscopic damage to the fracture surface, and thus should be avoided.

8.1.2 Chemical Damage

This type of damage to fractures can be prevented in a number of ways, each using common sense and requiring an awareness of the necessity of protecting the surface from chemical contamination or degradation. Since the identification of a foreign material (such as release agent) present on a fracture surface may be critical in the overall interpretation of the cause of fracture, all chemical protection schemes such as plastic coatings or desiccants are to be avoided. If such a condition exists where a substance must be cleaned from the part prior to shipment, such as fire retardant foams, the most desirable solvent is plenty of clean water.

8.1.3 Laboratory Cleaning

Usually some sort of cleaning of the fracture surface is required prior to examination, since small pieces of fibers and matrix are present due to either the fracture process or mechanical cutting operations. However, to prevent potential loss of contamination evidence, cleaning should be avoided early in the investigations if possible. Numerous cleaning procedures have been attempted, each suited for the extent and type of deposit, or the preference of a particular laboratory. The most commonly employed cleaning techniques, in order of least-to-most damage or destruction of evidence, are:

1. **Dry air blast:** This method will remove many loosely adhering materials. If possible, canned air for laboratory use is preferred over the piped-in compressed air which can often contain oils and moisture. A soft artist's brush will assist in the removal, but extreme care must be exercised to see that no damage is done to the fracture surface.
2. **Detergent wash:** This method can effectively clean most specimens for high magnification investigations. A large, soft artist's brush can be used to apply a mild, water-base detergent (such as dishwashing detergent), followed by a thorough rinse in lukewarm tap water and drying by air blast. Stubborn deposits of particulate dust, which can occur on cyclically loaded parts, can be removed by ultrasonic agitation while the detergent solution is present. Ultrasonic durations of only a few seconds are usually satisfactory, although up to 15 minutes have been required to remove physically imbedded dust particles.
3. **Chemical solvents:** Chemical solvents should be avoided and used only when other techniques do not remove the tenacious deposits or chemical coatings. Prior to using chemical solvents on critical fracture surface regions, these solvents such as acetone, methyl ethyl ketone (MEK) or alcohols should be trial tested on fracture surfaces of the same material to check for degradation or loss of morphological details. Soak durations should be kept to a minimum. These solvents may also be used with ultrasonic agitation, which may shorten the soak duration quite significantly. This should be followed by detergent wash, rinse, and dry as above.

8.2 PHOTO MACROGRAPHY

Photography plays an important role in fractographic reporting as well as analysis of the physical features associated with a post-failure investigation. Photographic documentation always begins with several pictures of the broken part. This is followed by successively more detailed photography of the fracture surface and associated details, including the documentation of the successive steps carried out during the analyses.

Prior to photo documenting a fractured part, a detailed and thorough visual examination of the specimen in the as-received condition should be performed. This should determine which features are most important, which aspects are extraneous (such as post-failure damage), and whether any special treatment is necessary. This inspection should begin with unaided visual examination, followed with a hand-held magnifier. The fractured part should be scrutinized with a low power optical stereo widefield microscope if possible.

The next step should be to photograph the entire surface of the fractured part, with several angles and lighting conditions, to record the extent and type of damage relative to the components of the part. The documentation should begin with room overhead lighting and proceed using various angles of oblique lighting, to assess how the fracture characteristics can best be delineated and emphasized.

Accident related parts are often best photographed in the field and sometimes test parts are too large to be photographed in the laboratory. In such cases, outdoor photography using 35mm or 4-inch by 5-inch view cameras provide the best results. Where adequate daylight lighting exists, it should be utilized, although flash or flood lighting can provide necessary illumination of shadowed or fine details.

Where most of the photography in the laboratory consists of overall pictures of fractured parts and details of fracture surfaces at low magnification, a view camera offers the highest degree of flexibility. While 8-inch by 10-inch cameras are available, the 4-inch by 5-inch cameras are most popular, lending themselves to a wider range of photographic media such as Polaroid and cut negative films. Other advantages include a wide range of magnifications with the use of the bellows and various lenses. The ground glass backing allows accurate framing and focusing, and film or lens planes can be tilted to provide focus or perspective on large components. The major disadvantages to these cameras are that they are slower to use than other smaller cameras and require a camera stand or tripod. A workable setup for photographing fracture surfaces or small specimens is a view camera mounted on an enlarger type stand. This allows vertical, or top-down view of the specimen and conveniently provides a fairly quick setup and photo documentation time.

The 35mm single lens reflex (SLR) cameras offer ease of use with small size and, as stated above, offer a particular advantage for field work and color photography. The 35mm SLR provides a quick, "see what you get" feature. With the closeup "macro" lenses, magnifications less than 1X can be obtained. The major disadvantages are that they offer a small viewing port which provides a limited assessment of the lighting and focus, the small negative may not always be adequate for enlargements with high speed/large grain film, and the tilt and swing functions of the lens and film planes are not available as in the view cameras.

Low magnification stereo microscopes with attached cameras are often required to provide a light optical view and documentation of the fracture features at magnification ranges beyond those

possible for the 35mm and view cameras. These systems also permit three dimensional viewing at magnifications up to and beyond the lower limits offered by the light optical microscopes. The practical ranges of magnification for these systems range from 5X to 80X. These systems often have the additional advantage that detailed macroscopic examinations of the fracture surface details and origin regions can be performed, while allowing documentation of the features identified.

8.3 OPTICAL MICROSCOPY

Optical microscopy has proven itself as a most critical tool for failure analyses, for the examination of both fracture surfaces and cross sections. For cross sections, the optical microscope remains the most important technique available. The analyses of cross sections provide insight into the microstructural features related to construction, crack propagation, and defect conditions. For fracture surfaces, particularly the delamination surfaces, the optical microscope is possibly the best technique, and at the least should be used in conjunction with the SEM and TEM, rather than as a substitute. The fractography of delaminations by optical microscopy can provide information regarding the crack growth direction, loading conditions at fracture, the origin locations, and anomalous conditions related to the origin. Undoubtedly, this information is considered paramount to the determination of the cause and sequence of failure and thus should be required for all investigations of delamination surfaces.

8.3.1 Microscope Systems

Optical microscopes are available from a wide variety of sources and range considerably in cost and capability. Reflected light is the illumination mode used for composites. These microscopes are classified as upright or inverted, relative to the location of the stage with respect to the objective lenses. The upright microscope is the preferred type for examination of fracture surfaces, as the fracture surface does not contact the stage which can potentially damage the surface. The inverted stage, however, can accept an extremely large specimen, whereas the upright stage is limited to approximately 6 inches by 6 inches maximum size.

The bench type microscope is the least expensive type and often can provide all of the capabilities required to perform the investigations during fractographic analyses of composites. Various metallographs, although usually more expensive, provide more flexibility and resolution. These can range from simple to full-scale research units, with assorted illumination modes, objectives, light sources, hot stages, and other features.

8.3.2 Illumination

A variety of light sources for optical microscopy are available. The low voltage tungsten filament lamp is most often used on bench microscopes and has adequate light intensity for most observation and photography requirements. Where more light intensity is required for photo documentation, xenon arc sources (intensity adjusted by neutral density filters) and tungsten halogen filament lamps (adjusted by filters or electrical current) are the most common.

8.3.3 Diaphragms

Two diaphragms are available within all systems to provide improved image quality. A field diaphragm is placed near the light source to minimize internal reflections and glare within the microscope. This diaphragm is stopped down to the edge of the field of view, while not impairing examination or photography. A second diaphragm, the aperture, is placed in the light path just before the vertical illuminator. Opening or closing this diaphragm alters the amount and the cone shape of light, varying the contrast, sharpness, and depth of field. As magnification is increased, the aperture should be stopped down. At a given magnification, closing the aperture increases contrast and depth of field while reducing the image sharpness. A general rule of thumb for aperture setting on rough fracture surfaces, which require maximum available depth of field, is to stop down the aperture until there is a noticeable decrease in image quality and then open it slightly to eliminate most of the aberration.

8.3.4 Objective Lens

This forms the primary image and is therefore the most important component of the optical microscope. The apochromatic and plano type objectives provide the highest degree of correction for aberrations, produce the best results, and reduce eye strain. There are long-distance-working objectives which are particularly valuable for examination of fracture surfaces with rough topography, and are usually only necessary for objectives in the upper ranges of magnification such as 20 to 60X. Other desirable features for fractographic examinations are parfocal lenses (maintains focus when objectives are changed) and spring loaded lenses (moves when contacted with specimen to reduce damage to lenses).

8.3.5 Specimen Preparation

Reflected light illumination mode requires a relatively flat surface due to depth of field limitations and therefore specimen preparation is important to provide the best situation for examination and documentation. Specimen preparation for cross sections are presented earlier, with descriptions of the steps for cutting, mounting, and polishing. Specimen preparation for fracture surface examinations involve cutting the desired fracture region from the remaining structure followed by cleaning.

8.3.6 Fracture Surface Inspections

Optical fractography is by far the most efficient and cost-effective method for examination of delamination surfaces. Since the specimen setup and examination times are very short, an enormous amount of fracture surface is covered with this technique. As a result, a reliable and accurate determination of the typical and representative fracture surface features is obtained in a relatively quick fashion. Translaminar fractures, on the other hand, are too rough and the features (fiber ends) are too fine for optical microscopy. Low magnification inspections can be used on delaminations to verify the plane of fracture and the location of crack growth features such as beach marks and transverse cracking. More detailed, higher magnification inspections provide resolution of the fine matrix resin fracture features. These features are used to identify the direction of crack growth (by evaluating river marks), the fracture mode (tension versus shear), and indications of contamination and

environmental extremes. Bright field illumination, a stopped-down aperture, and long working distance objective lenses provide the best combination for examination at high magnifications required for crack mapping and identification of the fracture modes. Crack mapping methods and interpretation of the fracture features are presented in Part 2, Volume II, Section 1. The features found with the optical microscope, even though they are visible through the eyepiece, are often too small to document with photographic film. In these situations where photomicrographs are desired, the SEM is required.

8.3.7 Cross-Section Analysis

Metallographically prepared cross sections provide the following types of information:

1. Determination of the overall laminate quality
2. Quantitative evaluations of:
 - a. Extent of porosity
 - b. Relative percent and morphology of phases or microconstituents
 - c. Ply count and orientations
3. Origin examinations
4. Inspections of interfacial conditions
5. Crack propagation regions (intraply versus interply)
6. Extent of degradation due to wear, thermal cycling, and fatigue.

Where possible, specimens should be selected from at least two areas to most accurately characterize features, particularly when anomalous conditions are identified. These two areas include (1) as close to the origin as possible, and (2) at an area away from damage.

Several illumination methods are available for cross-section analyses, with bright-field being the most widely used. Dark-field or oblique illumination provides an excellent image contrast for differentiating surface topographical features such as microcracks and phase interfaces. Polarized light can be used to enhance differences between ply orientations for easier ply count and orientation analyses.

8.4 SCANNING ELECTRON MICROSCOPY

Since its relatively recent origin, SEM has found a wide range of applications in failure analysis, materials research and development, and quality control. Fractography is probably the most popular application of the SEM. The three dimensional appearance of SEM fractographs, the large depth of focus, large magnification range, and simple specimen preparation with direct inspection make the SEM a versatile and indispensable tool in failure studies and fracture mechanism research. This unique instrument offers possibilities for image formation of fractured parts that are usually easy to interpret and provides clear photomicrographs of rough surfaces as well as polished cross sections. The development of an assortment of related capabilities such as stereo viewing, quantitative microchemical analyses, in situ fracture studies and image formation that is easy to interpret all contribute to the value of this investigative and research tool. Energy dispersive X-ray (EDX) analysis equipment is

routinely attached to the SEM, providing semiquantitative and, in favorable situations, quantitative analysis of composition from a small volume. For composites, EDX analysis is usually only required for contamination analysis.

The SEM is capable of magnifications from about 5X to 250,000X, although the majority of composite fractography analyses do not go beyond 20,000X. SEM is normally a resolution of approximately 100 angstroms. The depth of field is about 300 times that of the light optical microscope, providing an excellent three-dimensional view of the specimen at focal depths of over 1000 microns at 100X and 5 microns at 20,000X. Specimens can be tilted up to approximately 70 degrees to the incident beam, while maintaining focus over most of the surface. The working depth ranges from 8mm to about 25mm, allowing an extremely rough surface (such as with protruding fibers) to be examined. The specimen size is usually limited by the size of the chamber door. The maximum size for the latest SEM equipment is approximately 6 inches by 6 inches, with limitations in tilt and thickness at this size. Usually specimens are much smaller (0.5 to 1.0 inch square), so that thicker specimens and maximum tilting may be allowed. Since the specimen size is limited, very large specimens must be partially destroyed. This particular limitation indicates that lower magnifications and less destructive inspection methods such as optical macroscopy and microscopy should be employed prior to SEM analyses.

8.4.1 SEM Specimen Preparation

Proper specimen preparation is basically simple and requires only a small amount of time. The preparation sequence is usually as follows:

1. Specimen selection: Commonly visual or optical inspections of the fracture surfaces to define areas of interest for analyses or documentation
2. Specimen cutting/removal: Involves mechanical methods such as abrasive cutoff machines or hand saws
3. Specimen cleaning: Used to remove dust particulate (from the fracture and cutting processes) and oils, etc., as discussed earlier; cleaning and coating should not be performed if contamination is a concern
4. Specimen mounting: Involves adhering the specimen to a mounting stub to secure it and to provide a conductive path from the specimen to the SEM chamber
5. Specimen coating: Usually required for nonconducting materials such as composites when high KeVs are used.

Good imaging requires careful specimen preparation, such that electrical charging, electron beam damage, and outgasing of volatiles are minimized. Composites, due to their laminated construction and organic structure, are subject to all of these problems if the proper preparation procedures are not followed. Because of this, the latter two preparation steps (mounting and coating) are discussed in detail below.

To prevent charging, conductive adhesives such as silver, carbon, or aluminum containing glues are used to bond the specimen to the stub. Drying times are on the order of 30 minutes, although time can be significantly reduced with the aid of a warm air blower. In order to maintain proper specimen identification, labeling the stub with a scribe is often recommended.

Nonconducting materials such as composites are usually coated to prevent electron charging, caused by a buildup of a space charge region of absorbed electrons. This charging appears dark at the site of absorbed electrons and deflects the incident beam, leading to image distortion and significantly changes the emission of secondary electrons so that the surrounding region appears washed out or over-bright. Charging can be prevented by operating at low acceleration voltages (less than 5 KeV) or applying conductive coatings. The latter method is preferred by most laboratories, since the magnification ranges do not ever approach conditions where the coating would affect microstructural resolution. It should be noted that non-coated low KeV analyses offer shorter preparation times and do not cover or obstruct surface contaminations, but do usually require an image enhancement system to properly process the limited image output.

The coating layer must be thin as feasible to minimize the possibility of obscuring fine details and thick enough to provide a conductive path for the impinging electrons. The minimum thickness is dependent upon the general roughness of the specimen surface, and may range from 10 nanometers for relatively flat specimens to 50 nanometers for extremely rough topographies. Carbon, copper aluminum, platinum, palladium, silver, gold, or gold-palladium (Au-Pd) are applied by high vacuum vapor deposition or sputtering. The gold-palladium sputtered is the preferred method, since sputtered layers provide better adhesion and more even condensation, and it provides the finest microstructure and lowest possibility of obscuring fine details. A combination that seems to work well for most fractures is to sputter coat approximately 20 nm of Au-Pd using the DC-pulse mode for five minutes after backfilling the vacuum chamber to 4.0 to 7.0 Pascal (30 to 50 millitorr) with argon.

It should be noted that a nondestructive method for SEM examination is available for situations where destructive cutting examination is not possible or the fracture surface may not be removable from the structure. In these situations, a two stage acetate replica may be produced with the same techniques described for TEM analyses. The only difference is that the specimen must be made conductive, and therefore requires an additional layer of vapor deposited gold or similar material.

8.4.2 SEM Techniques

The basic features of the SEM are presented in Figure 8-2. This instrument is a combination of electron-optical, vacuum, and electronic control devices for impinging a narrow beam of electrons from a heated cathode and focused by a system of magnets to a pinpoint spot on the surface of the specimen. An image is gained from collecting, modifying, and displaying the resulting emission from the specimen's surface. The cathode, or filament, is usually tungsten. Acceleration voltages range from 1,000 to 50,000 volts, although the usual range for composites are 2 to 30 KeV. A more effective and longer life electron source is lanthanum hexaboride (LaB_6). This new cathode requires more care and warm-up time, a better vacuum, and higher initial cost. To generate the required vacuum, a diffusion pump or a turbomolecular pump is used.

The electron beam scans the specimen similarly to the way a cathode ray tube is used to image a scanning raster on a television screen. A scanning generator controls the current to the scanning coils, which, in turn, deflect the incident beam along closely spaced lines. The magnification is controlled by

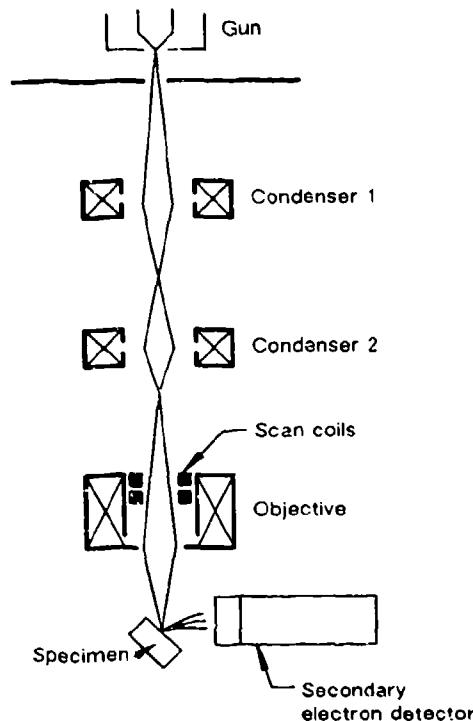


Figure 8-2. Basic Features of the SEM

varying the current in the deflection coils. The electron beam impacts the specimen surface, and the electrons that return from the specimen surface are collected by a detector. Amplification of this electron signal is required for imaging the scanning cathode ray tube.

When the primary electron beam is impinged upon the specimen, electrons and other radiations are emitted from the surface that can be used to produce images and to microchemically determine the elements present. Figure 8-3 shows the types of emissions radiated from the surface and the relationship to the type of detection modes available. The most common detection modes for composite materials are: (1) the secondary electron (SE) mode, (2) the backscatter electron (BSE) mode, (3) the pseudo backscatter electron (PBE) mode, and (4) X-ray spectroscopy. These are used routinely with a sound understanding of the types of information available and the limitations of each detection mode. Each of these detection techniques is described below except X-ray spectroscopy, which is presented in Section 6.

Although both secondary and backscatter electrons are used for fractography, the secondary electrons are usually the preferred source since they offer better resolution, provide an abundant signal, permit viewing areas of the specimen that are not in direct line with the detector, and provide a better three dimensional effect due to the shadowing loss of electrons at topographical features. There are situations where it is necessary to sacrifice resolution for improved image contrast and differentiation of features or phases by their atomic number. In such a case, backscatter electrons provide image contrast in specimens which are especially smooth or are viewed at low magnifications.

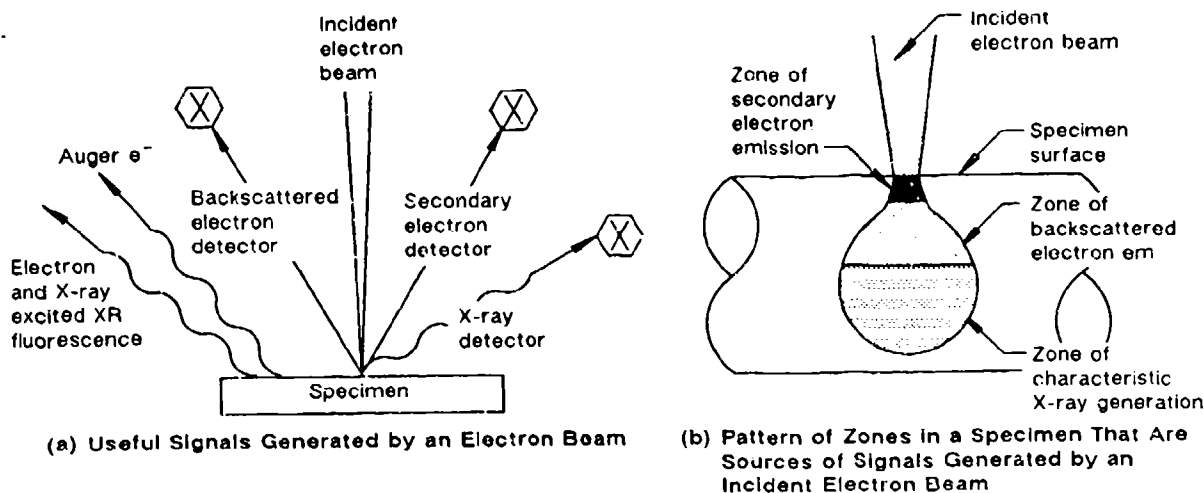


Figure 8-3. SEM Beam-Specimen Interaction Details

Secondary electrons are produced by interaction of the primary electrons with the atoms in the first 1 to 10 nm, resulting in emission of the loosely bound atomic electrons. The energy spectrum of these secondary electrons is independent of the energy of the incident beam and material type. The energy spectrum is fairly limited in range, with a pronounced maximum at approximately 3 eV. As a general rule, all electrons below 50 eV are considered to be secondary electrons and electrons with more energy are in the backscatter range. The primary factor for secondary yield is due to topographical features such as small variations in the surface angle. Since the secondary are emitted from the top few nanometers, the envelope of the excited and emitted electron volume moves closer to the surface when the beam contacts the surface at an angle, thus increasing secondary electron yield, and therefore brightness on the visual image.

As shown in Figure 8-3, the backscatter electrons are produced by single large-angle or multiple small-angle elastic scattering of the primary electrons as they impact the atoms from 0.1 to 1.0 μm beneath the surface of the specimen. Different than secondary electrons, the energy distribution of the backscatter electrons depend directly on the energy of the primary electrons and the atomic number of the material. In a similar manner, although with a more pronounced effect, surface inclination of the specimen provides an accentuation of the topographical features of the specimen. In specimens with high atomic numbers, which have larger atomic sizes, a larger percentage of the electrons are backscattered from atoms closer to the surface, with little change in energy. Therefore, the yield and thus the brightness are increased with materials that have higher atomic numbers. For those specimens which have a very smooth topography, the use of pseudo-backscatter electron is employed. This involves using the secondary electron detector with gating of the allowed electron energies for those electrons with more than 50 eV. This detection mode does not "see" the secondary electrons that have energies around 3 eV. Figure 8-4 illustrates the use of secondary, backscatter, and pseudo-backscatter for the imaging of a composite fracture surface.

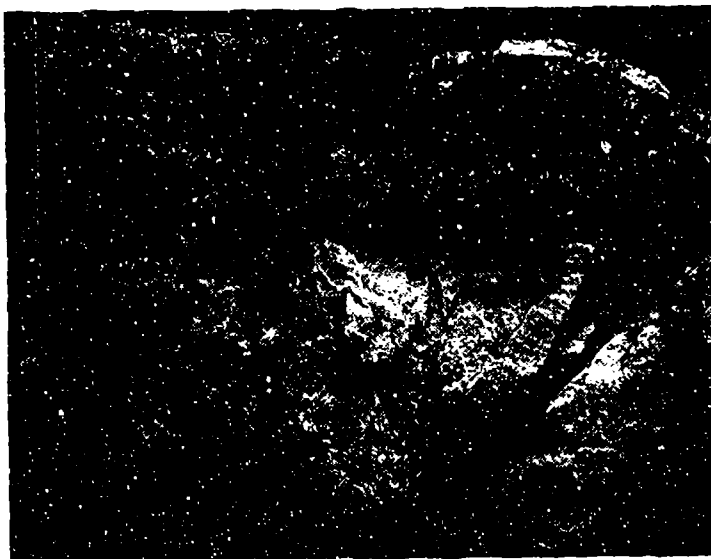
Optimization of imaging can enhance the image for analysis and documentation. Some components of a scanning electron microscope have their own characteristics of resolution and noise, which determine the image quality, however, most instrument parameters are fixed by the designer to



Backscatter electron detector image. Note increased contrast but lack of general feeling of depth.



Secondary electron detector image of trans laminate flexure specimen. Note high degree of resolution but lacking contrast.



Pseudo-backscatter electron detector image. Note significant contrast for fine features.

Figure 8-4. Contrasting Differences in SEM Photomicrographs

achieve maximum performance. The SEM provides flexibility so that the operator can adjust the instrument parameters for a specific specimen and investigation. Several commonly adjusted parameters which are available include:

1. Object tilt angle
2. Aperture size and working distance
3. Beam characteristics such as beam KeV and spot size
4. Detection method such as SE or BE.

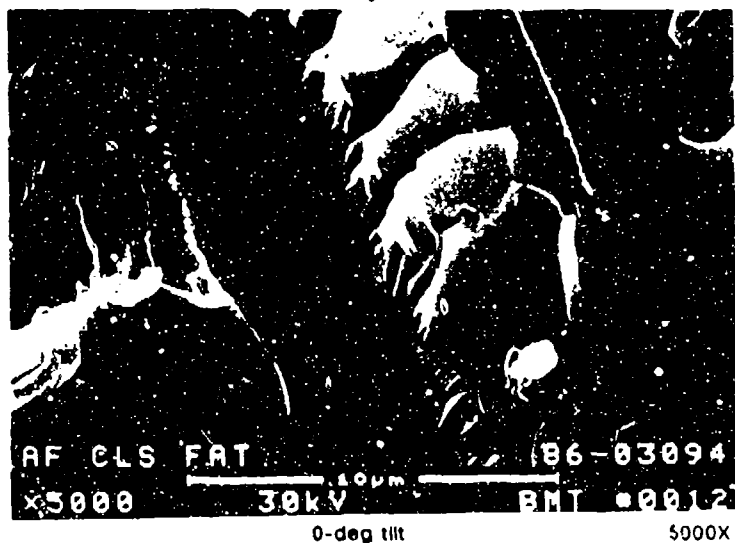
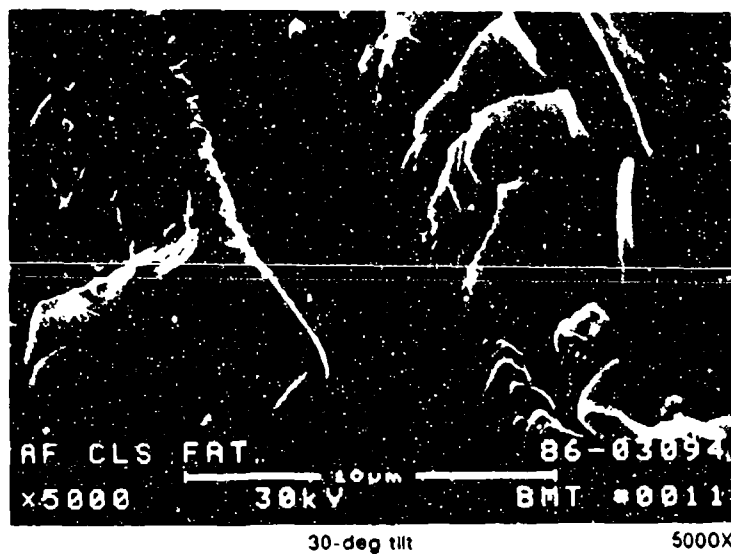
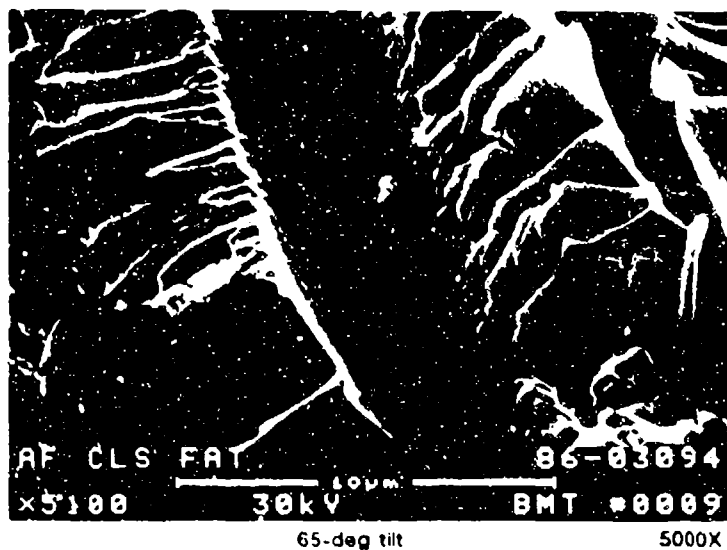
Object tilt probably provides the greatest effect on the overall image and thus should be optimized. Specimen tilt, which causes the beam penetration depth and scattering to vary, results in contrast between topographical features, similar to side lighting in optical macroscopy or shadowing for the TEM. The effect of tilting is more pronounced for the backscatter mode than the secondary emission mode. Since tilting can be used to enhance subtle features on smooth fractures, the use of high tilts is often required for examination of fatigue features, as shown in Figure 8-5, where fatigue striations are not visible until tilts beyond 30 degrees are employed. Similarly, the use of tilt often provides a quite different perspective of the fracture morphology such as hackles, as shown in Figure 8-6.

The aperture size and working distance determine the depth of focus. For rough surfaces at low magnifications, a small aperture and large working distance are selected. For high magnifications, a short working distance, small aperture, and high lens currents must be used to minimize the spot size.

Interlaminar Fractures. The basic fracture types and the general SEM instrument optimization for each type are presented below:

1. Crack mode and direction of propagation: Magnification in the range of 400X to 2,000X is used to inspect the direction of river marks, resin microflow, and tilt of hackles. For most observations, a tilt of approximately 30 degrees in the SE detection mode appears to be best.
2. Fatigue: Where this crack growth mode is suspected, high tilts beyond 60 degrees are often required, with viewing angle perpendicular to the striation. For instance, Mode II shear striations usually appear within the fiber matrix separation region, and therefore the viewing angle should be running parallel to the direction of fibers in a tape material. Pseudo backscatter and backscatter detection modes have been used successfully to identify and provide accentuated contrast to striations that are not easily detected using the secondary electron detector.
3. Disbond or contamination: For areas suspected of contamination or regions suspected of having a thin coating with different atomic number, the use of backscatter is invaluable. Usually a tilt is not required for this detection method.

Translaminar Fractures. For these fractures which have a very rough topography, the use of small apertures is desirable to increase the depth of field. Increasing the working distance also provides increased depth of field, although the resolution is degraded at extremely long distances and higher magnifications. Higher accelerating voltages do not provide any additional benefit since the secondary



Induced crack growth direction

Figure 8-5. SEM Photomicrographs of Effect of Tilt on Striation Resolution

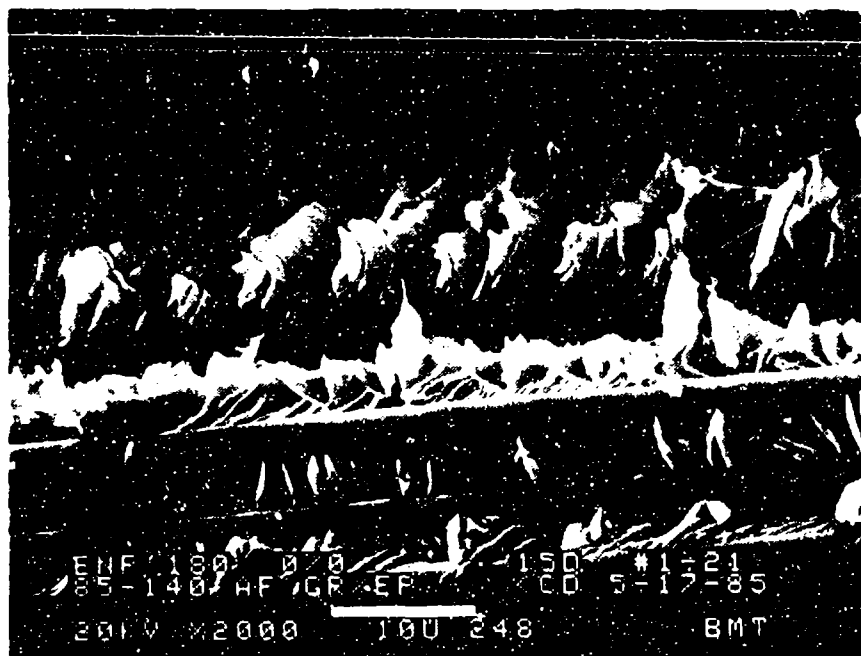
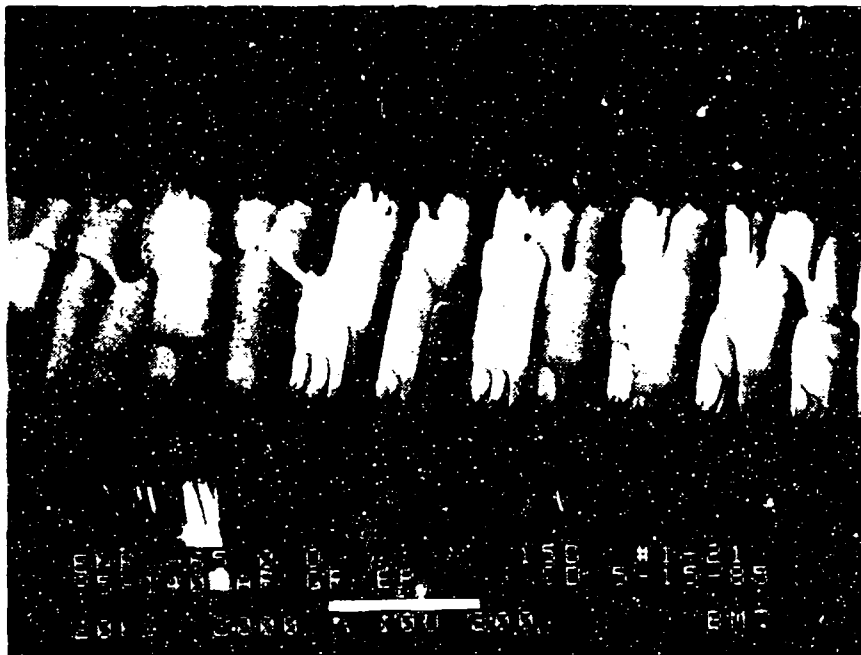


Figure 8-6. SEM Fractographs of Mode II Deamination Between Adjacent 0-deg Plies Illustrating the Effect of Tilt Angle

electron emission is independent of the beam energy. For most of these investigations, the magnification range is from 5X (for macroscopic view to differentiate between compression or tension) to 2,500X (to identify the individual fiber end fracture morphology). Translaminar fractures provide an enormous amount of contrast and topography changes. Accordingly, the SE detection mode is most useful since it is least sensitive to roughness extremes.

8.5 TRANSMISSION ELECTRON MICROSCOPY

The use of transmission electron microscopy (TEM) is fairly limited in investigation of composite fracture surfaces. Since the application of the SEM, which provides an excellent view of the fracture morphology, the TEM has been only applied to analyses of interlaminar fatigue. For this failure type, the striations related to cyclic crack growth are usually faint and limited to small zones in the fracture surface. The TEM has advantages over the SEM in that extremely fine resolution and a high degree of image enhancement is available through the specimen preparation methods and specimen tilt during analyses. The TEM however, requires a labor intensive specimen preparation and a trained operator to interpret the features observed. Quite different than the SEM, the transmitted electrons provide an image that is difficult to interpret and differentiate the actual fracture features from artifacts created during the replication process and microscope operation.

8.5.1 TEM Specimen Preparation

The basic specimen used for TEM analyses is the two-stage replica. Direct examination of the fracture surface can be made with the other techniques discussed above, but replicas offer the unique capability of transposing topographical information of composite delaminations to a high-fidelity facsimile that can be conveniently handled and transported, and readily examined in the TEM, SEM, or light optical microscope. The use of replication has significant value when the fracture surface of the failed part cannot be transported to the laboratory. Additional value is the ability to generate several replicas of the fracture surface, all of which may be destructively analyzed to determine the physical features relative to the determination of the cause of failure.

The initial cleaning of the composite fracture surface was covered in the beginning of Section 8. This usually involves detergent wash with ultrasonic agitation to displace particulate that may be physically impacted into the fracture surfaces during fatigue cyclic loading. The final stage of cleaning usually consists of successively applying and stripping several acetate tape replicas. The thin acetate tape is first wetted with a small amount of acetate solution, allowed to soften, and then applied to the fracture surface which also has some acetated solution applied to the area. Hand pressure is maintained without moving for at least a full minute. Following full drying of the replica, it is carefully removed to limit the damage from lifting fibers from the fracture surface. Usually two replicas are required to properly clean the fracture surface.

For most composite laminates, the matrix material can withstand short periods of contact with solvent, even those within their own functional chemical groups. This is particularly true for chemically stable epoxy resins that are thermosetting and are highly cross-linked. For these resin systems, the use of the most common replication materials, acetate film and acetone, do not exhibit damage of even the

finest fracture details. Other matrix materials, particularly those that are thermoplastic and are not cross-linked, should be spot tested in an area in the replication technique.

Following the generation of several clean replicas, they are then prepared in the same manner that is used for metals, in which the plastic replica is first shadowed with a high Z (atomic number) material such as germanium, and then coated with carbon. Figure 8-7 illustrates the two stage replication technique. For fatigue striation evaluation and maximum enhancement of the subtle features involved, the direction of germanium shadowing should be parallel to the direction of anticipated fatigue crack growth.

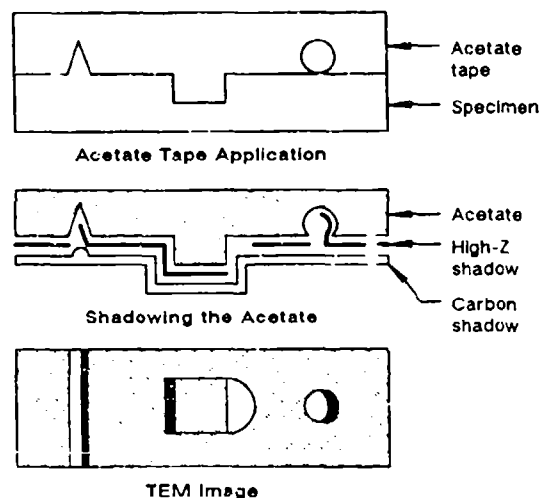


Figure 8-7. Two-Stage TEM Replication Technique

These replicas are then cut to size, for fit to the copper grids, and then floated in an acetone solution to remove the plastic portion from the replica. This stage is the most difficult and often very frustrating. Due to the fiber reinforcements, the replicas have a pronounced tendency to curl along the ridges formed by the fibers. Laminate tape fractures are extremely sensitive to this problem, particularly when the fracture involves only unidirectional fiber orientation. Specialized methods can be attempted, which include:

1. Dilute the acetone solution with distilled water to reduce the chemical mixing and curling, thus reducing the possibility of tearing and breakup.
2. Provide more than one carbon coating, each at different angles, to provide a more complete covering of the specimen. This increases the thickness which tends to reduce the curling.
3. When the above methods fail, scribe the specimen in the direction perpendicular to the fiber direction, creating a crosshatched effect, also reducing the chance of curling or breakup. The crosshatching has been successfully performed using a hot blade, attached to the tip of a small soldering gun, so that the damage is lessened by the smooth cutting action on the plastic film. The cuts should be made very close together, as close as 0.01 to 0.02 inches, with very light pressure to the coated side of the replica.

4. Place the small replica specimen between two copper grids. (There are butterfly types for this purpose.) The plastic may be removed overnight by acetone vapor. (There are instruments sold for this purpose.)

8.5.2 TEM Techniques

The TEM shown in Figure 8-8 contains an electron source, or filament, that emits a stream of electrons into a vacuum chamber. The filament is held at high accelerating potential relative to the grounded anode beneath it. The electrons pass through the hole located in the center of the anode and then through a condenser lens which consists of an electrically variable magnet. The condenser lens focuses the beam on the specimen. The electrons are either reflected, absorbed, or transmitted. The electrons which are transmitted through the specimen are allowed to pass through three magnetic lenses, forming a succession of three images, each magnified in turn to yield the intended overall magnification. The range of magnification is from 200X to about 25,000X for two-stage replicas; however the limit of use for composite laminate resin is about 10,000X.

The quality of the TEM image is affected by magnification, image intensity, image contrast, and the resolution obtainable. For increased resolution, higher magnification and better focus is necessary. For increased contrast, the objective-lens aperture may be varied, lower KeV's can be used, or the specimen can be tilted. Specimen tilt is usually the best method for identifying the faint striations present in the resin fracture regions. Figure 8-9 presents fractographs of a specimen which had been subjected to a compression-compression fatigue cyclic loading. The faint striations are barely visible and lie perpendicular to the localized crack growth directions. River marks and resin microflow are also evident. The river marks and resin microflow features can be used to identify the localized direction so that the tilting of the specimen can be made on the correct plane to maximize the enhancement of the striations. Figure 8-10 illustrates the striations evident at the fiber/matrix interface region for crack lap shear specimens (80 percent interlaminar Mode II shear). Tilts between 15 and 30 degrees were required for creating enough contrast and striation enhancement for the fractograph examples presented in this paragraph.

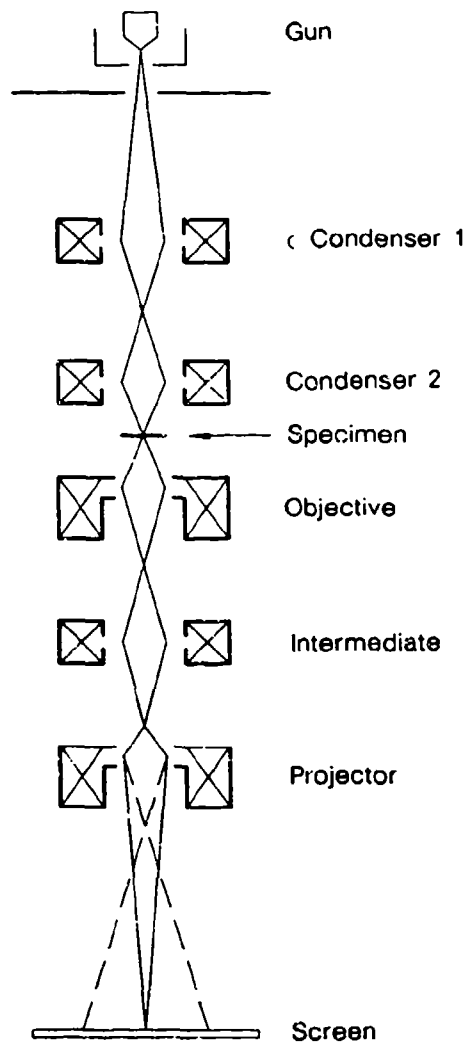


Figure 8-8. Basic Features of the Transmission Electron Microscope



Resin fracture
microplanes

7050X

Fiber



Striations

Striations

13,500X

Note: Striations are an indication of fatigue growth.

Figure 8-9. High-Magnification TEM Photomicrographs Showing Fatigue Striations



Note the curved striations equally spaced along the fiber surface

Figure 8-10. TEM Photomicrograph of Striation Features From a Crack Tip Shear Specimen

SECTION 9

STRESS ANALYSIS

9.1 INTRODUCTION TO COMPOSITE STRESS ANALYSIS

The purpose of stress analysis in the context of this compendium is to provide information which may lead to defining the cause of failure damage in a composite structural component. Although other methods of analysis may identify the origin, direction, and mode of crack propagation, stress analysis most often provides a quantitative explanation for the cause of failure initiation.

Stress Analysis Techniques. In the following paragraphs, literature on stress analysis is reviewed in detail. While these writings by no means encompass the entire field of stress analysis, they provide a perspective on the techniques and procedures available for composite materials. Before discussing the application of these techniques, however, it is important to recognize the role of stress analysis in a postfailure investigation.

Most components are subjected to detailed stress analyses as part of their initial design. Consequently, in the as-designed configuration, failure should not occur as long as the component is operated within its design life and envelope. However, real-world experience indicates that component fractures do occur in service. Common causes of such failures include:

1. Design deficiencies, such as insufficient assessment of loads and stresses, either of design details or individual plies; also, oversimplification of loads, load paths, and combined effects of load, damage, and environment
2. Manufacturing and process discrepancies, such as mismatched radii, ply layup errors, and mislocated or misdrilled fastener holes
3. Service damage, including foreign object impact, subcritical cracking, and improper maintenance or repair.

For each case, the objective in analyzing stress is to determine if the occurrence of a failure not predicted during initial design can be explained and understood. While techniques such as fractography may be able to identify the origin and mode of fracture, it is stress analysis that most often determines the cause of failure.

The stress analysis required to investigate part failure can be relatively complex, but from the point of view of the failure analyst, the process involved can be divided into two discrete tasks, thus making the review of available literature most straightforward. The two tasks are:

1. Assessment of the component strength in the as-fabricated condition
2. Assessment of component residual strength considering flaws, damage, and subcritical cracks.

Table 9-1 illustrates the relationship between the methods identified in the literature and these two tasks. The first task, assessing the part strength in the as-fabricated condition, evaluates stresses at a greater level of detail than during initial design. In most cases, this assessment focuses on the crack origin, with special attention to discrepant manufacturing and production conditions. Principal techniques at this level of assessment, likely to be of value, include individual-ply, point, and average-failure criteria, laminate strength criteria, and the Damaged Zone Model.

The individual-ply failure criterion examines stresses at the individual ply level and establishes the onset of first-ply failure. The chief benefit of this analysis method to failed structures is its ability to predict the point of initial failure on a microscale. This ability is particularly significant since most initial design analyses consider stresses on a gross average basis. However, even though there is potential value in this methodology, some drawbacks exist. The most significant of these is that to examine edge-effect stresses of individual-ply failure criterion requires a knowledge of plan view stress distributions (surface stress flow) and detailed finite-element grids. For organizations with experts in stress analysis, neither of these factors is a limitation. More significantly, however, the individual-ply failure criterion predicts failure initiation, not catastrophic failure. It also exhibits significant inaccuracies when applied to predicting strengths of multidirectional laminates. Consequently, failure onset cannot be meaningfully determined based on the individual-ply failure criterion. As a result, prediction of the stress required for catastrophic failure is more likely to be calculated by gross area stress calculations with fine, finite-element grid structures placed in the area of failure origin.

Other considerations in estimated gross area stress are the point and the average-failure stress criteria and the Damaged Zone Model. As described in the works of Daniel (Reference 7), Mikulas (Reference 8), or Aronsson (Reference 9) on laminate failure criteria, the stress at failure can be determined for any hole, given a characteristic parameter for the particular material and layup. Based on results reported in these researchers' works, this method appears to work relatively well, its only apparent constraints being that it requires empirical measurement of the characteristic parameter and knowledge of the plan view stresses for the area of interest. In actual application, neither of these constraints should be significant; however, additional concerns that must be addressed include the effects of environment, absorbed moisture, and resin formulation on the validity of a single value used as a characteristic material property.

Table 9-1 depicts the second major task involved in the stress analysis of a failed component — assessing its residual strength. Considerable investigation has been done that can be directly translated to the analysis of through-thickness flaws such as cracks emanating from holes. Either the Damaged Zone Model or point-stress failure criterion appear to work well for predicting the onset of crack instability. The limit in applying either of these methodologies lies in the ability of disciplines such as fractography to identify and define the size of original damage. Given this measurement, establishing

Table 9-1. Stress Analysis Methods

ANAL. TASK	METHOD	DESCRIPTION	AUTHORS (ref. number)	COMMENTS
Assessment of as-fabricated strength	Laminate theory and first ply failure criteria	Laminate theory is used to identify two-dimension stresses; one of several failure criteria are applied to define occurrence of first ply failure	<ul style="list-style-type: none"> • Chamis (10) • Craddock (11) • McLaughlin (12) • Tsai (13) • Jones (14) 	<ul style="list-style-type: none"> • Valuable for simple prediction of ply failure • Laminate theory requires knowledge of local stresses • Laminate theory cannot handle edge effects/complex geometries • Predicted failure stresses vary widely with criterion used • Failure criterion not accurate • Does not predict catastrophic failure
	Finite element analysis and first ply failure criteria	Finite element analysis is used to define stresses in three dimensions for edge effects/environments/bolted joint configurations; one of several criteria are applied to define occurrence of first ply failure	<ul style="list-style-type: none"> • Crossman (15) • Herakovich (16) • Wu (17) 	<ul style="list-style-type: none"> • Valuable for simple prediction of ply failure • Finite element techniques can be used to define local stresses • Method accounts for edge effects, environment, complex geometries • Predicted failure stresses vary widely with criterion used • Failure criterion not accurate • Does not predict full failure
	Point or average failure stress criteria, DZM	A semiempirical method for describing the strength of open or filled holes, failure occurs when point or average stress at a characteristic distance from hole equals material strength	<ul style="list-style-type: none"> • Mikulas (8) • Wilson (18) • Daniel (7) • Aronsson (9) 	<ul style="list-style-type: none"> • Valuable for prediction of strength with holes • Requires knowledge of characteristic distances for material • Requires knowledge of stress distribution around hole
Assessment of residual strength	Point failure stress criterion, DZM	Adapted semiempirical method from predicting strength with holes; failure occurs when stress at a characteristic distance from damage radius equals material strength	<ul style="list-style-type: none"> • Mikulas (8) • Starnes (19) • Aronsson (9) 	<ul style="list-style-type: none"> • Valuable for predicting residual strength with impact of through-thickness cracks • Requires knowledge of characteristic distance for material • Requires knowledge of stress distribution around hole • Requires estimation of initial damage size to predict strength
	K_{IC} fracture toughness	Fracture toughness method commonly used with metals	<ul style="list-style-type: none"> • Bathias (20) • McGarry (21) • Awerbuch (22) 	<ul style="list-style-type: none"> • Valuable for predicting residual strength with through-thickness cracks under tension loads • Requires knowledge of K_{IC} for material • Requires estimation of initial crack size to predict strength
	G strain energy release rate	Predicts onset of delamination instability based on G_{IC} for material and G level generated by applied load	<ul style="list-style-type: none"> • O'Brien (23) • Whitcomb (24) • Rothschilds (25) 	<ul style="list-style-type: none"> • Valuable for predicting delamination instability • Requires knowledge of G for material layup • Requires calculation of buckle stability for compression case • At present, can handle only very simple geometries
	CODSTRAN	Integrated computer program that incorporates finite element model, first ply failure, and point or average failure criteria; program is iterative, allowing prediction of failure sequence and residual strength	<ul style="list-style-type: none"> • Chamis (10) 	<ul style="list-style-type: none"> • Attempts to meld various techniques discussed above • Requires expert computer programmer • Requires material data, as described above • Inaccurate prediction of strength

the point of stress necessary to cause failure requires only that values for the characteristic parameter be known. The literature shows that these values have been measured for a variety of layups. However, these characteristic material properties may vary with resin system and environment, making the calculation of residual strength more difficult.

Methods of evaluating the criticality of interlaminar defects has been maturing rapidly in the last five years. To accompany this, researchers have identified characteristic surface morphologies for pure Mode I or Mode II crack growth. Crack growth directions under Mode I loading can be determined quite readily from the surface microfeatures. These emerging technologies in the area of delamination provide the failure analyst with useful tools for determining the cause of a structural failure.

In summary, reviewing the stress analysis literature revealed several techniques for assessing the strength of failed components either as-fabricated, or with through-thickness damage or fracture. These techniques, their value and their limitations are summarized in Table 9-1. Some of these techniques are somewhat inaccurate, or may require measured properties not readily available; however, at the very least, the techniques define the applicable methodologies and their attributes.

Stress Analysis Failure Analysis Logic Network. Defining the cause of component failure requires the accurate understanding of the loads and stresses involved as a part functions. In metals, this understanding is commonplace. Fracture mechanic calculations are usually carried out during initial design stages as well as after component failure. Stress analyses are run after failure to review initial design stresses in more detail, to evaluate configurational and material errors, and to determine if damage (cracking) was incurred in service or during maintenance. The logical investigative sequence for metals and composites is similar. Figure 9-1 illustrates the detailed stress analysis FALN based upon existing metals procedures and inputs from experts in the area of composite materials stress analysis.

Stress analysis of a failed component is carried out at three different levels: initial design review, a structural level, and a lamina level.

At the initial design review, the analyst's objective is to verify initial design assumptions and calculations with respect to the available service history and the location of fracture. This review establishes what analyses were performed and their adequacy.

The next level of investigation encompasses the most critical stage. At the structural level, inputs from the main FALN are incorporated, and detailed strains and stability at fracture origin area are defined. Since most components are designed to gross average strain and stability criteria, the information from this analysis usually provides adequate detail to understand the cause of failure. For the analyst, investigations at this level may involve detailed finite-element modeling, depending upon the level of initial analyses.

Investigation of stress at the lamina level is unique to composite materials. Because of the highly anisotropic nature of laminated composites, internal stresses can exist on a ply-by-ply level, and individual ply stresses and failure predictions can be handled with varying degrees of detail. The simplest level of investigation employs laminate theory combined with relatively simple failure criteria. However, since individual ply failure does not usually constitute catastrophic fracture, additional iterative analyses are required. These analyses can be performed with a variety of computer programs

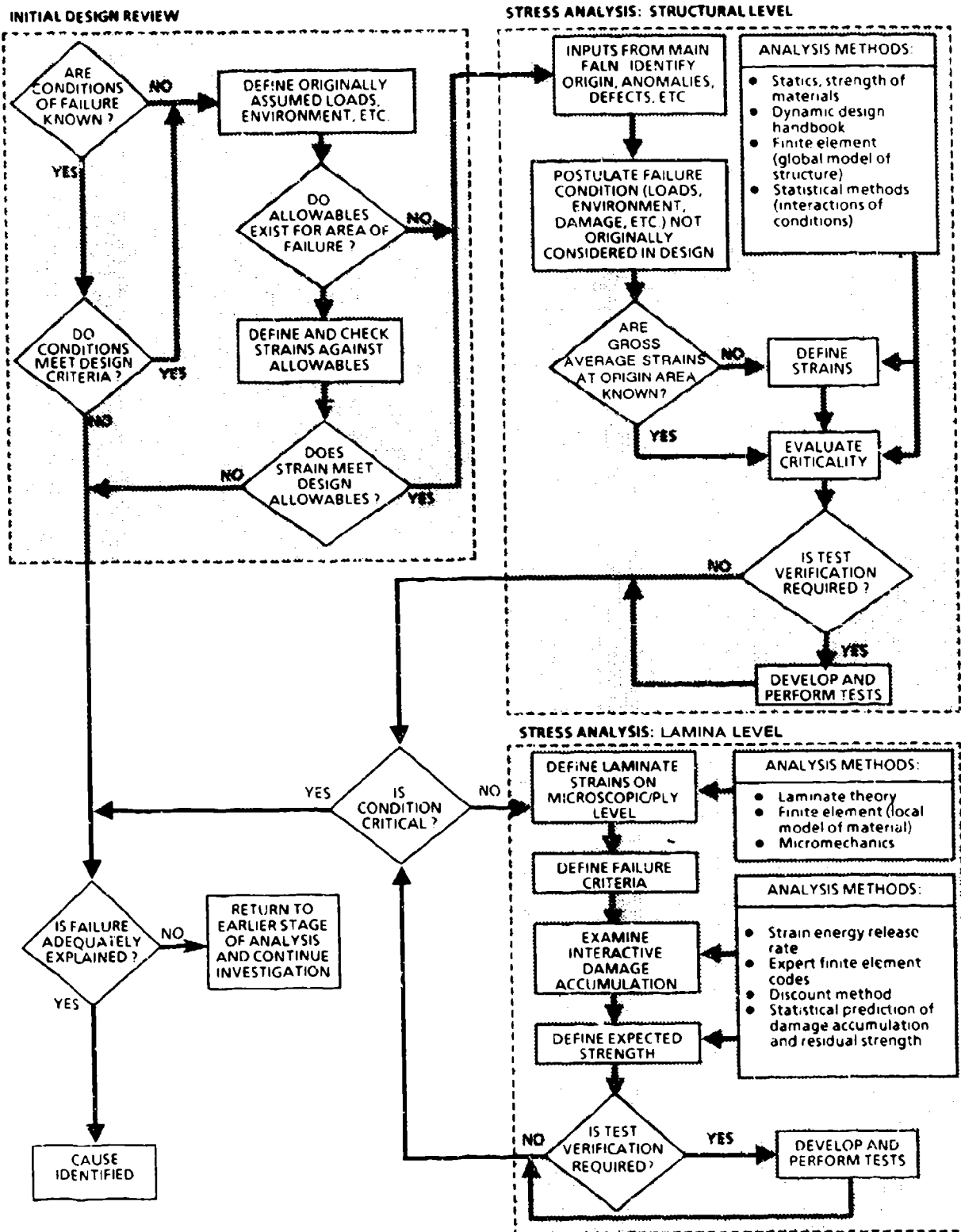


Figure 9-1. Stress Analysis Sub-FALN

(Figure 9-1); however, using such programs requires a detailed understanding of the methods used, their accuracy, and most importantly, their limitations.

9.1.1 Relevance to Stress Analysis FALN

Stress analysis as depicted by the Stress Analysis FALN (see Table 9-2) is conducted at one or more of the following levels of complexity depending on the type of damage and economic considerations: (1) initial design review, (2) a structural level analysis, and (3) a lamina or microstructural level analysis. Throughout the investigation the failure analyst must communicate with the stress analyst to understand how the structure was loaded in the damage region (for example, tension, compression, shear, flexure).

Table 9-2. Computer Analysis Programs

NAME	FEATURES	USER MANUAL	COMPUTER	APPLICATION
AC-50	Inplane laminate allowable stress	Rockwell TFD-75-1180 Nov. 1975	CDC 6600	Advanced composite analysis
NASTRAN	<ul style="list-style-type: none"> Finite element analysis Resize for minimum weight 	NASA SP-222 (01) 1972		Analysis and resizing of complex structures
BOP (Buckling of panels)	Combined compression and shear of stiffened, variable-thickness flat rectangular orthotropic panels on discrete springs	NASA TND-7996 Oct. 1975	CDC 6600	Graphite-epoxy composite panels
SO S	Point stress analysis of laminated composites for: <ul style="list-style-type: none"> Inplane loads Moments Temperature Transverse shear 	AFFDL tech memo FBC-74-107 July 1974	CDC 6600	Advanced composite analysis
STAGS	Stress analysis and panel stability evaluations	Lockheed document, Structural Analysis of General Shells, Volume 3, Dec 1975	CDC 6600	Plotting of buckling mode shapes
VIPASA (Vibration and instability of plate assemblies including shear and anisotropy)	Natural frequencies of loaded structures <ul style="list-style-type: none"> Critical buckling loads Thin, flat rectangular plates Thermal stress 	COSMIC file ISCL Doc ID 00 17437 Jan 1973 NASA TMX-73914 May 1976	CDC 6600	Compression loaded stiffened graphite-epoxy panels

During the initial design review, the stress analyst's objective is to verify initial design assumptions and calculations with respect to the available loading history, the location of fracture, and

environmental conditions. This review establishes what analyses were performed during original design and evaluates their adequacy.

The next level of investigation encompasses the most critical analysis. At the structural level the analyst's understanding of the loads and stresses derived from the initial design review will help evaluate the significance of inputs or anomalies from the main FALN (for example, load types or errors in number of plies or ply orientation). It may be determined that these defects significantly affect the stresses or strengths in the damaged region. In this case, parts of the initial stress analysis would be repeated to assess the impact of the anomalies at the origin of failure. At the structural level, the stress analyst employs finite elements and analytical models to compare the gross average strain to strength critical strain and stability conditions. This information, incorporating the effect of anomalies, usually provides adequate detail to understand the cause of failure. Redesigns at this level of analysis would be focused towards reducing gross average design strain to account for anomalies discovered during the initial design review.

If the cause of failure has not been adequately explained in terms of gross average strains, stress analysis at the microstructural or lamina level is required. This is often the case when failure may have initiated at a design detail such as a hole, edge, or other stress concentrator. At the lamina level, highly refined finite element meshes in the region of failure initiation are employed to determine detailed three-dimensional strain distributions. Loads or displacements applied to the finite element meshes are derived from the stress analysis at the structural level. This detailed type of analysis, although not often done during the initial design, provides information needed to evaluate interlaminar normal and shear stress concentrations at free edges. Fracture mechanics, coupled with finite element analysis, have been successful at predicting the onset of interlaminar crack growth (see Reference 24 and Reference 25). Redesigns, resulting from lamina level studies, may be required to eliminate or reduce the effect of design details that cause stress concentrations.

The thermoelastic properties of the anisotropic, or more specifically, orthotropic plies or lamina can be predicted from the properties of the fiber and matrix constituents with micromechanics. Lamination theory is then employed to calculate the thermoelastic properties of a group of lamina bonded together into a laminate. References (13, 26, 27 and 28) provide lucid descriptions of the limitations and value of lamination theory. Stress analysis of fiber reinforced polymers is quite different than that of metals for the following reasons:

1. Lamina stiffness in the fiber direction is typically greater than 10 times the stiffness transverse to the fibers.
2. Lamina strength in the fiber direction is generally greater than 30 times the strength transverse to the fibers.
3. The differences in the stiffness coefficients between plies within a laminate cause interlaminar stresses.
4. The differences in the hygrothermal expansion coefficients between fiber and matrix within a ply and between plies within a laminate may lead to significant residual stresses due to changes in temperature or moisture content.

Lamination theory can be used to determine the strains and stresses in a composite structure without considering interlaminar stresses. Finite element, finite difference and analytical methods beyond the scope of this text have been used to evaluate interlaminar stresses. However, the failure analyst must recognize that these stresses exist in composite structures and that the resistance to interlaminar crack growth is hundreds of times less than the resistance to transply crack growth. This result is expected since the fracture of fibers requires far greater energy than that needed to propagate an interlaminar crack in which matrix fracture dominates.

9.1.2 Overview of Topics

The following paragraphs provide the failure analyst with an overview of the techniques used to determine the stresses in laminated composites. These tools vary widely in their ease of application and accuracy of results. In addition, it is intended to familiarize the reader with design details, manufacturing and processing defects, and other considerations which must be applied to composite failure analysis.

Paragraph 9.1.3 deals with predicting the strength of unnotched multi-directional laminates with and without edge effects. Criteria for predicting failure of an individual ply are discussed and then applied to predicting laminate strength. Paragraph 9.2 addresses the influence of ply thickness and orientation on transverse cracking and delamination. Paragraph 9.3 describes some of the approaches for predicting reductions in strength caused by inplane stress concentrators such as cutouts and notches are described. Other strength reductions incorporated into design such as environmental effects and impact damage are also discussed. Semi-empirical fracture mechanics and stress based approaches are discussed with respect to their ease of use and generality of application. Paragraph 9.4 discusses, in more detail, design details causing interlaminar stress concentrations (unique to composites), such as holes and free edges. This is important because interlaminar stresses cause delamination to grow under fatigue or static loading leading to significant reductions in compressive strength. Paragraph 9.5 is designed to familiarize the reader with some of the extrinsic factors (for example manufacturing defects) which may reduce the strength of laminated composites. The stress analyst would then evaluate the significance of these factors or anomalies with respect to the cause of failure.

9.1.3 Analytical Prediction of Strength (of Unnotched Multidirectional Laminates)

Methods for predicting the strength of laminates composed of plies at various angles are needed to allow designers to orient the fibers in the load bearing and stiffness critical directions. The methods are semi-empirical in that they rely on measured strengths in the principal material directions for calibration. The theories are focused toward the strength of an orthotropic laminate under in-plane loading. Laminate level analysis is always based on ply level analysis. This is fundamental to the concept of lamination theory.

9.1.4 Individual Ply Failure Criteria

At this level of analysis the failure of an individual ply is predicted in terms of the strengths in the principal material directions and an appropriate failure criterion. The overview presented here is drawn from the excellent discussions given in References 13, 14, and 26.

Maximum Stress and Maximum Strain Theories. The maximum stress theory states that fracture occurs when the stress in any of the principal laminate orientations exceeds its respective strength. This criterion defines a failure envelope described by the following equations:

$$\sigma_1 < X^t \text{ for } \sigma_1 > 0 \text{ and } |\sigma_1| < X^c \text{ for } \sigma_1 < 0 \quad (\text{Eq. 6})$$

and

$$\sigma_2 < Y^t \text{ for } \sigma_2 > 0 \text{ and } |\sigma_2| < Y^c \text{ for } \sigma_2 < 0 \quad (\text{Eq. 7})$$

and

$$\sigma_{12} < S \quad (\text{Eq. 8})$$

where:

σ_1 = stress along the fiber direction

σ_2 = stress transverse to fiber direction

σ_{12} = in-plane shear stress

X^t, X^c = tension and compression strength along the fiber direction

Y^t, Y^c = tension and compression strength transverse to the fiber direction

S = in-plane shear strength

For in-plane loading of an off-axis ply, the principal stresses can be calculated by the transformation equations below and then substituted into the failure criteria in the previous equations.

$$\sigma_1 = M^2\sigma_x + n^2\sigma_y + 2mn\sigma_{xy} \quad (\text{Eq. 9})$$

$$\sigma_2 = N^2\sigma_x + M^2\sigma_y - 2mn\sigma_{xy} \quad (\text{Eq. 10})$$

$$\sigma_{12} = -MN\sigma_x + mn\sigma_y + (m^2 - n^2)\sigma_{xy} \quad (\text{Eq. 11})$$

where:

$m = \cos$

$n = \sin$

An analogous failure criterion in terms of strains (see Reference 13) generates strength predictions in close agreement with the maximum stress theory. Figure 5-2 illustrates data taken by Tsai (Reference 29) that shows there are significant discrepancies between theoretical strength predictions based on the maximum stress failure criteria and experimental data for glass/epoxy. This is expected since interactions between stress components are not accounted for.

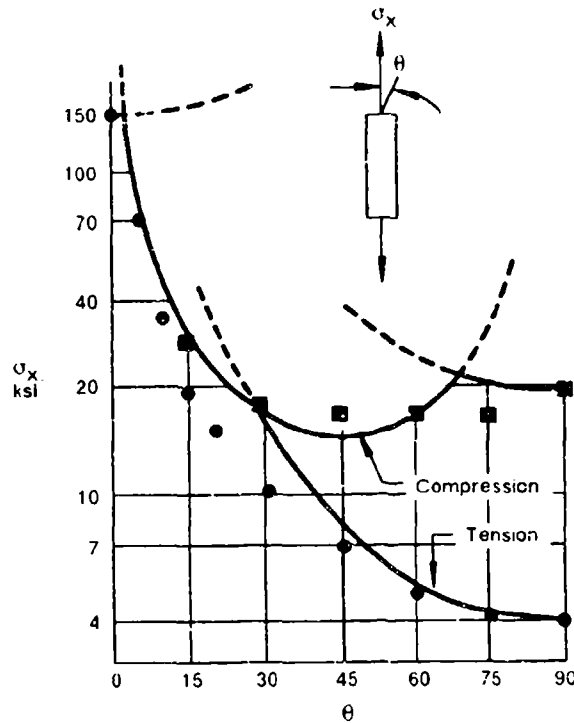


Figure 9-2. Maximum Stress Failure Theory

Tsai-Hill Theory. A strength criterion based on von Mises' isotropic yield criterion was proposed by Hill (Reference 30) for anisotropic materials. For biaxial loading and plane stress conditions, lamina failure would occur when,

$$\frac{\sigma_1^2}{X^2} - \frac{\sigma_1 \sigma_2}{(X)^2} + \frac{\sigma_2^2}{Y^2} + \frac{\sigma_{12}^2}{S^2} = 1 \quad (\text{Eq. 12})$$

where:

$X = X^t$ when σ_1 is positive

$X = X^c$ when σ_1 is negative

$Y = Y^t$ when σ_2 is positive

$Y = Y^c$ when σ_2 is negative

X^t, X^c = tension and compression strength along the fiber direction

Y^t, Y^c = tension and compression strength transverse to the fiber direction

S = in-plane shear strength.

The Tsai-Hill strength criterion for uniaxial loading of an off-axis ply is developed by substituting Equations (9), (10), and (11), into Equation (12). The resulting criterion shown below provides an excellent fit to the experimental data for glass/epoxy (Reference 29) as shown in Figure 9-3.

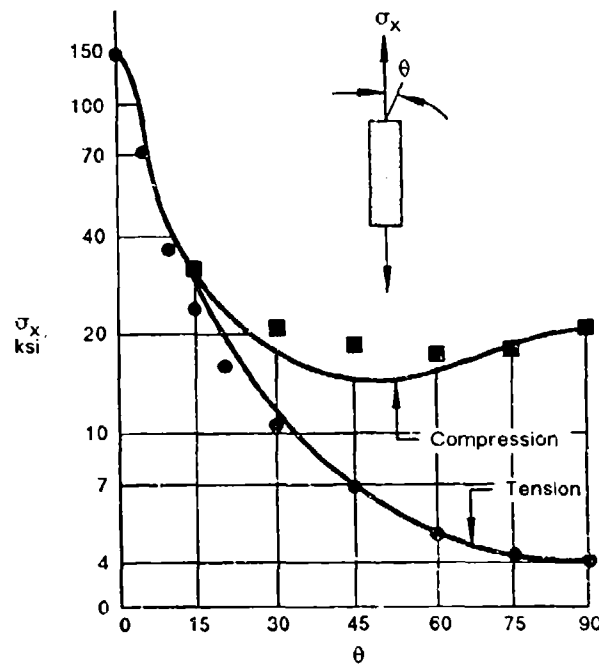


Figure 9-3. Tsai-Hill Theory

$$\frac{m^4}{(X)^2} + \frac{m^2 n^2}{(X)^2} + \frac{n^4}{(Y)^2} + \frac{m^2 n^2}{S^2} = \frac{1}{(\sigma_x)^2} \quad (\text{Eq. 13})$$

It should be noted that the Tsai-Hill criterion provides for interactions between stresses and yields a smooth curve when compared to the maximum stress or strain criteria. However, von Mises isotropic yield criterion and hence the Tsai-Hill theory is related to distortional energy as opposed to dilatational (volume change) energy. The disadvantage to Tsai-Hill's criterion is that biaxial loading of orthotropic materials always causes distortional and dilatational energy. Hence failure may not be directly related to distortional energy as it was for isotropic materials. A more general strength criterion including additional interaction terms is discussed in the next paragraph.

Tsai-Wu Quadratic Interaction Failure Criterion. The Tsai-Wu strength criterion reduces to the equation below for inplane loading of a thin (plane stress conditions) orthotropic ply.

$$F_{11}\sigma_1^2 + F_{22}\sigma_2^2 + F_{66}\sigma_6^2 + 2F_{12}\sigma_1\sigma_2 + F_1\sigma_1 + F_2\sigma_2 + F_6\sigma_6 = 1 \quad (\text{Eq. 14})$$

and

$$F_1 = \frac{1}{x^t} - \frac{1}{x^c}$$

$$F_2 = \frac{1}{y^t} - \frac{1}{y^c}$$

$$F_6 = 0$$

$$F_{11} = \frac{1}{X^t X^c}$$

$$F_{22} = \frac{1}{Y^t Y^c}$$

$$F_{66} = \frac{1}{S^2}$$

where X^t , X^c , Y^t , Y^c , and S have the same meanings as denoted previously.

F_{12} , which represents the interaction between normal stresses, must be determined by performing a biaxial stress test. Since this test is relatively complicated, it has been recommended in References 13 and 26 to use:

$$F_{12} = F_{xy} (F_{11} F_{22})^{\frac{1}{2}} \quad (\text{Eq. 15})$$

where:

$$F_{xy} = -0.5$$

It should also be emphasized that for uniaxial loading of a unidirectional lamina the failure strength is insensitive to values of F_{12} within the stability limits in the following equation.

$$-(F_{11} F_{22})^{\frac{1}{2}} < F_{12} < (F_{11} F_{22})^{\frac{1}{2}}$$

This insensitivity is demonstrated in Figure 9-4 where predicted strengths are in excellent agreement with experimental data for boron/epoxy (Reference 31). Figure 9-4 also demonstrates that for uniaxial loading there is little difference between the Tsai-Hill and Tsai-Wu criteria. Although the Tsai-Wu strength theory is more complicated, the well founded mathematical operations of tensor theory can be used to transform the strength parameters in these equations. This is important since it leads to straightforward computer implementation. References 13 and 26 provide invaluable discussions and examples on the Tsai-Wu strength theories in terms of stress and an analogous strain criteria.

Christensen has recently developed a new failure criterion for continuous fiber composites that represents a major departure from traditional analyses (Reference 32). This theory was developed from an effort to extend conventional laminate theory to thick composite sections. To include out-of-plane stresses that are present in thick laminates, Christensen postulated the simplifying assumption that the out-of-plane stresses in a laminate were independent of the orientation of the fibers. In doing so, Christensen reported that the failure criterion consisted of one in which fiber-dominated failure could be separated from matrix failure, and matrix-interface failure. Thus fiber failure and matrix failure could be treated as two separate events. A more detailed summary of this theory has been presented in Volume I, Appendix A, of this report.

Lamina level strength theories presented in these paragraphs differ primarily in the number of empirically determined coefficients used in the curve fitting equations. The relatively simple maximum stress or strain criteria indicate the failure mode while the others do not. However, the Tsai-Hill and

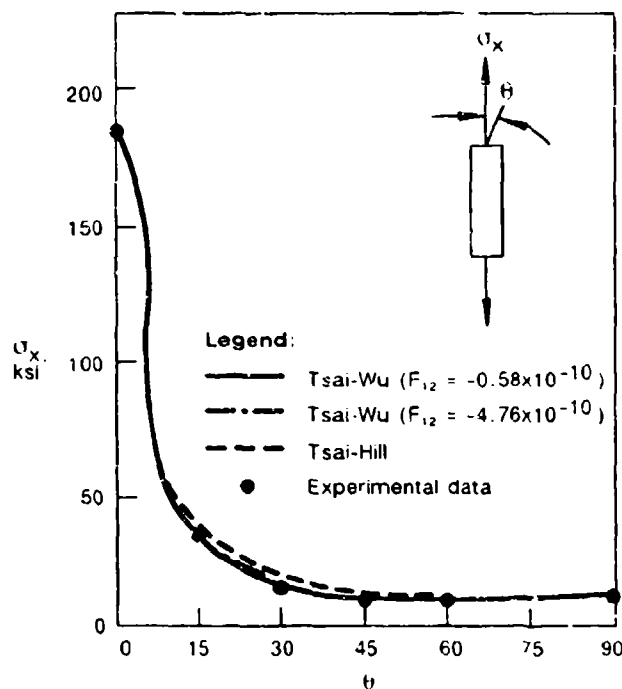


Figure 9-4. Tsai-Wu Tensor Theory

Tsai-Wu strength criteria are recognized as useful design tools. Predicting strength using the strain based analogies of the theories presented here is a generally accepted practice in the aircraft industry. This results from the fact that design allowables are given in terms of strain. The lamina strength theories in this paragraph will be applied to predicting laminate strength in the next paragraph.

9.1.5 Laminate Level Strength Criteria

First Ply Failure. At some point during loading of a multidirectional laminate, the ply or group of plies with the lowest strength will start accumulating damage. This event, often described as first ply failure, can be predicted using the lamina level theories presented in this section. Figure 9-5 shows a comparison between predicted strengths for plies in a uniaxially loaded multidirectional graphite/epoxy laminate based on the quadratic interaction criterion (Reference 33). It is seen that first ply failure (that is, the 90-degree plies) occurs at a lower load level than catastrophic laminate failure. This is expected, since load shedding from the damaged 90-degree plies to the rest of the plies continues until the laminate cannot carry additional load. In this case, a more accurate, but nonconservative, prediction of the strength would be based on the strength of the 0-degree plies as shown in Figure 9-5. The first ply failure envelope for a multidirectional laminate is the intersection of the failure envelopes for each ply angle in the laminate. This is shown schematically in Figure 9-6 based on the quadratic interaction criterion and ply strength data from (Reference 13).

Ply Discount Methods. First ply failure is quite conservative because the initial damage in a multidirectional laminate is cracks running parallel to the fibers. These cracks are modeled by reducing the matrix modulus of the cracked ply group. Micromechanics (References 13 and 26) can then be used

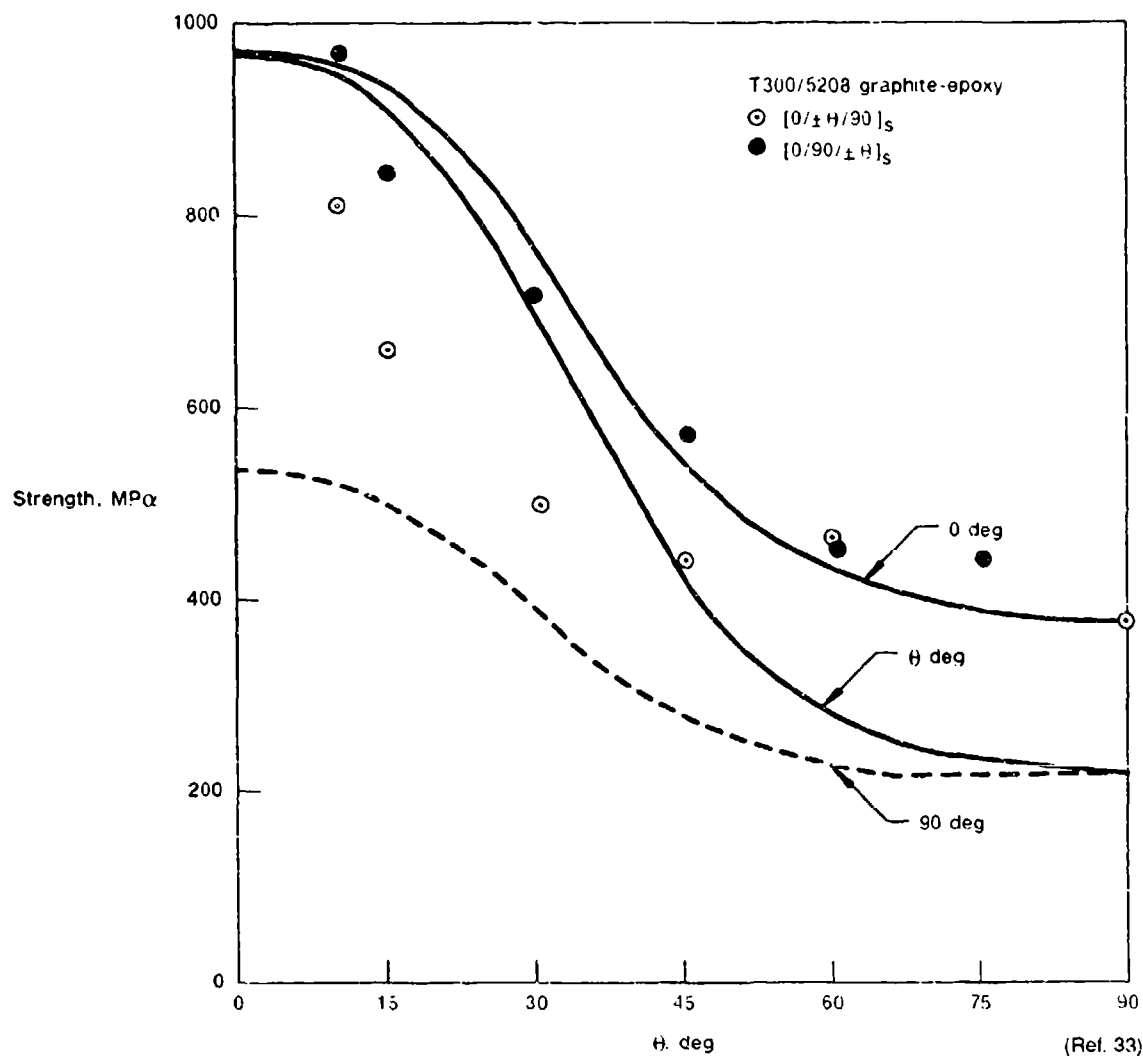


Figure 9-5. Comparison of Calculated In-plane Tensile Strength With Experiment

to calculate the reduced transverse and shear modulus of the plies. In the next step, lamination theory is employed to predict the redistribution of loads within the laminate. Loads are then reapplied incrementally until compressive or tensile fiber failure occurs. Since the fibers carry most of the load, this point often corresponds to the peak load or strength of the laminate. Ply discount methods incorporating the effect of hygrothermal stresses are being used with limited success by designers.

It should be noted that these methods are based on lamination theory which does not account for the interlaminar stress concentrations at the free edges. Transverse cracks also cause interlaminar stress concentrations which may lead to delamination and significant reductions in laminate strength. Two or three dimensional finite element modeling, discussed in the next paragraph, is one of the methods employed to investigate these microstructural failure modes.

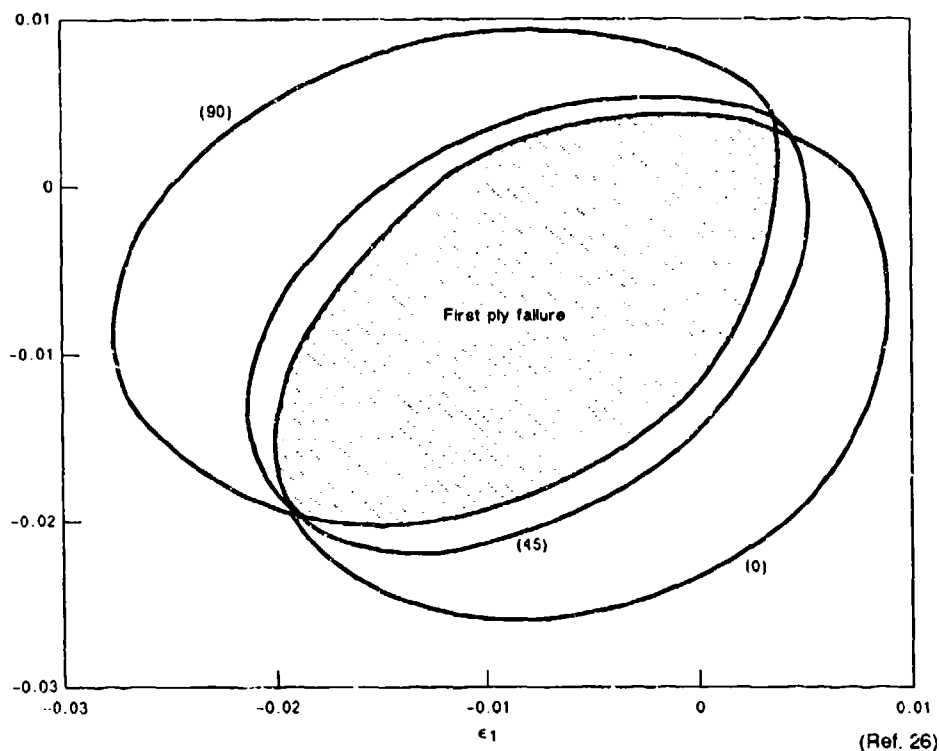


Figure 9-6. Quadratic Interaction First Ply Failure Envelope for T300/5208

Finite Element Modeling. Incorporating the effects of free edge interlaminar stress concentrations with environmental and cure stress considerations represents the next level of complexity in predicting failure onset using individual-ply failure criteria. For the failure analyst, these works are useful in that they embody considerations likely to be necessary with real-world structures. Both Crossman and Herakovich (References 15 and 16, respectively) observed that significant variations in stresses and strains can occur at the free edge of specimens. Both authors show the magnitude of these stresses for relatively simple layups and specimen geometries. Generally, the most significant stresses are those developed near the specimen's free edge. In analyzing these stresses, both authors employed two dimensional finite-element grids arranged along the specimen cross-section. Using these grids illustrates the degree of complexity involved in determining the interlaminar stresses (or strains) in microscale with such design details. As noted by Crossman, particularly large gradients can occur in both Z and Y directions near the free edge (Figure 9-7). Regarding the application of individual-ply failure criteria, the large increase in σ_z , σ_x and τ_{xz} stresses near the edge of the specimen are particularly significant, since laminate theory methods would have ignored these increases.

Furthermore, Crossman and Herakovich predicted that stresses would be further influenced by internal cure stress, test temperature, and conditions of moisture absorption or desorption (Figure 9-8). In Herakovich's work, the relationship of these stresses to failure prediction were considered. Since his finite-element model examined stresses along three dimensions, it was necessary to develop a full three-dimensional failure criterion. Herakovich used the tensor polynomial criteria advanced by Tsai-Wu, in which strength tensors are given in terms of material principal strengths. As illustrated in Figure 9-9, Herakovich predicted that the onset of failure depends quite strongly on edge stresses,

particularly for small ($\pm \theta$) laminate angles. While not verified against actual test data, these results, when considered with Crossman's, clearly indicate that both edge and environmental stress effects must be carefully evaluated in predicting the onset of failure for whichever individual-ply criteria are employed.

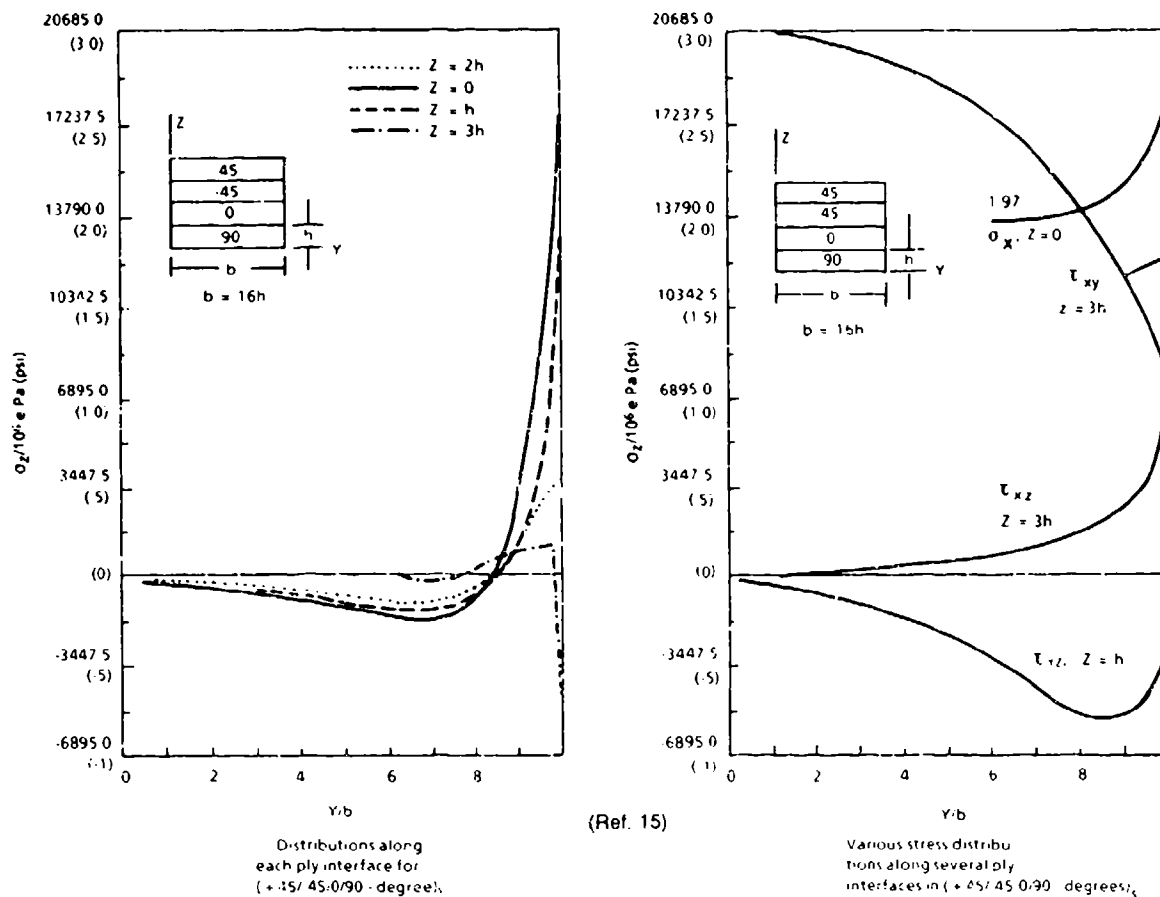


Figure 9-7. Stress Gradients Resulting From Edge Effects

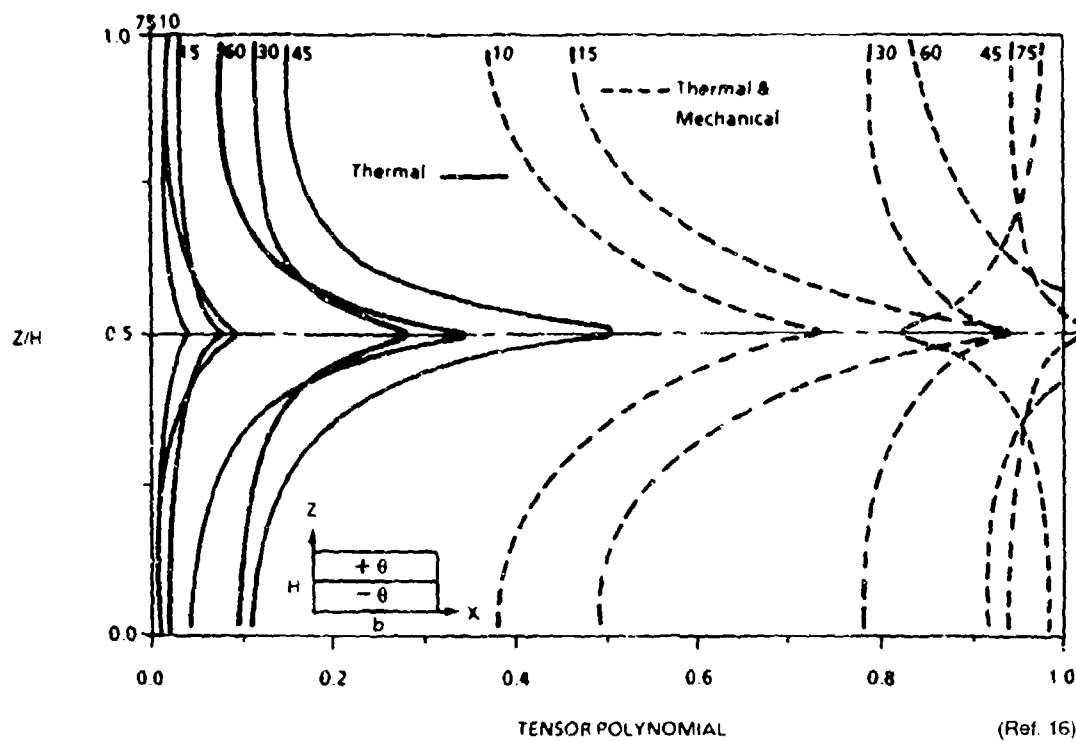


Figure 9-8. Through-Thickness Tensor Polynomial Distributions for Curing Stresses and Stresses at the First Failure (+/-) Laminates

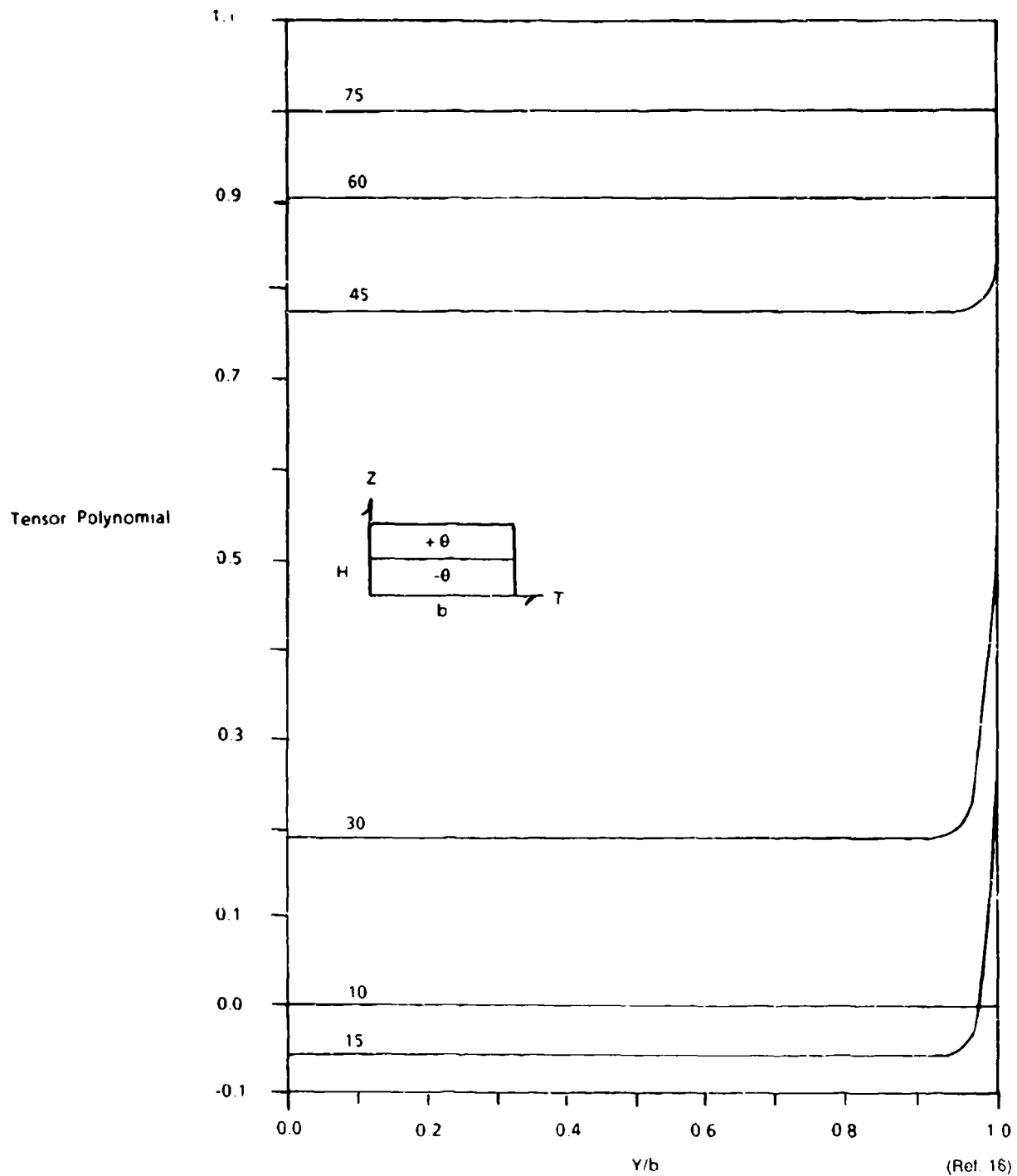


Figure 9-9. Tensor Polynomial Distributions Along the Interface of (+/-) Laminates

Perhaps the farthest advancement of first-ply failure criteria as a method of prediction has been made by Chamis (Reference 10). In attempting to predict the defect growth and damage of composite materials subjected to load, Chamis developed an integrated computer program called CODSTRAN. Within this program, a detailed finite-element grid is constructed and evaluated for failure using both individual first-ply failure criteria and laminate-level fracture criteria. In the case of individual-ply failures, Chamis' program incorporates both general quadratic and modified distortional energy (Von Mises') criteria to predict the occurrence of failure for each element of the overall finite element model. What is unique about Chamis' work, however, is that failed-ply elements are eliminated, and the analysis process is reiterated. As a result, CODSTRAN describes the sequence of events leading to failure, and an approximate prediction of the load at failure.

9.1.6 Summary – Unnotched Laminate Strength

The failure modes of composites are far more complex than those discussed in these paragraphs. At the ply-level, Tsai-Wu's quadratic interaction failure criterion seems to provide sufficiently accurate results for unidirectional laminate strength under biaxial loading. Prediction of multidirectional laminate strength is quite complex since free-edge interlaminar stress concentrations and hygrothermal stresses must be considered. Finite elements and interactive ply discount methods have been used with limited success.

It can be seen from the discussions above that computers play an important role in the stress analysis of composites. Lamination theory predictions of stiffness and the laminate strength theories discussed here have been implemented on microcomputers (that is, References 26 and 34).

The methods presented in the following paragraphs can provide criteria for selecting the laminate geometry providing optimum strength in the load bearing directions. However, predictions of laminate strength, at this time, are not quantitatively accurate. Thus, the designer must rely on coupon or full scale tests to determine the actual strength for a particular laminate geometry. This requires large and expensive databases to design structural composite parts. If needed, the failure analyst should consult designers or stress analysts to find out what methods were used to establish the allowables. The overview presented in this section is intended to familiarize the reader with some of the considerations, many of which are unique to composites, that must be applied to predicting laminated composite strength.

9.2 INFLUENCE OF PLY THICKNESS ON TRANSVERSE CRACKING

In the previous paragraph, it was noted that transverse cracking and free-edge delamination reduce laminate strength. In this paragraph, the influence of ply thickness and orientation on these microstructural failure modes is discussed. It is intended to provide the reader with an introduction to microstructural failure features unique to laminated composites.

In the previous paragraphs, the strain required to cause cracks parallel to the fibers (transverse matrix cracking) was assumed equal to the transverse failure strain of a 90-degree ply. However, it has been shown by numerous researchers (References 35 to 39) that the strain to cracking of an off-axis ply group depends upon its thickness. Flaggs and Kural (Reference 55) have clearly demonstrated that the in situ strain to cracking decreases as the thickness of an off-axis ply group (30-, 60- or 90-degree)

increases (see Figure 9-10). The fact that the in situ strength of a 90-degree ply is greater than that of a laminate composed only of 90-degree plies has been attributed to the constraint provided by the stiffer surrounding ply groups. Flaggs (Reference 39) used a fracture mechanics approach combined with 2-D shear lag analysis to successfully model the in situ strain to cracking as shown in Figure 9-10. This model has also been applied successfully to predicting in situ cracking of 30- and 60-degree ply groups (Reference 39).

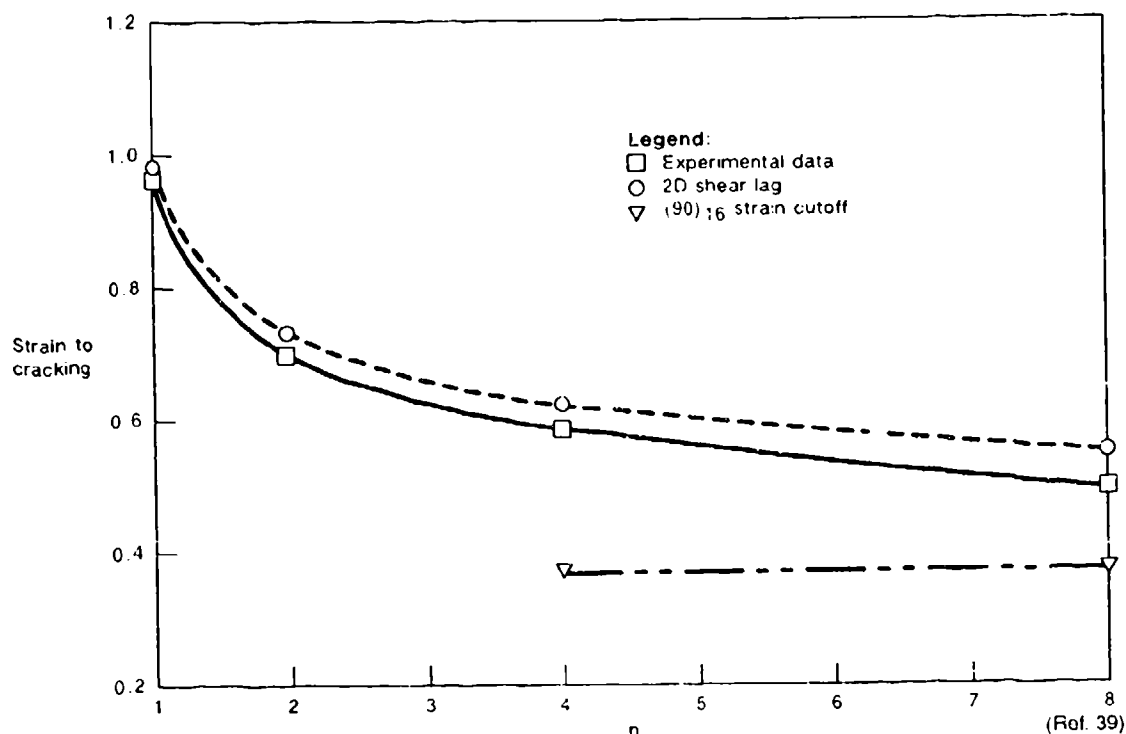


Figure 9-10. Comparison of Experimentally Derived In Situ Lamina Elastic Strains at Onset of Matrix Cracking With 2D Shear Lag Model Predictions for (0/90) T300/934 Laminate Family

With this type of analysis, the first ply failure predictions of laminate strength could be made more accurate. To accomplish this, Flaggs' model would be used to predict the in situ strain to cracking of the off-axis ply groups in a multidirectional laminate. Then these strains would be used as the strain to failure transverse to the fibers in the lamina level failure models. This represents an effort to integrate the prediction of microstructural failure with gross laminate failure features.

9.3 STRENGTH REDUCTIONS INCORPORATED INTO DESIGN

The methods described in Section 9 are commonly used to predict the strength of an unnotched laminate (that is, without in-plane stress concentrations). However, composite structural components may contain cutouts, fastener holes, or impact damage which reduce the in-plane strength below that of the virgin laminate. These laminates must be designed "a priori" such that the residual strength will be greater by some safety factor than the operating stresses. Some of the more popular approaches applied to predicting residual strength are reviewed in the following paragraphs.

Most of the analytic techniques for predicting residual strength employ semi-empirical approaches similar to the fracture toughness methods commonly used with metal structures. These methods typically involve the experimental determination of an intrinsic material property related to crack growth — such as material fracture toughness. This value, when considered with the size and geometry of the flaw, allows the stress at the fracture to be calculated.

The anisotropy of composites complicates the analyses considerably. Critical stress intensity factors used in metals analysis are independent of the direction of crack growth. However, the translaminal toughness of composites may be hundreds of times greater than the interlaminar toughness. This is expected since breaking fibers is a much higher energy fracture mode than matrix cracking. Often, the interaction of these two failure modes occurs as in impact damage. In this case the assessment of residual strength becomes so complicated that the designer must rely on empirical data. However, when the translaminal and interlaminar modes are acting independently, the rapidly maturing fracture mechanics approach for composites are being used successfully.

Notched Laminate Strength. The easiest-to-understand methodologies for determining laminate failure are those adapted directly from metals fracture toughness analyses.

These analyses predict the onset of component fracture through the experimental determination of a characteristic K_{Ic} fracture toughness value. In these cases, K_{Ic} indicates the stress intensity factor at which fracture occurs, based on the initial crack length and maximum load at failure. (For reference, this value is often referred to as $K_{Ic,apparent}$ in metals fracture toughness.) In works by Bathias (Reference 20), McGarry (Reference 21), and Awerbuch (Reference 22), K_{Ic} values have been determined for a variety of layups. In measuring values, these researchers used specimens adapted directly from traditional metals toughness testing, such as compact tension coupons or large center-crack tension panels. In Bathias' work, K_{Ic} values were measured for a variety of layups. As illustrated in Table 9-3, values ranging from 16 to 43 MPa times the square root of m were measured, and demonstrated a clear dependence on the ply stacking sequence and orientations examined. (For 7075-T7351 aluminum, K_{Ic} typically equals 80 to 90 MPa times the square root of m.) Each author suggests that knowledge of this material property for a layup can be used to estimate the stress at fracture instability for a given crack and component geometry.

Table 9-3. Fracture Toughness of Various Orientations

FRACTURE TOUGHNESS (MPa√m)	LAYUP (DEGREES)		
	0/45/90/135/90/45/0 16 plies	0/30/60/90/120/150/0 13 plies	0/45/135/0/135/45/0 16 plies
K_{Ic}	29-43	23-35	16-22

(Ref 20)

This point of instability can be defined by using the equation:

$$K_{Ic} = Y\sigma_c \text{ times the square root of } \pi a \quad (\text{Eq. 17})$$

where:

Y = geometric factor related to the crack length and location within component being examined

σ_c = stress at instability

a = full crack length

K_{Ic} = material fracture toughness

A more detailed review of this technology can be found in any of several texts dealing with the fracture behavior of metals.

Numerous researchers have also attempted to predict the criticality of holes, cracks, and damage by empirically measuring other characteristic fracture properties, in much the same way as is done with fracture toughness (References 7 to 9 and 40 to 51). Two of the significant efforts include failure criteria which assume failure occurs when the stress at some distance away from the flaw reaches the ultimate material strength. These two are the average stress, and the point stress failure criteria models presented by Whitney and Nuismer (References 43, 44). As described in Daniel's paper (Reference 7), the average stress failure criterion proposes that failure occurs when the average stress over a characteristic material dimension (a_0) equals the material strength. This criterion is illustrated in Figure 9-11, where a_0 represents the length dimension of a particular layup and material. Similarly, the point-stress failure criterion presented by Mikulas (Reference 8) predicts that panel failure occurs when the axial stress at some distance (d_0) from the hole boundary equals the strength of the unnotched laminate as shown in Figure 9-12. Daniel, Mikulas, and other investigators measured both a_0 and d_0 for a variety of layups and found a relatively good correspondence of predicted and measured strengths for open holes (Figure 9-13). The disadvantage of the point or average stress criteria is that they require different characteristic lengths for various notch sizes in the same type laminate (References 45 to 48).

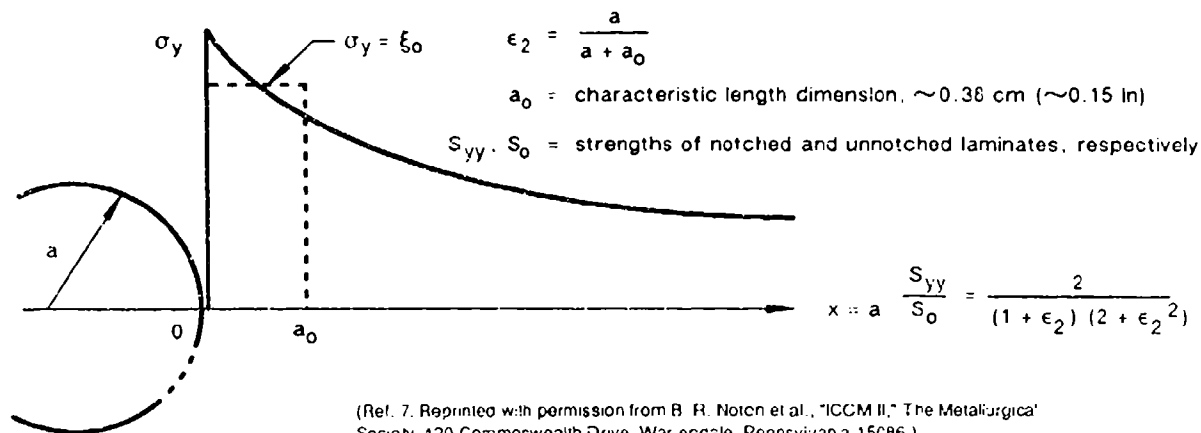


Figure 9-11. Strength Reduction of Uniaxially Loaded Plate With Circular Hole According to Average Stress Criterion

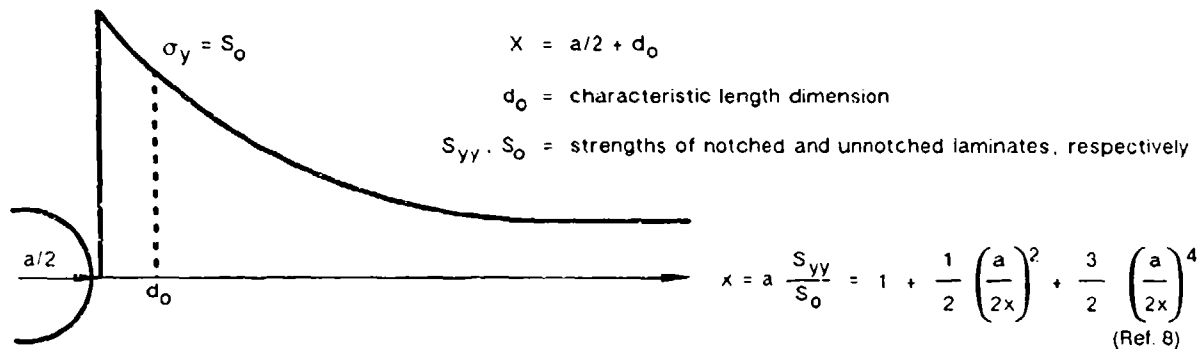
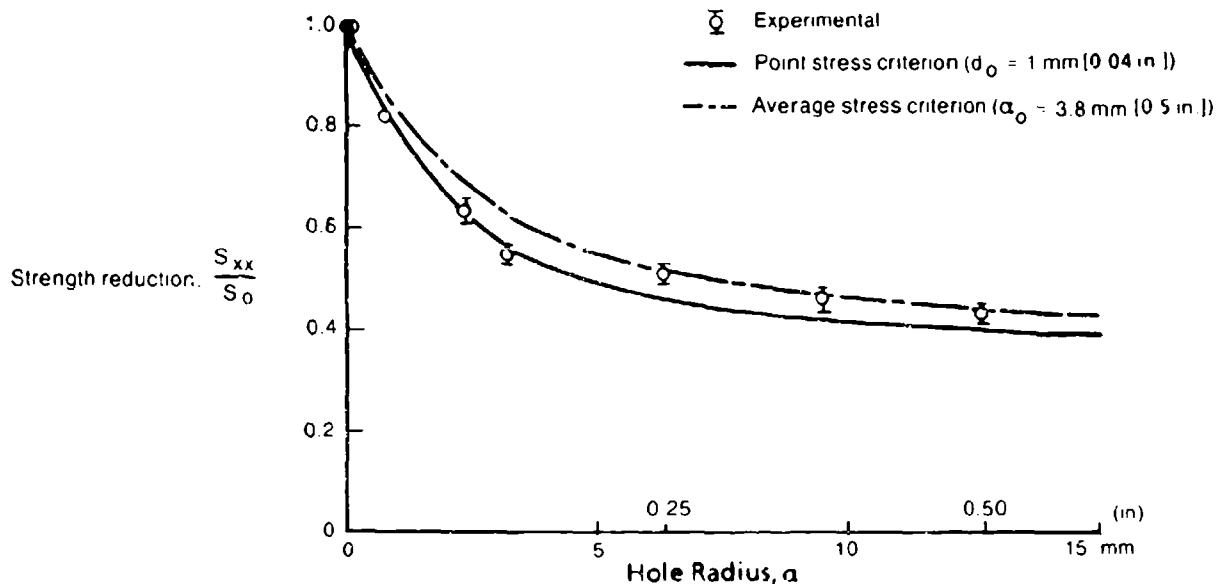


Figure 9-12. Strength Reduction of Uniaxially Loaded Hole According to Point Failure Stress Criteria



(Ref. 7. Reprinted with permission from B. R. Noton et al., "ICCM II," The Metallurgical Society, 420 Commonwealth Drive, Warrendale, Pennsylvania 15086.)

Figure 9-13. Strength Reductions as a Function of the Hole Radius for $(0/+45/-45/90 \text{ deg})$ Graphite-Epoxy Plates With Circular Holes Under Uniaxial Tensile Loading

The more general Damaged Zone Model discussed by Aronsson in (Reference 9) requires only basic laminate properties (strength and stiffness) and the apparent fracture energy to predict the fracture behavior of brittle and ductile notched three point bend specimens.

In this model, the damaged (as opposed to a crack in metals) zone which develops in composites around a crack or hole is modeled by a crack with cohesive stresses acting on its surfaces. As the applied load is increased, the damage grows. This is approximated by reducing the cohesive forces on the cracked region in the model. The Damaged Zone Model (DZM) and the Point Stress Criteria (PSC) (Reference 9) accurately predict the failure load for brittle and ductile matrix three-point bend

specimens. The real utility of the DZM lies in its ability to analyze complex geometries. The PSC, which relies on exact calculations of the stress distribution around a flaw, is limited to very simple flaw geometries such as holes. Tensile failure loads have been predicted by the DZM to within 10 percent of the experimental values for laminates with the hole geometries in Figure 9-14 (Reference 52). The DZM should be a tool for the aerospace industry that can be used for predicting the residual strength of laminates with cutouts.

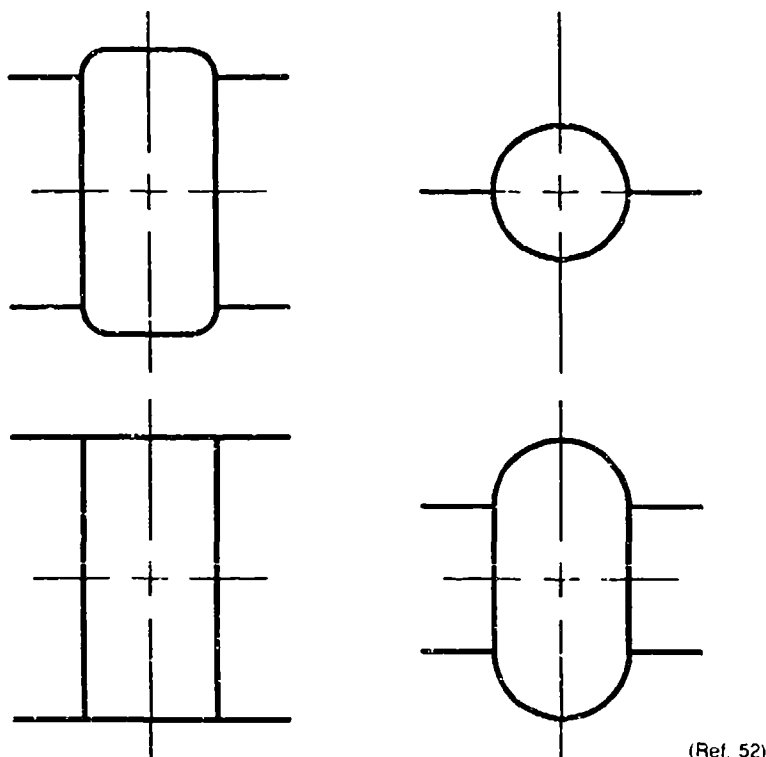


Figure 9-14. Hole Geometries Analyzed With the Damaged Zone Model (DZM)

Of particular concern to the failure analyst, however, is the ability to predict failure onset for flaw conditions such as through-cracks or impact damage. In this area, Mikulas (Reference 8) examined the applicability of the point stress failure criteria; for the case of a through-crack, stress as a function of distance from the crack was expressed as:

$$\frac{\sigma_y}{\sigma_\infty} = \frac{X}{\text{the square root of } X^2 - \left(\frac{a}{2}\right)^2} \quad (\text{Eq. 18})$$

where:

$$x = X_1 + \frac{a}{2}$$

X = distance along the x-axis, away from the crack

a = crack length

σ_∞ = stress at infinite distance from crack

σ_y = stress in the y direction

As a result, Mikulas indicated that the residual strength for a given crack of size a can be determined if X is set equal to d_0 .

With respect to impact damage, Mikulas reported that the characteristic length d_0 depends on the toughness of the resin system examined. As illustrated in Figure 9-15, a relatively good correlation exists for tough resin chemistries, but not for brittle, delamination-prone resin systems. These observations indicate that the accuracy of failure predictions will depend strongly on the resin system used, and the configuration of damage examined. An excellent discussion of impact damage with respect to failure modes and the effects of resin toughness has been given by Starnes, Williams, and Rhodes in References 19, 53, 54, and 55. Their studies have clearly shown that:

1. Tough resins reduce the size of the damage zone caused by impact
2. Several graphite/epoxy systems with varying toughness exhibited similar residual post-impact compression strength for the same damage zone size
3. The dominant failure mechanisms causing post-impact compression failure are delamination and shear crippling.

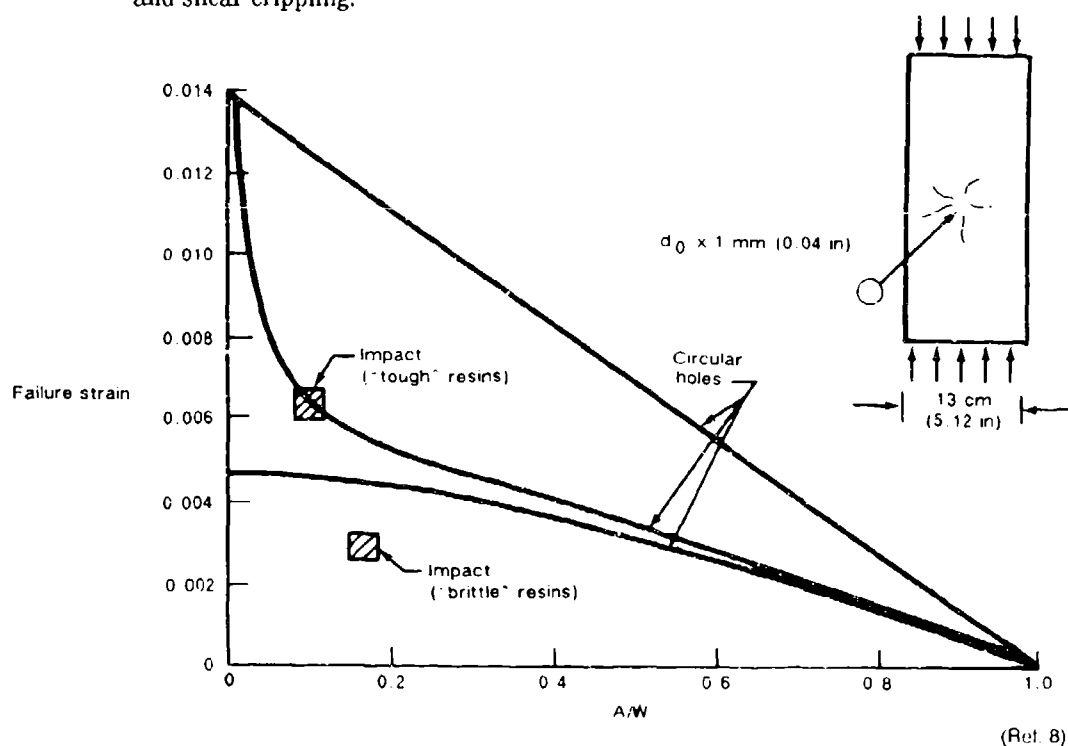


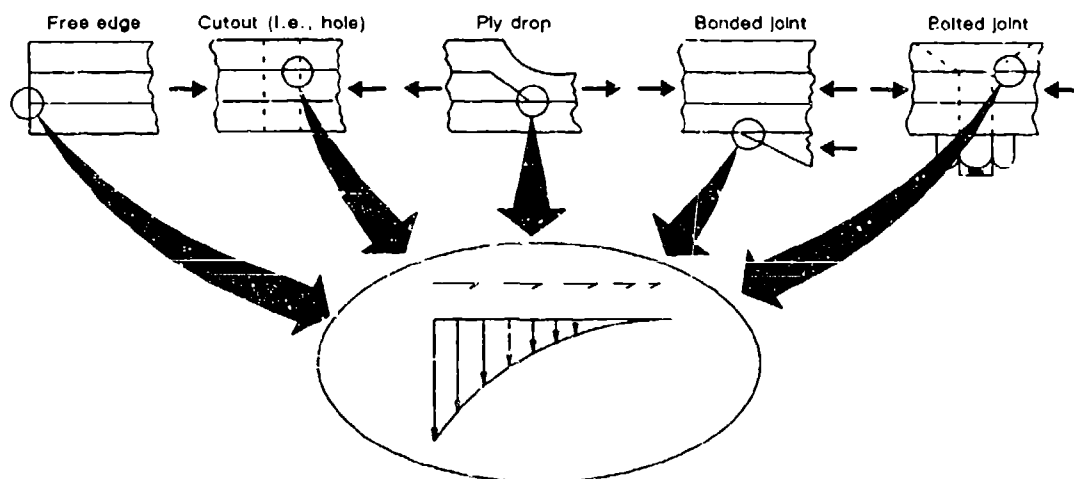
Figure 9-15. Effect of Impact Damage on the Compressive Strength of a Quasi-Isotropic Laminate (Ref. 8)

9.4 INTRODUCTION TO DELAMINATION

While the works discussed earlier in this section examined the residual strength of the laminates with trans laminar through-thickness flaws, other investigators have considered the criticality of interlaminar defects. This paragraph has been included to acquaint the reader with some of the

significant results and tests applicable to assessing the criticality of interlaminar defects in composites. Delaminations may grow and initiate component failure due to sudden loss of stiffness and strength. Fractography can be used to detect delamination and interlaminar crack growth directions, but the methods discussed here can be employed to evaluate the criticality of delaminations.

As a result of processing and service conditions, delaminations may be introduced into composite structures. Fatigue and static loading of laminated composite structure may initiate delaminations near interlaminar stress concentrations. Some of the common design features found in composite structures such as bolted joints, ply drops, and cutouts contain interlaminar stress concentrations (see Figure 9-16). In addition, multiple delaminations represent characteristic post-impact damage. Local instability of a delaminated subregion in composite structures under compressive loading precipitates out-of-plane deformations and may lead to subsequent crack growth. Under these circumstances, it has been well documented that structural strength and stiffness reductions are significant (References 57 to 65).



(Ref. 53)

Figure 9-16. Design Details That Cause Interlaminar Stress Concentrations

9.4.1 Fracture Analysis and Specimens (For Interlaminar Toughness)

In the presence of interlaminar stress singularities, the fracture mechanics approach is now frequently used to assess defect criticality in composites. Double cantilever beam (DCB), Mode I, and end notched flexure (ENF) Mode II specimens, as shown in Figure 9-17 (a and b), are being used to evaluate the pure mode critical strain energy release rates. Strain energy release rates are utilized in these pure mode tests because G is a physically well defined quantity experimentally measurable with compliance calibration techniques. But, in general, cracks in composite structures are subjected to all three modes of loading at the crack tip as shown in Figure 9-18.

To study mixed-mode crack growth criteria, the imbedded through-width delamination (ITWD) and cracked lap shear (CLS) specimens shown in Figure 9-19 have been used by a number of researchers.

The opening moment and the eccentricity in load path at the crack tip of the CLS and ITWD specimens are the mechanisms causing interlaminar normal (Mode I) and shear (Mode II) stress concentrations (see Figure 9-20).

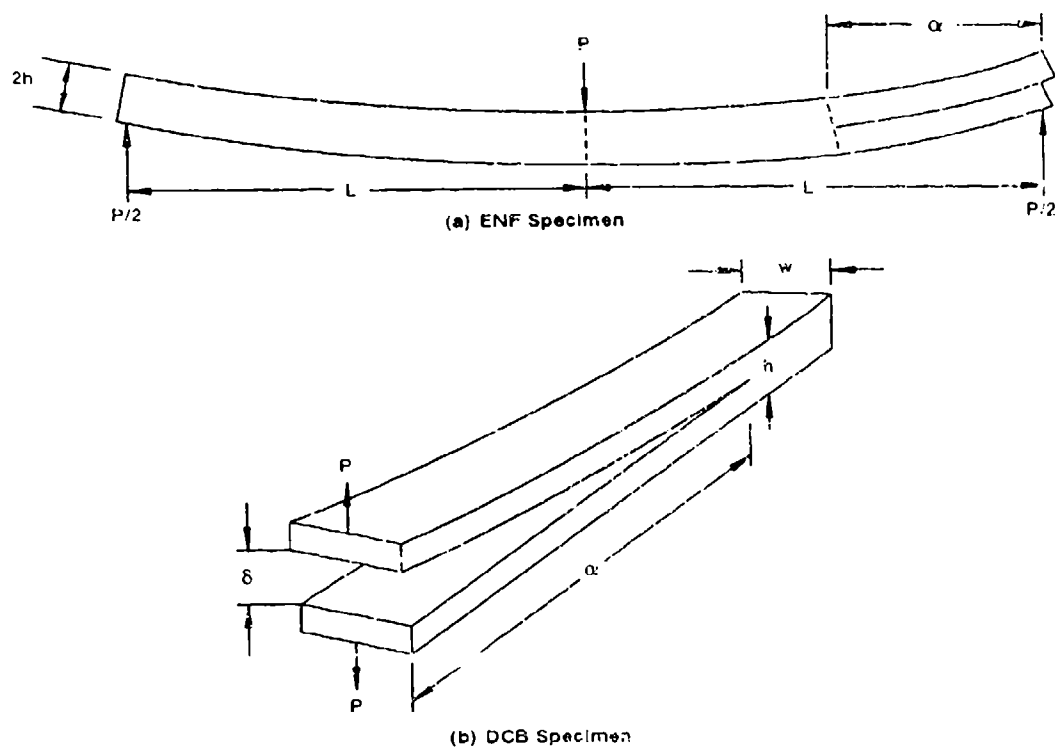


Figure 9-17. End-Notched Flexure (ENF) and Double-Cartridge Beam (DCB) Specimens

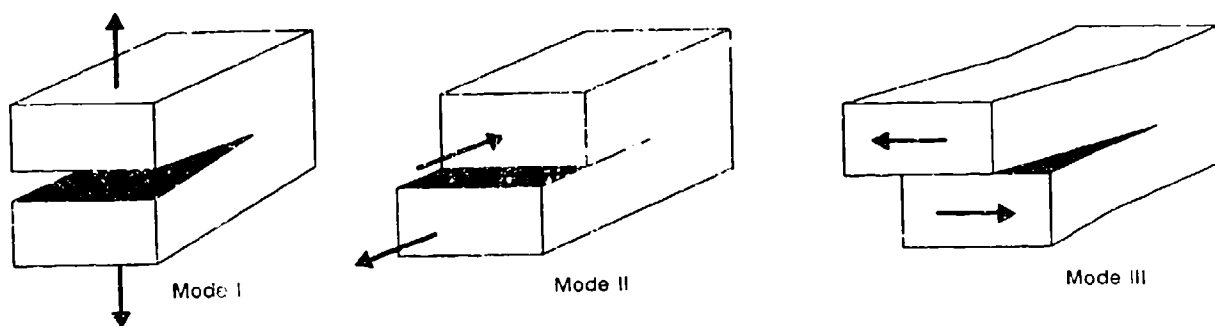


Figure 9-18. Modes of Crack Propagation

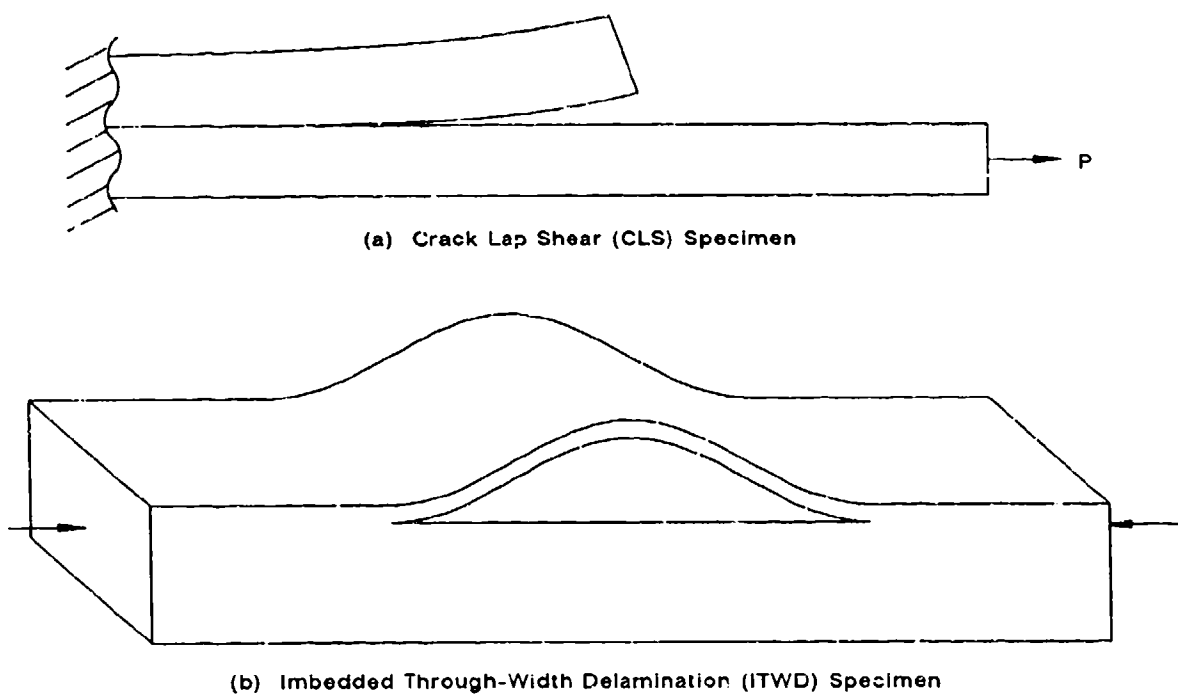


Figure 9-19. Mixed Modes I and II Delamination Specimens

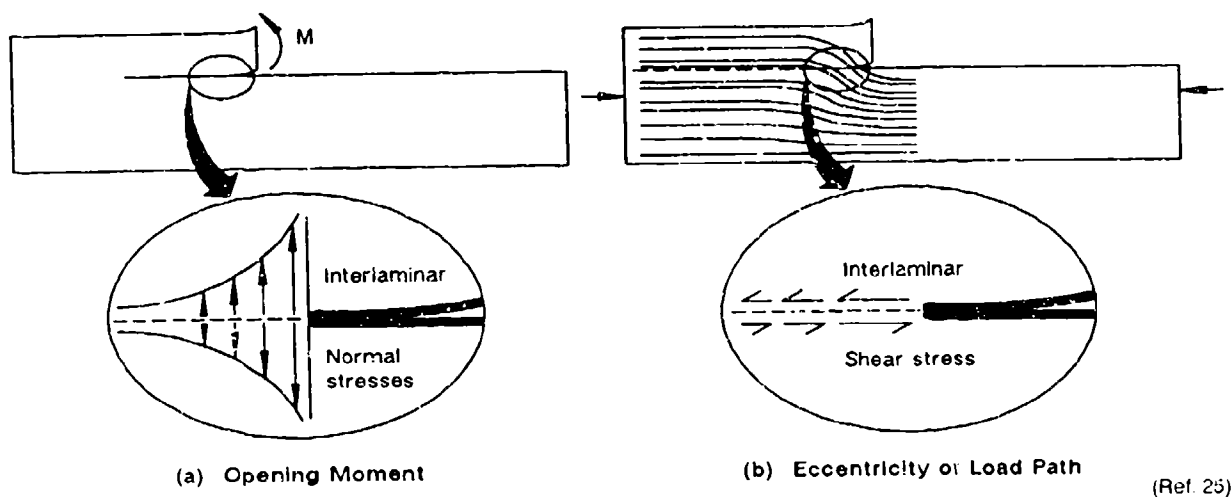


Figure 9-20. Crack Tip Loading Mechanisms Causing Interlaminar Normal and Shear Stress Concentrations

The strain energy release rate methods for evaluating the criticality of delaminations assume that G_c is a material property. This type of analysis is based on the equation below presented by Griffith (Reference 66).

$$G = \frac{P^2}{2b} \frac{dC}{da} \quad (\text{Eq. 19})$$

where:

b = width of crack

G = strain energy release rate

C = compliance

a = crack length

P = load

For a single mode of loading at the crack tip, the load on the specimen, P , is increased until G reaches its critical value G_c at the onset of crack growth. In this case, the failure criterion can be stated as crack growth occurs when G reaches G_c . Once G_c has been measured, the fracture load, P_c , can be found for any other crack length or geometry by evaluating the change in compliance with respect to crack length (dC/da). Then, dC/da can be adequately determined analytically for simple pure Mode I or Mode II geometries such as the DCB and ENF, respectively; however, finite element methods combined with the virtual crack closure analysis (Reference 67) are required to evaluate dC/da in more complicated structural applications. These types of complex geometries often have more than one mode of loading present at the crack tip (that is, mixed mode). In this case the interaction of modes must be considered, thus invalidating the simple crack growth criterion mentioned above. The mixed mode fracture criterion becomes more complicated since the critical value of the Mode II interlaminar toughness of composites can range from one to ten times that in Mode I as shown in Table 9-4. However it has been recently shown by Rothschilds (Reference 25) and Johnson (Reference 68) that the linear mixed-mode crack growth criterion, in the following equation, provides accurate predictions of the critical loads at the onset of mixed mode crack growth.

Table 9-4. G_{IC} and G_{IIC} Values Obtained From DCB and ENF Testing Reported in Literature

Material	G_{IC} kJ/m ² *	Ref. number	G_{IIC} kJ/m ² *	Ref. number
AS-4/PEEK	1.75 ± 0.13	65	1.89 ± 0.16	61
AS-4/PEEK	2.1 - 2.4	66		
AS-4/PEEK	1.54 ± 0.06	63	1.77 ± 0.24	63
T300/5208	0.103	67	0.92 ± 0.14	64
AS-1/3506-6	0.131	62		
AS-1/3501-6	0.19 ± 0.01	63	0.61 ± 0.3	63
Cellon 6000/ CYCOM 982	0.25 ± 0.02	65	0.77 ± 0.07	65

*1 kJ/m² = 5.71 in lb/in².

$$\frac{G_I}{G_C} + \frac{G_{II}}{G_{IIC}} = 1 \quad (\text{Eq. 20})$$

(Where the values are as defined for the previous equation.)

With this criterion, the criticality of interlaminar cracks can be evaluated in complex mixed-mode geometries. It should be noted that the criterion in the above equation reduces to the desired result in the case of pure mode loading. It is also seen that the mixed-mode criterion above requires the pure Mode I, Mode II, and or Mode III critical strain energy release rates. Fracture testing exhibits rate dependence, material nonlinearity, and subcritical crack growth. To be consistent, these effects must be considered when using the results of pure mode fracture testing in the analysis of fracture in structural components.

9.4.2 Interlaminar Fatigue Crack Growth

The previous paragraph discussed methods used to evaluate the criticality of interlaminar cracks under quasi-static loading. Some excellent investigations on interlaminar fatigue crack growth were performed by Wilkins (Reference 69) and Russell (Reference 70). They have shown that a power law relation exists between the change in G during a fatigue cycle and the crack growth rate. Table 9-5 shows the crack growth rate equations in Mode I and Mode II for AS-1/3501-6 (Gr/Ep). Similar equations for other materials could be used in conjunction with the methods for predicting G (discussed above) to evaluate the criticality of interlaminar fatigue in laminated composites. Figure 9-21 shows rather surprisingly that over a certain range of cyclic Mode II crack loading, the tougher thermoplastic AS4/PEEK has a higher crack growth rate than the relatively brittle epoxy. The characteristic surface microfeatures have been documented in a thorough investigation of composite interlaminar crack growth by Russell (Reference 70). Failure analysts can use this information to characterize the loading (static or fatigue) and interlaminar stress state (Mode I or Mode II) in the region of failure initiation. Recreating the loads at the onset of failure may illuminate the cause of failure.

Table 9-5. Fatigue Crack Growth of AS-1/3501-6

Mode	Governing equation	Reference number	B	n	G_{TH} , J/m ²	$\frac{\Delta G_{TH}}{G_{TC}}$
Mode I	$\left(\frac{da}{dn}\right)_I = B(\Delta G_I)^n$	62	1.47×10^{-64}	28.6	105	0.6
Mode II	$\left(\frac{da}{dn}\right)_{II} = B(\Delta G_{II})^n$	63	22.3×10^{-18}	5.8	82	0.14
Mode II	$\left(\frac{da}{dn}\right)_{mm} = B(\Delta G_T)^n$	62	1.04×10^{-20}	7.7	74	0.16

* G_{TH} is the cyclic strain energy release rate corresponding to a threshold crack growth rate of 2.54×10^{-6} mm/cycle.

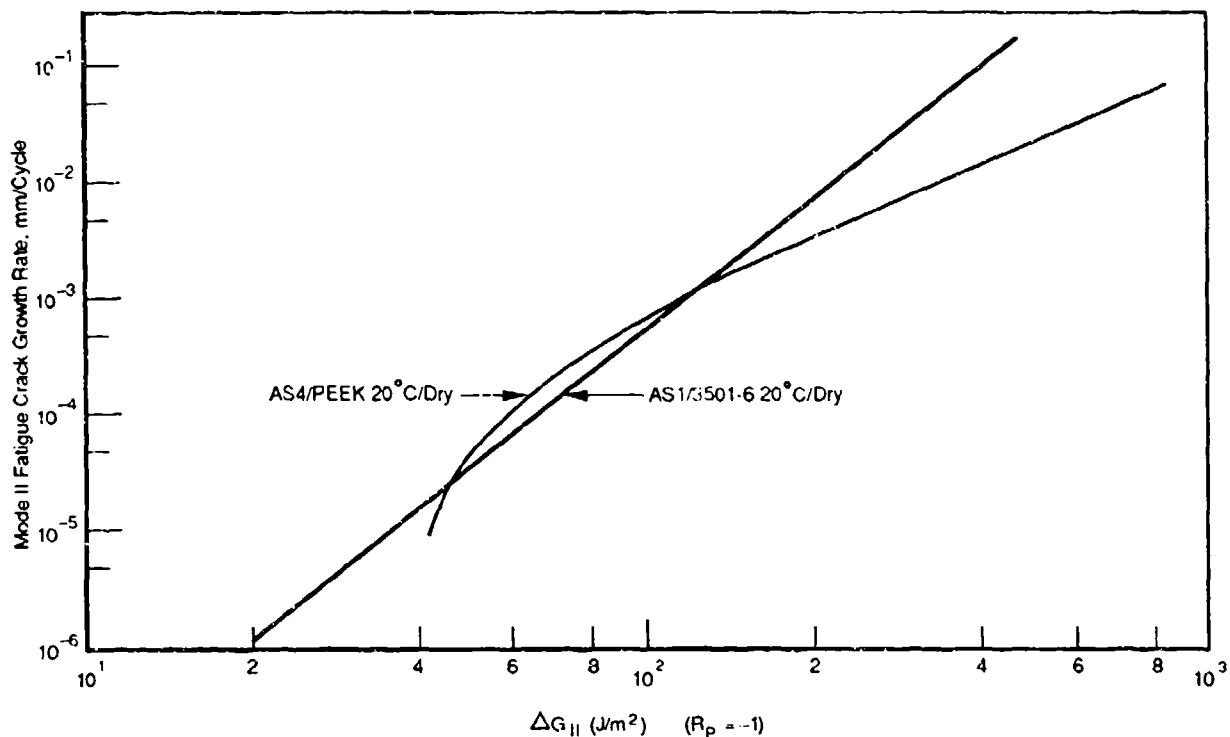

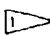









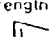

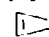



Figure 9-21. Mode II Fatigue

9.4.3 Reductions in Strength Due to Manufacturing Defects

While the strength reductions due to holes, cutouts, and impact damage are incorporated into design, manufacturing defects are not accounted for. Some of the typical manufacturing defects that may cause strength reductions are listed in Table 9-6. This chart also lists the mechanical properties likely to be affected by the defects and some of the methods and data needed to evaluate the criticality of the flaw. Although the list in Table 9-6 is incomplete, it provides the failure analyst with an understanding of some causes and effects related to typical manufacturing defects.

Table 9-6. Manufacturing Defects

Defect	Type of defect	Cause	Mechanical properties	Stress analysis method used to evaluate criticality of defects	Data needed to perform analysis
Small error in ply angle	Laminate fabrication defect	Layup technique	Strength, stiffness, and hygrothermal stability	Lamination theory, laminate fracture criterion, finite element	
Error in number or size of plies, gross error in ply direction	Laminate fabrication defect		Strength, stiffness, resistance to edge delamination, hygrothermal stability	Lamination theory, laminate fracture criterion, finite element	
Low-level porosity (i.e., 2%-5%)	Laminate fabrication defect	Layup technique—ply not compacted correctly, interply porosity in tapes, intraply and interply porosity in fabric	Reduction in interlaminar shear strength and interlaminar toughness	Empirical evaluation, lamination theory, finite elements, crack growth criterion	Interlaminar shear strength and/or interlaminar toughness versus percentage of porosity 
Low-level porosity (i.e., 2%-5%)	Outline-laminate held above storage temperature too long before final curing	Schedule improper or not followed, freezer malfunction	Reduction in interlaminar shear strength and interlaminar toughness	Empirical evaluation, lamination theory, finite elements, crack growth criterion	Interlaminar shear strength and/or interlaminar toughness versus percentage of porosity 
Low-level porosity (i.e., 2%-5%)	Processing error	Prepreg resin content too low, too much resin flow during cure	Reduction in interlaminar shear strength and interlaminar toughness	Empirical evaluation, lamination theory, finite elements, crack growth criterion	Interlaminar shear strength and/or interlaminar toughness versus percentage of porosity 
Low-level porosity (i.e., 2%-5%)	Processing error	Cure pressure too low	Reduction in interlaminar shear strength and interlaminar toughness	Empirical evaluation, lamination theory, finite elements, crack growth criterion	Interlaminar shear strength and/or interlaminar toughness versus percentage of porosity 
Low-level porosity (i.e., 2%-5%)	Processing error	Poor impregnation of resin into fiber tow	Interlaminar toughness—susceptible to transverse cracking	Empirical evaluation, lamination theory, finite elements, crack growth criterion	Interlaminar shear strength and/or interlaminar toughness versus percentage of porosity 
High-level porosity (i.e., 5%-10%)	Same as for low-level porosity	Same as for low-level porosity	All	Empirical evaluation, lamination theory, finite elements, crack growth criterion	Interlaminar shear strength and/or interlaminar toughness versus percentage of porosity 
Low glass transition temperature (T _g)	Processing error, fabrication defects, solvent sensitivity	Incorrect processing temperature, incorrect material exposure to solvents	Strength and stiffness at temperatures near T _g	Empirical evaluation, lamination theory, finite elements, crack growth criterion	Strength and stiffness versus temperature 
Incorrect material	Laminate fabrication defects	Layup technique	All	Lamination theory, finite elements, laminate fracture criterion, crack growth criterion	Inplane and interlaminar fracture toughness 
Implanted defect or contamination causing delamination	Laminate fabrication defects	Layup technique	Compression and interlaminar shear strength susceptible to static or fatigue delamination growth	Finite elements, analytical fracture mechanics, crack growth criterion	Interlaminar toughness 
Incorrect—size fastener or hole, hole or cutout, countersink depth	Assembly error	Machining error, design error, procurement error	Joint strength, laminate strength	Lamination theory, laminate strength criterion, finite elements, notched strength criterion	Notched strength data 
Incorrect fastener material	Assembly error	Machining error, design error, procurement error	Joint strength susceptible to galvanic corrosion	Lamination theory, laminate strength criterion, finite elements, notched strength criterion	Notched strength data 
Contamination, bond line thickness, improperly cured adhesive, improper surface preparation	Defective bonding	Assembly error	Bonded joint strength	Lamination theory, analytical fracture mechanics, finite elements, crack growth criterion	Fracture toughness of adhesive and interface 

 Basic laminate properties: strength, stiffness, coefficient of thermal expansion, etc.

SECTION 10

INVESTIGATIVE AND REPORTING FORMATS

This section presents formats for reporting failure analysis and fractographic data, with the intent that eventually all the information can be incorporated into a computerized database.

FAILURE ANALYSIS COLLECTION
AND TRACKING SYSTEM (FACTS)
DATA INPUT SHEET

OPERATOR: _____ DATE: _____

REPORT NUMBER: _____ DESIGN DRAWING PART NAME/NUMBER: _____

PART LOCATION ON AIRCRAFT: _____

MATERIAL/PROCESSING INFORMATION/SPECIFICATION: _____

AIRPLANE INFORMATION: CUSTODIAN AFB: _____

MODEL: _____ FLIGHT HOURS: _____

NUMBER OF LANDINGS: _____

BACKGROUND/INFORMATION:

LOCATION OF DAMAGE: _____

ENVIRONMENTAL CONCERNS: _____

(OTHERS): _____

DATA: _____

ANALYSES CONDUCTED _____

RESULTS: _____

RECOMMENDATIONS: _____

KEYWORDS: _____

Figure 10-1. Figure Analysis Collection and Tracking System (FACTS) Data Input Sheet

NON-DESTRUCTIVE
EXAMINATION
DATA INPUT SHEET

OPERATOR: _____ DATE: _____

PART NAME/NUMBER: _____

MATERIALS & CONSTRUCTION: _____

LOCATION OF ANALYSIS: _____

REASON FOR ANALYSIS: _____

ANALYTICAL INSTRUMENT/SETTINGS: _____

SUPPORTIVE DATA: _____

RESULTS/INTERPRETATIONS: _____

KEYWORDS: _____

Figure 10-2. Nondestructive Examination Data Input Sheet

MATERIALS CHARACTERIZATION
DATA INPUT SHEET

OPERATOR: _____ DATE _____

PART NAME/NUMBER: _____

MATERIALS/SPECIFICATIONS: _____

SPECIFICATION REQUIREMENTS: _____

CURE TEMP: _____

FIBER/RESIN DENSITIES: _____

VERIFICATION DATA

- T_g DETERMINATION-
INSTRUMENTATION: _____

RESULTS: _____

- RESIN CHARACTERIZATION-
INSTRUMENTATION _____

RESULTS: _____

- RESIN CONTENT-
INSTRUMENTATION _____

RESULTS _____

- SPECIALIZED ANALYSES METHODS USED (HPLC, GPC, DSC, SURF ANALYSIS, ETC.) _____

RESULTS _____

KEYWORDS _____

Figure 10-3. Materials Characterization Data Input Sheet

MATERIALS CHARACTERIZATION
DATA INPUT SHEET
(FIGURE ATTACHMENT)

- Diagram of specimen location
- Data/Graphs from analysis

COMMENTS _____

Figure 10-4. Materials Characterization Data input Sheet (Figure Attachment)

FRACTOGRAPHY
MACROSCOPIC ANALYSIS
DATA INPUT SHEET

OPERATOR _____ DATE _____

PART NAME/NUMBER: _____

MATERIAL: _____

VISUAL OBSERVATIONS. _____

KEYWORDS. _____

10-6

FRACTOGRAPHY MACROSCOPIC ANALYSIS
DATA INPUT SHEET
(PHOTO ATTACHMENT)

- Diagram or photo of part location on structure
- Photo of overall part
- Closeup of fracture origin or defect

MAG

MAGNIFICATION: _____

COMMENTS: _____

Figure 10-6. Fractography Macroscopic Analysis Data Input Sheet (Photo Attachment)

FRACTOGRAPHY
MICROSCOPIC ANALYSIS
DATA INPUT SHEET

OPERATOR: _____ DATE: _____

PART NAME/NUMBER: _____

MATERIAL: _____

RESIN/FIBER SYSTEM: _____

LAYUP: _____

MICROSCOPIC OBSERVATIONS: _____

KEYWORDS: _____

10-8

FRACTOGRAPHY MICROSCOPIC ANALYSIS
DATA INPUT SHEET
(PHOTO ATTACHMENT)

- Optical photomicrograph
- Low-Mag photomicrograph
 - SEM
 - TEM
 - STEM
- High-Mag photomicrograph
 - SEM
 - TEM
 - STEM

MAG

MAGNIFICATION: _____

COMMENTS: _____

Figure 10-8. Fractography Microscopic Analysis Data Input Sheet (Photo Attachment)

STRESS ANALYSIS
DATA INPUT SHEET

OPERATOR: _____ DATE: _____

PART NAME/NUMBER: _____

MATERIALS/SPECIFICATION/CONSTRUCTION: _____

ENVIRONMENTAL AND LOAD CONDITIONS (PRIOR TO AND DURING FRACTURE): _____

INPUTS FROM FRACTOGRAPHY (ORIGIN, LOAD TYPES, DEFECTS): _____

INITIAL STRUCTURAL REVIEW:

- GROSS STRAIN AT ORIGINS: _____
- ALLOWABLES AT ORIGINS: _____
- ANALYSIS METHODS: _____
- RESULTS/COMMENTS: _____

LAMINA LEVEL REVIEW:

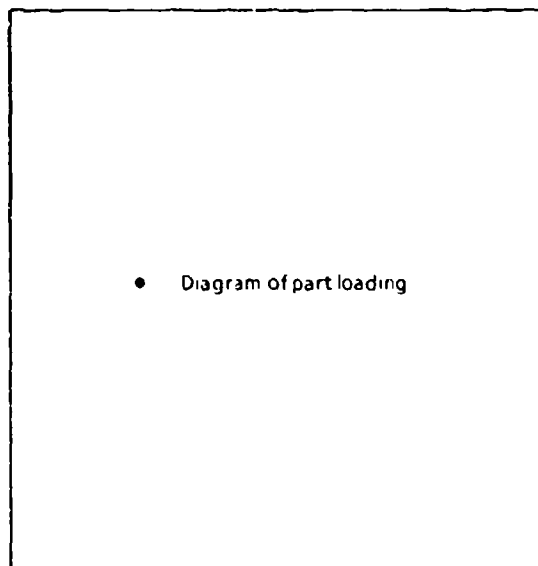
- FAILURE CRITERIA USED: _____
- ANALYSIS METHODS USED: _____
- RESULTS: _____

SUMMARY/INTERPRETATIONS: _____

KEYWORDS: _____

Figure 10-9. Stress Analysis Data Input Sheet

STRESS ANALYSIS
DATA INPUT SHEET
(DIAGRAM ATTACHMENT)



COMMENTS: _____

Figure 10-10. Stress Analysis Data Input Sheet (Diagram Attachment)

- 1.0 INTRODUCTION
- 2.0 MATERIAL
 - Prepreg Type (Fiber/Resin)
 - Laminate/Orientation
 - Processing Information
- 3.0 MECHANICAL TEST INFORMATION
 - Test Specimen Configuration
 - Loading Condition
 - Test Conditions
 - Mechanical Test Data
- 4.0 FRACTOGRAPHIC DATA
 - Visual /Microscopic Observations
 - SEM Macroscopic Observations
 - SEM Microscopic Observations
 - Analysis of Data - Initiation Site
 - Analysis of Data - Crack Propagation Direction
- 5.0 SUMMARY AND CONCLUSIONS

Figure 10-11. Fractographic Data Reporting Format

1.0 ABSTRACT

2.0 BACKGROUND

- Part Identification
- Manufacturing History
- Service History
- Field Information Relating To Fracture
- Detection of Problem

3.0 ANALYSIS OF FAILURE

- NDI Techniques Used and Results
- Fractographic Techniques Used and Results
- Chemical Properties
- Mechanical Properties
- Engineering Analysis

4.0 CONCLUSIONS

5.0 RECOMMENDATIONS

Figure 10-12. Failure Analysis Data Reporting Format

SECTION 11

GLOSSARY

A-Basis. The mechanical property value above which at least 99 percent of the population of values is expected to fall, with a confidence of 95 percent.

A-Stage. An early stage in the polymerization reaction of a thermosetting resin in which the material is still soluble and fusible.

Adhesive. A substance capable of holding two materials together by surface attachment. Structural adhesives produce attachments capable of transmitting significant structural loads.

Advanced Composites. A family of high-performance materials that consists of a high-strength, high-modulus continuous fiber system embedded within an essentially homogeneous matrix material.

Advanced Filaments. Continuous filaments made from high-strength, high-modulus materials for use as a reinforcement constituent in advanced composites.

Angle-Ply Laminate. A laminate in which the fiber orientations in successive plies alternate between "+" and "-" with respect to the global reference coordinates.

Anisotropic. Not isotropic; having mechanical and/or physical properties which vary with orientation at any point within the material.

Aramid Fibers. A class of aromatic polyamide fibers, presently including Kevlar, Kevlar 29, Kevlar 49, and Nomex, all products of the DuPont Company.

Autoclave. A closed vessel that produces an environment of gas pressure, with or without heat.

B-Basis. The mechanical property value above which at least 90 percent of the population of values is expected to fall, with a confidence of 95 percent.

B-Stage. An intermediate stage in the reaction of a thermosetting resin in which the material softens when heated and swells when in contact with certain solvents, but does not entirely fuse or dissolve. Materials are usually precured to this stage to facilitate handling and lay-up prior to final cure.

Bagging. An operation consisting of thermocouple placement, bleeder cloth, and blanket arrangement over a laminate lay-up, placement of a caul sheet (if required), installation of vacuum bag and vacuum lines, and sealing of the vacuum bag.

Balanced Laminate. A laminate in which laminae at angles other than 0 degree and 90 degrees occur only in +- pairs (not necessarily adjacent to one another). Every "+" lamina has a corresponding "-" lamina.

Batch (or Lot). In general, a quantity of material formed using the same process and having identical characteristics throughout. A batch of prepreg tape is produced from a single batch of matrix material. The prepreg tape batch is not necessarily produced at one time, but all sub-batches are produced in the same equipment under identical conditions.

Binders. Either liquid emulsions or pulverized resin solids, directly applied to virgin blown fibers to form mat products.

Bleeder Cloth. A nonstructural layer of material used in the manufacture of composite parts to allow the escape of excess gas and resin during cure. The bleeder cloth is removed after the laminate layup is cured, and is not part of the final laminated part.

Bond. The adhesion of one surface to another, with or without the use of an adhesive as a bonding agent.

Braid. Yarn that is interlaced by a process similar to that used in the weaving of fabrics; available in flat, round, or tubular forms; often referred to as "sleeving" or "braided fabric."

Broadgoods. A term loosely applied to prepreg material greater than 12 inches in width, usually furnished by suppliers in continuous rolls, applied to both collimated uniaxial tape and woven fabric prepreps.

Carbon fibers. Fibers produced via pyrolytic degradation of synthetic organic fibers, rayon, or polyacrylonitrile (PAN), which have about 92-99% carbon content. The fibers have moduli greater than or equal to 70 GPa (10 million psi).

C-Stage. The final stage of curing of a thermosetting resin in which the material is infusible and insoluble in common solvents. Fully cured thermosets are in this stage.

Cable. Yarn that is plied more than once; yarn made by plying two or more previously plied yarns.

Caul Plate. Smooth metal plate, free of surface defects, the same shape as a composite layup; used to transmit normal pressure during the curing process and to provide a smooth surface on the finished laminate.

Chemical Size. A surface finish applied to the fiber that contains some chemical constituents other than water.

Cocuring. The process of curing a composite laminate and simultaneously bonding it to some other prepared surface during the same cure cycle.

Collimated. Rendered parallel.

Composite Material. A material composed of two or more different constituent materials. Current structural composites consist of any combination of fibers, whiskers, and particles in a common matrix material. Composite materials may be classified as follows:

1. Fibrous composites — Fibers in a matrix
2. Laminated composites — Layers of the same or various materials
3. Particulate composites — Particles in a matrix
4. Hybrid composites — Composed of more than one kind of fiber/matrix material system.

Consolidated Monolayer. A form of metal matrix prepoly in which the fiber system and the encapsulating metallic matrix material are fully or partially consolidated into a stable lamina. Monolayers are combined into oriented stacks which are then further consolidated into a finished laminate.

Constituent Class. A group of fiber or matrix constituents of the same generic chemical type or family; e.g., graphite is a generic fiber class and epoxy is a generic matrix class.

Continuous Filament Yarn. A yarn formed by twisting two or more continuous filaments into a single, continuous strand.

Core. A sandwich filler material, generally cellular in nature, resembling a honeycomb and referred to by that name. The core material may be paper, nylon, phenolic, aluminum foil, etc.

Coupling Agent. That part of a sizing or finish which is designed to provide a bond between the reinforcement and the matrix material.

Cure. To change the properties of a thermosetting resin irreversibly by chemical reaction which may be condensation, ring closure, or addition. Cure may be accomplished by the addition of curing (cross-linking) agents, with or without catalyst, and with or without heat.

Debond or Disbond. An adhesive failure or separation along a bonded interface between two adherends.

Debulk (Densification). The compacting of plies and removal of air pockets from a laminate lay-up prior to curing. This is generally done in stages, under full vacuum, under ambient or elevated temperature conditions.

Delamination. A separation between adjacent layers of material in a laminate.

Drape. The ability of tape and broadgoods to conform to a contoured shape.

End. An individual warp yarn, fiber, thread, monofilament, or roving.

Fabric (Woven Fabric). A generic material construction manufactured by interlacing two yarns at right angles. The warp is the system of yarn or threads running lengthwise in the fabric, and the fill or filling is the system of yarn or threads running crosswise in the fabric. Warp is also referred to as "warp ends" or simply "ends." Filling is also referred to as "filling picks," "weft," or "picks."

Fiber. A single homogenous strand of material, essentially one-dimensional in the macromechanical sense, used as a principal constituent in advanced composites because of its high axial strength and modulus.

Fiber Content. The amount of fiber present in a composite, usually expressed as volume fraction or weight fraction of the composite.

Fiber Direction. The orientation or alignment of the longitudinal axis of the fiber with respect to a selected global reference axis (X).

Fiber System. The type of arrangement of the fiber constituent of an advanced composite. Examples of fiber systems are collimated filaments or filament yarns, woven fabric, randomly oriented short-fiber ribbons, random fiber mats, whiskers, etc.

Filament. A fiber characterized by extreme length, such that there is normally no filament end within a part except at geometric discontinuities. Filaments are used in filamentary composites and are also used in filament winding processes, which require long continuous strands.

Filamentary Composite. One form of advanced composites in which the fiber constituent consists of continuous filaments. Specifically, a filamentary composite is a laminate composed of a number of laminae, each of which consists of a nonwoven, parallel, unidirectional planar array of filaments (or filament yarns) embedded in the selected matrix material.

Fill. Yarn oriented at right angles to the warp in the woven fabric.

Finish. A material with which filaments are treated, containing a coupling agent to improve the bond between the filament surface and the resin matrix in a composite material. A finish often contains ingredients which provide high-temperature lubricity to the filament surface preventing abrasive damage during handling, and a binder which promotes strand integrity and facilitates packing of the filaments.

Flame-Sprayed Tape. A metal matrix prepoly form in which the fiber system is held in place on a foil sheet of matrix alloy by a metallic flame-spray deposit.

Flash. Excess material which forms at the parting line of a mold or a die, or that which is extruded from a closed mold.

Foamed Plastics. Resins in sponge form, flexible or rigid, with closed or interconnected cells that vary in density from that of the solid parent resin to 2 pounds/cubic foot; good heat barriers, and the fiber compressive strength of rigid foams makes them useful as core materials for sandwich constructions. Also, a chemical cellular plastic whose structure is produced by gases generated from the chemical interaction of its constituents.

Fugitive Binder. A resinous material used in the fabrication of metal matrix preplies to hold the fiber system in place on the metallic foil sheet during shipping, storage, handling, and layup. During laminate consolidation, the fugitive binder decomposes and the products completely vaporize.

Gel. A semisolid system consisting of a network of solid aggregates in which liquid is held; the initial jelly-like solid phase that develops during the formation of a resin from a liquid.

Gel Coat. A quick-setting resin used in molding processes to provide an improved surface for the composite. It is applied to the mold after the mold-release agent.

Graphite Fibers. A group of carbon fibers with a carbon content of 99 percent and high modulus values (greater than 20 GPa or 3 million psi).

Green Tape. A metal matrix prepoly form in which the fiber system is held in place on a foil sheet of matrix alloy by a resinous fugitive binder.

Greige. Loom state fabric that has received no finishing.

Hand Layup. The process of placing and working successive plies of prepreg in position on a mold by hand.

Homogeneous Material. A material of uniform composition throughout with no internal physical boundaries; a material whose properties are constant at every point within the material (but not necessarily with respect to directional coordinates).

Hybrid Laminate. A laminate composed of laminae of two or more composite material systems (intraply or interply).

Impregnate. To apply resin onto fibers or fabrics by one of several processes: hot melt, solution coat, or hand lay-up.

Integral Composite Structure. A composite structure in which several structural elements, which would conventionally be assembled together by bonding or mechanical fastening after separate fabrication, are instead laid up and cured as a single, complex, continuous structure.

Interlaminar. A descriptive term referring to a location between adjacent laminae.

Intralaminar. A descriptive term referring to a location entirely within a single lamina without reference to any adjacent laminae.

Isotropic. Having properties that are uniform in all directions at any point within the material (independent of the axis of testing).

Kevlar. Trade name for Aramid Fibers from DuPont.

Lamina. A single ply or layer in a laminate.

Laminae. Plural of lamina.

Laminate. A product obtained by bonding together two or more laminae of the same material or of different materials.

Layup. A fabrication process involving the placement of successive layers of materials. Also, the arranged set of laminae.

Mandrel. A form fixture or a male mold used as a base in the production of a part by layup or filament winding.

Matrix. The essentially homogeneous material in which the fiber system of a composite material is imbedded.

Matrix Class. The generic type of matrix material; organic, metallic, or ceramic.

Mold Release Agent. A lubricant applied to the mold surface to facilitate the release of the molded article.

Molding. The process of forming a polymer or a composite into a solid mass of prescribed shape and size by the application of pressure and heat.

Orthotropic. Having three mutually perpendicular planes of elastic (material property) symmetry.

Peel Ply. A layer of resin-free material used to protect a laminate for later secondary bonding.

Pitch Fibers. Fibers derived from pitch precursor and not as strong as the low-modulus PAN fibers, but easily processed to increase their modulus and excellent for stiffness-critical applications.

Plastic. An organic substance of large molecular weight which is solid in its finished state and, at some stage during its manufacture or its processing into a finished article, can be shaped by flow.

Plasticizer. A material of lower molecular weight which, when added to a polymer, separates the molecular chains and results in a lowering of the polymer glass transition temperature (with concomitant property degradation).

Piled Yarn. An assembly of previously twisted yarns.

Polymer. A high molecular weight organic material, natural or synthetic, formed by the linking together of a large number of repeating chemical units (monomers). When two or more monomers are involved, the product is called a copolymer.

Porosity. A distribution of trapped pockets of air, gas, or vacuum within a solid material, usually expressed as a percentage of the total nonsolid volume to the total volume (solid plus nonsolid) of a unit quantity of material. Also referred to as voids or microvoids.

Postcure. After the initial cure, an additional elevated temperature exposure, usually above the cure temperature and without pressure, to improve final properties and/or complete the cure. In certain resins, complete cure and ultimate mechanical properties are attained only by exposure of the cured resin to higher temperatures than those of curing.

Pot Life (of a resin). The length of time that a resin system retains viscosity that is low enough to be used in processing.

Precursor. Organic material from which carbon fibers are prepared via pyrolysis. Polyacrylonitrile (PAN), rayon, and pitch are commonly used precursor materials.

Preply. A lamina in the "raw material" stage, as furnished by a materials supplier, including all of the fiber system placed in position relative to all or part of the required matrix material. An organic matrix prepoly is called a prepreg. Metal matrix preplies include green tape, flame-sprayed tape, and consolidated monolayers.

Prepreg, Preimpregnated. A mat, a fabric, nonwoven material, or a roving, with resin usually advanced to the B-stage (when it is a thermoset resin), ready for lay-up and cure.

Quasi-Isotropic Laminate. A laminate that approximates isotropic mechanical behavior on a macro-scale.

Reinforced Plastics. Composite materials which have a polymer matrix and a modulus that is less than 20 GPa (3 million psi).

Resin. A solid, semisolid, or pseudosolid organic material which has an indefinite and often high molecular weight, exhibits a tendency to flow when subjected to stress, usually has a softening or melting range, and usually fractures conchoidally. Most resins are polymers.

Roving. An assembly of two or more strands, without a twist.

Sandwich Construction. A structural panel concept consisting in its simplest form of two relatively thin, parallel sheets (face sheets) of structural material bonded to and separated by a relatively thick, lightweight core.

Scrim Cloth (also called glass cloth, carrier). A reinforcing prepreg fabric woven into an open mesh construction, used in the processing of a tape or any other B-staged material to facilitate handling.

Secondary Bonding. The joining together of two or more already-cured composite parts by the process of adhesive bonding, during which the only chemical or thermal reaction is the curing of the adhesive itself.

Shelf Life. The length of time a material can be stored under specified environmental conditions and meet all applicable specification requirements and/or remain suitable for its intended function.

Sizing. Chemical compounds which, when applied to manufactured filaments, create a loose bond between the filaments, and provide the desired handling and processing properties.

Strand. A primary bundle of untwisted filaments.

Symmetric Laminate. A laminate in which the ply properties (material and geometric) and fiber orientation are symmetrical about the laminate midplane (midplane symmetry).

Tack. Stickiness of a prepreg or an adhesive.

Tape. Narrow fabric or material that ranges in width from 1/4 to 12 inches.

Thermoplastic Material. A material that is capable of being repeatedly softened by an increase in the temperature and hardened by a decrease in the temperature with no accompanying chemical change.

Thermoset Material. A material which becomes substantially infusible and insoluble when cured by the application of heat or by chemical means.

Tow. A loose, untwisted bundle of filaments.

Typical Basis. A "typical basis" property value is the average value. No statistical assurance is associated with this value.

Unidirectional Laminate. A laminate with nonwoven prepreg plies that are all laid up in the same direction.

Vacuum Bag Molding. A fabrication process in which the lay-up is cured under pressure generated by drawing a vacuum in the space between the lay-up and a flexible sheet that is placed over it and sealed at the edges.

Verifilm. A nonadhesive curing film used to check the bond line thickness of mating parts prior to adhesive bonding.

Void. A physical discontinuity in the form of a gaseous pocket, occurring within a material or part.

Volatiles. Materials in the sizing or the resin formulation in a prepreg which are released as a vapor at temperatures near or above room temperature.

Warp. The longitudinally oriented yarn in a woven fabric.

Whisker. A single filamentary crystal. Whisker diameters range from 1 to 25 microns, with length to diameter (aspect) ratios between 100 and 14,000.

X-Axis. The axis in the plane of a laminate which is used as the 0 degree reference for designating the fiber orientation of a lamina.

XY Plane. The reference laminate midplane that is parallel to the plane of the laminae.

Y-Axis. The axis in the plane of the laminate which is perpendicular to the X-axis.

Yarn. A yarn is produced by twisting and plying either strands of fiber or continuous filaments in a form suitable for weaving.

Z-Axis. The reference axis normal to the plane of the laminate.

SECTION 12

REFERENCES

1. Altman, J., et al., "Advanced Composite Serviceability Program," AFWAL TR-80-4092, July 1980.
2. Sewell, T.A., "Chemical Composition Processing for Air Force/Navy Advanced Composite Matrix Material," AFWAL TR-81-4180, 1982.
3. Carpenter, J.F., "Test Program Evaluation of Hercules 3501-6 Resin," N00019-77-C-0155, May 1978.
4. Young, P.R., Stein, B.A., and Chang, A.C., "Resin Characterization in Cured Graphite Fiber Reinforced Composites Using Diffuse Reflectance-FTIR," 28th National SAMPE Symposium and Exhibition, Vol. 28, 1983, pp. 824-837.
5. Handbook of Chemistry and Physics, 65th edition, R.C. Weast (ed.), CRC Press Inc., Boca Raton, Florida, 1985, p. E-130.
6. Ratner, B.D., McElroy, B.J., in Spectroscopy in the Biomedical Sciences, R.M. Gendreau (ed.), CRC Press Inc., Boca Raton, Florida, 1986, pp. 107-140.
7. Daniel, I.M., "The Behavior of Uniaxial Loaded Graphite/Epoxy Plates With Holes," Proceedings of the Second International Conference on Composite Materials, published by the Metallurgical Society of AIME, 1978, pp. 1019-1034.
8. Mikulas, M.M., "Failure Prediction Techniques for Compression-Loaded Composite Laminates With Holes," Selected NASA Research in Composite Materials and Structures, NASA Conference Publication 2142, August 1980.
9. Aronsson, C.G., and Bachklund, J., "Damage Mechanics Analysis of Matrix Effects in Notched Laminates," Composite Materials: Fatigue and Fracture, ASTM STP 907, H.T. Hahn (ed.), ASTM, Philadelphia, Pennsylvania, 1986, pp. 134-157.
10. Chamis, C.C., and Smith, G.T., "CODSTRAN: Composite Durability Structural Analysis," NASA-TM-79070, 1978.
11. Craddock, J.N., and Champagne, P.J., "A Comparison of Failure Criteria for Laminate Composite Materials," Structures, Structural Dynamics and Materials Conference, American Institute of Aeronautics and Astronautics, 1982, pp. 268-278.
12. McLaughlin, P.V., and Dasgupta, A., "BILAM: A Composite Laminate Failure Analysis Code Using Bilinear Stress Strain Approximations," UCRL-15371, October 1980.
13. Tsai, S.W., and Hahn, H.T., Introduction to Composite Materials, Technomic Pub. Co, Inc., Westport, Connecticut, 1980.
14. Jones, R.M., Mechanics of Composite Materials, Scripta Book Co., Washington, D.C., 1975.

15. Crossman, F.W., "Analysis of Free Edge Induced Failure of Composite Laminates," First USA-USSR Symposium on Fracture of Composite Materials, Sijthoff and Noordhoff International Publishers, 1979, pp. 291-302.
16. Herakovich, C.T., "On Failure Modes in Finite Width Angle Ply Laminates," Advances in Composite Materials; Proceedings of the Third International Conference on Composite Materials, Vol 1, Pergamon Press, 1980, pp. 425-435.
17. Wu, E.M., "Failure Analysis of Composites With Stress Gradients," First USA-USSR Symposium on Fracture of Composite Materials, Sijthoff and Noordhoff International Publishers, 1979, pp. 63-76.
18. Wilson, D.W., Gillespie, J.W., York, J.L, and Pipes, R.B., "Failure Analysis of Composite Bolted Joints," NASA-CR-16372, July 1980.
19. Starnes, J.H., Jr., Rhodes, M.D., and Williams, J.G., "Effect of Impact Damage and Holes on the Compressive Strength of a Graphite-Epoxy Laminate," ASTGM STP 696, 1979, pp. 145-171.
20. Bathias, C., Esnault, R., and Pellas, J., "Application of Fracture Mechanics to Graphite Fibre-Reinforced Composites," Composites, Vol. 12, July 1981, pp. 195-200.
21. McGarry, F.J., Mandell, J.F., and Wang, S.S., "Fracture of Fiber-Reinforced Composites," Polymer Engineering and Science, Vol. 16, No. 9, September 1976, pp. 609-613.
22. Awerbuch, J., et al., "Determination Characteristics and Failure Modes of Notched Graphite Polyimide Composites at Room and Elevated Temperatures," NASA-CR-159375, August 1980.
23. O'Brien, T.K., "Analysis of Local Delaminations and Their Influence on Composite Laminate Behavior," NASA-TM-85728, January 1984.
24. Whitcomb, J.D., "Analysis of Instability Related Growth of a Through-Width Delamination," NASA-TM-86301, September 1984.
25. Rothschilds, R.J., "Instability-Related Delamination Growth in Thermoset and Thermoplastic Composites," Presented at ASTM Composite Materials Testing and Design: Eighth Symposium, Charleston, South Carolina, April 1986.
26. Tsai, S.W., Composites Design — 1986, Think Composites, Dayton, Ohio, 1986.
27. Halpin, J.C., Primer on Composite Materials, Technomic Pub. Co., Inc., Lancaster, Pennsylvania, 1984.
28. Ashton, J.E., and Whitney, J.M., Theory of Laminated Plastics, Technomic Pub. Co., Inc., Stanford, Connecticut, 1970.
29. Tsai, S.W., "Strength Theories of Filamentary Structures," in Fundamental Aspects of Fiber Reinforced Plastic Composites, R.T. Schwartz and H.S. Scharts (eds.), Wiley Interscience, New York, 1968, pp. 3-11.
30. Tsai, S.W., and Wu, E.M., "A General Theory of Strength for Anisotropic Materials," J. Composite Materials, January 1971, pp. 58-80.
31. Pipes, R.B., and Cole, B.W., "On Off-Axis Strength Tests for Anisotropic Materials," J. Composite Materials, April 1973, pp. 246-256.

32. Christensen, R.M., "Tensor Transformations and Failure Criteria for the Analysis of Fiber Composite Materials," J. Composite Materials, September 1988, pp. 874-897.
33. Kim, R.Y., "In-Plane Tensile Strengt. Multidirectional Composite Laminates," Technical Report UDR-TR-81-84, University of Dayton Research Institute, 1981.
34. Gillespie, J.W., Jr., Microcomputer Software, Center for Composites Manufacturing, Science, and Engineering, Newark, Delaware, 1984.
35. Flaggs, D.L., and Kural, M.H., "Experimental Determination of the In Situ Transverse Lamina Strength in Graphite/Epoxy Laminates," J. Composite Materials, Vol. 16, March 1982, pp. 103-116.
36. Parvizi, A., Garrett, K.W., and Bailey, J.E., "Constrained Cracking in Glass Fibre-reinforced Epoxy Cross-ply Laminates," J. Materials Science, 13, 1978, pp. 195-201.
37. Bader, M.G., Bailey, J.E., Curtis, P.T., and Parvizi, A., "The Mechanisms of Initiation and Development of Damage in Multi-Axial Fibre-Reinforced Plastic Laminates," ICCM3, Vol. 3, Cambridge, England, August 1979, pp. 227-239.
38. Bailey, J.E., Curtis, P.T., and Parvizi, A., "On the Transverse Cracking and Longitudinal Splitting Behavior of Glass and Carbon Fibre Reinforced Epoxy Cross Ply Laminates and the Effect of Poison and Thermally Generated Stain," Proc. R. Soc. Lond., 366, 1979, pp. 599-623.
39. Flaggs, D.L., "Prediction of Tensile Matrix Failure in Composite Laminates," J. Composite Materials, Vol. 19, January 1985, pp. 29-50.
40. Lagace, P.A., "Notch Sensitivity and Stacking Sequence of Laminated Composites," Composite Materials: Testing and Design (Seventh Conference), ASTM STP 893, J.M. Whitney (ed.), ASTM, Philadelphia, Pennsylvania, 1986, pp. 161-176.
41. Wu, E.M., "Fracture Mechanics of Anisotropic Plates," in Composite Materials Workshop, S.W. Tsai, J.C. Halpin, and N.J. Pagano (eds.), Technomic Pub. Co., Inc., Stanford, Connecticut, 1968, pp. 20-43.
42. Waddoups, M.E., Eisemann, J.R., and Kaminski, B.E., "Macroscopic Fracture Mechanics of Advanced Composite Materials," J. Composite Materials, Vol. 5, 1971, pp. 446-454.
43. Whitney, J.M., and Nuismer, R.J., "Stress Fracture Criteria for Laminated Composites Containing Stress Concentrations," J. Composite Materials, Vol. 8, 1974, pp. 253-265.
44. Nuismer, R.J., and Whitney, J.M., "Uniaxial Failure of Composite Laminates Containing Stress Concentrations," in Fracture Mechanics of Composites, ASTM STP 593, American Society of Testing and Materials, 1975, pp. 117-142.
45. Karlak, R.F., "Hole Effects in a Related Series of Symmetrical Laminates," in Proceedings of Failure Modes in Composites, Vol. IV, The Metallurgical Society of AIME, Chicago, Illinois, 1977, pp. 105-117.
46. Pipes, R.B., Wetherhold, R.C., and Gillespie, J.W., Jr., "Notched Strength of Composite Materials," J. Composite Materials, Vol. 12, 1979, pp. 148-160.
47. Pipes, R.B., Gillespie, J.W., Jr., and Wetherhold, R.C., "Superposition of the Notched Strength of Composite Laminates," Polymer Engineering and Science, Vol. 19, No. 16, 1979, pp. 1151-1155.

48. Pipes, R.B., Wetherhold, R.C., and Gillespie, J.W., Jr., "Macroscopic Fracture of Fibrous Composites," Materials Science and Engineering, Vol. 45, 1980, pp. 247-253.
49. Lin, K.Y., "Fracture of Filamentary Composite Materials," PhD Dissertation, Department of Aeronautics and Astronautics, M.I.T., Cambridge, Massachusetts, January 1976.
50. Mar, J.W., and Lin, K.Y., "Fracture Mechanics Correlation for Tensile Failure of Filamentary Composites With Holes," J. of Aircraft, Vol. 14, No. 7, July 1977, pp. 703-704.
51. Poe, C.C., Jr. and Sova, J.A., "Fracture Toughness of Boron/Aluminum Laminates With Various Proportions of 0° and $\pm 45^\circ$ Plies," NASA Technical Paper 1707, November 1980.
52. Aronsson, C.G., "Tensile Fracture of Composite Laminates With Holes and Cracks," The Royal Institute of Technology, Report No. 84-5, Stockholm, Sweden, 1984.
53. Williams, J.G., and Rhodes, M.D., "Effect of Resin on the Impact-Damage Tolerance of Graphite-Epoxy Laminates," ASTM STP 787, 1983, pp. 450-480.
54. Starnes, J.H., Jr. and Williams, J.G., "Failure Characteristics of Graphite-Epoxy Structural Components Loaded in Compression" Mechanics of Composite Materials — Recent Advances, Hashin and Herakovich (eds.), Pergamon Press, 1983.
55. Williams, J.G., "Effect of Impact Damage and Open Holes on the Compression Strength of Tough Resin/High Strain Fiber Laminates," in Tough Composite Materials — Recent Developments, Noyes Publications, Park Ridge, New Jersey, 1985.
56. Wilkins, D.J., "A Preliminary Damage Tolerance Methodology for Composite Structures," in Failure Analysis and Mechanisms of Failure of Fibrous Composite Structures, NASA CP 2278, 1983, pp. 67-93.
57. Gillespie, J.W. Jr. and Pipes, R.B., "Compressive Strength of Composite Laminates With Interlaminar Defects," Composite Structures, Vol. 2, 1984, pp. 49-69.
58. Webster, J.D., "Flaw Criticality of Circular Disbond Defects in Composite Laminates," CCM-81-03, Center for Composite Materials, University of Delaware, 1981.
59. Ashizawa, M., "Fast Interlaminar Fracture of a Compressively Loaded Composite Containing a Defect," Douglas Paper 6994, January 1981.
60. Ashizawa, M., "Improving Damage Tolerance of Laminated Composites Through the Use of New Tough Resins," Douglas Paper 7250, January 1983.
61. Ramkumar, R.L., "Performance of a Quantitative Study of Instability Related Delamination Growth," NASA Contractor Report 166046, March 1983.
62. Ramkumar, R.L., Kulkarni, S.W., and Pipes, R.B., "Definition and Modeling of Critical Flaws in Graphite Fiber Reinforced Epoxy Resin Matrix Composite Materials," Naval Air Development Center Report No. NADC-76228-30, January 1978.
63. Chatterjee, S.N., Hashin, Z., and Pipes, R.B., "Definition and Modeling of Critical Flaws in Graphite Fiber Reinforced Resin Matrix Composite Materials," Naval Air Development Center Report No. NADC 77278-30, August 1979.

64. Chatterjee, S.N., and Pipes, R.B., "Composite Defect Significance," Proceedings of the Mechanics of Composites Review Meeting, Dayton, Ohio, October 1982.
65. Yin, W.L., Sallam, S.N., and Simites, G.J., "Ultimate Axial Load Capacity of a Delaminated Beam-Plate," AIAA Journal, Vol. 24, No. 1, January 1986.
66. Griffith, A.A., "The Phenomena of Rupture and Flow in Solids," Phil. Trans. Royal Soc. of London, A221, 1921.
67. Rybicki, E.F., and Kanninen, M.F., "A Finite Element Calculation of Stress Intensity Factors by a Modified Crack Closure Integral," Engineering Fracture Mechanics, Vol. 9, No. 4, 1977, pp. 931-938.
68. Johnson, W.S., and Mangalgiri, P.D., "Influence of the Resin on Interlaminar Mixed-Mode Fracture," NASA TM 87571, July 1985.
69. Wilkins, D.J., "A Comparison of the Delamination and Environmental Resistance of a Graphite/Bismaleimide," NAV-GD-0037, General Dynamics, Fort Worth, Texas, September 1981.
70. Russell, A.M., and Street, K.N., "The Effect of Matrix Toughness on Delamination: Static and Fatigue Fracture Under Mode II Shear Loading of Graphite Fiber Composites," presented at NASA/ASTM Symposium on Toughened Composites, Houston, Texas, March 13-15, 1985.

APPENDIX A

CHEMICAL AND MECHANICAL PROPERTIES OF FIBER-REINFORCED COMPOSITE MATERIALS COMPILED BY NORTHROP

This section presents a compilation of chemical and mechanical properties of fiber-reinforced composite materials. Literature searches were performed on the Defense Technical Information Center (DTIC), the Plastics Center, and NASA databases. The keywords used and associated source(s) and abstracts that were found are shown in Table A-1. Northrop requested copies for review and compiled properties obtained into database files using a personal computer. These were subsequently condensed into tabular forms.

Table A-1. Keywords, Sources and Abstracts in Literature Search of DTIC, NASA and Plastics Center Data Bases

KEYWORD(S)	SOURCE(S)	NO. OF ABSTRACTS
CHEMICAL/MECHANICAL PROPERTIES - THERMOSETTING RESINS THERMOPLASTIC RESINS FIBERS EPOXY RESINS	DTIC	21
CHEMICAL/MECHANICAL PROPERTIES - FIBER REINFORCED COMPOSITES	DTIC, PLASTICS CENTER DATABASE	103
EPOXY/GRAPHITE	NASA	598
PEEK/GRAPHITE	NASA	86
BISMALEIMIDE/GRAPHITE	NASA	28
FIBER REINFORCED COMPOSITES - MULTI-PLY LAMINATES	DTIC	3
TOTAL		839

Table A-2. Commercial Fiber Properties

COMMERCIAL NAME	ULT. TENSILE STRENGTH (KSI)	ELASTIC MODULUS (MSI)	ELONGATION (%)	FIBER DENSITY (lb/in ³)	GENERIC TYPE
Celion G30-500	550	34.0	1.62	0.064	C Pan Fiber + Epoxy Sizing
Celion G30-600	630	34	1.85	0.064	C Pan Fiber + Epoxy Sizing
Celion G40-600	620	43.5	1.43	0.062	C Pan Fiber + Epoxy Sizing
Celion G40-700	720	43.5	1.66	0.064	C Pan Fiber + Epoxy Sizing
Celion G30-400	470	34	1.4	0.064	High Strength C Fiber for Weaving
Celion G50-300	360	52	0.7	0.064	High Modulus Carbon Fiber
Celion GY-70	270	75	0.36	0.071	Ultra High Modulus C Fiber Unidirectional Tape
Celion GY-70SE	270	75	0.36	0.071	Ultra High Modulus C Fiber Tow
Celion GY-80	270	83	0.32	0.071	Ultra High Modulus C Fiber Unidirectional Tape
Celion GY-80SE	270	83	0.32	0.071	Ultra High Modulus C Fiber Tow
Celion 6-S	550	33.5	1.64	0.064	Sized, Chopped High Strength C Fiber
Amoco T1000	1024	42	2.47	0.066	High Strength High Modulus C Fiber
Amoco T650/42	731	41.5		0.064	Low Strength Intermediate Modulus C Fiber
Kevlar 49	400	17.5	2.5	0.051	High Tensile Modulus Organic Fiber
Magnumite AS1	450	33	1.32	0.065	Continuous PAN fiber, high strength, surface treated
Magnumite AS4	520	34	1.53	0.065	Continuous PAN fiber, high strength, surface treated

Table A-3. Properties of Carbon/Epoxy Prepreg (Page 1 of 2)

Manufacturer	Product Number	Prepreg Type/ Orientation	Prepreg Cure	Resin Content (%)
AMERICAN CYANAMID	CYCOM 907/T-300	UNIDIRECTIONAL	-	40 ± 3
	CYCOM 919/T-300	F-134 WEAVE	-	45 ± 2
	CYCOM 985/CELION	UNIDIRECTIONAL TAPE 145	-	37 ± 2
	CYCOM 985/CELION	7 MIL PLAIN WEAVE	-	40 ± 2
	CYCOM 985/T-300	UNIDIRECTIONAL TAPE	-	37 ± 3
	CYCOM 985/T-300	F-134 WEAVE	-	42 ± 2
	CYCOM 980/T-300	YARN F-134 WEAVE	-	42 ± 2
	CYCOM 980/T-300	UNIDIRECTIONAL TAPE	-	37 ± 3
CIBA-GEIGY	R6268	-	-	40 ± 2
	RAC 6350	-	-	43 ± 3
	R6378	UNIDIRECTIONAL	-	35
FERRO CORPORATION	CE-9000-1/T-300	2424 8H SATIN WEAVE	-	40 ± 3
	CE-9000-2	2424	-	40 ± 3
	CE-9000-9/T-300	UNIDIRECTIONAL	-	39 ± 3
	CE-343/CELION 6000	UNIDIRECTIONAL	-	40
	CE-3201/T-300	UNIDIRECTIONAL	-	39 ± 4
	CE-9000-9/P-75S	-	-	40.3
	CE-339/HMS	UNIDIRECTIONAL	-	41.3
	CE-339/GY-70	-	-	36.6
	CE-339/T-300	UNIDIRECTIONAL	-	39 ± 4
	CE-324/T-300	UNIDIRECTIONAL	-	39 ± 4
	CE-324/T-300	2424	-	40 ± 3
HERCULES	A*370 5H/3501-5A	5H WEAVE	-	42 ± 3, 35 ± 3
	A*370 5H/3501-6	5H WEAVE	-	42 ± 3, 35 ± 3
	A*370 8H/3501-5A	8H WEAVE	-	42 ± 3, 35 ± 3
	A*370 8H/3501-6	8H WEAVE	-	42 ± 3, 35 ± 3
	A*183 P/3501-5A	PLAIN WEAVE	-	42 ± 3, 35 ± 3
	A*183 P/3501-6	PLAIN WEAVE	-	42 ± 3, 35 ± 3
	HMS/1900	UNIDIRECTIONAL	-	38 ± 3
	HMS/3501-6	UNIDIRECTIONAL	-	42 ± 3
	HMS/3501-5A	UNIDIRECTIONAL	-	42 ± 3
	AS4/1908	UNIDIRECTIONAL W/O GLASS SCRIM	-	38 ± 3
	AS4/1908	UNIDIRECTIONAL/108 GLASS SCRIM	-	38 ± 3
	AS4/3502	UNIDIRECTIONAL	-	42 ± 3, 35 ± 3
	AS4/3501-6	UNIDIRECTIONAL	-	42 ± 3, 35 ± 3
	AS/3501-6	UNIDIRECTIONAL	-	42 ± 3, 35 ± 3
	AS4/3501-5A	UNIDIRECTIONAL	-	42 ± 3, 35 ± 3
	AS/3501-5A	UNIDIRECTIONAL	-	42 ± 3, 35 ± 3
	IG300 5H/3501-6	5H SATIN WEAVE	-	32 - 42
	AS4 OR IM7X/8551-7	TAPE	-	32 - 42
	AS4/8551-7	TAPE & FABRIC	-	33 - 46
	AS4/2220-3	UNIDIRECTIONAL TAPE	-	37 ± 3
	AS4/4502	UNIDIRECTIONAL TAPE	-	42 ± 3, 35 ± 3
	AS4/1919	UNIDIRECTIONAL TAPE	-	38 ± 3
	HMS4/3501-5A	UNIDIRECTIONAL TAPE	-	42 ± 3, 35 ± 3
	HMS4/3501-6	UNIDIRECTIONAL TAPE	-	42 ± 3, 35 ± 3
	IM6/3501-6	UNIDIRECTIONAL TAPE	-	32 - 42
	A*185-CSW/3501-5A	CROW'S FOOT SATIN WEAVE	-	42 ± 3, 35 ± 3
	A*185-CSW/3501-6	CROW'S FOOT SATIN WEAVE	-	42 ± 3, 35 ± 3
	A*185-CSW/3502	CROW'S FOOT SATIN WEAVE	-	42 ± 3, 35 ± 3
	A*370 5H/3502	5H WEAVE	-	42 ± 3, 35 ± 3
	A*370 8H/3502	8H WEAVE	-	42 ± 3, 35 ± 3
	A*183-P/3502	PLAIN WEAVE	-	42 ± 3, 35 ± 3
	A*260-5H/3501-5A	5H WEAVE	-	42 ± 3, 35 ± 3
	A*260-5H/3501-6	5H WEAVE	-	42 ± 3, 35 ± 3
	A*260-5H/3502	5H WEAVE	-	42 ± 3, 35 ± 3
HEXCEL	T-300/F263	UNIDIRECTIONAL 3000 TOW	-	42 ± 3
	T-300/F250	UNIDIRECTIONAL 3000 TOW	-	42 ± 3
	T-300/F263	BIDIRECTIONAL WOVEN 3000 TOW	-	43 ± 3
	T-300/F163	UNIDIRECTIONAL 3000 TOW	OVEN CURE	33 ± 3
	T-300/F163	UNIDIRECTIONAL 3000 TOW	AUTOCLAVE	42 ± 3
	T8T190/F584	T-300 8K	-	36 - 40
	T4A145/F584	AS6 12K	-	26 - 30
	T5A145/F584	IM6 12K	-	32 - 36
	T5A190/F584	IM6 12K	-	32 - 36
	T6U145/F584	T-700 6K	-	32 - 36
	T8A145/F584	AS4 12K	-	27 - 30
HITCO	EM-7125A	CHOPPED STRAND MOLDING CMPD	-	37 - 43
	E787HM	UNIDIRECTIONAL TAPE	-	36
	E787	3K PLAIN WEAVE	-	40

Table A-3. Properties of Carbon/Epoxy Prepreg (Page 2 of 2)

Resin Flow (%)	Volatile Content (%)	Tack	Drape	Fiber Areal Weight (g/m ²)	Shelf Life (months at 0 F)	Out Time (days at 77 F)	Gel Time (min)
15 ± 5 (50 PSI/350 F)	1	-	-	-	6 (70 F)	-	-
12 ± 5 (50 PSI/250 F)	1.5	-	-	-	6	-	-
24 ± 7 (50 PSI/500 F)	2.0	-	-	-	-	-	-
16 ± 7 (50 PSI/500 F)	2.0	-	-	-	-	-	-
18 ± 6 (50 PSI/350 F)	1.0	-	-	-	6	-	15 ± 3 (350 F)
18 ± 6 (50 PSI/350 F)	1.0	-	-	-	6	-	15 ± 3 (350 F)
15 ± 6 (50 PSI/350 F)	1.0	-	-	-	6	-	15 ± 3 (350 F)
15 ± 6 (50 PSI/350 F)	1.0	-	-	-	6	-	15 ± 3 (350 F)
5 - 18 (50 PSI/275 F)	2	-	-	-	-	14	3 - 14 (275 F)
15 ± 5 (50 PSI/350 F)	2	-	-	-	6 (40 F)	14	-
15 ± 5 (100 PSI/350 F)	1.5	-	-	-	6	21	18 ± 5 (350 F)
20 ± 4 (10 MIN/100 PSI/325 F)	2	-	-	-	-	-	4 - 13 (325 F)
17 ± 5 (15 PSI/325 F)	2 (10 MIN/325 F)	MEDIUM	MEDIUM	-	-	-	4 - 10 (350 F)
7 (15 PSI/250 F)	1 (10 MIN/350 F)	-	-	-	-	-	10 - 18 (350 F)
4 - 15 (15 PSI/324 F)	2 (250 F)	-	-	-	-	-	13 (250 F)
16.2 (15 PSI/350 F)	1.5 (10 MIN/325 F)	-	-	-	-	-	4 - 20 (325 F)
17.5 (10 MIN/15 PSI/250 F)	1.1 (15 MIN/275 F)	-	-	-	-	-	10.25 (350 F)
9.8 (10 MIN/15 PSI/250 F)	0.1 (10 MIN/250 F)	-	-	-	-	-	7.66 (250 F)
5 - 20 (15 PSI/275 F)	0.9 (10 MIN/250 F)	MEDIUM	-	-	-	-	12.8 (250 F)
4 - 15 (10 PSI/275 F)	1.5 (10 MIN/275 F)	-	-	-	-	-	4 - 20 (275 F)
10 (10 MIN/15 PSI/250 F)	1.5 (10 MIN/275 F)	-	-	-	-	-	4 - 20 (275 F)
-	2 (10 MIN/250 F)	-	-	-	-	-	8 (250 F)
-	1.5	-	-	370 ± 14	12	10	3 - 7 (350 F)
-	1.5	-	-	370 ± 14	12	10	6 - 12 (350 F)
-	1.5	-	-	370 ± 14	12	10	3 - 7 (350 F)
-	1.5	-	-	370 ± 14	12	10	6 - 12 (350 F)
-	1.5	-	-	193 ± 8	12	10	3 - 7 (350 F)
-	1.5	-	-	193 ± 8	12	10	6 - 12 (350 F)
-	1.5	-	-	146	12	14	7 - 14 (250 F)
-	1	-	-	146	12	10	6 - 12 (350 F)
-	1	-	-	146	12	10	3 - 7 (350 F)
-	1.5	-	-	146	12	14	7 - 14 (250 F)
-	1.5	-	-	146	12	14	7 - 14 (250 F)
-	1	-	-	164	12	10	12 - 32 (350 F)
-	1	-	-	150	12	10	6 - 12 (350 F)
-	1	-	-	150	12	10	6 - 12 (350 F)
-	1	-	-	150	12	10	6 - 12 (350 F)
-	1	-	-	150	12	10	3 - 7 (350 F)
-	1.5	-	-	-	12	10	6 - 12
-	1.5	-	-	75 - 200	12	7	8 - 20 (350 F)
-	1.5	-	-	355 - 385	12	7	8 - 20 (350 F)
-	1.0	-	-	150	12	14	2.5 (350 F)
-	1	-	-	150	12	17	19 (350 F)
-	1.5	-	-	145	12	14	5 - 12 (250 F)
-	1	-	-	150	12	10	3 - 7 (350 F)
-	1	-	-	146	12	10	6 - 12 (350 F)
-	1	-	-	150	12	10	6 - 12 (350 F)
-	1.5	-	-	185 ± 8	12	10	3 - 7 (350 F)
-	1.5	-	-	185 ± 8	12	10	6 - 12 (350 F)
-	1.5	-	-	185 ± 8	12	10	12 - 32 (350 F)
-	1.5	-	-	370 ± 14	12	10	12 - 32 (350 F)
-	1.5	-	-	370 ± 14	12	10	12 - 32 (350 F)
-	1.5	-	-	193 ± 8	12	10	12 - 32 (350 F)
-	1.5	-	-	280 ± 10	12	10	3 - 7 (350 F)
-	1.5	-	-	280 ± 10	12	10	6 - 12 (350 F)
-	1.5	-	-	280 ± 10	12	10	12 - 32 (350 F)
22 ± 4 (100 PSI/350 F)	2	GOOD	-	-	-	-	1 - 8 (350 F)
22 ± 4 (100 PSI/250 F)	2	GOOD	-	-	-	-	4 - 10 (250 F)
20 ± 4 (100 PSI/350 F)	2	GOOD	GOOD	-	-	-	1 - 8 (350 F)
10 ± 4 (15 PSI/350 F)	2	GOOD	GOOD	-	-	-	6 - 10 (350 F)
17 ± 4 (50 PSI/350 F)	2	GOOD	GOOD	-	-	-	6 - 10 (350 F)
5 - 15 (50 PSI/350 F)	1 - 4 (350 F)	-	-	180	-	-	-
5 - 15 (50 PSI/350 F)	1 - 4 (350 F)	-	-	145	-	-	-
5 - 15 (50 PSI/350 F)	1 - 4 (350 F)	-	-	145	-	-	-
5 - 15 (50 PSI/350 F)	1 - 4 (350 F)	-	-	180	-	-	-
5 - 15 (50 PSI/350 F)	1 - 4 (350 F)	-	-	145	-	-	-
5 - 15 (50 PSI/350 F)	1 - 4 (350 F)	-	-	145	-	-	-
-	0.5	-	-	-	12	90	-
-	2.0	-	-	145	-	-	-
-	-	-	-	183	-	-	-

Table A-4. Properties of Glass/Epoxy Prepreg (Page 1 of 2)

Manufacturer	Product Number	Prepreg Type/ Orientation	Resin Content (%)	Resin Flow (%)
AMERICAN CYANAMID	CYCOM 5143	-	35 - 40	20 ± 4 (50 PSI/325 F)
	CYCOM 5105	-	36 - 40	10 - 20
	CYTRON 5104	REGULAR GEL-GRADE C/104	75 ± 5	50 ± 7 (200 PSI/340 F)
	CYTRON 5104	REGULAR GEL-GRADE C/108	65 ± 5	44 ± 7 (200 PSI/340 F)
	CYTRON 5104	REGULAR GEL-GRADE C/112	60 ± 5	40 ± 7 (200 PSI/340 F)
	CYTRON 5104	REGULAR GEL-GRADE C/113	60 ± 5	40 ± 7 (200 PSI/340 F)
	CYTRON 5104	REGULAR GEL-GRADE C/116	55 ± 5	35 ± 7 (200 PSI/340 F)
	CYTRON 5104	MEDIUM GEL-GRADE D/104	75 ± 5	45 ± 7 (200 PSI/340 F)
	CYTRON 5104	MEDIUM GEL-GRADE D/108	65 ± 5	40 ± 7 (200 PSI/340 F)
	CYTRON 5104	MEDIUM GEL-GRADE D/112	60 ± 5	36 ± 7 (200 PSI/340 F)
	CYTRON 5104	MEDIUM GEL-GRADE D/113	60 ± 5	36 ± 7 (200 PSI/340 F)
	CYTRON 5104	MEDIUM GEL-GRADE D/116	55 ± 5	32 ± 7 (200 PSI/340 F)
	CYTRON 5150B	104	75 ± 5	50 ± 5 (200 PSI/340 F)
	CYTRON 5150B	108	65 ± 5	36 ± 5 (200 PSI/340 F)
	CYTRON 5150B	112	60 ± 5	30 ± 5 (200 PSI/340 F)
	CYTRON 5150B	113	55 ± 5	30 ± 5 (200 PSI/340 F)
	CYTRON 5150B	116	52 ± 5	22 ± 5 (200 PSI/340 F)
	CYCOM 985/E-GLASS	7781 B-H SATIN	36 ± 2	20 ± 7 (50 PSI/350 F)
	CYCOM 980/E-GLASS	7781 A1100	34 ± 2	20 ± 5 (50 PSI/350 F)
	CYCOM 5102/E-GLASS	7581	35 - 45	15 - 25 (50 PSI/325 F)
	CYCOM 5134	7581	38 ± 2	13 ± 7 (77 F)
CIBA-GEIGY	R1604	-	35 ± 2	13 ± 4
	R2520	-	38	18 ± 5 (50 PSI/260 F)
	RAC 7350	-	30	15 ± 5 (50 PSI/350 F)
	R7373	-	35 ± 3	10 ± 5 (15 PSI/325 F)
FERRO CORPORATION	CE-9018A	7781	36	17 (15 MIN/50 PSI/330 F)
	CE-9000-1	7781	36.2	14.0 (10 MIN/15 PSI/325 F)
	CE-9000-2	120	43 - 53	15 - 30 (15 PSI/325 F)
	CE-6000-2	7781	35.6	15.3 (10 MIN/15 PSI/325 F)
	CE-3330	7781	38.0	14.7 (15 PSI/250 F)
	CE-3201	7781	36 - 44	10 - 20 (10 MIN/15 PSI/325 F)
	CE-347/E GLASS	456 UNIDIRECTIONAL	35 - 42	28 ± 4 (10 MIN/50 PSI/325 F)
	CE-345	7781	38.7	9.0 (15 PSI/250 F)
	CE-339	7781	35.1	8.1 (15 PSI/250 F)
	CE-339	120	49.4	19.3 (15 PSI/250 F)
	CE-324	7781	37 ± 3	10 ± 5 (10 MIN/15 PSI/250 F)
	CE-306	7781	38 ± 2	15 ± 4 (50 PSI/275 F)
	E-293	7781	40 ± 3	15 - 25 (5 MIN/15 PSI/325 F)
	CE-9000/MPC-4	7781	35 - 39	9 - 15 (10 MIN/15 PSI/325 F)
	CE-9000/VOL. A	1543	32 - 36	10 - 18 (10 MIN/15 PSI/325 F)
	CE-9000/MPC-5	7576	32 - 36	10 - 16 (10 MIN/15 PSI/325 F)
	CE-307HM	7544	34.3	5.0 (15 PSI/250 F)
	CE-307HM	1582	32.2	3.0 (15 PSI/250 F)
	CE-307HM	76281	32.7	21.5 (15 PSI/250 F)
	CE-307	7781	46.0	22.0 (15 PSI/250 F)
	CE-3201/VOLAN A	112	45.3	15 (15 PSI)
	CE-9000/S 2 GLASS	6581	36.8	20.2 (50 PSI/325 F)
	E-9300	7781	33.4	8.65
	EF-2/S-901	ROVING	17 - 23	5 - 12 (325 F)
	EF-2/S-2	ROVING	17 - 23	5 - 12 (10 MIN/325 F)
FIBERITE	MXB-7018	181	32	14 (100 FSI/325 F)
	MXB-7203	7581	41.0	22.0 (50 PSI/250 F)
	MXB-7701	1581	38	16 (50 PSI/275 F)
HITCO	EM-7205A	-	34 ± 3	5 - 20
	EM-7302LD	-	41 - 47	-
	EM-7302-XLD	-	41 - 47	-
	EM-7302	-	33 - 39	-
	E718LT/1583	-	35	-

Table A-4. Properties of Glass/Epoxy Prepreg (Page 2 of 2)

Volatile Content (%)	Tack	Drape	Shelf Life (days)	Out Time (days at 77 F)	Gel Time (minutes)
0 - 9 (325 F)	-	-	-	10 - 14	1 - 1.68 (325 F)
1.5	-	-	90 (40 F)	-	-
0.75	-	-	-	-	3.66 ± 0.3 (340 F)
0.75	-	-	-	-	3.66 ± 0.3 (340 F)
0.75	-	-	-	-	3.66 ± 0.3 (340 F)
0.75	-	-	-	-	3.66 ± 0.3 (340 F)
0.75	-	-	-	-	3.66 ± 0.3 (340 F)
0.75	-	-	-	-	2 ± 0.3 (340 F)
0.75	-	-	-	-	2 ± 0.3 (340 F)
0.75	-	-	-	-	2 ± 0.3 (340 F)
0.75	-	-	-	-	2 ± 0.3 (340 F)
0.75	-	-	-	-	2 ± 0.3 (340 F)
0.75	-	-	-	-	4 ± 0.5 (340 F)
0.75	-	-	-	-	4 ± 0.5 (340 F)
0.75	-	-	-	-	4 ± 0.5 (340 F)
0.75	-	-	-	-	4 ± 0.5 (340 F)
0.75	-	-	-	-	4 ± 0.5 (340 F)
2.0	-	-	-	-	-
1.0	-	-	180 (0 F)	-	12 ± 4 (350 F)
3 (325 F)	-	-	90 (40 F)	-	-
1.5	-	-	90 (0 F)	-	-
2.2	-	-	180 (40 F)	30	-
2	-	-	180 (40 F)	10	3 - 6 (275 F)
2	-	-	180 (40 F)	14	-
1	-	-	180	14	6 ± 2 (325 F)
1.5 (10 MIN/350 F)	-	-	10 (80 F)	-	-
0.8 (10 MIN/325 F)	-	-	10 (80 F)	-	-
3 (10 MIN/325 F)	MEDIUM	MEDIUM	-	-	-
0.4 (10 MIN/325 F)	-	-	10 (80 F)	-	12
1.4 (10 MIN/325 F)	MEDIUM	EXCELLENT	30 (80 F)	-	3.9 (280 F)
3 (10 MIN/325 F)	-	-	14 (80 F)	-	-
1.5 (20 MIN/325 F)	MEDIUM	MEDIUM	10 (80 F)	-	31 ± 2 (300 F)
0.8 (10 MIN/250 F)	MEDIUM	-	30 (80 F)	-	4 (250 F)
0.4 (250 F)	-	-	60 (80 F)	-	6.25 (250 F)
0.3 (250 F)	-	-	60 (80 F)	-	5.33 (250 F)
2 (10 MIN/250 F)	-	-	60 (80 F)	-	8 (250 F)
1.5 (375 F)	-	-	30 (80 F)	-	2 - 10 (250 F)
2 - 6 (10 MIN/325 F)	LIGHT	-	-	-	1.5 - 2.5 (325 F)
2 (15 MIN/325 F)	-	-	-	-	-
2 (10 MIN/15 PSI/325 F)	-	-	-	-	-
2 (10 MIN/325 F)	-	-	-	-	-
0.3 (250 F)	MEDIUM	MEDIUM	-	-	12.5 (250 F)
0.3 (250 F)	MEDIUM	MEDIUM	-	-	12.5 (250 F)
0.3 (250 F)	MEDIUM	MEDIUM	-	-	12.25 (250 F)
0.28	-	-	-	142	12.5 (250 F)
0.7 (10 MIN/325 F)	-	-	-	-	15.5 (325 F)
0.8 (15 MIN/325 F)	-	-	-	-	11.6 (325 F)
1.08	-	-	-	30	0.833
3 (10 MIN/325 F)	-	-	-	-	1 - 3.5 (325 F)
3.0 (10 MIN/325 F)	-	-	-	-	1 - 4 (325 F)
1.2	-	-	-	-	-
1.2	-	-	-	-	9 (250 F)
1	-	-	-	-	4 (275 F)
2.0	-	-	-	-	-
0.5	-	-	-	-	-
0.5	-	-	-	-	-
0.5	-	-	-	-	-
1.5	-	-	-	-	-

Table A-5. Properties of Kevlar/Epoxy Prepreg (Page 1 of 2)

Manufacturer	Product Number	Prepreg Type/ Orientation	Resin Content (%)	Resin Flow (%)
AMERICAN CYANAMID	CYCOM 5118L/KEVLAR 49	181	50-55	17-25
	CYCOM 5105B/KEVLAR 49	181	50-55	27-35 (15 MIN/325 F)
	CYCOM 950/KEVLAR 49	281	45 \pm 4	18 \pm 7 (50 PSI/250 F)
	CYCOM 950/KEVLAR 49	UNIDIRECTIONAL	50 \pm 4	25 \pm 10 (50 PSI/250 F)
	CYCOM 983/KEVLAR 49	K-285	50 \pm 2	33 \pm 7 (50 PSI/350 F)
	CYCOM 985/KEVLAR 49	281	45 \pm 4	20 \pm 7 (50 PSI/350 F)
	CYCOM 989/KEVLAR 49	281	45 \pm 4	18 \pm 7 (50 PSI/350 F)
	CYCOM 5102/KEVLAR 49	181	54.5	22.5 (10 PSI/350 F)
CIBA-GEIGY	R9256-1	285	55 \pm 3	10-40 (50 PSI/250 F)
	R9256-2	120 CROWFOOT	63 \pm 3	10-40 (50 PSI/250 F)
	R9257	181	51 \pm 3	17-37 (50 PSI/250 F)
	R9269	285	52 \pm 3	15-30 (50 PSI/275 F)
	R9269	120	57 \pm 3	15-30 (50 PSI/275 F)
	RAC 9350	281, 285	50 \pm 3	20 \pm 5
	RAC 9350	120	60 \pm 3	20 \pm 5
	R9369	285	50 \pm 3	33 \pm 6 (50 PSI/325 F)
	R9369	120	55 \pm 3	30 \pm 6 (50 PSI/325 F)
	R9521	181, 285	54 \pm 3	15-35 (50 PSI/275 F)
FERRO CORPORATION	CE-9010A	181	54.1	28.4 (10 MIN/50 PSI/325 F)
	CE-9010	181	52	22.5 (10 MIN/15 PSI/325 F)
	CE-9010	120	56	25 (10 MIN/15 PSI/325 F)
	CE-9000-2/KEVLAR 49	285	45-55	20-35 (15 PSI/325 F)
	CE-9000/KEVLAR 49	181	49.5	17.9 (15 PSI/325 F)
	CE-345/KEVLAR 49	281	53	25.2 (15 PSI/250 F)
	CE-345/KEVLAR 49	181	52.3	25.2 (15 PSI/250 F)
	CE-345/KEVLAR 49	UNIDIRECTIONAL TAPE	57.7	28.1 (15 PSI/250 F)
	CE-343/KEVLAR	4560 UNIDIRECTIONAL TAPE	58.1	9.4 (50 PSI/250 F)
	CE-306	281	53 \pm 2	30 \pm 5 (50 PSI/260 F)
	CE-306	281	47.1	19.5
	CE-321R	4560 UNIDIRECTIONAL TAPE	45 \pm 3	15 \pm 6 (50 PSI/250 F)
	CE-324/KEVLAR 49	285	52	23 (50 PSI/250 F)
FIBERITE	MXM-7880/KEVLAR 49	120	55	28.8 (50 PSI/325 F)
	MXM-7880/KEVLAR 49	285	52	28.9 (50 PSI/325 F)
	MXM-7978/KEVLAR 49	120	51	24 (100 PSI/350 F)
	MXM-7978/KEVLAR 49	285	49	30 (100 PSI/350 F)
	MXM-7669/KEVLAR 49	285	49.1	29 (50 PSI/325 F)
	MXM-7764/KEVLAR 49	181, 285	51-57	15-35 (50 PSI/275 F)
	MXM-7064/KEVLAR 49	181, 285	51-57	2-7 (50 PSI/275 F)
	MXM-7714/KEVLAR 49	120	54-60	20-30 (50 PSI/250 F)
	MXM-7714/KEVLAR 49	285	49-55	20-30 (50 PSI/250 F)
	MXM-7251/KEVLAR 49	285	55	30 (50 PSI/250 F)

Table A-5. Properties of Kevlar/Epoxy Prepreg (Page 2 of 2)

Volatile Content (%)	Wick	Drape	Fiber Areal Weight (g/m ²)	Shelf Life (months)	Out Time (days at 77 F)	Gel Time (min)
2	-	-	-	3 (40 F)	-	10-15
2 (10 MIN/325 F)	-	-	-	3 (40 F)	-	-
1.0	-	-	-	6 (0 F)	10	17 ± 3 (250 F)
1.0	-	-	-	6 (0 F)	10	17 ± 3 (250 F)
2.0	-	-	-	-	-	-
1.0	-	-	-	6 (0 F)	-	15 ± 3 (350 F)
1.0	-	-	-	6 (0 F)	-	15 ± 3 (350 F)
1.4	-	-	-	3 (40 F)	-	2.0 (325 F)
1.5	LIGHT	-	-	6 (40 F)	15	2-12 (250 F)
1.5	LIGHT	-	-	6 (40 F)	15	2-12 (250 F)
1.5	LIGHT	-	-	6 (10 F)	15	3-8 (250 F)
2	-	-	-	6 (10 F)	15	2-12 (275 F)
2	-	-	-	6 (10 F)	15	2-12 (275 F)
2	-	-	-	6 (40 F)	14	-
2	-	-	-	6 (40 F)	14	-
2	-	-	-	6 (40 F)	10	18 ± 6 (325 F)
2	-	-	-	-	-	18 ± 6 (325 F)
2	-	-	-	6 (40 F)	10	2-7 (275 F)
1.14 (10 MIN/325 F)	-	-	-	-	-	8.5 (325 F)
1.0 (10 MIN/325 F)	-	-	-	-	-	18 (325 F)
1.2 (10 MIN/325 F)	-	-	-	-	-	18 (325 F)
3 (10 MIN/325 F)	MEDIUM	MEDIUM	-	-	-	4-10 (350 F)
2.0 (10 MIN/325 F)	-	-	-	-	-	-
1.1 (10 MIN/250 F)	MEDIUM	-	-	-	-	3.5 (250 F)
1.1 (10 MIN/250 F)	MEDIUM	-	-	-	-	3.5 (250 F)
1.4 (10 MIN/250 F)	MEDIUM	-	-	-	-	3.3 (250 F)
3.8 (250 F)	-	-	11.3	-	-	10.08 (250 F)
2 (15 MIN/280 F)	MEDIUM	MEDIUM	-	-	-	8 (280 F)
0.8	-	-	-	-	-	-
3.5 (250 F)	-	-	21-23	-	-	10 ± 4 (250 F)
1.5 (10 MIN/250 F)	-	-	-	-	-	9 (250 F)
1 (8 MIN/325 F)	-	-	-	-	-	24.3
1 (8 MIN/235 F)	-	-	-	-	-	27.9
1 (15 MIN/325 F)	-	-	-	-	-	16 (350 F)
1 (15 MIN/325 F)	-	-	-	-	-	16 (350 F)
1.2	-	-	-	-	-	2.4 (325 F)
2 (8 MIN/275 F)	-	-	-	-	-	2-7 (275 F)
2 (8 MIN/275 F)	-	-	-	-	-	-
2 (8 MIN/275 F)	-	-	-	-	-	4-10 (275 F)
2 (8 MIN/275 F)	-	-	-	-	-	4-10 (275 F)
1 (10 MIN/250 F)	-	-	-	-	-	10 (250 F)

Table A-6. Properties of Glass/Polyimide Prepreg (Page 1 of 2)

Manufacturer	Product Number	Prepreg Type/ Orientation	Laminate Cure	Resin Content (%)
AMERICAN CYANAMID	CYCOM 3001	112	-	50-55 (8 MIN/325 F)
	CYCOM 3001	120	-	35-40 (8 MIN/325 F)
	CYCOM 3001	143	-	35-40 (8 MIN/325 F)
	CYCOM 3002	108	-	-
	CYCOM 2507	104	-	-
	CYCOM 3002	7781	-	27-33
	CYCOM 3003	A1100 E GLASS/7781	-	32-36
CIBA-GEIGY	R7451	-	-	36 \pm 2
FERRO CORPORATION	CPI-2274	7781	-	40.1
	CPI-2272	7781	-	37.0
	CPI-2249	7781	VACUUM BAG	48-50
	CPI-2249	7781	HIGH PRESSURE	42-44
	CPI-2237	7781	-	35 \pm 3
	CPI-2214	7781	-	41.7
FIBERITE	MXB-5004	181-150	-	28.6
HEXCEL	F174	-	-	25-45

Table A-6. Properties of Glass/Polyimide Prepreg (Page 2 of 2)

Resin Flow (%)	Volatiles Content (%)	Shelf Life (months at 40 F)	Out Time (days at 77 F)	Gel Time (min)
35-45 (5 MIN/15 PSI/350 F)	9-12 (8 MIN/325 F)	-	-	3-4 (350 F)
20-25 (5 MIN/15 PSI/350 F)	6-9 (8 MIN/325 F)	-	-	3-4 (350 F)
25-35 (5 MIN/15 PSI/350 F)	6-9 (8 MIN/325 F)	-	-	3-4 (350 F)
52 ± 7 (5 MIN/15 PSI/450 F)	31 ± 3 (2.5 MIN/750 F)	-	-	-
33 ± 4 (5 MIN/15 PSI/450 F)	33 ± 4 (2.5 MIN/750 F)	-	-	-
20-29 (15 PSI/450 F)	17-21 (2.5 MIN/750 F)	-	-	-
32-38	18-21 (2.5 MIN/750 F)	-	-	-
19 (85 PSI/350 F)	8 (325 F)	-	-	14 (350 F)
-	8.7 (5 MIN/800 F)	3	10	-
20-22 (10 MIN/15 PSI/350 F)	-	3	7	30 (300 F)
20-30 (10 MIN/15 PSI/350 F)	12-18 (10 MIN/350 F)	3	7-10	-
11-17 (10 MIN/15 PSI/350 F)	8-8.5 (10 MIN/350 F)	3	7-10	-
NOT APPLICABLE	9 ± 3 (5 MIN/800 F)	3	10	-
17.5 (10 MIN/200 PSI/370 F)	0.37 (10 MIN/370 F)	-	90	-
12.1 (10 MIN/15 PSI/350 F)	9 (10 MIN/325 F)	-	-	-
-	9-15	3	-	-

Table A-7. Properties of Carbon/Epoxy Laminates (Page 1 of 2)

Manufacturer	Product Number	Fiber	Resin	Laminate Cure	Laminate Type/ Orientation	UFS Long (ksi)	UFS Trans (ksi)	UTS Long (ksi)
AMERICAN CYANAMID	CYCROM 807/T-300	THORNEL 300	-	-	UNIDIRECTIONAL	203	13.7	-
	CYCROM 819/T-300	THORNEL 300	-	-	-	107	-	85
	CYCROM 885	CELION/E-32 MS	CYCROM 885	-	UNIDIR./GRADE 145	-	-	250
	CYCROM 885	CELION/E-32 MS	CYCROM 885	-	3K70 PLAIN WEAVE	-	-	95
	CYCROM 885/T-300	THORNEL 300	CYCROM 885	-	UNIDIRECTIONAL	265	-	216
	CYCROM 885/T-300	THORNEL 300	CYCROM 885	-	-	95	-	83
	CYCROM 880/T-300	THORNEL 300	CYCROM 880	-	UNIDIRECTIONAL	159	-	88
	CYCROM 880/T-300	THORNEL 300/F134	CYCROM 880	-	FABRIC STYLE F134	100	-	58
CIBA GEIGY	RAC 8350	AS	-	-	-	240	-	200
	RAC 8350	HMS	-	-	-	185	-	135
	RAC 8350	AS/104 GLASS	-	-	-	240	-	198
	RAC 8350	HTS	-	-	-	265	-	215
	R8378	HERCULES AS-8	-	-	TAPE	262	-	380
	R8378	HERCULES IM6	-	-	TAPE	272	-	381
FERRO CORPORATION	CE 8000-1	THORNEL 300/2424	CE 8000-1	-	FABRIC	104	-	80
	CE 8000-2	2424	CE 8000-2	-	FABRIC	121.6	108.1	82.3
	CE 8000-8/T-300	THORNEL 300	CE 8000-8	-	UNIDIRECTIONAL	280	-	240
	CE 343/CELION 6000	CELION 6000	CE 343	-	-	245	-	245
	CE 3201/T-300	THORNEL 300	CE 3201	-	UNIDIRECTIONAL	237	-	-
	CE 8000-9/P-75S	-	CE 8000-9	-	-	80.3	-	110.3
	CE 336/HMS	HMS	CE 336	-	-	153	142	-
	CE 336/GY-70	GY-70	CE 336	-	-	109.5	-	95.8
	CE 336/T-300	THORNEL 300	CE 336	-	UNIDIRECTIONAL	229.3	-	-
	CE 324/T-300	THORNEL 300/BK	CE 324	-	UNIDIRECTIONAL	247	-	-
	CE 324/2424	THORNEL 300/2424	-	-	FABRIC	119	109	84
FIBERITE	HY-E 1334	GY-70	834	-	UNIDIRECTIONAL	134	-	85
	HY-E 1334A	HM-3	834	-	UNIDIRECTIONAL	190	-	120
	HY-E 1334B	HT-3	834	-	UNIDIRECTIONAL	230	-	205
	HY-E 1334C	A-8	834	-	UNIDIRECTIONAL	260	-	235
	HY-E 1034C	THORNEL 300/3K	834	-	UNIDIRECTIONAL	270	-	230
	HY-E 1078C	THORNEL 300/3K	878	-	UNIDIRECTIONAL	298	-	233
	HY-E 1078E	THORNEL 300/BK	878	-	UNIDIRECTIONAL	287	-	215
	HY-E 1034C	THORNEL 300/3K	834	-	CROSS PLY TAPE	120	-	98
	HMF 133/34	-	-	-	FABRIC	100	-	90
	HMF 330C/34	-	-	-	QUASI-ISOTROPIC	-	-	88.7
	T300/834	-	-	-	QUASI-ISOTROPIC	-	-	71.7
	HMF 178/34	THORNEL 300/1000	-	-	SH SATIN	-	-	90
	HMF 134/34	THORNEL 300/3000	-	-	PLAIN WEAVE	-	-	30
	HMF 705/34	THORNEL 300/8000	-	-	PLAIN WEAVE	-	-	200
	HMF 1133/78	CELION/3000	-	-	SH SATIN	-	-	90
	HMF 131/48A	THORNEL 300/3000	-	-	SH SATIN	-	-	85
	HMF 1133/86A	CELION/3000	-	-	SH SATIN	-	-	80
	HMF 133/80	THORNEL 300/3000	-	-	SH SATIN	-	-	80
HERCULES	A370-SH/3501-5A	A370-SH	3501-5A	-	SH SATIN	150	-	100
	A370-BH/3501-5A	A370-BH	3100-5A	-	SH SATIN	130	-	90
	A183-P/3501-5A	A183-P	3501-6A	-	PLAIN WEAVE	-	-	100
	HMS/1908	HMS	1908	-	TAPE	185	-	180
	HMS/3501-6	HMS	3501-6	-	TAPE	190	-	180
	HMS/3501-5A	HMS	3501-6A	-	TAPE	188	-	198
	AS4/1908	AS4 W/O SCRIM	1908	-	TAPE	240	-	250
	AS4/1908	AS4 W/ 108 SCRIM	1908	-	TAPE	210	-	225
	AS4/3502	AS4	3502	-	TAPE	280	-	280
	AS4/3501-6	AS4	3501-6	-	TAPE	280	-	310
	AS/3501-6	AS	3501-6	-	TAPE	280	-	230
	AS4/3501-5A	AS4	3501-5A	-	TAPE	250	-	310
	AS/3501-5A	AS	3501-5A	-	TAPE	280	-	250
	STYLE A370-SH	AS4/8K	-	-	SH SATIN	150	-	100
	STYLE A370-BH	AS4/3K	-	-	SH SATIN	130	-	90
	STYLE A183-P	AS4/3K	-	-	PLAIN	-	-	100
	TYPE HMS	TYPE HMS/10K	-	-	-	188	-	198
	TYPE AS1	TYPE AS1/10K	-	-	-	250	-	280
	TYPE AS4	TYPE AS4	-	-	-	280	-	315
	A370-SH/3501-6	A370-SH	3501-6	-	SH SATIN	150	-	100
	A370-SH/3502	A370-SH	3502	-	SH SATIN	150	-	100
	A370-BH/3501-6	A370-BH	3501-6	-	-	130	-	90
	A370-BH/3502	A370-BH	3502	-	-	130	-	90
	A183-P/3501-6	A183-P	3501-6	-	PLAIN	-	-	100
	IG380-SH/3501-6	IG380-SH	3501-6	-	SH FABRIC	-	-	-
	AS4/8551-7	AS4	8551-7	-	-	-	-	315
	IM7/8551-7	IM7	8551-7	-	-	-	-	400
	IM8/8551-7	IM8	8551-7	-	-	-	-	400
	AS4/8552	AS4	8552	-	-	-	-	305
	IM7/8552	IM7	8552	-	-	-	-	365
	IM8/8552	IM8	8552	-	-	-	-	375
	IM7/3501-6	IM7	3501-6	-	-	-	-	370
	IM8/3501-6	IM8	3501-6	-	-	-	-	380
	AS4/2220-3	AS4	2220-3	-	UNIDIRECTIONAL	280	-	310
	AS4/4502	AS4	4502	-	UNIDIRECTIONAL	280	-	270
	AS4/1919	AS4	1919	-	UNIDIRECTIONAL	230	-	320
	HMS4/3501-5A	HMS4	3501-5A	-	UNIDIRECTIONAL	188	-	198
	HMS4/3501-6	HMS4	3501-6	-	UNIDIRECTIONAL	160	-	180
	IM8/3501-6	IM8	3501-6	-	UNIDIRECTIONAL	280	-	370
	A*185-CSW/3501-5A	A*185-CSW	3501-5A	-	CSW FABRIC	-	-	120
	A*185-CSW/3502	A*185-CSW	3501-6	-	CSW FABRIC	-	-	120
	A*183-P/3501-5A	A*183-P	3501-6A	-	P FABRIC	-	-	129
	A*183-P/3501-6	A*183-P	3501-6	-	P FABRIC	-	-	100
	A*183-P/3502	A*183-P	3502	-	P FABRIC	-	-	100
	A*280-SH/3501-5A	A*280-SH	3501-6A	-	SH FABRIC	150	-	100
	A*280-SH/3501-6	A*280-SH	3501-6	-	SH FABRIC	150	-	100
	A*280-SH/3502	A*280-SH	3502	-	SH FABRIC	150	-	100
HIXEL	THORNEL 300/F283	T-300/3000 TOW	F283	-	UNIDIRECTIONAL	280	-	220
	THORNEL 300/F250	T-300/3000 TOW	F250	-	UNIDIRECTIONAL	260	-	220
	THORNEL 300/F283	T-300/3000 TOW	F283	-	BIDIR. FABRIC	120	-	80
	THORNEL 300/F183	T-300/3000 TOW	F183	-	UNIDIRECTIONAL	228	-	180
	THORNEL 300/F183	T-300/3000 TOW	F183	-	UNIDIRECTIONAL	251	-	210
	-	T8T190	F584	-	TAPE	-	-	218
	-	T4A145	F584	-	TAPE	285	-	404
	-	T5A145	F584	-	TAPE	265	-	414
	-	T5A190	F584	-	TAPE	-	-	445
	-	T8U145	F584	-	TAPE	242	-	340
	-	T8A145	F584	-	TAPE	-	-	341
HITCO	EM 7125A	1/2" CHOP LENGTH	MOLDING CMPO	-	-	50	-	25
	EM 7125A	1" CHOP LENGTH	MOLDING CMPO	-	-	74	-	35
	E787HM	-	-	-	UNIDIRECTIONAL	-	-	180
	E787JK	-	-	-	PLAIN WEAVE	104	-	68

UFS - Ultimate Flexural Strength
 UTS - Ultimate Tensile Strength
 UCS - Ultimate Compressive Strength

USS - Ultimate Shear Strength
 ISS - Interlaminar Shear Strength

FM - Flexural Modulus
 TM - Tensile Modulus
 CM - Compressive Modulus
 SM - Shear Modulus

TFS - Tensile Failure Strain
 CFS - Compressive Failure Strain
 SFS - Shear Failure Strain

Table A-7. Properties of Carbon/Epoxy Laminates (Page 2 of 2)

UTS Trans (ksi)	UCS Long (ksi)	UCS Trans (ksi)	USS (ksi)	ISS (ksi)	FM Long (ksi)	FM Trans (ksi)	TM Long (ksi)	TM Trans (ksi)	CM Long (ksi)	CM Trans (ksi)	SM (ksi)	Major Poisson Ratio	TFS Long (in/in)	TFS Trans (in/in)	CFS Long (in/in)
-	101	-	14.5 HORIZONTAL	-	16800	-	-	-	18100	-	-	-	-	-	-
-	67	-	10.5 SBS	-	7800	-	9100	-	9300	-	-	-	-	-	-
5.8	180	-	17.0 SBS	-	-	-	18500	1200	17900	-	-	-	-	-	-
-	103	-	11 SBS	-	-	-	8800	-	8800	-	-	-	-	-	-
-	-	-	17.7 SBS	-	18000	-	21800	-	-	-	-	-	-	-	-
-	62	-	8.7 SBS	-	8000	-	9800	-	8500	-	-	-	0.008135	-	-
-	71	-	10.5 SAS	-	11300	-	9800	-	11800	-	-	-	0.00877	-	-
-	70	-	8.9 SBS	-	8700	-	8800	-	11800	-	-	-	-	-	-
-	-	-	18.0 HORIZONTAL	-	18000	-	19500	-	-	-	-	-	-	-	-
-	125	-	8.8 HORIZONTAL	-	27300	-	13000	-	30000	-	-	-	-	-	-
-	-	-	18 HORIZONTAL	-	17300	-	19200	-	-	-	-	-	-	-	-
-	-	-	15.9 HORIZONTAL	-	20600	-	21800	-	-	-	-	-	-	-	-
12.1	228	-	19.3 SBS	-	19800	-	19700	1380	-	-	-	-	0.0182	0.0085	-
10.8	234	-	18 SBS	-	22500	-	23000	1300	-	-	-	-	0.0156	0.0078	-
-	72	-	9.8 HORIZONTAL	-	6200	-	10500	-	9200	-	-	-	-	-	-
63.4	80	77.5	8.9 SBS	-	7310	8010	10000	7240	9810	8080	-	-	-	-	-
7.8	190	-	16 SBS	-	10000	1200	19000	1700	18000	-	-	-	-	-	-
6	-	-	15 SBS	-	18500	-	19000	-	-	-	-	-	-	-	-
-	-	-	12.4 SBS	-	24000	-	-	-	-	-	-	-	-	-	-
-	-	-	8.1 SBS	-	33100	-	48400	-	-	-	-	-	-	-	-
-	-	-	9.46 SBS	-	24800	-	23500	-	-	-	-	-	-	-	-
6.5	80.3	-	8.8 SBS	-	39000	-	38800	780	35400	-	-	-	-	-	-
-	-	-	8.36	-	17000	-	-	-	-	-	-	-	-	-	-
-	88.7	-	12.8 SBS	-	22400	-	-	-	15400	-	-	-	-	-	-
81	74	-	9.9 HORIZONTAL	-	10000	9700	11100	11100	8500	-	-	-	-	-	-
-	-	-	7.5	-	38000	-	40000	-	-	-	-	-	-	-	-
-	-	-	8	-	30000	-	32000	-	-	-	-	-	-	-	-
-	-	-	12	-	21000	-	23000	-	-	-	-	-	-	-	-
-	-	-	17.5	-	19000	-	21000	-	-	-	-	-	-	-	-
-	-	-	17	-	20000	-	22000	-	-	-	-	-	-	-	-
-	-	-	17	-	21500	-	21600	-	-	-	-	-	-	-	-
-	-	-	14	-	20000	-	-	-	-	-	-	-	-	-	-
-	-	-	8.5BR	-	11500	-	-	-	-	-	-	-	-	-	-
90	-	-	8 SBS	-	-	-	10500	10500	-	-	4500	0.8	-	-	-
-	82	-	-	-	-	-	8000	-	7.5	-	-	0.89	-	-	-
-	65.4	-	-	-	-	-	7800	-	7	-	-	-	-	-	-
90	-	-	8.5 SBS	-	-	-	10000	10000	-	-	-	-	-	-	-
80	-	-	8.5 WAPP, 8500 FILL	-	-	-	9500	9500	-	-	-	-	-	-	-
10	-	-	11 WAPP, 3 FILL SBS	-	-	-	20600	1500	-	-	-	-	-	-	-
90	-	-	10 SBS	-	-	-	10500	10500	-	-	-	-	-	-	-
85	-	-	9.5 SBS	-	-	-	10000	10000	-	-	-	-	-	-	-
80	-	-	8.5 SBS	-	-	-	8000	8000	-	-	-	-	-	-	-
80	-	-	8 SBS	-	-	-	8000	8000	-	-	-	-	-	-	-
-	100	-	9.1 SBS	-	10000	-	10500	-	10200	-	-	-	0.0095	-	0.01
-	100	-	9.5 SBS	-	8600	-	10000	-	8900	-	-	-	0.0088	-	0.0113
-	86	-	8.75 SBS	-	-	-	10000	-	8900	-	-	-	0.0103	-	0.0110
-	-	-	8.0	-	26700	-	29000	-	-	-	-	-	-	-	-
-	-	-	7.8 SBS	-	28000	-	30000	-	-	-	-	-	-	-	-
-	-	-	13 SBS	-	26000	-	30000	-	-	-	-	-	-	-	-
-	-	-	12 SBS	-	19800	-	20500	-	-	-	-	-	-	-	-
-	-	-	17.5 SBS	-	13200	-	15500	-	-	-	-	-	-	-	-
-	-	-	18.5 SBS	-	18500	-	21500	-	-	-	-	-	-	-	-
-	-	-	17.5	-	18500	-	21500	-	-	-	-	-	-	-	-
-	-	-	18.5 SBS	-	17500	-	20000	-	-	-	-	-	0.0085	-	0.01
-	-	-	18.5 SBS	-	19500	-	21500	-	-	-	-	-	0.0088	-	0.0113
-	-	-	18.5 SBS	-	17500	-	19500	-	-	-	-	-	0.0103	-	0.0110
-	100	-	9.1 SBS	-	13000	-	10500	-	10200	-	-	-	-	-	-
-	100	-	9.5 SBS	-	9500	-	10000	-	8600	-	-	-	-	-	-
-	95	-	9.5 SBS	-	-	-	10000	-	8900	-	-	-	-	-	-
-	-	-	7.8	-	28000	-	30000	-	-	-	-	-	-	-	-
-	-	-	19	-	18000	-	20000	-	-	-	-	-	0.0095	-	0.01
-	-	-	18	-	18000	-	21000	-	-	-	-	-	0.0095	-	0.01
-	100	-	9.1 SBS	-	10000	-	10500	-	10200	-	-	-	0.0088	-	0.0113
-	100	-	9.1 SBS	-	10700	-	10500	-	10200	-	-	-	0.0088	-	0.0113
-	100	-	9.5 SBS	-	8000	-	10000	-	8900	-	-	-	0.0103	-	0.0110
-	100	-	9.5 SBS	-	9500	-	10000	-	8900	-	-	-	-	-	-
-	95	-	9.5 SBS	-	-	-	10000	-	8900	-	-	-	-	-	-
148	130	-	10.5 WAPP, 10.2 FILL	-	-	-	14000	-	11500	-	-	-	-	-	-
-	230	-	15.5 SBS	-	-	-	21000	-	20000	-	-	-	0.014	-	-
-	21.5	-	14.5 SBS	-	-	-	23000	-	21500	-	-	-	0.0182	-	-
-	240	-	-	-	-	-	28500	-	22100	-	-	-	0.0148	-	-
-	220	-	19.2 SBS	-	-	-	20500	-	17500	-	-	-	0.0153	-	-
-	-	-	-	-	-	-	25000	-	-	-	-	-	0.0157	-	-
-	245	-	19800	-	-	-	28000	-	23000	-	-	-	0.0135	-	-
-	270	-	17.5 SBS	-	-	-	24000	-	22000	-	-	-	0.0143	-	-
-	280	-	19.0	-	-	-	27000	-	22500	-	-	-	0.0125	-	-
-	-	-	17.0 SBS	-	18100	-	20000	-	-	-	-	-	-	-	-
-	-	-	15.3 SBS	-	18800	-	20000	-	-	-	-	-	0.0133	-	-
-	-	-	13.0 SBS	-	18000	-	20000	-	-	-	-	-	-	-	-
-	-	-	7.8 SBS	-	26000	-	30000	-	-	-	-	-	-	-	-
-	-	-	8.0 SBS	-	26000	-	30000	-	-	-	-	-	-	-	-
-	229	-	18.0 SBS	-	21000	-	24000	-	21700	-	-	-	0.0144	0.0108	-
-	115	-	12.3 SBS	-	-	-	10500	-	-	-	-	-	0.0103	-	-
-	115	-	12.3 SBS	-	-	-	10500	-	-	-	-	-	0.0103	-	-
-	115	-	12.3 SBS	-	-	-	10500	-	-	-	-	-	0.0103	-	-
-	96	-	9.5 SBS	-	-	-	10000	-	8900	-	-	-	0.0103	-	0.0110
-	95	-	9.5 SBS	-	-	-	10000	-	8900	-	-	-	0.0103	-	0.0110
-	95	-	9.5 SBS	-	-	-	10000	-	8900	-	-	-	0.0103	-	0.0110
-	100	-	10.0 SBS	-	10000	-	10500	-	8900	-	-	-	0.0095	-	0.010
-	100	-	10.0 SBS	-	10000	-	10500	-	8900	-	-	-	0.0095	-	0.010
-	100	-	10.0 SBS	-	10000	-	10500	-	8900	-	-	-	0.0095	-	0.010
-	230	-	18	-	19000	-	20000	-	20000	-	-	-	-	-	-
-	200	-	-	-	17500	-	20500	-	20000	-	-	-	-	-	-
78	88	85	9.5	9	8100	-	10000	9500	10000	9500	-	-	-	-	-
-	180	-	11	-	18000	-	17000	-	17000	-	-	-	0.01110	-	-
-	218	-	13	-	20000	-	19000	-	19000	-	-	-	0.0189	-	-
-	198	-	18.2	-	-	-	18400	-	17800	-	-	-	0.0184	-	-
-	260	-	16.8	-	26500	-	21900	-	22700	-	-	-	0.0154	-	-
6.34	251	-	16.2	-	22400	-	25800	1210	-	-	-	-	0.0162	-	-
9.14	274	-	16.5	-	-	-	26800	1310	28400	-	-	-	0.0166	-	-
-	208	-	15.2	-	18200	-	21100	-	-	-	-	-	-	-	-
-	278	-	19.2	-	-	-	19800	-	17200	-	-	-	-	-	-
-	30	-	-	-	7500	-	7400	-	-	-	-	-	0.011	-	-
-	35	-	-	-	7800	-	7500	-	-	-	-	-	-	-	-
-	180	-	12 SBS	-	-	-	17800	-	16800	-	-	-	-	-	-
-	75	-	9.1 SBS	-	6800	-	8100	-	6800	-	-	-	-	-	-

Table A-8. Properties of Glass/Epoxy Laminates (Page 1 of 2)

Manufacturer	Product Number	Fiber	Resin	Laminate Cure	UFS Long (ksi)	UFS Trans (ksi)	UTS Long (ksi)	UTS Trans (ksi)
AMERICAN CYANAMID	CYCOM 5143	7581	CYCOM 5143		95	-	65	-
	CYCOM 5108	-	CYCOM 5108	250 F	80	-	55	-
	CYCOM 985	84 SATIN/7781	CYCOM 985	350 F	90	-	72	-
	CYCOM 980	E GLASS/7781	CYCOM 980		102	-	60	-
	CYCOM 5134	7581	CYCOM 5134		78.0	-	65.0	-
CIBA GEIGY	R1804/1581	1581	R1804		73	-	60	-
	R2520/7781	7781	R2520		77	-	59	-
	R2520/120	120	R2520		65.0	-	44.8	-
	RAC 7350 UNIDIR	463 S 2 GLASS	RAC 7350		225	-	210	-
	RAC 7350 UNIDIR	458 E GLASS	RAC 7350		201	-	158	-
FERRO CORPORATION	R7373	7781	R7373		110	-	79	-
	CE 9010A/7781	7781	CE 9010A		69.1	65.5	70.3	60
	CE 9000-1/7781	7781	CE 9000-1	1 HR/350 F/VACUUM BAG	90	-	74	-
	CE 9000-1/7781	7781	CE 9000-1	1 HR/350 F/200 PSI/AUTOCLAVE	63	-	64	-
	CE 9000-2/120	120	CE 9000-2		66.8	73.9	65	54.2
FERRO CORPORATION	CE 9000-2/7781	7781	CE 9000-2		93.1	-	60.8	-
	CE 3330/7781	7781	CE 3330		88.2	-	56.3	-
	CE 3201/7781	7781	CE 3201		90	-	58	-
	CE 347 UNIDIR	458 E GLASS	CE 347		155	-	140	-
	CE 345/7781	7781	CE 345	AUTOCLAVE	77.7	-	60.3	-
FERRO CORPORATION	CE 345/7781	7781	CE 345	100 F/VACUUM BAG	-	-	-	-
	CE 345/7781	7781	CE 345	250 F/VACUUM BAG	-	-	59.0	-
	CE 330/7781	7781	CE 330		-	-	63.6	-
	CE 330/120	120	CE 330		-	-	71.1	-
	CE 324/7781	7781	CE 324		108	-	63	-
FERRO CORPORATION	CE 308/7781	7781/MPC-4	CE 308	AUTOCLAVE	89.6	-	63.4	-
	CE 308/7781	7781/MPC-4	CE 308	VACUUM BAG	73.9	-	52.9	-
	E 263/7781	7781	E 263	PRESS CURED	78.66	-	51.84	-
	E 263/7781	7781	E 263	AUTOCLAVE	66	-	66	-
	E 263/7781	7781	E 263	VACUUM BAG	62.7	-	-	-
FERRO CORPORATION	CE 9000/7781	7781/MPC-4	CE 9000	50 PSI/AUTOCLAVE	95.5	-	71	-
	CE 9000/7781	7781/MPC-4	CE 9000	35 PSI/VACUUM/AUTOCLAVE	97.5	-	71.3	-
	CE 9000/1581	1581/MPC-4	CE 9000	35 PSI/VACUUM/AUTOCLAVE	88.5	-	58	-
	CE 9000/7781	7781/MPC-4	CE 9000	60 MIN/350 F/15 PSI/PRESSED	90.8	-	55.1	-
	CE 9000/7781	7781/MPC-4	CE 9000	60 MIN/350 F/VACUUM	82.1	-	52.5	-
FERRO CORPORATION	CE 9000/1543	1543/VOL A	CE 9000		144.6	-	-	-
	CE 9000/7376	7376/MPC-5	CE 9000		181.4	-	147.2	-
	CE 9000/581	581/9073 QUARTZ	CE 9000		95.5	-	74.9	-
	CE 307HM/7544	7544	CE 307HM		63.4	-	47.1	-
	CE 307HM/1582	1582	CE 307HM		77.9	-	64.9	-
FERRO CORPORATION	CE 307HM/76261	76261	CE 307HM		98.9	-	61.7	-
	CE 307HM/76261	76261/PIGMENTED	CE 307HM		30	-	59.6	-
	CE 307/7781	7781	CE 307		75.2	-	78.8	-
	CE 3201/112	112 VOLAN A	CE 3201		83.8	-	-	-
	CE 9000/8581	6581/S-2	CE 9000		110.2	-	94	-
FERRO CORPORATION	E 9300/7781	7781	E 9300		92.2	-	63.6	-
	EF 2/S/901	S 901 ROVING	EF-2		-	-	180.0	20.0
	EF 2/S-2	S 2 ROVING EF-2	EF-2		-	-	-	-
					-	-	-	-
					-	-	-	-
FIBERITE	MKB-7010/1581	1581	-		94.4	-	68.0	-
	MKB-7203/7581	7581	-	PRESS CURE	73.1	-	54.4	-
	MKB-7203/7581	7581	-	VACUUM BAG	59.9	-	43.4	-
	MKB-7701/1581	1581	-		-	-	67.1	-
	HY E 9034B	S GLASS UNIDIR	934		270	-	235	-
FIBEXCEL	F181/S 904	S 904	F181		105	-	90	-
	F181/S 2	S 2/442 PREFINISH	F181		91	-	85	-
	F181/S 2	S 2/PREFINISH	F181		80	-	75	-
	F255/7781	7781	F255		95	-	75	-
	F255/1581	1581	F255		85	-	57	-
FIBEXCEL	F258/7781	7781	F258	VACUUM OVEN	72	-	50	-
	F258/7781	7781	F258	AUTOCLAVE	83	-	50	-
	F250/7781	7781	F250		98	-	94	-
	F184/7781	7781	F184		84	-	68	-
	F184/1581	1581	F184		78	-	60	-
FIBEXCEL	F180/1581	1581	F180		67	-	55	-
	F158/7781	7781	F158		90	-	70	-
	F158/1581	1581	F158		78	-	58	-
	F158/7781	7781	F158	VACUUM OVEN	71	-	55	-
	F158/7781	7781	F158	AUTOCLAVE	62	-	64	-
FIBEXCEL	F157/116	7781	F157		70	-	54	-
	F158/7781	7781	F158	VACUUM	87	-	69	-
	F158/7781	7781	F158	AUTOCLAVE	95	-	71	-
	F158/1581	1581	F158		78	-	56	-
	TEF 7/F 155	TEF7	F155		-	-	28	-
FIBEXCEL	TSF 181/F155	-	F155		-	-	41.2	-
	TSF 181/1581/F155	TSF 181/1581 1.1	F155		-	-	47.4	-
	METAFIL G/F 550	METAFIL G	F550		62	-	54.6	-
	METAFIL G/S 2/F 550	METAFIL G/S 2 1.1	F550		126	-	110	-
	METAFIL G/S 2/F 550	METAFIL G/S 2 1.1	F550		146	-	132	-
FIBEXCEL	S 2 GLASS/F 550	S-2	F550		182	-	180	-
	EM 7200A	S 2/8581	E 900		115	-	98	-
	EM 7302/LD	-	-		22	-	11	-
	EM 7302	-	-		16	-	6.5	-
	E773/S 2	S 2 ROVING	E773		65	-	25	-
FIBEXCEL	E718LT/1583	-	-		-	-	290	6.9
					78	-	62	-

UFS - Ultimate Flexure Strength
 ULS - Ultimate Tensile Strength
 UCS - Ultimate Compressive Strength
 USS - Ultimate Shear Strength
 ISS - Ultimate In-plane Shear Strength

FM - Flexural Modulus
 TM - Tensile Modulus
 CM - Compressive Modulus
 SM - Shear Modulus

Table A-8. Properties of Glass/Epoxy Laminates (Page 2 of 2)

UCB Long (ksi)	UCB Trans (ksi)	USL (ksi)	ISB (ksi)	FM Long (ksi)	FM Trans (ksi)	TM Long (ksi)	TM Trans (ksi)	CM Long (ksi)	CM Trans (ksi)	SM (ksi)	Major Poisson Ratio
72	-	-	7.7	3600	-	-	-	-	-	-	-
80	-	-	-	3600	-	3600	-	4000	-	-	-
83	-	-	-	3700	-	-	-	-	-	-	-
88	-	10.6	-	-	-	3700	-	3700	-	-	-
84	-	11.6 HORIZONTAL	-	-	5000	-	4500	-	4200	-	-
73.0	-	9.0	4.8	3300	-	3000	-	5000	-	-	-
48	-	-	-	3400	-	-	-	-	-	-	-
45	-	-	3.4	3600	-	3600	-	-	-	-	-
43.6	-	-	3.3	2600	-	2500	-	-	-	-	-
-	-	11.5 HORIZONTAL	-	-	6400	-	7000	-	-	-	-
-	-	14.6 HORIZONTAL	-	-	5600	-	6200	-	-	-	-
88	-	-	3.5	4200	-	4500	-	4400	-	-	-
85.1	-	-	-	3660	-	3670	-	-	-	-	-
58	-	6.00	-	3600	-	-	-	-	-	-	-
70	-	9.1R	-	3300	-	-	-	-	-	-	-
80.4	66.3	-	-	3640	3440	3300	3050	4230	3610	-	-
88.2	-	-	-	3600	-	3050	-	-	-	-	-
84.3	-	-	-	-	-	-	-	-	-	-	-
55	-	-	-	3700	-	-	-	-	-	-	-
-	-	-	12.3	5370	-	6020	-	-	-	-	-
62.4	-	-	-	3500	-	3700	-	3600	-	-	-
51.4	-	-	-	-	-	-	-	3700	-	-	-
-	-	-	8.31	-	-	-	-	-	-	-	-
-	-	-	6.59	-	-	-	-	-	-	-	-
52	-	9.8	-	4400	-	3600	-	-	-	-	-
88.3	-	-	-	3700	-	-	-	-	-	-	-
57.1	-	-	3.8	3100	-	2610	-	3240	-	-	-
57.54	-	-	-	3300	-	-	-	-	-	-	-
60	-	-	4.2	4060	-	-	-	-	-	-	0.16
-	-	-	-	4060	-	-	-	-	-	-	-
84	-	-	3.2	4500	-	4000	-	4400	-	-	-
75	-	-	-	3600	-	4100	-	4600	-	-	-
75	-	-	-	3700	-	3600	-	-	-	-	-
60.2	-	-	-	3670	-	3370	-	4320	-	-	-
65.6	-	-	-	3670	-	3310	-	4030	-	-	-
-	-	-	-	-	-	-	-	-	-	-	-
110.4	-	-	-	5600	-	5700	-	7800	-	-	-
86.4	-	-	-	3270	-	3140	-	3430	-	-	-
56.6	-	-	-	3500	-	3500	-	3400	-	-	-
60.4	-	-	-	3700	-	3600	-	3500	-	-	-
67.8	-	-	-	3600	-	3700	-	3700	-	-	-
56.4	-	-	-	3600	-	3400	-	3400	-	-	-
73.7	-	-	-	3600	-	3480	-	4580	-	-	-
54.7	-	-	-	2960	-	-	-	-	-	-	-
81.1	-	8.7	-	-	-	-	-	-	-	-	-
68.9	-	2.41	-	3600	-	3660	-	-	-	-	-
120.0	30.0	-	-	-	-	6700	1450	5600	2000	-	0.26
-	-	10.2 HORIZONTAL	-	-	-	-	-	-	-	-	-
51.4	-	-	-	3750	-	-	-	-	-	-	-
82	-	-	-	3400	-	3200	-	3200	-	-	-
44.9	-	-	-	2800	-	2800	-	3050	-	-	-
73.5	-	-	5.6	5300	-	5300	-	3500	-	-	-
-	-	14	-	8500	-	8500	-	-	-	-	-
88	-	-	-	4000	-	4600	-	5400	-	-	-
63	-	-	-	4000	-	4200	-	4400	-	-	-
62	-	-	-	4000	-	4200	-	4600	-	-	-
65	-	-	3.6	3400	-	4000	-	4000	-	-	-
74	-	-	4.5	3300	-	3300	-	3400	-	-	-
56	-	-	3.2	3000	-	3300	-	3400	-	-	-
63	-	-	3.5	3300	-	3500	-	3600	-	-	-
58	-	-	-	4500	-	4100	-	4400	-	-	-
59	-	-	1.6	3500	-	3400	-	3400	-	-	-
67	-	-	2.0	3400	-	3370	-	3200	-	-	-
60	-	-	-	2900	-	3000	-	3100	-	-	-
70	-	-	3.6	3400	-	4400	-	4000	-	-	-
48	-	-	4.2	3200	-	3200	-	3400	-	-	-
57	-	-	2.6	3300	-	3400	-	4000	-	-	-
55	-	-	-	3100	-	2900	-	3000	-	-	-
56	-	-	5.0	3400	-	3000	-	3100	-	-	-
61	-	-	3.3	4000	-	3400	-	3400	-	-	-
60	-	-	3.5	3700	-	3700	-	3200	-	-	-
61.5	-	-	-	-	-	3010	-	3140	-	-	-
62.5	-	-	-	-	-	3350	-	3670	-	-	-
65.6	-	-	-	-	-	3450	-	3610	-	-	-
79.6	-	0.74	-	3660	-	3620	-	4610	-	-	-
140	-	7.2	-	4610	-	4900	-	4850	-	-	-
162	-	7.54	-	4650	-	5230	-	5400	-	-	-
175	-	8.5	-	5400	-	6200	-	6100	-	-	-
-	-	-	-	-	-	-	-	-	-	-	-
91	-	10	-	5100	-	6200	-	6700	-	-	-
27	-	-	-	-	-	-	-	-	-	-	-
22	-	-	-	1800	-	-	-	-	-	-	-
40.5	-	-	-	4100	-	3000	-	-	-	-	-
176	33.2	11	-	-	-	7500	1800	8400	2200	-	-
-	-	-	9.0	3700	-	-	-	-	-	-	-

Table A-9. Properties of Kevlar/Epoxy Laminates (Page 1 of 2)

Manufacturer	Product Number	Fiber	Resin	Laminate Type/ Orientation	Laminate Cure	UFS Long (ksi)
AMERICAN CYANAMID	5118L	KEVLAR 49/181	5118L	-	-	47.6
	5105B	KEVLAR 49/181	5105B	-	-	64.0
	950	KEVLAR 49/281	950	FABRIC	50 PSI/250 F/1 HR	-
	950	KEVLAR 48/281	950	FABRIC	14.7 PSI/250 F/1 HR	-
	950	KEVLAR 49	950	UNIDIRECTIONAL	50 PSI/250 F/1 HR	-
	950	KEVLAR 49	950	UNIDIRECTIONAL	100 PSI/250 F/1 HR	-
	985	KEVLAR 49	CYCOM 985	K-285/FABRIC	-	-
	985	KEVLAR 49	CYCOM 985	281/FABRIC	-	-
	985	KEVLAR 49	CYCOM 985	181/FABRIC	-	-
	980	KEVLAR 49	CYCOM 980	STYLE 281	-	63
	5102	KEVLAR 49	CYCOM 5102	181/FABRIC	-	-
	5134	KEVLAR 49	CYCOM 5134	181/FABRIC	-	-
	5134	KEVLAR 49	CYCOM 5134	120/FABRIC	-	-
	5134	KEVLAR 49	CYCOM 5134	281/FABRIC	-	-
CIBA-GEIGY	R9256-1	KEVLAR	-	FABRIC	-	-
	R9257	KEVLAR/181	-	FABRIC	-	-
	R9259	KEVLAR/285	-	-	-	-
	R9289	KEVLAR/120	-	-	-	-
	RAC 9350	KEVLAR/120	-	-	-	63.3
	RAC 9350	KEVLAR/281	-	-	-	68.0
	RAC 9350	KEVLAR/285	-	-	-	55.0
	R9369	KEVLAR/285	-	-	-	-
	R9369	KEVLAR/120	-	-	-	-
	R9521	KEVLAR/181	-	8H FABRIC	-	52
	R9521	KEVLAR/285	-	CROWFOOT FABRIC	-	52
DUPONT	-	KEVLAR 49	-	STYLE 243	-	45.2
	-	KEVLAR 49	-	STYLE 281	-	45.1
	-	KEVLAR 49	-	STYLE 285	-	50.6
	-	KEVLAR 49	-	STYLE 328	-	20.3
	-	KEVLAR 49	-	STYLE 1050X	-	43.9
	-	KEVLAR 49	-	STYLE 1033X	-	34.6
FERRO CORPORATION	CE-9010A/181	STYLE 181	CE-9010A	FABRIC	-	51.2
	CE-9010/181	STYLE 181	CE-9010	FABRIC	-	45.6
	CE-9010/120	STYLE 120	CE-9010	FABRIC	-	47.7
	CE-9000-2/285	KEVLAR 49/285	CE-9000-2	FABRIC	-	55.4
	CE-9000/181	KEVLAR 49/181	CE-9000	FABRIC	-	62
	CE-345/281	KEVLAR 49/281	CE-345	12 PLY FABRIC	AUTOCCLAVE	62
	CE-345/281	KEVLAR 49/281	CE-345	12 PLY FABRIC	VACUUM BAG	55
	CE-345/KEVLAR 49	KEVLAR 49	CE-345	UNIDIRECTIONAL	-	73.5
	CE-343/4560	4560	CE-343	UNIDIRECTIONAL	-	91.1
	CE-308/281	STYLE 281	CE-308	-	-	53.7
	CE-321R/KEVLAR 4560	KEVLAR 4560	CE-321R	UNIDIR. TAPE	-	92.5
	CE-324/KEVLAR 49	KEVLAR 49/285	CE-324	-	-	62.8
	CE-9000/KEVLAR	-	CE-9000	STYLE 181	13 PLY/50 PSI/350 F/1 HR	58.9
	CE-9000/KEVLAR	-	CE-9000	STYLE 181	12 PLY/35 PSI/350 F/1.5 HR	62.0
FIBERITE	MXM-7669/KEVLAR 49	KEVLAR 49	MXM-7669	STYLE 285	-	-
	MXM-7676/KEVLAR 49	KEVLAR 49	MXM-7676	STYLE 120	-	61.0
	MXM-7676/KEVLAR 49	KEVLAR 49	MXM-7676	STYLE 285	-	65.0
	MXM-7669/KEVLAR 49	KEVLAR 49	MXM-7669	-	-	60.13
	MXM-7764/KEVLAR 49	KEVLAR 49	MXM-7764	STYLE 181	-	57.0
	MXM-7764/KEVLAR 49	KEVLAR 49	MXM-7764	STYLE 285	-	56.0
	MXM-7064/KEVLAR 49	KEVLAR 49	MXM-7064	STYLE 181	-	56.0
	MXM-7064/KEVLAR 49	KEVLAR 49	MXM-7064	STYLE 285	-	57.0
	MXM-7714/KEVLAR 49	KEVLAR 49	MXM-7714	STYLE 120	-	-
	MXM-7714/KEVLAR 49	KEVLAR 49	MXM-7714	STYLE 285	-	-
	MXM-7251/KEVLAR 49	KEVLAR 49	MXM-7251	STYLE 285	-	-
	1734A	KEVLAR 49	934	UNIDIR. TAPE	-	100

UFS - Ultimate Flexural Strength
 UTS - Ultimate Tensile Strength
 UCS - Ultimate Compressive Strength

USS - Ultimate Shear Strength
 ISS - Interlaminar Shear Strength

FM - Flexural Modulus
 TM - Tensile Modulus
 CM - Compressive Modulus

Long - Longitudinal
 Trans - Transverse

Table A-9. Properties of Kevlar/Epoxy Laminates (Page 2 of 2)

UTS Trans (ksi)	UTS Long (ksi)	UTS Trans (ksi)	UCS Long (ksi)	UCS Trans (ksi)	USS (ksi)	ISS (ksi)	FM Long (ksi)	FM Trans (ksi)	TM Long (ksi)	TM Trans (ksi)	CM Long (ksi)	CM Trans (ksi)
-	71.0	-	17.2	-	-	-	3300	-	-	-	-	-
-	67.0	-	29.0	-	5.0 SBS	2.4	4000	-	4100	-	4200	-
-	72	-	26	-	5.1 SBS	-	-	-	4500	-	4500	-
-	64	-	21	-	5.3 SBS	-	-	-	4000	-	4100	-
-	140	-	33	-	6.6 SBS	-	-	-	10000	-	8800	-
-	120	-	36	-	11 SBS	-	-	-	10000	-	10000	-
-	95	-	31	-	5.4 SBS	-	-	-	4300	-	4200	-
-	74	-	24	-	4.3 SBS	-	-	-	4700	-	4200	-
-	78	-	26	-	4.1 SBS	-	4100	-	4700	-	-	-
-	73	-	24	-	4.7 HORIZONTAL	-	-	-	-	4600	-	4600
-	78.3	-	23.5	-	-	-	-	-	5100	-	4400	-
-	70.0	-	25.7	-	7.0 SBS	-	4400	-	-	-	4400	-
-	70.0	-	20.0	-	-	-	4500	-	-	-	-	-
-	65.0	-	20.0	-	-	-	4500	-	-	-	-	-
-	80	-	17	-	-	-	-	-	3300	-	3300	-
-	75	-	23	-	-	-	-	-	4000	-	3500	-
-	70	-	25	-	7.4	-	-	-	3800	-	4400	-
-	67	-	23	-	7.7	-	-	-	3700	-	4700	-
-	49.6	-	-	-	4.2	-	4110	-	4400	-	-	-
-	46.0	-	-	-	6.0 SBS	-	4200	-	4300	-	-	-
-	49.0	-	-	-	5.2	-	3400	-	4400	-	-	-
-	67	-	26	-	4.8	2.3	-	-	3500	-	3700	-
-	70	-	23	-	5.4	2.7	-	-	3900	-	3600	-
-	81	-	27	-	-	-	3000	-	4200	-	3700	-
-	75	-	24	-	-	-	2800	-	4100	-	3500	-
-	81.4	-	-	-	-	5.24	4350	-	5620	-	-	-
-	72.4	-	-	-	-	5.12	3830	-	3780	-	-	-
-	72.6	-	-	-	-	4.47	3460	-	3360	-	-	-
-	53.7	-	-	-	-	2.85	2320	-	2950	-	-	-
-	74.4	-	-	-	-	4.61	3280	-	3710	-	-	-
-	54.3	-	-	-	-	4.2	2770	-	3540	-	-	-
45	75.7	64.2	19.1	-	-	-	3860	3800	436	3700	-	-
44.2	67	61.2	22.3	-	-	-	3400	3000	3600	3600	-	-
46.6	59.5	51.7	26.8	-	-	-	3300	3200	3500	3200	-	-
53.3	67.2	60.3	25.3	24	4.4 SBS	-	2630	2480	4600	4730	3810	3630
-	72	-	25	-	-	-	4150	-	5100	-	3700	-
-	82	-	32	-	5.8 SBS	-	4000	-	-	-	-	-
-	67.7	-	23	-	4.7 SBS	-	3500	-	-	-	-	-
-	117.2	-	-	-	8.96 SBS	-	5300	-	6600	-	-	-
-	180.2	1.53	39.5	-	8.2 SBS	-	9410	-	9980	610	-	-
-	75.9	-	26.2	-	-	-	2630	-	4000	-	-	-
-	186.2	-	39.6	-	8.4	-	9200	-	9800	-	-	-
-	78.9	-	24.8	-	6.5 SBS	-	3600	-	4600	-	4600	-
-	52.1	-	33.3	-	-	-	3180	-	3500	-	3100	-
-	72.0	-	25.0	-	-	-	4150	-	5100	-	3700	-
-	62	-	24	-	4.7 SBS	1.598	-	-	3500	-	3800	-
-	76.0	-	28.0	-	4.2 SBS	-	3400	-	5100	-	4000	-
-	76.0	-	26.0	-	4.0 SBS	-	3100	-	4300	-	3700	-
-	76.53	-	24.7	-	4.3 SBS	-	3100	-	4300	-	4100	-
-	66.0	-	26.0	-	-	-	3200	-	4300	-	4400	-
-	85.0	-	23.0	-	-	-	1600	-	5200	-	4200	-
-	76.0	-	25.0	-	-	-	3400	-	4800	-	3700	-
-	72.0	-	22.0	-	-	-	2300	-	4400	-	4800	-
-	64	66	24	-	6.8 SBS	-	-	-	3800	4000	3500	-
-	67	-	26	-	6.0 SBS	-	-	-	3500	-	3500	-
-	87.3	-	20.0	-	-	-	-	-	3800	-	3800	-
-	190	-	-	-	5 SBS	-	10500	-	11000	-	-	-

Table A-10. Properties of Glass/Polyimide Laminates (Page 1 of 2)

Manufacturer	Product Number	Fiber	Resin	Laminate Type/ Orientation
AMERICAN CYANAMID	CYCOM 3002	-	3002	7781 FABRIC
	CYCOM 3003	E GLASS	3003	A1100-7781 FABRIC
CIBA-GEIGY	R7451	-	R7451 (BMI)	7781 FABRIC
	R7451	QUARTZ	R7451 (BMI)	581 FABRIC
FERRO CORPORATION	CPI-2274/7781	-	CPI-2274	7781 FABRIC
	CPI-2272/7781	-	CPI-2272	7781 FABRIC
	CPI-2249/7781	-	CPI-2249	7781 FABRIC
	CPI-2248/7781	-	CPI-2249	7781 FABRIC
	CPI-2237/7781	-	CPI-2237	7781 FABRIC
	CPI-2214/7781	-	CPI-2214	7781 FABRIC
FIBERITE	PI-750	1/2" GLASS	PI-750 CMPD	MOLDED
	PI-740	< 1/2" GLASS	PI-740 CMPD	MOLDED
	PI-730	SEED FORM	PI-730 CMPD	MOLDED
	MXB-5004	E GLASS	-	181-150 FABRIC
HEXCEL	F174	-	F174	7781 FABRIC
	F174	-	F174	7781 FABRIC

UFS - Ultimate Flexural Strength
UTS - Ultimate Tensile Strength
UCS - Ultimate Compressive Strength

USS - Ultimate Shear Strength
ISS - Interlaminar Shear Strength

FM - Flexural Modulus
TM - Tensile Modulus
CM - Compressive Modulus

Long - Longitudinal
Trans - Transverse

Table A-10. Properties of Glass/Polyimide Laminates (Page 2 of 2)

Laminate Cure	UFS Long (ksi)	UTS Long (ksi)	UCS Long (ksi)	USS (ksi)	IBS (ksi)	FM Long (ksi)	TM Long (ksi)	CM Long (ksi)
VACUUM BAG	65.0	53.0	55.0	5.4 SBS	-	3500	-	-
"	65.0	65.0	70.0	8.0 SBS	-	3500	2000	4000
"	61.4	-	73.8	-	-	-	3900	4100
"	64.1	64.2	53.9	5.26 SBS	-	3160	-	3910
"	66.9	-	-	7.55	-	-	-	-
"	64.2	63.4	70.7	5.07	-	4370	3920	4230
HIGH PRESSURE	65.5	57.0	-	-	-	3200	-	-
VACUUM BAG	63.5	50.0	-	-	-	2800	-	-
"	103	62.0	76.4	10.6	-	4230	-	4450
"	64.0	-	78.8	-	3.11	3610	-	3840
COMPRESSION MOLDED	36.0	21.0	32.0	-	-	3100	-	-
TRANSFER MOLDED	36.0	15.0	34.0	-	-	2800	-	-
INJECTION MOLDED	19.0	8.0	35.0	-	-	2000	-	-
"	76.2	64.6	-	-	-	3500	3700	-
VACUUM CURE	79.2	60.8	59.8	10.61 HORIZONTAL	3.65	3350	3300	4470
AUTOCLAVE	61.8	61.2	63.1	10.68 HORIZONTAL	3.15	3500	4040	4670

Table A-11. Properties of Carbon/Polyimide Laminates (Page 1 of 2)

Manufacturer	Product Number	Fiber	Resin	Laminate Type/ Orientation	UFS Long (ksi)	UFS Trans (ksi)	UTS Long (ksi)
BOEING	PMR-15	-	-	UNIDIRECTIONAL	269	-	-
CIBA-GEIGY	R6451	T-3000	-	UNIDIRECTIONAL	278	15.0	308.0
FERRO CORPORATION	CPI-2237/HTS-II CPI-2237/CELION 3000 CPI-2237	HTS-II	CPI-2237	UNIDIRECTIONAL	210	-	180
		CELION 3000	CPI-2237	2424 WOVEN	133	121.5	67
		T-300	CPI-2237	2424 WOVEN	126.5	-	-
GENERAL DYNAMICS	NR150B2	-	-	UNIDIRECTIONAL	264	-	-
	NR150B2S5X	-	-	UNIDIRECTIONAL	264	-	-
HEXCEL	F178/T-300	T-300 HMG	F178	3K UNIDIRECTIONAL	260	-	220
	F650/T300	T300	F650	FABRIC	134	-	91
	F650/T500	T500	F650	FABRIC	161	-	67
	F650/T300	T300	F650	TAPE	288	17.8	251
HITCO	USPMR-15	CELION	USPMR-15	TAPE	236	-	210
	USPMR-15	CELION	USPMR-15	FABRIC	117	-	112
U. S. POLYMERIC	V-378A/T-300	T-300	V-378A	6K UNIDIRECTIONAL	248.3	-	-
	V-378A/T-300	T-300 HMG	V-378A	6K TAPE	265.0	-	228.9
	V-378A/T-300	T-300 HMG	V-378A	6K	268	-	-
	V-378A/PW-70	PW-70 HMG	V-378A	BIDIRECTIONAL FABRIC	99.8	-	-

UFS - Ultimate Flexural Strength
UTS - Ultimate Tensile Strength
UCS - Ultimate Compressive Strength

USS - Ultimate Shear Strength
ISS - Interlaminar Shear Strength

FM - Flexural Modulus
TM - Tensile Modulus
CM - Compressive Modulus

TFS - Tensile Failure Strain
Long - Longitudinal
Trans - Transverse

Table A-11. Properties of Carbon/Polyimide Laminates (Page 2 of 2)

UTS Trans (ksi)	UCS Long (ksi)	UCS Trans (ksi)	USS (ksi)	ISS (ksi)	FM Long (ksi)	FM Trans (ksi)	TM Long (ksi)	TM Trans (ksi)	CM Long (ksi)	TFS Long (in/in)
-	-	-	14.5	-	-	-	-	-	-	-
8.2	-	-	16.3 SBS	-	266000	8800	181000	-	-	-
10	136	34	14	-	1830	-	2200	1.1	-	-
-	84.8	-	5.6 SBS	-	8560	8300	9630	-	9020	-
-	83	-	5.88 SBS	-	9690	-	-	-	11800	-
-	-	-	12.1 SBS	-	-	-	-	-	-	-
-	-	-	7.5	-	-	-	-	-	-	-
-	210	-	18.5 SBS	-	19000	-	20200	-	20	-
-	108	-	8.8 SBS	-	9100	-	10100	-	-	0.0083
-	112	-	10.0 SBS	-	9000	-	10200	-	-	0.0085
-	238	-	20.2 SBS	-	18400	1500	21500	-	-	-
-	-	-	-	-	19100	-	20500	-	-	-
-	79	-	-	5.6 C	8900	-	10400	-	9600	-
-	-	-	17.9 HORIZONTAL	-	-	-	-	-	-	-
9.0	-	-	18.3 HORIZONTAL	-	19800	-	21800	1400	-	0.01047
-	-	-	18.6 HORIZONTAL	-	19500	-	-	-	-	-
-	58.8	-	7.0 HORIZONTAL	-	9600	-	-	-	8100	-

Table A-12. Properties of Ablative/Phenolic Prepreg (Page 1 of 2)

Manufacturer	Product Number	Prepreg Type/ Orientation	Resin Content (%)	Resin Flow (%)
FERRO CORPORATION	CA-2204	PHENOLIC/SILICA	27-33	6-12 (10 MIN/325 F/150 PSI)
	CA-2221	PHENOLIC/SILICA	26-32	6-12 (325 F/150 PSI)
	CA-2221 MC	PHENOLIC/SILICA	27-32	10
	CA-2230	PHENOLIC/SILICA	28-32	6-12 (10 MIN/325 F/150 PSI)
	CA-2230 MC	PHENOLIC/SILICA	28-32	3-11 (60 MIN/300 F/1000 PSI)
	CA-2212	PHENOLIC/ASBESTOS	40-50	14-22 (10 MIN/325 F/15 PSI)
	CA-2228	PHENOLIC/ASBESTOS	40-50	14-22 (10 MIN/325 F/15 PSI)
	CA-2248	PHENOLIC/ASBESTOS	37-48	2-12 (10 MIN/325 F/15 PSI)
	CA-8207	PHENOLIC/CARBON	34-40	2-8 (10 MIN/325 F/15 PSI)
	CA-8208	PHENOLIC/CARBON	36-40	5-11 (10 MIN/325 F/15 PSI)
	CA-8214	PHENOLIC/CARBON	32-40	1-8
	CA-8217	PHENOLIC/CARBON	31-36	3-11 (10 MIN/325 F/150 PSI)
	CA-8220	PHENOLIC/CARBON	31-36	3-11 (10 MIN/325 F/15 PSI)
	CA-8203	PHENOLIC/CARBON	32-38	5-7 (10 MIN/325 F/15 PSI)
	CA-2270	PHENOLIC/QUARTZ	27-33	7-13 (10 MIN/325 F/15 PSI)
	CA-2227	PHENOLIC/QUARTZ 581	28-32	6-11 (10 MIN/325 F/150 PSI)
HITCO	FM-5503	PHENOLIC/SILICA	24-30	10-12.0 (150 PSI)

Table A-12. Properties of Ablative/Phenolic Prepreg (Page 2 of 2)

Volatile Content (%)	Tack	Drape	Shelf Life (months at 0 F)	Out Time (days at 77 F)	Gel Time (min)
6.0 (10 MIN/325 F)	-	-	3 (40 F)	30	-
4 (10 MIN/325 F)	-	-	3 (40 F)	30	-
4 (10 MIN/325 F)	-	-	3 (40 F)	30	-
6 (10 MIN/325 F)	-	-	3 (40 F)	30	-
4 (15 MIN/325 F)	-	-	3 (40 F)	30	-
7-13 (10 MIN/325 F)	-	-	3 (40 F)	30	-
6-13 (10 MIN/325 F)	-	-	3 (40 F)	30	-
5 (10 MIN/325 F)	-	-	3 (40 F)	30	-
2-6 (10 MIN/325 F)	-	-	3 (40 F)	30	-
2-6 (10 MIN/325 F)	-	-	3 (40 F)	30	-
9.0 (10 MIN/325 F)	-	-	3 (40 F)	30	-
4-7 (10 MIN/325 F)	-	-	3 (40 F)	30	-
4-7 (10 MIN/325 F)	-	-	3 (40 F)	30	-
2-7 (10 MIN/325 F)	-	-	3 (40 F)	30	-
6 (10 MIN/325 F)	-	-	3 (40 F)	30	-
5 (10 MIN/325 F)	-	-	3 (40 F)	7	-
6.0-9.0	-	-	-	-	-

Table A-13. Properties of Ablative/Phenolic Laminates (Page 1 of 2)

Manufacturer	Fiber/Resin System	Product Number	Fiber	Laminate Type/ Orientation
FERRO CORPORATION	SILICA/PHENOLIC	CA-2204	48	FABRIC
	SILICA/PHENOLIC	CA-2221	48	FABRIC
	SILICA/PHENOLIC	CA-2221 MC	48	FABRIC
	SILICA/PHENOLIC	CA-2230	48	FABRIC
	SILICA/PHENOLIC	CA-2230 MC	48	FABRIC
	ASBESTOS/PHENOLIC	CA-2212	RPD 40 RAYBESTOS-MANHATTAN	-
	ASBESTOS/PHENOLIC	CA-2226	RPD 40 RAYBESTOS-MANHATTAN	-
	ASBESTOS/PHENOLIC	CA-2248	RPD 40 RAYBESTOS-MANHATTAN	-
	GRAPHITE/PHENOLIC	CA-8207	-	FABRIC
	GRAPHITE/PHENOLIC	CA-8208	-	FABRIC
	CARBON/PHENOLIC	CA-8214	-	-
	CARBON/PHENOLIC	CA-8220	-	FABRIC
	CARBON/PHENOLIC	CA-8203	-	FABRIC
	QUARTZ/PHENOLIC	CA-2270	ASTROQUARTZ 570	FABRIC
	QUARTZ/PHENOLIC	CA-2227/581	-	FABRIC
	CARBON/PHENOLIC	CA-8217	-	FABRIC
HITCO	SILICA/PHENOLIC	FM-5503	-	FABRIC

Table A-13. Properties of Ablative/Phenolic Laminates (Page 2 of 2)

UFS Long (ksi)	UFS Trans (ksi)	UTS Long (ksi)	UTS Trans (ksi)	UCS Long (ksi)	UCS Trans (ksi)	ISS (ksi)	FM Long (ksi)	TM Long (ksi)
28.0	-	16.0	-	25.0	-	-	2900	-
25.5	-	14.8	-	28.0	-	-	3100	-
13.0	-	5.0	-	31.0	-	-	2750	-
27.0	-	15.0	-	26.0	-	-	2900	-
12.0	-	4.5	-	29.5	-	-	2700	-
37.0	-	34.0	-	-	-	-	3100	-
37.0	-	34.0	-	20.0	-	-	3100	-
36.5	-	29.0	-	-	-	-	3000	-
23.0	-	18.5	-	18.0	-	-	1850	2000
26.0	-	18.0	-	13.0	-	-	1680	-
13.6	15.4	23.4	14.1	-	-	1.45	-	-
36.0	-	17.0	-	38.0	-	-	2700	-
38.6	-	19.0	-	49.4	-	3.56	-	-
80.0	-	54.0	-	-	-	-	-	3500
104.1	-	68.0	-	-	-	-	-	4150
35.0	-	18.0	-	42.0	-	-	2900	-
-	-	-	-	34.2	19.7	2.5	-	-

Table A-14. Properties of Glass/Phenolic Laminates (Page 1 of 2)

Manufacturer	Product Number	Fiber	Resin	Laminate Type/ Orientation	Laminate Cure	UFS Long (ksi)
AMERICAN CYANAMID	6101-2	7581 (A1100 FINISH)	CYCOM 6101-2	FABRIC	-	73.0
	6102	181	CYCOM 6102	FABRIC	-	73.0
CIBA-GEIGY	R7273	120	-	WOVEN PREPREG	-	-
	R7273	7781	-	WOVEN PREPREG	-	-
FERRO CORPORATION	AC	-	-	FABRIC	VACUUM BAG	70.5
	AC	-	-	FABRIC	PRESS MOLDED	78.8
	CPH-2208/7781	7781	CPH-2208	-	-	71.0
	CPH-2224/7781	7781	CPH-2224	-	-	-
	CPH-2251/120	120	CPH-2251	-	-	73.4
	CPH-2251/7781	7781	CPH-2251	-	-	74.9
	CPH-2280/7781	7781	CPH-2280	-	-	88.2
FIBERITE	MXB-6032	1581	-	FABRIC	-	66.3
	MXB-60C1	181	-	FABRIC	-	87.2
	MXB-6032	181-150S	-	FABRIC	-	66.3
	MXB-6032	1581	-	FABRIC	-	66.3
HITCO	FM-5042	181 (A1100 FINISH)	-	FABRIC	-	75

Table A-14. Properties of Glass/Phenolic Laminates (Page 2 of 2)

UTS Trans (ksi)	UTS Long (ksi)	UTS Trans (ksi)	UCS Long (ksi)	ISS (ksi)	FM Long (ksi)	TM Long (ksi)	CM Long (ksi)
-	52.0	-	59.0	-	3700	-	-
-	52.0	-	59.0	-	4100	3900	3600
-	47	-	36.1	-	-	2400	2400
-	44.5	-	37.3	-	-	2500	2500
-	56.1	-	38.0 EDGEWISE	-	3300	-	-
-	51.96	-	47.3 EDGEWISE	-	3660	-	-
-	48.0	-	50.0	-	3200	-	-
-	52.2	-	67.0	-	-	3560	4610
-	56.7	-	51.4	-	3300	-	-
-	56.4	-	44.1	-	3840	2850	-
-	58.5	-	69.3	1.1	4100	4500	5100
-	43.0	-	51.7 EDGEWISE	-	3700	-	-
-	57.2	-	65.7	-	4600	-	-
-	43.0	-	-	-	3700	-	-
-	43.0	-	51.7 EDGEWISE	-	3700	-	-
-	60	-	45	-	3500	3300	3000

Table A-15. Properties of Glass/Polyester Laminates (Page 1 of 2)

Manufacturer	Product Number	Fiber	Resin	Laminate Type/ Orientation
AMERICAN CYANAMID	CYCOM 4104	GLASS	-	-
	CYCOM 4104/581 QUARTZ	581 QUARTZ	-	-
	CYCOM 4102/1543	1543 FIBERGLASS	-	-
	4102	7581 FIBERGLASS	-	-
	4101	-	-	-
FERRO CORPORATION	CP-1304/7781	7781 FIBERGLASS	CP-1304	FABRIC
	CP-1301/7781	7781	CP-1301	FABRIC
	PE-285/7781	7781	PE-285	-
	PE-285/7781	7781	PE-285	-
	UVFR/7781	7781	UVFR	-
	IFRR/7781	7781	IFRR	-
	IFRR/7781	7781	IFRR	-
	H-200C/7781	7781	H-200C	-
	H-200C/7781	7781	H-200C	-
	OS/7781	7781	OS	-

Table A-15. Properties of Glass/Polyester Laminates (Page 2 of 2)

Laminate Cure	UFS Long (ksi)	UTS Long (ksi)	UCS Long (ksi)	IRS (ksi)	FM Long (ksi)
-	66.0	54.0	44.0	-	3000
-	65.0	70.0	35.0	-	-
-	-	85.0	70.0	-	-
-	68.0	54.4	56.0	-	3800
-	68.0	64.0	45.0	-	-
-	85.0	47.0	46.0	-	3300
-	70.0	47.0	40.0	-	3800
VACUUM BAG MCLDED	65.48	44.82	48.08 EDGEWISE	-	2750
PRESS MOLD (30 psi)	79.4	52.4	52.3 EDGEWISE	-	3420
-	66.7	63.7	50.5 EDGEWISE	3.82	3050
VACUUM BAG	65.4	64.0	41.1 EDGEWISE	-	3320
PRESS MOLD	80.7	52.0	52.8	-	3400
VACUUM BAG	96.0	71.0	60.0 EDGEWISE	-	3800
AUTOCCLAVE CURED	116.0	72.4	68.9 EDGEWISE	-	4060
-	58.8	41.2	57.3 EDGEWISE	-	2700

APPENDIX B

CHEMICAL AND MECHANICAL PROPERTIES OF FIBER-REINFORCED COMPOSITE MATERIALS COMPILED BY BOEING

This appendix lists a compilation of chemical and mechanical properties of composite materials compiled by Boeing under Air Force Contract F33615-86-C-5071.

Table B-1. Mechanical Properties of Hercules Fibers

Typical fiber properties	A51	A52	A54	A55	IM6	IM7
Tensile strength, ksi MPa	451 3105	401 2760	551 3795	601 4140	636 4382	684 4713
Tensile modulus, ksi GPa	33 228	33 228	34 235	35 242	40 276	41 283
Ultimate elongation, %	1.32	1.20	1.53	1.65	1.50	1.60
Carbon content, %	92	94	94	94	94	—
Density, g/cm ³	1.80	1.80	1.80	1.83	1.73	1.78

Typical epoxy composite properties at RT	A51	A52	A54	A56	IM6	IM7
Tensile strength, ksi MPa	280 1932	290 2001	342 2353	373 2567	395 2719	424 2922
Tensile modulus, ksi GPa	20 138	20 138	21 145	22 151	20 138	25 175
Flexural strength, ksi MPa	250 1725	240 1656	260 1794	272 1877	250 1725	237 1635
Flexural modulus, ksi GPa	18 124	18 124	19 131	20 139	22 150	24 166
Short beam shear, ksi MPa	19 131	18 124	18 124	19 129	18 124	19 129
Fiber volume, %	62	62	62	62	62	62

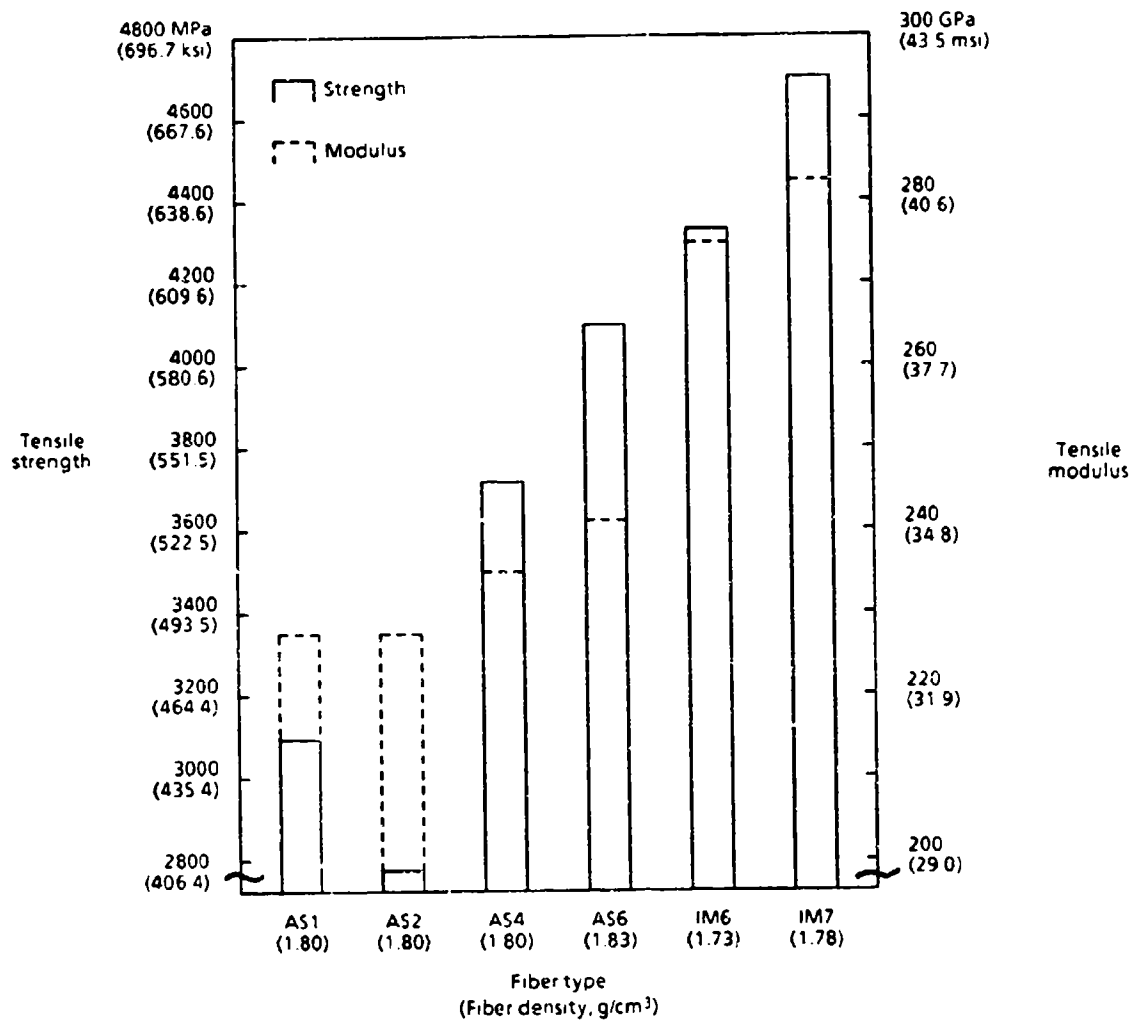


Figure B-1. Hercules Fiber Properties at Room Temperature

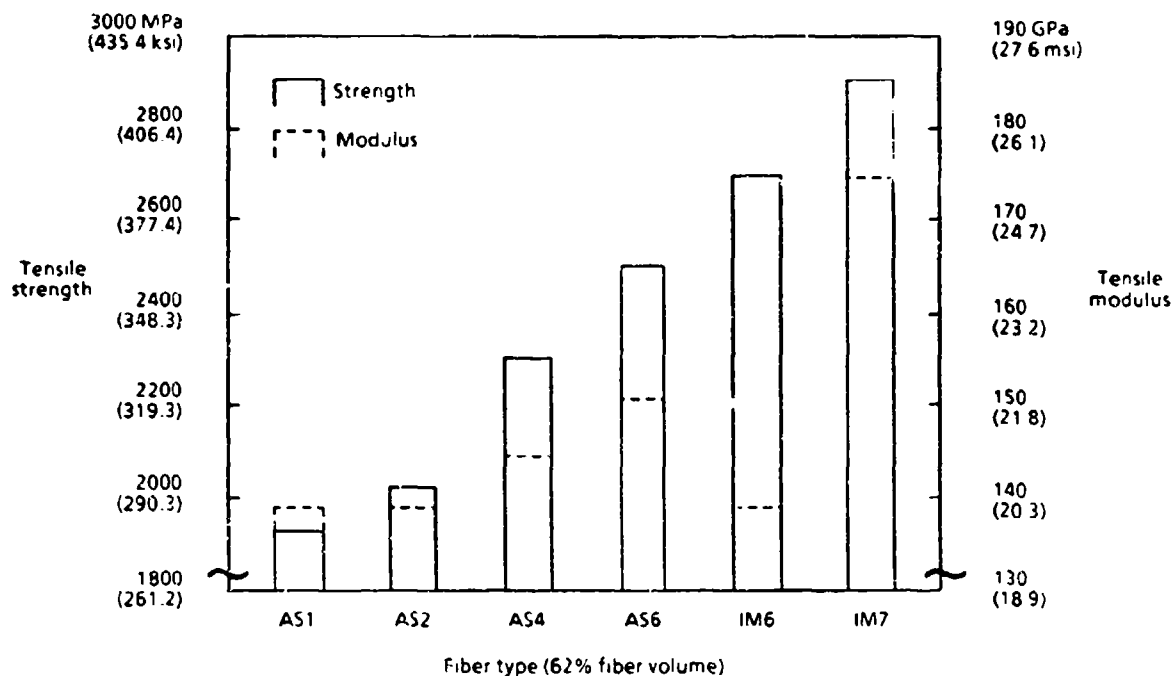


Figure B-2. Typical Epoxy Composite Properties at Room Temperature

Table B-2. Properties of Typical Epoxy Composites at Room Temperature

Fiber type *	Tensile strength				Young's modulus				Poisson's ratio	Density	
	0°		90°		0°		90°			g/cm³	lb/in³
	MPa	ksi	MPa	ksi	GPa	msi	GPa	msi			
E-Glass	1020	150	40	7	45	6.5	12	1.8	0.28	2.08	0.075
S-Glass	1620	230	40	7	55	8.0	16	2.3	0.28	2.02	0.073
Boron	1240	180	70	10	210	30.0	19	2.7	0.25	2.02	0.073
Kevlar 49	1240	180	280	40	76	11.0	5.5	0.8	0.34	1.39	0.050

* Fiber volume, $V_f = 60\%$

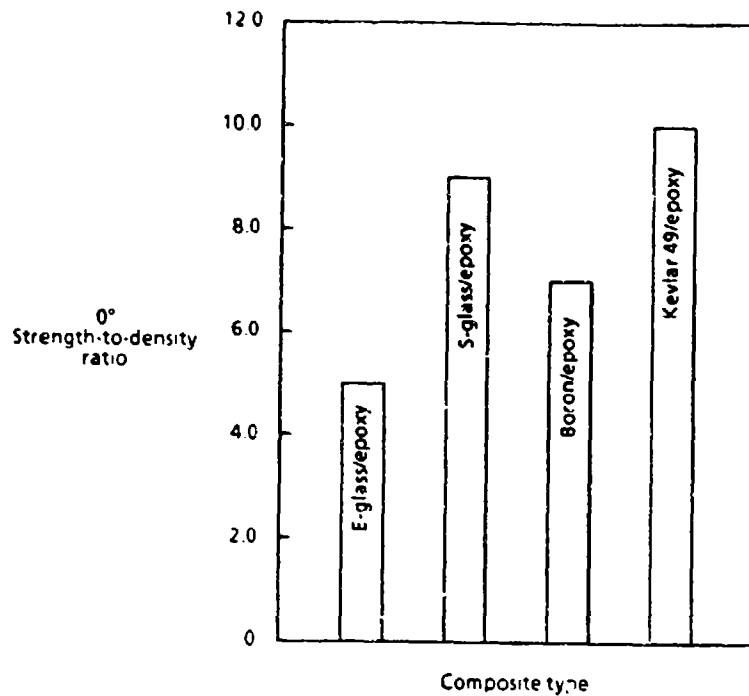


Figure B-3. 0° Strength-to-Density Ratio of Typical Epoxy Composites

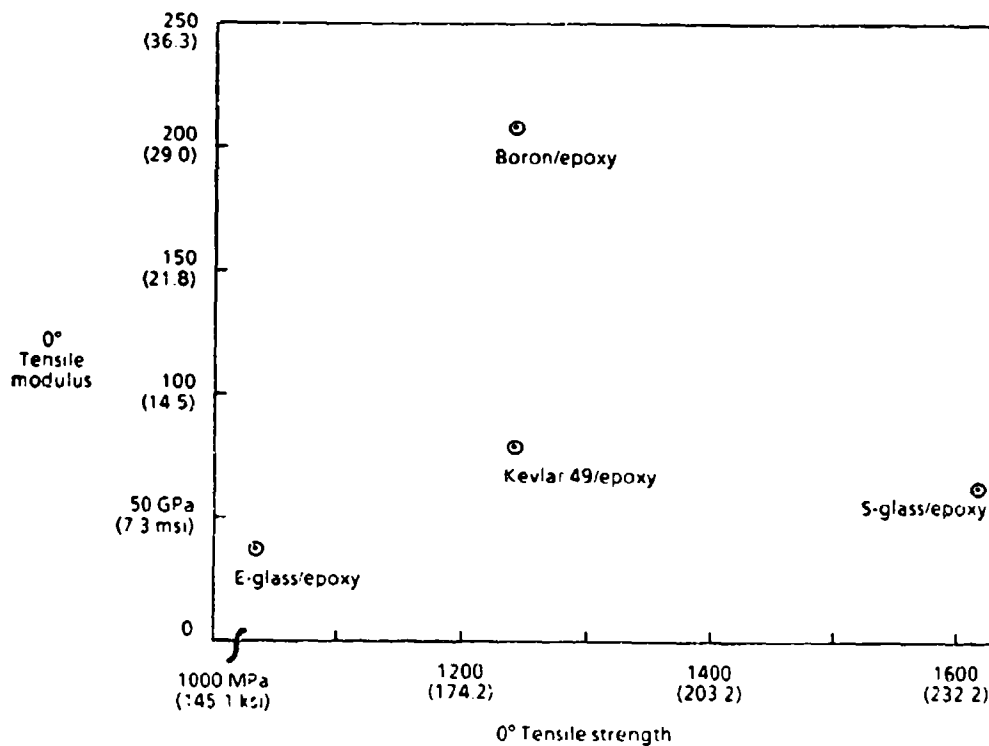
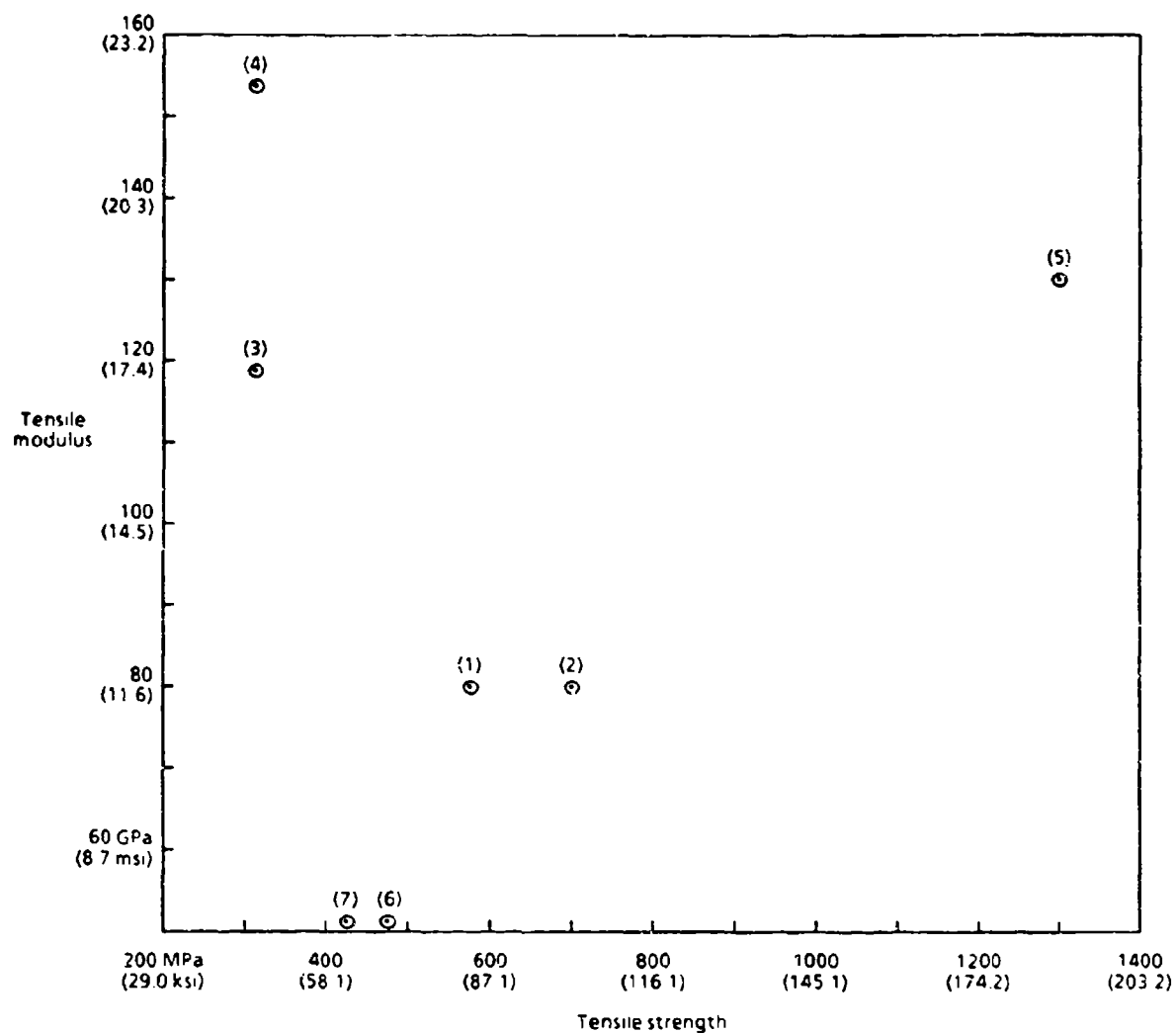


Figure B-4. 0° Tensile Properties of Typical Epoxy Composites

Table B-3. Physical Properties of Graphite Fabric Prepreg (Data From Fiberite Corp.)

Type	Ultimate tensile strength		Tensile modulus		Poisson's ratio (ν_{12})	Ultimate compressive strength		Compressive modulus		Transverse shear strength		Shear modulus		Interlaminar shear strength		Specific gravity, g/cm ³	Cured ply range	
	MPa	ksi	GPa	msi		MPa	ksi	GPa	msi	MPa	ksi	GPa	msi	MPa	ksi		μm	mils
Standard bidirectional graphite/epoxy	586	85	68.9	10.0	0.09	565	82	62.1	9.0	93.1	13.5	4.8	0.7	67.6	9.8	1.59	127-381	5-15
1 5%-strain bidirectional graphite/epoxy	690	100	68.9	10.0	0.09	586	85	62.1	9.0	93.1	13.5	4.8	0.7	66.2	9.6	1.60	178-381	7-15
High-modulus bidirectional graphite/epoxy	345	50	117.0	17.0	0.09	152	22	110.0	16.0	34.5	5.0	4.8	0.7	31.0	4.5	1.80	203-381	8-15
Ultrahigh-modulus bidirectional graphite/epoxy	345	50	152.0	22.0	0.09	152	22	152.0	22.0	34.5	5.0	4.8	0.7	34.5	5.0	1.80	152-330	6-13
Standard woven unidirectional graphite/epoxy	1310	190	129.0	18.7	0.25	1105	160	124.0	18.0	62.1	9.0	4.1	0.6	82.7	12.0	1.60	178-254	7-10
Standard bidirectional hybrid graphite/5-2 glass	483	70	51.7	7.5	0.09	565	82	48.3	7.0	34.5	5.0	4.1	0.6	65.5	9.5	1.80	254-381	10-15
Standard bidirectional hybrid graphite/Kevlar 49	448	65	51.0	7.4	0.09	276	40	41.4	6.0	-	-	-	-	34.5	5.0	1.55	254-381	10-15



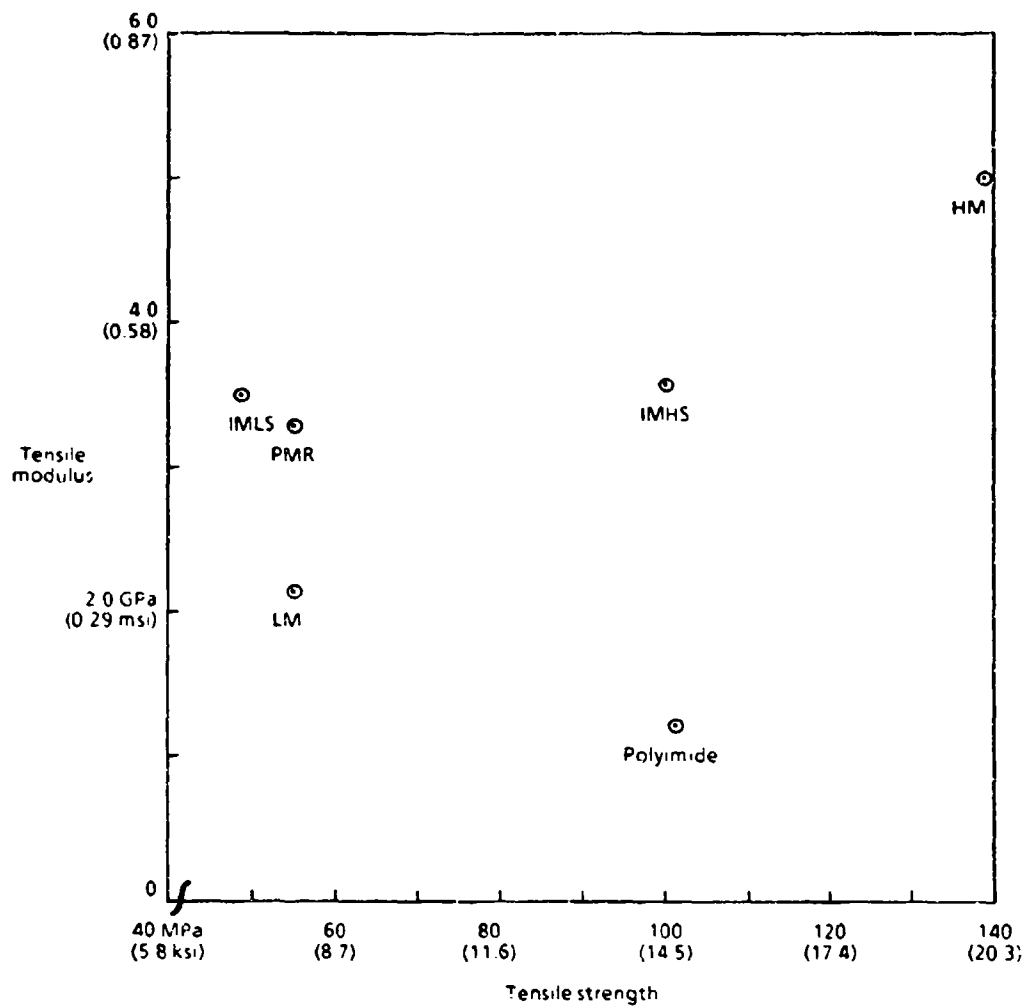
- | | |
|--|--|
| (1) Standard bidirectional graphite/epoxy | (5) Standard woven unidirectional graphite/epoxy |
| (2) 1.5%-strain bidirectional graphite/epoxy | (6) Standard bidirectional hybrid graphite/S-2 glass |
| (3) High-modulus bidirectional graphite/epoxy | (7) Standard bidirectional hybrid graphite/Kevlar 49 |
| (4) Ultrahigh-modulus bidirectional graphite/epoxy | |

Figure B-5. Tensile Properties of Graphite Fabric Prepreg

Table B-4. Properties of Matrices

Property	Units	LM	IMLS	IMHS	HM	Polyimide	PMR
Density	lb/in. ³ g/cm ³	0.042 1.16	0.046 1.27	0.044 1.22	0.045 1.25	0.044 1.22	0.044 1.22
Modulus	ksi GPa	0.32 2.20	0.50 3.45	0.50 3.45	0.75 5.17	0.50 3.45	0.47 3.24
Glass transition temperature (dry)	°C °F	177 350	216 420	216 420	216 420	371 700	371 700
Poisson's ratio	—	0.43	0.41	0.35	0.35	0.35	0.36
Thermal expansion coefficient	10 ⁻⁶ in/in °F	57	57	36	40	20	28
Moisture expansion coefficient	in/in m	0.33	0.33	0.33	0.33	0.33	0.33
Tensile strength	ksi MPa	8 55.1	7 48.2	15 103.4	20 137.8	15 103.4	8 55.1
Compression strength	ksi MPa	15 103.4	21 144.7	35 241.2	50 344.5	30 206.7	16 110.2
Shear strength	ksi MPa	8 55.1	7 48.23	13 89.57	15 103.4	13 89.57	8 55.1

Legend:
 LM = Low modulus
 IMLS = Intermediate modulus low strength
 IMHS = Intermediate modulus high strength
 HM = High modulus



Legend:

- LM = Low modulus
- IMLS = Intermediate modulus low strength
- IMHS = Intermediate modulus high strength
- HM = High modulus

Figure B-6. Tensile Properties of Matrices

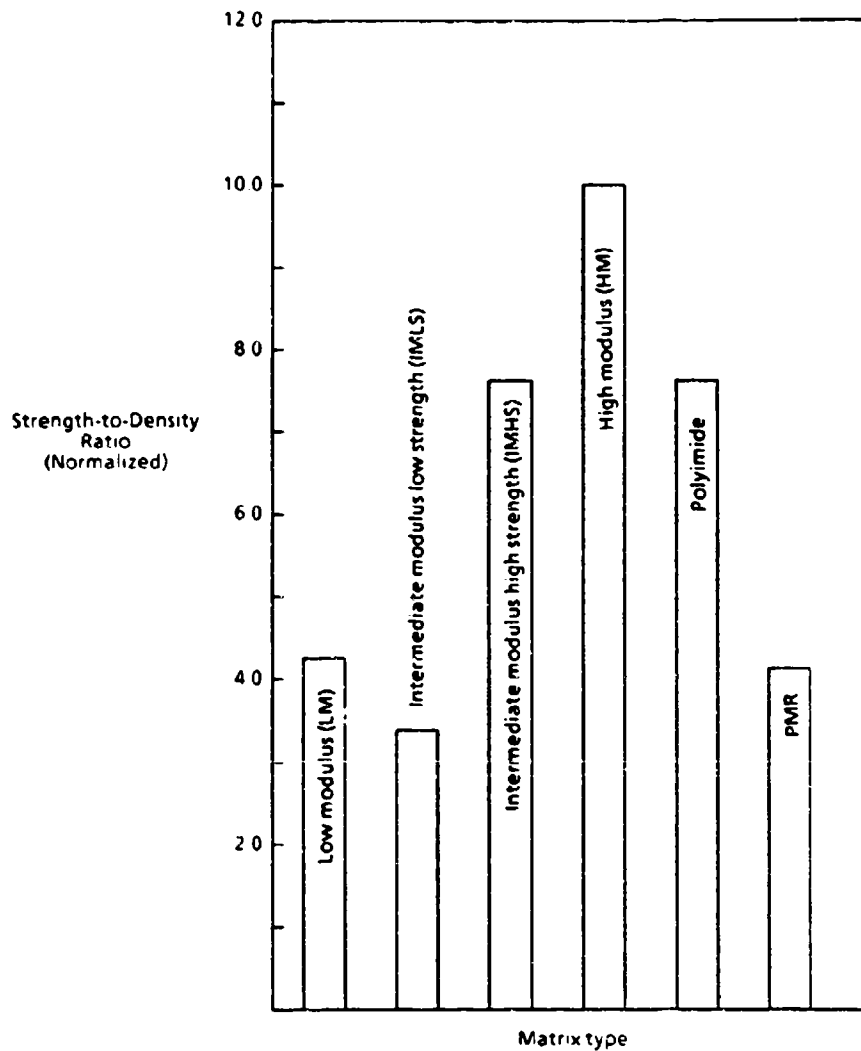


Figure B-7. Strength-to-Density Ratio of Matrices

Table B-5. Table of Neat Resin Properties at Room Temperature

Resin	Type	Specific gravity	Tensile modulus, GPa (msi)	Tensile strength, MPa (ksi)
Epoxy	Thermoset	1.1 - 1.4	2.1 - 5.5 (0.3 - 0.8)	40 - 85 (6 - 12)
Phenolic	Thermoset	1.2 - 1.4	2.7 - 4.1 (0.4 - 0.6)	35 - 60 (5 - 9)
Polyester	Thermoset	1.1 - 1.4	1.3 - 4.1 (0.2 - 0.6)	40 - 85 (6 - 12)
Acetal	Thermoplastic	1.4	3.5 (0.5)	70 (10)
Nylon	Thermoplastic	1.1	1.3 - 3.5 (0.2 - 0.5)	55 - 90 (8 - 13)
Polycarbonate	Thermoplastic	1.2	2.1 - 3.5 (0.3 - 0.5)	55 - 70 (8 - 10)
Polyethylene	Thermoplastic	0.9 - 1.0	0.7 - 1.4 (0.1 - 0.2)	20 - 35 (3 - 5)
Polyester	Thermoplastic	1.3 - 1.4	2.1 - 2.8 (0.3 - 0.4)	55 - 60 (8 - 9)

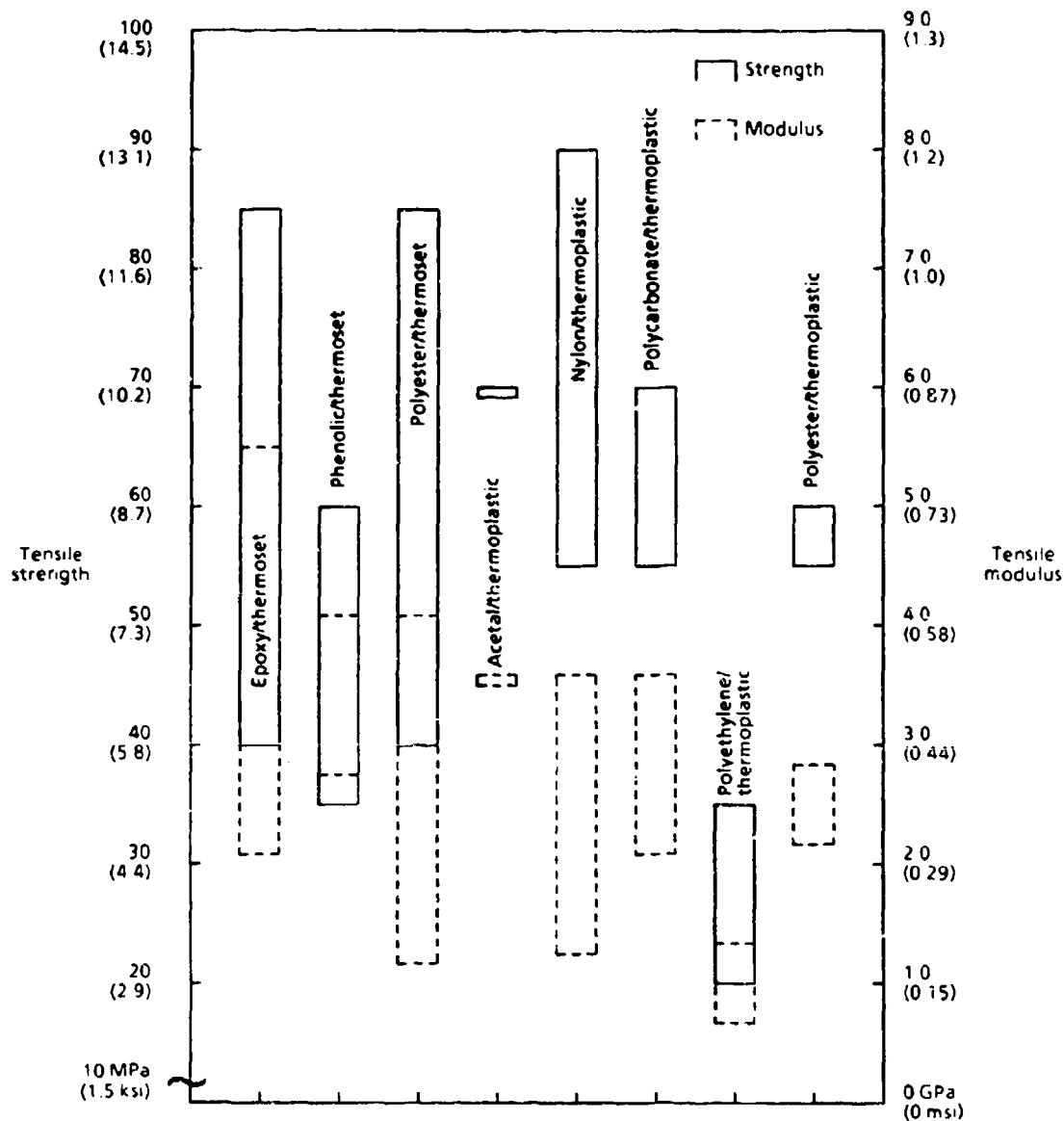
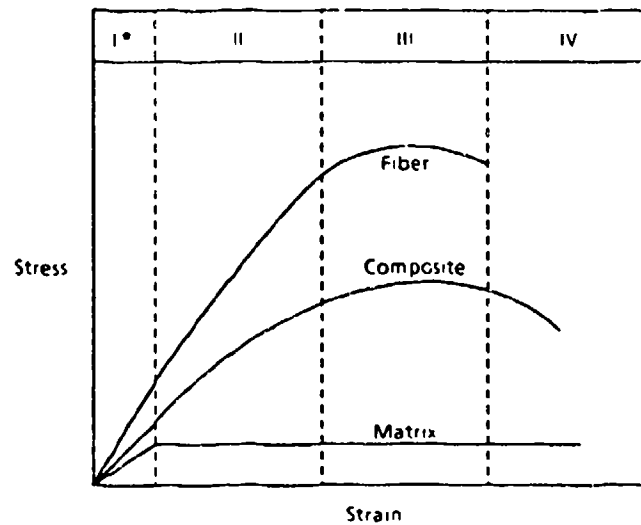


Figure B-8. Neat Resin Properties at Room Temperature



* Four stages of deformation of fibers, matrix, and composite.

- Stage I - elastic deformation of both fibers and matrix
- Stage II - elastic deformation of fibers, plastic deformation of matrix
- Stage III - plastic deformation of both fibers and matrix
- Stage IV - failure of both fibers and matrix

Figure B-9. Deformation Stages of Fiber, Matrix, and Composite

Table B-6. Properties of Graphite (Carbon) Fibers

	High strength	High modulus	Ultra-high modulus
Specific gravity, γ	1.8	1.9	2.0 - 2.1
Modulus, E , ksi (GPa)	34 (230)	53 (370)	75 - 90 (520 - 620)
Tensile strength*, σ , ksi (MPa)	360 (2480)	260 (1790)	150 - 190 (1030 - 1310)
Tensile elongation, %	1.1	0.5	0.2
Specific modulus, E/γ , ksi (GPa)	19 (130)	20 (190)	38 - 45 (260 - 310)
Specific strength*, σ/γ , ksi (MPa)	200 (1380)	137 (940)	75 - 90 (520 - 620)
Longitudinal CTE, 10^{-6} in/in°F (10^{-6} m/m °C)	-0.2 (-0.4)	-0.3 (-0.5)	-0.6, est. (-1.1, est.)

* In a typical composite

Table B-7. Properties of Kevlar and Glass Fibers

Properties	E-glass	S-glass	Kevlar 29	Kevlar 49
Specific gravity, γ	2.60	2.5	1.44	1.44
Modulus, E, msi (GPa)	10.5 (72)	12.6 (87)	12** (83)	18 (124)
Tensile strength*, σ , ksi (MPa)	250 (1,720)	360 (2,530)	330 (2,270)	330 (2,270)
Tensile elongation*, %	2.4	2.9	2.8	1.8
Specific modulus, E/ γ msi (GPa)	4.1 (28)	5.1 (35)	8.3 (57)	12.5 (86)
Specific strength*, σ/γ ksi (MPa)	96 (661)	145 (1,000)	230 (1,580)	230 (1,580)
Longitudinal, CTE, 10^{-6} in/in $^{\circ}$ F (10^{-6} m/m $^{\circ}$ C)	2.8 (5.0)	3.1 (5.6)		-1.1 (-2)

* In a typical composite

Table B-8. Tensile Strength of Neat Resins

Neat Resin System	23°C (73.4°F)				82°C (179.6°F)				121°C (249.8°F)			
	Dry		Wet		Dry		Wet		Dry		Wet	
	MPa	ksi	MPa	ksi	MPa	ksi	MPa	ksi	MPa	ksi	MPa	ksi
Hercules 3502 - epoxy	41	6.0	36	5.2	42	6.1	25	3.6	54	7.8	15	2.2
Fibredux 914 - epoxy	28	4.0	48	7.0	32	4.6	32	4.6	19	2.9	8	1.2
Hercules 2220-1 - epoxy	43	6.3	68	9.9	73	10.6	46	6.7	60	8.7	23	3.4
Hercules 2220-3 - epoxy	46	6.7	67	9.7	70	10.2	44	6.4	62	9.0	21	3.0
Hexcel 1504 - epoxy	77	11.2	51	7.4	71	10.3	48	6.9	62	9.0	16	2.3
Narmco 5245C - Bismaleimide	74	10.7	47	6.8	62	9.0	57	8.2	76	11.0	28	4.0
American Cyanamid CYCOM 907 - multiphase epoxy, formerly BP907	85	12.5	59	8.4	67	9.7	2	0.3	1	0.1	-	-
Union Carbide 4901A - epoxy cured with MDA (Methylenedianiline)	109	15.8	79	11.5	57	8.2	3	0.4	10	1.4	-	-

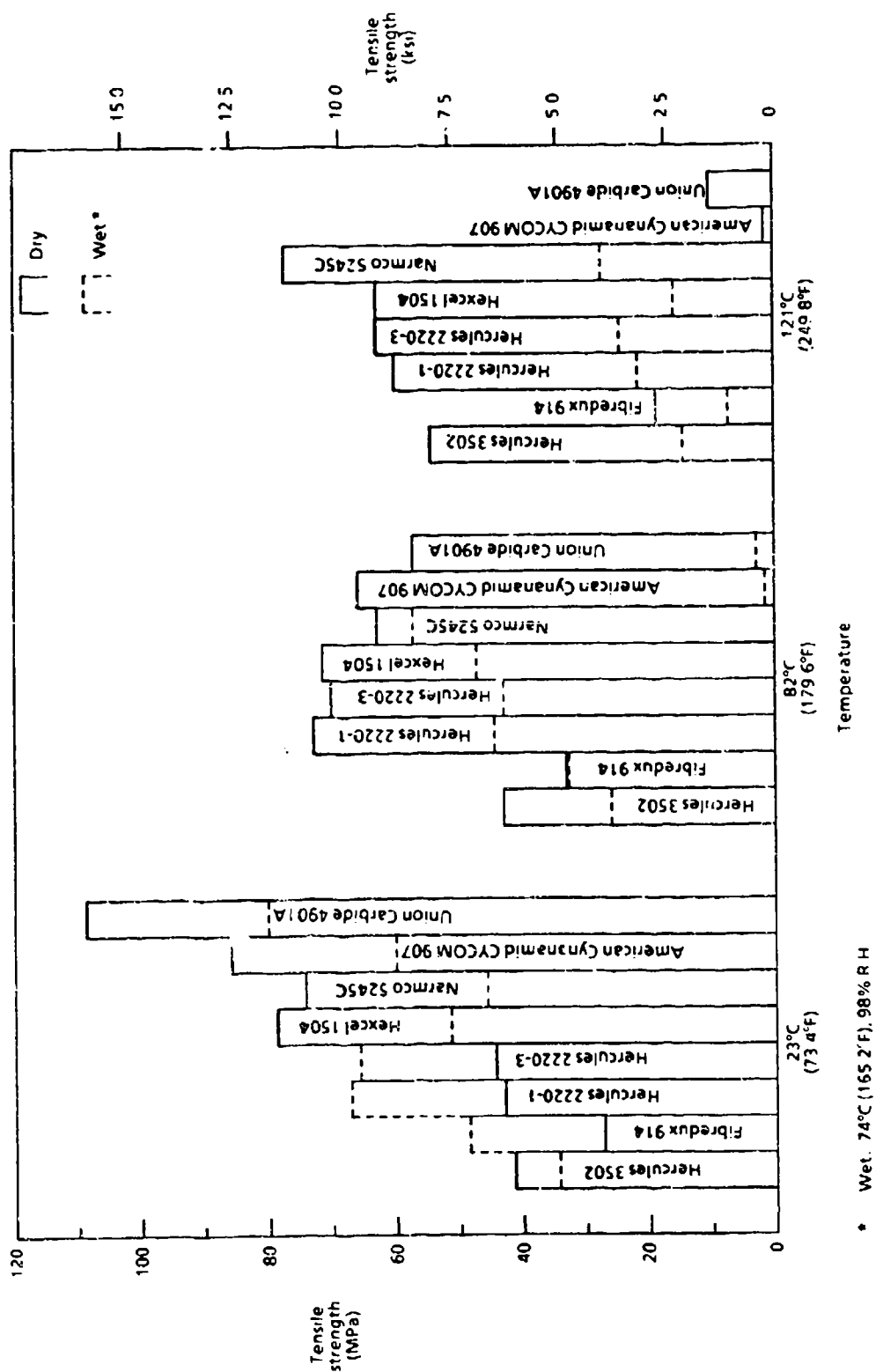
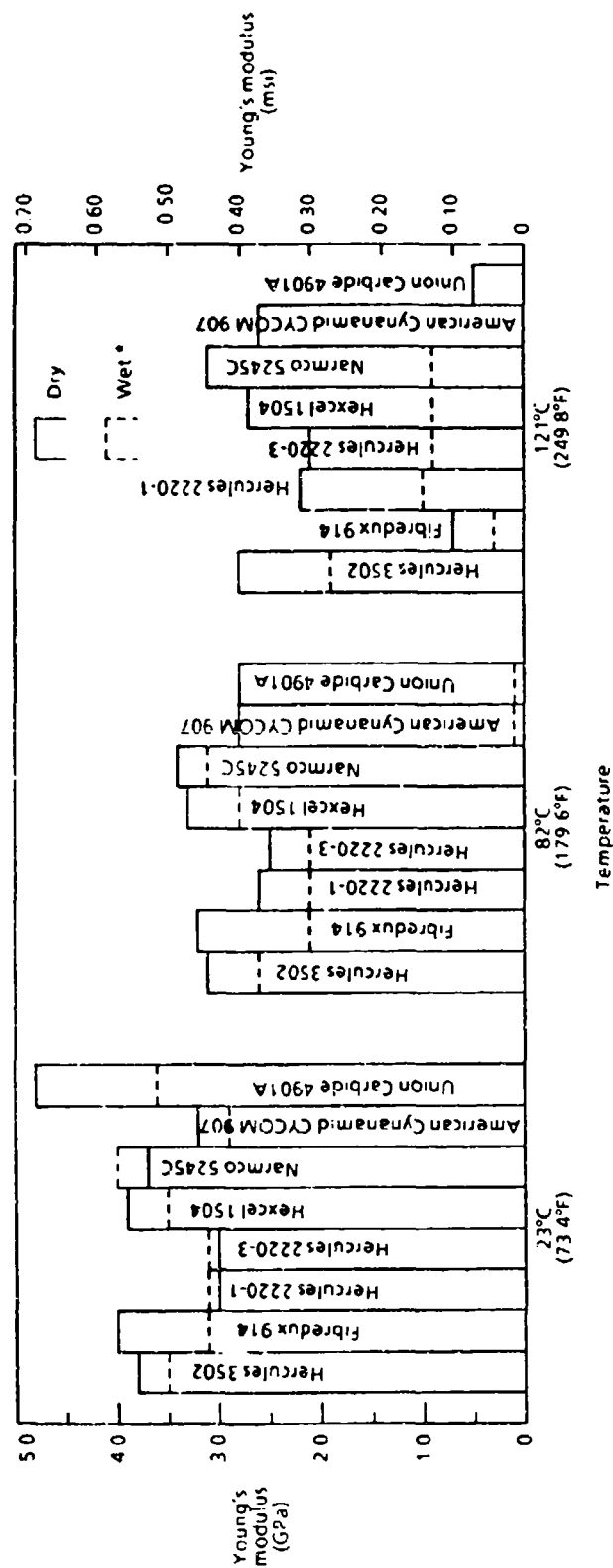


Figure B-10. Tensile Strength of Neat Resins

Table B-9. Young's Modulus of Neat Resins

Neat Resin System	23°C (73.4°F)				82°C (179.6°F)				121°C (249.8°F)			
	Dry		Wet		Dry		Wet		Dry		Wet	
	GPa	msi	GPa	msi	GPa	msi	GPa	msi	GPa	msi	GPa	msi
Hercules 3502 - epoxy	3.8	0.55	3.5	0.51	3.1	0.45	2.6	0.37	2.8	0.40	1.9	0.28
Fibredux 914 - epoxy	4.0	0.58	3.1	0.45	3.2	0.46	2.1	0.31	0.7	0.10	0.3	0.04
Hercules 2220-1 - epoxy	3.0	0.43	3.1	0.45	2.6	0.38	2.1	0.30	2.2	0.32	1.0	0.15
Hercules 2220-3 - epoxy	3.0	0.44	3.1	0.45	2.5	0.36	2.1	0.31	2.1	0.31	0.9	0.13
Hexcel 1504 - epoxy	3.9	0.57	3.5	0.51	3.3	0.48	2.8	0.40	2.7	0.39	0.9	0.13
Narmco 5245C - Bismaleimide	3.7	0.54	4.0	0.58	3.4	0.50	3.1	0.45	3.1	0.45	0.9	0.13
American Cyanamid CYCOM 907 - multiphase epoxy, formerly BP907	3.2	0.47	2.9	0.42	2.8	0.40	0.1	0.01	2.6	0.38	-	-
Union Carbide 4901A - epoxy, cured with MUA (methylenedianiline)	4.8	0.70	3.6	0.52	2.8	0.41	0.1	0.01	0.5	0.07	-	-



• Wet: 74°C (165.2°F), 98% R.H.

Figure B-11. Young's Modulus of Neat Resins

Table B-10. Physical Properties of Epoxy Preimpregnated Unidirectional Tapes

Type	Ultimate tensile strength		Tensile modulus		Poisson's ratio (ν_{12})	Ultimate compressive strength		Compressive modulus		Transverse shear strength		Shear modulus		Interlaminar shear strength		Specific gravity, g/cm ³	Cured ply range	
	MPa	ksi	GPa	msi		MPa	ksi	GPa	msi	MPa	ksi	MPa	ksi	MPa	ksi		μm	mil
Standard graphite/epoxy	1515	220	131	19.0	0.3	1310	190	131	19.0	66	9.5	4.1	0.6	110	16.0	1.58	51-254	2-10
1 5%-strain graphite/epoxy	1895	275	134	19.4	0.3	1585	230	131	19.0	66	9.5	4.1	0.6	110	16.0	1.60	102-203	4-8
1 8%-strain graphite/epoxy	2585	375	138	20.0	0.3	1585	230	134	19.5	69	10.0	4.1	0.6	110	16.0	1.61	102-203	4-8
Intermediate modulus graphite/epoxy	2760	400	165	24.0	0.3	1380	200	145	21.0	66	9.5	4.1	0.6	110	16.0	1.60	102-203	4-8
High modulus graphite/epoxy	780	113	239	34.7	0.3	345	50	228	33.0	34	5.0	4.8	0.7	35	5.1	1.80	64-254	2.5-10
Ultrahigh modulus graphite/epoxy	760	110	314	45.6	0.3	338	49	316	45.9	37	5.4	4.8	0.7	66	9.5	1.83	64-254	2.5-10
Pitch-100/epoxy	1035	150	421	61.0	0.3	255	37	310	45.0	34	5.0	4.8	0.7	31	4.5	1.83	64-127	2.5-5
Kevlar 49/epoxy	1365	198	46	6.7	0.3	207	30	41	6.0	59	8.5	2.1	0.3	52	7.5	1.45	127-254	5-10
E glass/epoxy	1035	150	41	6.0	0.3	827	120	41	6.0	-	-	-	-	76	11.0	1.90	102-305	4-12
S-2 glass/epoxy	1690	245	52	7.6	0.3	827	120	60	8.7	-	-	-	-	76	11.0	2.02	102-305	4-12

Table B-11. Properties of Commercial Carbon Fibers

	Fiber diameter		Density		Tensile strength		Tensile modulus	
	μm	mils	g/cm^3	lb/in^3	MPa	ksi	GPa	msi
Magnamite AS1	8.00	0.315	1.80	0.065	3100	450	230	33
Magnamite AS4	8.00	0.315	1.80	0.065	3590	520	235	34
Magnamite AS6	-	-	1.82	0.066	4140	600	243	35
Magnamite IM6	-	-	1.74	0.063	4380	635	279	40
Celion GY-70	8.38	0.330	1.91-1.97	0.069-0.071	1520	220	485	70
Celion 3000	7.11	0.280	1.77	0.064	3790	550	231	34
Thornei T-300	6.93	0.273	1.77	0.064	3240	470	231	34

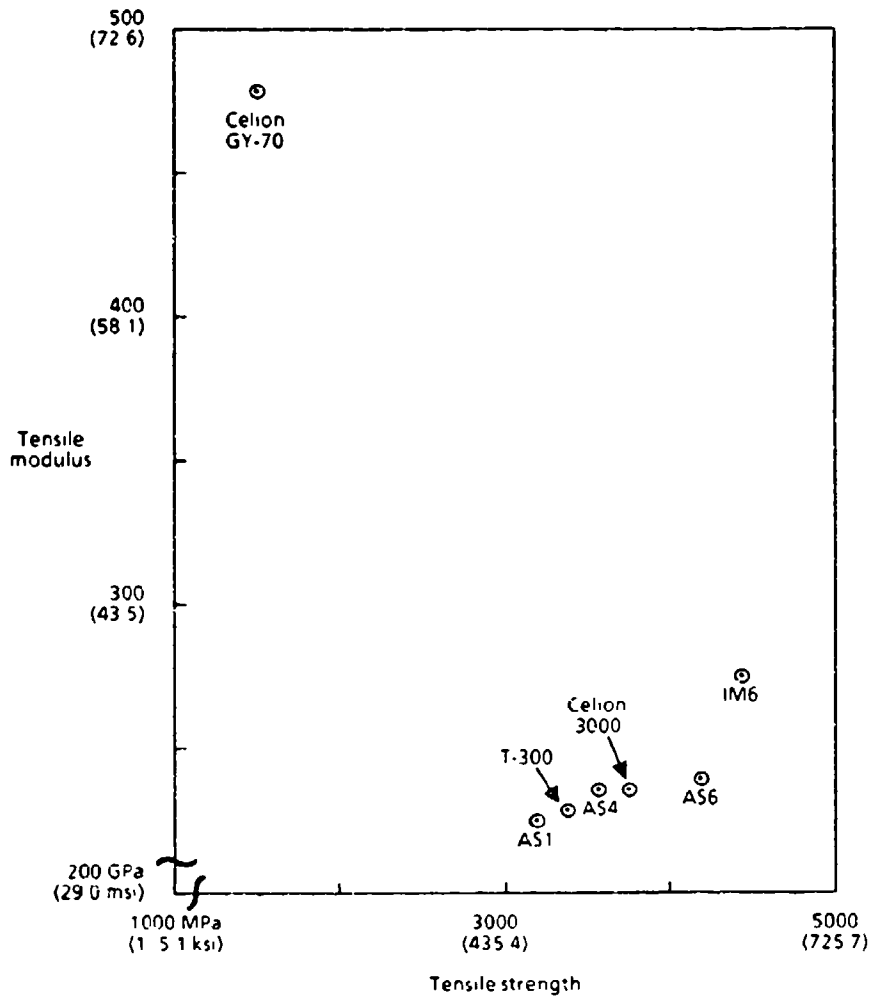


Figure B-12. Tensile Properties of Commercial Carbon Fibers

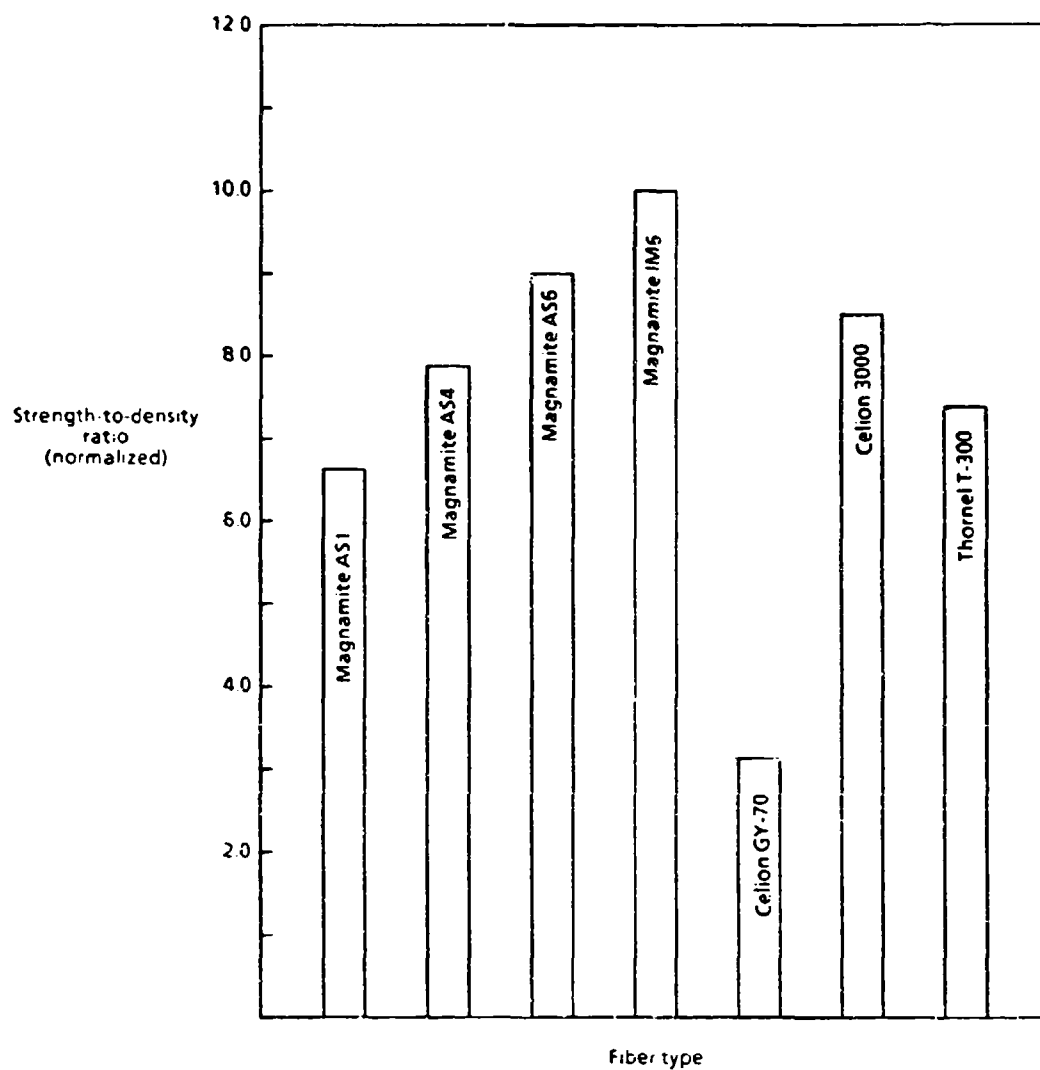


Figure B-13. Strength-to-Density Ratio of Commercial Carbon Fibers

Table B-12. Constituent Property Data of Fibers

	Kevlar 29	Kevlar 49	E-glass	S-glass	High-strength carbon fiber	High-modulus carbon fiber	Ultra-high-modulus carbon fibers
Specific gravity	1.44	1.44	2.60	2.50	1.8	1.9	2.0-2.1
Modulus, msi (GPa)	12** (83)	18 (124)	10.5 (72)	12.6 (87)	34 (230)	53 (370)	75-90 (520-620)
Tensile strength, ksi (MPa)	330* (2270)	330* (2270)	250* (1720)	360* (2530)	360* (2480)	260* (1790)	150-190* (1030-1310)
Tensile elongation, %	2.8*	1.8*	2.4*	2.9*	1.1*	0.5*	0.2*
Specific modulus, msi (GPa)	8.3 (57)	12.5 (86)	4.1 (28)	5.1 (35)	19 (130)	28 (190)	3.8-4.5 (260-310)
Specific strength, ksi (MPa)	230* (1580)	230* (1580)	96* (661)	145* (1000)	200* (1380)	137* (940)	75-90* (520-620)
Longitudinal CTE, 10 ⁻⁶ in/in°F (10 ⁻⁶ m/m°C)	----	-1.1 (-2)	2.8 (5.0)	3.1 (5.6)	-0.2 (0.4)	-0.3 (-0.5)	-0.6 (-1.1)

* In a typical composite

** Modulus increases with stress Initial value reported